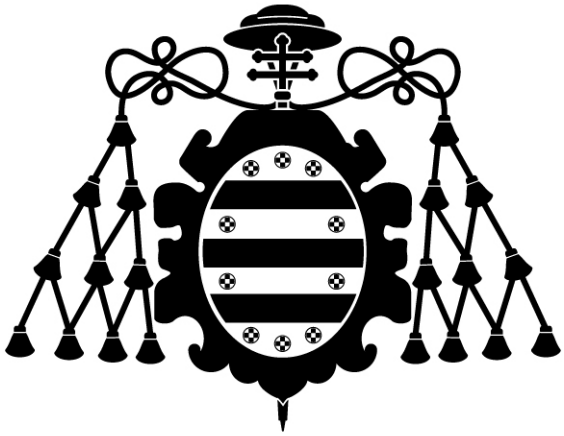

Universidad de Oviedo

Universidá d'Uviéu

University of Oviedo

Programa de Doctorado de Materiales

STUDY OF THE ADS/CFT CORRESPONDENCE AND ITS APPLICATIONS TO STRONGLY COUPLED PHENOMENA

TESIS DOCTORAL

David Rodríguez Fernández

Marzo 2018

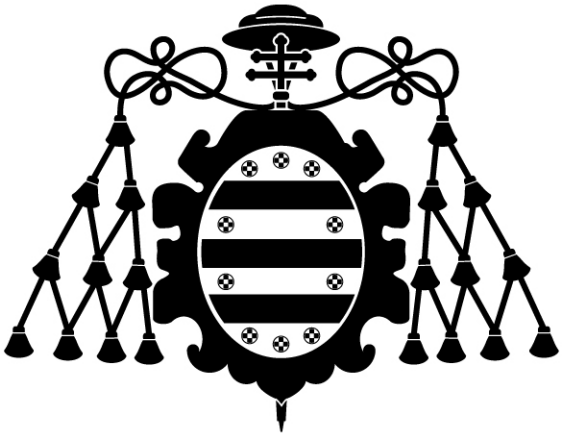

Universidad de Oviedo
Universidá d'Uviéu
University of Oviedo

Programa de Doctorado de Materiales

STUDY OF THE ADS/CFT CORRESPONDENCE AND ITS APPLICATIONS TO STRONGLY COUPLED PHENOMENA

TESIS DOCTORAL

Director de tesis:
Carlos Hoyos Badajoz

RESUMEN DEL CONTENIDO DE TESIS DOCTORAL

1.- Título de la Tesis	
Español: Estudio de la correspondencia AdS/CFT y sus aplicaciones a fenómenos fuertemente acoplados.	Inglés: Study of the AdS/CFT correspondence and its applications to strongly coupled phenomena.

2.- Autor	
Nombre: David Rodríguez Fernández	DNI:
Programa de Doctorado: Materiales	
Órgano responsable: Departamento de Ciencia de los Materiales e Ingeniería Metalúrgica	

RESUMEN (en español)

La correspondencia AdS/CFT, o también llamada dualidad holográfica, ha llegado a ser una de las herramientas más potentes para describir sistemas físicos en donde las interacciones entre sus constituyentes no se pueden describir mediante análisis perturbativo. En la presente tesis, se han examinado las aplicaciones de la correspondencia AdS/CFT a algunos de los más interesantes sistemas físicos en la actualidad, tales como el plasma de quarks y gluones (QGP), actualmente generado en colisiones de iones pesados, así como sistemas bidimensionales, con posibles aplicaciones a materia condensada.

Hemos examinado las relaciones entre coeficientes de transporte, i.e. cantidades que indican la respuesta a estímulos externos, existentes en sistemas que presentan simetría rotacional y de paridad en dos dimensiones espaciales, de acuerdo con el contexto de la dualidad holográfica, siendo capaces de plantear un procedimiento para obtener información acerca de dichas relaciones para este tipo de sistemas. Dicho procedimiento fue contrastado con sistemas ya conocidos, obteniendo los resultados esperados.

En cuanto al QGP, combinando un modelo holográfico para describir materia quarkionica en estado deconfinado, esto es, en estado libre, junto con un modelo usado para describir dicha materia en estado confinado (formando bariones), se ha modelizado el interior de una estrella de neutrones, hallando relaciones para la masa y radio globales que concuerdan con los datos experimentales. Predijimos además la existencia de una transición de primer orden a esas densidades tan brusca que la porción de materia deconfinada es prácticamente despreciable.

Además, existen argumentos (relacionados con el tamaño de las estrellas de neutrones y la viabilidad de que posean materia quarkionica) que establecen que el QGP a densidades intermedias pueda comportarse como un sistema de gran rigidez y fuertemente acoplado. Aunque la dualidad holográfica es exitosa para describir sistemas a acoplo fuerte, no ha sido capaz hasta ahora de describir sistemas extremadamente rígidos. En la presente tesis se presentan varios modelos válidos y precisos, de acuerdo con la correspondencia AdS/CFT, que caracterizan sistemas rígidos a acoplo fuerte, encontrando de hecho que pueden llegar a reproducir la máxima rigidez que un sistema físico pueda presentar, dictada por causalidad.

RESUMEN (en Inglés)

The AdS/CFT correspondence, also called holography, has become one of the most powerful tools to describe physical systems whose interactions between their constituents are non-perturbative. In the present thesis, we have examined some applications of the AdS/CFT correspondence to some of the most interesting and challenging systems in physics nowadays, such as the quark gluon plasma (QGP), which is currently generated in heavy ion collisions, as well as systems in two spatial dimensions, which could be related to real systems in that appear in condensed matter physics.

Within the context of holography, we have examined the relations between the transport coefficients, i.e. quantities that characterize the response against external perturbations, existing in systems that exhibit rotational and parity invariance in two spatial dimensions. In particular, we have been able to propose a method to draw information about such relations for these systems. Such prescription was tested with already known systems, obtaining the expected results.

In relation to the QGP, by combining a holographic model to describe deconfined quark matter, that is, free quarks, with a model employed to describe confined quark matter (that constitute baryons), we have modeled the interior of a neutron star, finding relations for the overall mass and radii that agree with the data from current astrophysical observations. In particular, we predicted the existence of a first order phase transition at densities so large, that only a tiny fraction of deconfined matter was allowed to be present.

In addition, there are some arguments (related to the size of neutron stars and the possibility of accommodating a deconfined quark core) that state that the QGP at intermediate densities may behave as a stiff system, i.e. rigid against compression, at strong coupling. Although holography has been successful in describing strongly coupled systems, it has been unable to model systems with large stiffness. In this thesis we presented several valid and accurate holographic models that reproduce stiff systems at strong coupling, finding actually that they can accommodate the largest possible stiffness, dictated by causality.

SR. PRESIDENTE DE LA COMISIÓN ACADÉMICA DEL PROGRAMA DE DOCTORADO EN MATERIALES

Contents

Acknowledgments

I wish to thank many people who greatly contributed to my development as a researcher, specially to my supervisor Carlos Hoyos, not only for sharing with me his wide knowledge on the AdS/CFT correspondence and physics in general, but also for his essential and skilled guidance, top-rate professionality and friendly treatment to me. I am also deeply thankful to Aleksi Vuorinen, for the great support that he gave me the times I have been at the University of Helsinki as a visitor, as well as for his pleasant character and strong involvement during the development of the works we share, in collaboration with Niko Jokela, to whom I wish also to thank. I would like to thank also my PhD colleagues and collaborators, Christian Ecker and Eemeli Annala, for their hard work and involvement, and for so many useful discussions with them.

I also would like to thank Yolanda Lozano and to the High Energy Theoretical Physics Group for supporting me with their GRUPIN 14-108 Ph.D. research grant, in order to carry out my activities as a Ph.D. student, and for supporting me when attending to conferences, Ph.D. schools and seminars, so essential and fruitful in my improvement as a researcher.

Finally, but not less important, I would like to give special thanks to my parents and to Lucía Rodríguez for the unconditional support they have been giving me to carry on.

About this thesis

This thesis is oriented towards the gauge/gravity duality and its applications to physical phenomena. It is presented as a compendium of publications that reflect the research activities that I carried out as a Ph.D student under the High Energy Physics Theory group at the Oviedo University from 2014 to 2017.

In this thesis, we shall begin by giving an introduction in section 2, in which we shall explain some issues regarding the holography and give an overview to some of its applications to phenomenology, providing also a complementary bibliography. In section 3 we present the papers just as they were published, leaving for section 4 a summary of the main results of the such papers, while in section 5 we comment on the conclusions that we have drawn from our research. Finally, in section 7 we give some additional information about the papers, such as their impact parameter according to the Journal Citation Reports.

Summary

The AdS/CFT correspondence, also called holography, has become one of the most powerful tools to describe physical systems whose interactions between their constituents are non-perturbative. In the present thesis, we have examined some applications of the AdS/CFT correspondence to some of the most interesting and challenging systems in physics nowadays, such as the quark gluon plasma (QGP), which is currently generated in heavy ion collisions, as well as systems in two spatial dimensions, which could be related to real systems in condensed matter physics.

Within the context of holography, we have examined the relations between the transport coefficients, i.e. quantities that characterize the response against external perturbations, existing in systems that exhibit rotational and parity invariance in two spatial dimensions. In particular, we have been able to propose a method to draw information about such relations for these systems. Such prescription was tested with already known systems, obtaining the expected results.

In relation to the QGP, by combining a holographic model to describe deconfined quark matter, that is, free quarks, with a model employed to describe confined quark matter (that constitute baryons), we have modeled the interior of a neutron star, finding relations for the overall mass and radii that agree with the data from current astrophysical observations. In particular, we predicted the existence of a first order phase transition at densities so large, that only a tiny fraction of deconfined matter was allowed to be present.

In addition, there are some arguments (related to the size of neutron stars and the possibility of accommodating a deconfined quark core) that state that the QGP at intermediate densities may behave as a stiff system, i.e. rigid against compression, at strong coupling. Although holography has been successful in describing strongly coupled systems, it has been unable to model systems with large stiffness. In this thesis we presented several valid and accurate holographic models that reproduce stiff systems at strong coupling, finding actually that they can accommodate the largest possible stiffness, dictated by causality.

Resumen

La correspondencia AdS/CFT, o también llamada dualidad holográfica, ha llegado a ser una de las herramientas más potentes para describir sistemas físicos en donde las interacciones entre sus constituyentes no se pueden describir mediante análisis perturbativo. En la presente tesis, se han examinado las aplicaciones de la correspondencia AdS/CFT a algunos de los más interesantes sistemas físicos en la actualidad, tales como el plasma de quarks y gluones (QGP), actualmente generado en colisiones de iones pesados, así como sistemas bidimensionales, con posibles aplicaciones a materia condensada.

Hemos examinado las relaciones entre coeficientes de transporte, i.e. cantidades que indican la respuesta a estímulos externos, existentes en sistemas que presentan simetría rotacional y de paridad en dos dimensiones espaciales, de acuerdo con el contexto de la dualidad holográfica, siendo capaces de plantear un procedimiento para obtener información acerca de dichas relaciones para este tipo de sistemas. Dicho procedimiento fue contrastado con sistemas ya conocidos, obteniendo los resultados esperados.

En cuanto al QGP, combinando un modelo holográfico para describir materia quarkionica en estado deconfinado, esto es, en estado libre, junto con un modelo usado para describir dicha materia en estado confinado (formando bariones), se ha modelizado el interior de una estrella de neutrones, hallando relaciones para la masa y radio globales que concuerdan con los datos experimentales. Predijimos además la existencia de una transición de primer orden a esas densidades tan brusca que la porción de materia deconfinada es prácticamente despreciable.

Además, existen argumentos (relacionados con el tamaño de las estrellas de neutrones y la viabilidad de que posean materia quarkionica) que establecen que el QGP a densidades intermedias pueda comportarse como un sistema de gran rigidez y fuertemente acoplado. Aunque la dualidad holográfica es exitosa para describir sistemas a acoplo fuerte, no ha sido capaz hasta ahora de describir sistemas extremadamente rígidos. En la presente tesis se presentan varios modelos válidos y precisos, de acuerdo con la correspondencia AdS/CFT, que caracterizan sistemas rígidos a acoplo fuerte, encontrando de hecho que pueden llegar a reproducir la máxima rigidez que un sistema físico pueda presentar, dictada por causalidad.

1 Preface

This thesis has been submitted to the Faculty of Science, University of Oviedo, as a partial fulfillment of the requirements to obtain the PhD degree. The work presented here has been developed during the years 2014-2017 under the supervision of Dr.Carlos Hoyos at the Department of Physics of Oviedo University.

Thesis objectives

The present thesis investigates the applications of holography to the description of physical systems in two and three spatial dimensions. By means of the gauge/gravity duality, the following aspects are examined:

- A general prescription to derive Ward identities for fluid hydrodynamics on a plane.
- The modeling of the deconfined state of the Quark Gluon Plasma, taking particular interest on the ultra-dense regime. The characterization, by means of a sensible holographic model (either stand-alone or combined with other complementary models), of the phase diagram at those densities.
- A prediction of allowed mass vs radius curves for stable neutron stars from holographic models. A comparison of the results with astrophysical observations.
- In holographic UV complete quantum field theories, it has been conjectured a bound on the speed of sound, v_s less than $1/\sqrt{3}$. Testing whether this bound is true. If not, present holographic models that describe relativistic matter at equilibrium with a speed of sound larger than $1/\sqrt{3}$.
- Determining if any other bound on the speed of sound may exist for UV complete holographic theories in four dimensions. This question is equivalent to determining what is the stiffest system that the gauge/gravity duality can model.

2 Introduction

In theoretical physics, important new results have often been found by realising that two different concepts are related to each other at a deep and fundamental level. Examples of such relations are *dualities*, which relate two seemingly different quantum field theories to each other by stating that the theories are in fact equivalent. The Anti-de Sitter/Conformal Field Theory correspondence (AdS/CFT) is one example of duality, which relates a quantum field theory on flat spacetime to a string theory.

In the so-called *weak form*, the AdS/CFT correspondence is an example of a strong-weak coupling duality, namely, if the field theory is strongly coupled, the dual gravity theory is classical and weakly coupled. Thanks to this, certain questions relating strongly coupled quantum field theories become computationally tractable on the gravity side and also conceptually clearer. The AdS/CFT correspondence and its generalizations [1–3] has become a unique tool to examine strongly coupled phenomena (see [4] for a review). The holographic duality has successfully been applied to obtain correlation functions and non-linear fluid dynamics for systems which were intractable before [5]. During the last ten years, its applications to condensed matter (CM) have become wide [6, 7], allowing to shed some light into some non-conventional materials, such as, topological systems [8], Weyl semimetals at strong coupling [9], certain superconductors [10], p-wave superfluids [11] or metal-insulator transitions [12]. Not only that, but it has also been used to the prediction of new states of matter with particular and unique properties, [13, 14], the modeling phase transitions [15–17] or to the characterization of the Kondo effect and Fano resonances for systems at strong coupling [18].

An important aspect has been the derivation of fluid properties, in particular those associated to the transport of conserved currents such as energy, momentum or charge. Transport is characterized by transport coefficients, that can be defined from correlators of conserved currents through Kubo formulas, or in other ways such as constitutive relations in hydrodynamics. An alternative way to identify the coefficients is through the derivative expansion of the equilibrium partition function as in [19, 20]. Moreover, not all the transport coefficients one can possibly define are independent. For correlators of conserved currents there are Ward identities that impose relations among them, thus constraining some of the transport coefficients. In some cases these relations lead to interesting effects, an example is the relation between Hall conductivity and Hall viscosity found in [21] for Quantum Hall systems with Galilean invariance. Both coefficients are interesting from the point of view of the characterization of topological phases.

However, in general, viscosities are much more difficult to measure than conductivities, since it is necessary to deform the material and measure the resulting stress, while the conductivities can be determined by a much simpler measurement of an electric current. This situation is helped by the relation between the two. In the presence of an inhomogeneous electric field, the Hall current receives a correction, which to leading order in derivatives is

$$J^i \sim \sigma_H E^i + \sigma_H^{(2)} \nabla^2 E^i. \tag{2.1}$$

The coefficient $\sigma_H^{(2)}$ depends on the Hall viscosity and other quantities that can be determined independently. This in principle allows to determine the Hall viscosity via highly inhomogeneous electric fields, which may be easier to realize experimentally than a direct measurement of the viscosity.

In terms of retarded 2-point functions of the energy-momentum tensor

$$\Gamma^{\mu\nu\alpha\beta}(x,\hat{x}) = \left\langle T^{\mu\nu}(x) T^{\alpha\beta}(\hat{x}) \right\rangle_R , \tag{2.2}$$

the relevant Ward identity is, in the absence of external sources ($i,j = 1,2$ label the spatial directions)

$$\partial_0 \hat{\partial}_0 \Gamma^{0i0j}(x,\hat{x}) + \partial_k \hat{\partial}_l \Gamma^{kilj}(x,\hat{x}) \simeq 0. \tag{2.3}$$

The right hand side might contain contact terms but otherwise it's zero because of the conservation of the energy-momentum tensor. The identity can be derived combining the two identities

$$\partial_\mu \Gamma^{\mu\nu\alpha\beta}(x,\hat{x}) \simeq 0, \quad \hat{\partial}_\alpha \Gamma^{\mu\nu\alpha\beta}(x,\hat{x}) \simeq 0. \tag{2.4}$$

In holography, some of these identities have been derived already from the holographic renormalization procedure [22,23], in particular the Ward identities for charged $2+1$ dimensional systems were studied in some detail in [10, 24, 25]. In the case of asymptotically AdS spacetimes[1] this follows from 'kinematics', it is not necessary to know the full geometry but the identity follows from the asymptotic expansion and the equations of motion. However, the second identity in (2.4) does not follow directly from the asymptotic expansion, it requires further input. So far the relations between viscosities and conductivities in the AdS/CFT correspondence could only be checked by direct computation of the correlators, but a general 'kinematic' argument should exist, since they follow from symmetries and will be valid in any field theory. In [32] we address to this question, by examining strongly coupled systems in $2+1$ dimensions with parity and rotational invariance.

[1] Generalizations for other geometries have been discussed in [26–31].

The holographic duality is not restricted to CM only. Quantitatively predicting the properties of Quantum Chromodynamics is one of the biggest challenges of modern physics [33, 34]. The complexity of the task originates from the need to non-perturbatively solve the theory of strong interactions, QCD; either at zero density, by means of Lattice QCD which, although accurate in the low density regime, requires the use of highly powerful computers and complex programming algorithms, and at finite baryon chemical potential μ_B, wherein the lack of knowledge becomes even greater. This combination of requirements is problematic, as it makes all the usual first principles tools fail: Lattice simulations suffer from the sign problem at finite baryon chemical potential [35], while perturbative QCD is invalidated by the sizable value of the gauge coupling at moderate densities [36]. At present, the Equation of State (EoS), i.e. the functional dependence of its energy density ε on the pressure p, which is the most fundamental quantity that governs the thermodynamic behavior of neutron star matter, is under quantitative control for cold strongly interacting matter at baryon densities below the nuclear saturation limit, $n_B \leq n_s \approx 0.16/\text{fm}^3$, where Chiral Effective Theory (CET) works [37, 38], as well as at baryon chemical potential above roughly 2.5 GeV where the perturbative EoS converges [39–42]. These limits unfortunately exclude the densities $n_s \leq n_B \leq 10n_s$, where it is possible that a deconfining phase transition to quark matter takes place [43]. Under these circumstances, it is a common approach in phenomenological physics to employ fixed EoS parametrized in a certain way (polytropic EoS, [44]). While they can provide some insight, they do not lean on a first-principle formulation.

Clearly, there is a need for fundamentally new approaches to the physics of strongly coupled quark matter — a challenge not unlike understanding the dynamics of hot quark-gluon plasma. In this context, a very promising approach has turned out to be to apply the holographic duality. Although limited by the fact of involving the large N limit, fundamentally different than QCD, with $N = 3$, it has been nevertheless successfully used to study the deconfined phases of QCD matter [45, 46] and to probe very nontrivial equilibration dynamics [47–49], giving useful insight on qualitative properties of QCD.

In the first formulation of the duality [1], the field theory is superconformal with degrees of freedom in the adjoint representation, however, there are several ways to capture the dynamics of fundamental flavors. One way in particular, which has been regarded in the present thesis, is to consider the addition of probe D-branes in the 't Hooft limit of $\lambda_{YM} \equiv g^2_{YM} N_c \gg 1$ and $N_c \gg N_f$. In this approach, the gluon sector continues to be described by classical supergravity (SUGRA) [50]. States with finite baryon density in the gauge theory correspond to gravity con-

figurations with a gauge field turned on in the D-brane worldvolume. The free energy can then be computed by evaluating the classical on-shell action of SUGRA together with the D-brane action. Given the relative simplicity of the calculations involved, the duality thus bestows us with a powerful tool to explore strongly coupled quark matter even at high density. In the present thesis we shall regard this model in particular when characterizing the inner core of a hybrid neutron star.

Astrophysical observations of neutron stars with masses up to two solar masses [51,52] imply that the EoS of the matter inside the stars should be very stiff—a property needed to build massive stars capable of resisting gravitational collapse into a black hole [53]. The stiffness can be measured by the thermodynamic derivative[2]

$$v_s^2 = \left(\frac{\partial p}{\partial \varepsilon}\right)_s \ , \tag{2.5}$$

where v_s can be identified as the speed of propagation of sound waves, naturally obeying the causal bound $v_s \leq 1$ (and thermodynamic stability guarantees that $v_s^2 > 0$), but it has been widely speculated that a more restrictive bound might exist as well. In particular, the lack of known physical systems in a deconfined phase with a speed of sound exceeding the conformal value $v_s^2 = 1/3$ has prompted a conjecture that this might represent a theoretical upper limit for this quantity [54, 55]. Some support for this argument comes from the fact that both the inclusion of a nonzero mass to a conformal system as well as the introduction of perturbatively weak interactions in an asymptotically free theory are known to lead to a speed of sound below the conformal limit. We should also note that a bound on the speed of sound *at fixed chemical potential* has been proposed in [56], and it seems to hold in holographic models that reproduce thermodynamic properties of QCD computed using lattice techniques at small densities [57].

Moreover, an interesting observation pointing towards neutron star matter indeed behaving like a strongly coupled system can be seen from the so-called Taub's inequality [58] (see also [59]), which states that in a relativistic kinetic theory, causality imposes the condition

$$\varepsilon(\varepsilon - 3p) \geq \rho^2 \ , \tag{2.6}$$

where ρ stands for the mass density. For instance, it is easy to check that degenerate fermionic matter satisfies Taub's inequality for any value of the chemical potential. It is far from being guaranteed that matter inside neutron stars would admit a quasiparticle description, therefore, any (holographic) theory candidate to model the interior of a neutron star, would presumably

[2]The symbol s denotes the entropy density here.

predict a violation of such bound.

The speed of sound conjecture has been widely discussed in the context of neutron star physics, and it has been shown to be in rather strong tension with the known existence of two-solar-mass neutron stars [51,52], which requires a very stiff EoS [53]. This points toward a highly nontrivial behavior of v_s as a function of the baryon chemical potential. Namely, at low densities the speed of sound is known to have a very small value, while its behavior at asymptotically large μ_B is a logarithmic *rise* toward $v_s^2 = 1/3$. This implies that should the speed of sound bound be violated somewhere, v_s needs to possess at least two extrema, a maximum and a minimum, between which the quantity may either behave continuously or jump discontinuously from above the conformal value to below it.

Despite the many achievements of the gauge/gravity duality applied to QCD, one however quickly realizes that the speed of sound bound is not easily violated for these models: previously examples of asymptotically AdS_5 geometries predict $v_s^2 \leq 1/3$ [55].[3] The known violations of the bound occur in theories that do not flow to a four-dimensional conformal field theory (CFT) in the UV, and thus do not correspond to ordinary renormalizable field theories in four dimensions. Such examples include the $3+1$-dimensional brane intersections $D4-D6$, $D5-D5$, and $D4-D8$ (the Sakai-Sugimoto model [62]), corresponding to the respective speeds of sound $v_s^2 = 1/2, 1, 2/5$ [63–65]. It is well known that even after a compactification to $3+1$ dimensions, it is not possible to disentangle four-dimensional dynamics from the additional degrees of freedom that live on the higher-dimensional color branes, and thus the thermodynamic properties may be very different from a *bona fide* four-dimensional theory.

For the reasons listed above, it has been very challenging to build a holographic description for dense strongly interacting quark matter that would allow for the existence of deconfined matter inside even the heaviest neutron stars observed. One possible resolution to the speed of sound puzzle is clearly that the quantity rises to a value $v_s > 1/\sqrt{3}$ in the nuclear matter phase, then discontinuously jumps to a low value at a first order deconfinement phase transition, and finally slowly rises toward the conformal limit in the deconfined phase. One can nonetheless propose another viable scenario, involving a violation of the speed of sound bound in the deconfined phase and thereby paving the way to the existence of quark matter in neutron star cores.

[3] For two exceptions to this that are, however, dynamically unstable, see [60, 61].

References

[1] J. M. Maldacena, *The large N limit of superconformal field theories and supergravity*, *Adv. Theor. Math. Phys.* **2** (1998) 231–252, [9711200].

[2] S. S. Gubser, I. R. Klebanov, and A. M. Polyakov, *Gauge theory correlators from noncritical string theory*, *Phys.Lett.* **B428** (1998) 105–114, [hep-th/9802109].

[3] E. Witten, *Anti-de Sitter space and holography*, *Adv.Theor.Math.Phys.* **2** (1998) 253–291, [hep-th/9802150].

[4] O. Aharony, S. S. Gubser, J. M. Maldacena, H. Ooguri, and Y. Oz, *Large N field theories, string theory and gravity*, *Phys. Rept.* **323** (2000) 183–386, [hep-th/9905111].

[5] S. Bhattacharyya, V. E. Hubeny, S. Minwalla, and M. Rangamani, *Nonlinear Fluid Dynamics from Gravity*, *JHEP* **02** (2008) 045, [arXiv:0712.2456].

[6] J. Zaanen, Y.-W. Sun, Y. Liu, and K. Schalm, *Holographic Duality in Condensed Matter Physics*. Cambridge Univ. Press, 2015.

[7] M. Cubrovic, J. Zaanen, and K. Schalm, *String Theory, Quantum Phase Transitions and the Emergent Fermi-Liquid*, *Science* **325** (2009) 439–444, [arXiv:0904.1993].

[8] C. Hoyos, K. Jensen, and A. Karch, *Holographic fractional topological insulators*, *Phys. Rev. D* **82** (Oct, 2010) 086001.

[9] M. Heinrich, A. Jiménez-Alba, S. Moeckel, and M. Ammon, *Surface states in holographic weyl semimetals*, *Phys. Rev. Lett.* **118** (May, 2017) 201601.

[10] C. P. Herzog, *Lectures on Holographic Superfluidity and Superconductivity*, *J. Phys.* **A42** (2009) 343001, [arXiv:0904.1975].

[11] M. Ammon, J. Erdmenger, V. Grass, P. Kerner, and A. O'Bannon, *On Holographic p-wave Superfluids with Back-reaction*, *Phys. Lett.* **B686** (2010) 192–198, [arXiv:0912.3515].

[12] S. Grozdanov, A. Lucas, S. Sachdev, and K. Schalm, *Absence of disorder-driven metal-insulator transitions in simple holographic models*, *Phys. Rev. Lett.* **115** (2015), no. 22 221601, [arXiv:1507.00003].

[13] N. Jokela, G. Lifschytz, and M. Lippert, *Striped anyonic fluids*, *Phys. Rev.* **D96** (2017), no. 4 046016, [arXiv:1706.05006].

[14] N. Jokela, M. Jarvinen, and M. Lippert, *Holographic sliding stripes*, *Phys. Rev.* **D95** (2017), no. 8 086006, [arXiv:1612.07323].

[15] S. Kobayashi, D. Mateos, S. Matsuura, R. C. Myers, and R. M. Thomson, *Holographic phase transitions at finite baryon density*, *JHEP* **02** (2007) 016, [hep-th/0611099].

[16] M. Ammon, J. Erdmenger, M. Kaminski, and P. Kerner, *Flavor Superconductivity from Gauge/Gravity Duality*, *JHEP* **10** (2009) 067, [arXiv:0903.1864].

[17] I. Amado, M. Kaminski, and K. Landsteiner, *Hydrodynamics of Holographic Superconductors*, *JHEP* **05** (2009) 021, [arXiv:0903.2209].

[18] J. Erdmenger, M. Flory, C. Hoyos, M.-N. Newrzella, A. O'Bannon, and J. Wu, *Holographic impurities and Kondo effect*, *Fortsch. Phys.* **64** (2016) 322–329, [arXiv:1511.09362].

[19] N. Banerjee, J. Bhattacharya, S. Bhattacharyya, S. Jain, S. Minwalla, and T. Sharma, *Constraints on Fluid Dynamics from Equilibrium Partition Functions*, *JHEP* **09** (2012) 046, [arXiv:1203.3544].

[20] K. Jensen, M. Kaminski, P. Kovtun, R. Meyer, A. Ritz, and A. Yarom, *Towards hydrodynamics without an entropy current*, *Phys. Rev. Lett.* **109** (2012) 101601, [arXiv:1203.3556].

[21] C. Hoyos and D. T. Son, *Hall Viscosity and Electromagnetic Response*, *Phys. Rev. Lett.* **108** (2012) 066805, [arXiv:1109.2651].

[22] S. de Haro, S. N. Solodukhin, and K. Skenderis, *Holographic reconstruction of space-time and renormalization in the AdS / CFT correspondence*, *Commun. Math. Phys.* **217** (2001) 595–622, [hep-th/0002230].

[23] I. Papadimitriou and K. Skenderis, *Correlation functions in holographic RG flows*, *JHEP* **10** (2004) 075, [hep-th/0407071].

[24] S. A. Hartnoll and C. P. Herzog, *Ohm's Law at strong coupling: S duality and the cyclotron resonance*, *Phys. Rev.* **D76** (2007) 106012, [arXiv:0706.3228].

[25] J. Lindgren, I. Papadimitriou, A. Taliotis, and J. Vanhoof, *Holographic Hall conductivities from dyonic backgrounds*, *JHEP* **07** (2015) 094, [arXiv:1505.04131].

[26] I. Kanitscheider, K. Skenderis, and M. Taylor, *Precision holography for non-conformal branes*, *JHEP* **09** (2008) 094, [arXiv:0807.3324].

[27] I. Papadimitriou, *Holographic Renormalization of general dilaton-axion gravity*, *JHEP* **08** (2011) 119, [arXiv:1106.4826].

[28] B. Gouteraux, J. Smolic, M. Smolic, K. Skenderis, and M. Taylor, *Holography for Einstein-Maxwell-dilaton theories from generalized dimensional reduction*, *JHEP* **01** (2012) 089, [arXiv:1110.2320].

[29] M. M. Caldarelli, J. Camps, B. Goutéraux, and K. Skenderis, *AdS/Ricci-flat correspondence*, *JHEP* **04** (2014) 071, [arXiv:1312.7874].

[30] W. Chemissany and I. Papadimitriou, *Lifshitz holography: The whole shebang*, *JHEP* **01** (2015) 052, [arXiv:1408.0795].

[31] J. Hartong, E. Kiritsis, and N. A. Obers, *Lifshitz space–times for Schrödinger holography*, *Phys. Lett.* **B746** (2015) 318–324, [arXiv:1409.1519].

[32] C. Hoyos and D. Rodríguez Fernández, *Ward identities and relations between conductivities and viscosities in holography*, *JHEP* **01** (2016) 013, [arXiv:1511.01002].

[33] J. M. Lattimer and M. Prakash, *The physics of neutron stars*, *Science* **304** (2004) 536–542, [astro-ph/0405262].

[34] N. Brambilla et al., *QCD and Strongly Coupled Gauge Theories: Challenges and Perspectives*, *Eur. Phys. J.* **C74** (2014), no. 10 2981, [arXiv:1404.3723].

[35] **AuroraScience** Collaboration, M. Cristoforetti, F. Di Renzo, and L. Scorzato, *New approach to the sign problem in quantum field theories: High density QCD on a Lefschetz thimble*, *Phys. Rev.* **D86** (2012) 074506, [arXiv:1205.3996].

[36] U. Kraemmer and A. Rebhan, *Advances in perturbative thermal field theory*, *Rept. Prog. Phys.* **67** (2004) 351, [hep-ph/0310337].

[37] I. Tews, T. Kruger, K. Hebeler, and A. Schwenk, *Neutron matter at next-to-next-to-next-to-leading order in chiral effective field theory*, *Phys. Rev. Lett.* **110** (2013), no. 3 032504, [arXiv:1206.0025].

[38] A. Gezerlis, I. Tews, E. Epelbaum, S. Gandolfi, K. Hebeler, A. Nogga, and A. Schwenk, *Quantum Monte Carlo Calculations with Chiral Effective Field Theory Interactions*, *Phys. Rev. Lett.* **111** (2013), no. 3 032501, [arXiv:1303.6243].

[39] B. A. Freedman and L. D. McLerran, *Fermions and Gauge Vector Mesons at Finite Temperature and Density. 3. The Ground State Energy of a Relativistic Quark Gas*, *Phys. Rev.* **D16** (1977) 1169.

[40] A. Vuorinen, *The Pressure of QCD at finite temperatures and chemical potentials*, *Phys. Rev.* **D68** (2003) 054017, [hep-ph/0305183].

[41] A. Kurkela, P. Romatschke, and A. Vuorinen, *Cold Quark Matter*, *Phys. Rev.* **D81** (2010) 105021, [arXiv:0912.1856].

[42] A. Kurkela and A. Vuorinen, *Cool quark matter*, *Phys. Rev. Lett.* **117** (2016), no. 4 042501, [arXiv:1603.00750].

[43] K. Fukushima and C. Sasaki, *The phase diagram of nuclear and quark matter at high baryon density*, *Prog. Part. Nucl. Phys.* **72** (2013) 99–154, [arXiv:1301.6377].

[44] K. Hebeler, J. M. Lattimer, C. J. Pethick, and A. Schwenk, *Equation of state and neutron star properties constrained by nuclear physics and observation*, *Astrophys. J.* **773** (2013) 11, [arXiv:1303.4662].

[45] J. Erdmenger, N. Evans, I. Kirsch, and E. Threlfall, *Mesons in Gauge/Gravity Duals - A Review*, *Eur. Phys. J.* **A35** (2008) 81–133, [arXiv:0711.4467].

[46] A. Adams, L. D. Carr, T. Schäfer, P. Steinberg, and J. E. Thomas, *Strongly Correlated Quantum Fluids: Ultracold Quantum Gases, Quantum Chromodynamic Plasmas, and Holographic Duality*, *New J. Phys.* **14** (2012) 115009, [arXiv:1205.5180].

[47] J. Casalderrey-Solana, M. P. Heller, D. Mateos, and W. van der Schee, *From full stopping to transparency in a holographic model of heavy ion collisions*, *Phys. Rev. Lett.* **111** (2013) 181601, [arXiv:1305.4919].

[48] H. Bantilan and P. Romatschke, *Simulation of Black Hole Collisions in Asymptotically Anti-de Sitter Spacetimes*, *Phys. Rev. Lett.* **114** (2015), no. 8 081601, [arXiv:1410.4799].

[49] P. M. Chesler and L. G. Yaffe, *Holography and off-center collisions of localized shock waves*, *JHEP* **10** (2015) 070, [arXiv:1501.04644].

[50] A. Karch and E. Katz, *Adding flavor to AdS / CFT*, *JHEP* **06** (2002) 043, [hep-th/0205236].

[51] P. Demorest, T. Pennucci, S. Ransom, M. Roberts, and J. Hessels, *Shapiro Delay Measurement of A Two Solar Mass Neutron Star*, *Nature* **467** (2010) 1081–1083, [arXiv:1010.5788].

[52] J. Antoniadis et al., *A Massive Pulsar in a Compact Relativistic Binary*, *Science* **340** (2013) 6131, [arXiv:1304.6875].

[53] P. Bedaque and A. W. Steiner, *Sound velocity bound and neutron stars*, *Phys. Rev. Lett.* **114** (2015), no. 3 031103, [arXiv:1408.5116].

[54] P. M. Hohler and M. A. Stephanov, *Holography and the speed of sound at high temperatures*, *Phys. Rev.* **D80** (2009) 066002, [arXiv:0905.0900].

[55] A. Cherman, T. D. Cohen, and A. Nellore, *A Bound on the speed of sound from holography*, *Phys. Rev.* **D80** (2009) 066003, [arXiv:0905.0903].

[56] Y. Yang and P.-H. Yuan, *Universal Behaviors of Speed of Sound from Holography*, arXiv:1705.07587.

[57] R. Rougemont, R. Critelli, J. Noronha-Hostler, J. Noronha, and C. Ratti, *Dynamical vs. Equilibrium Properties of the QCD Phase Transition*, arXiv:1704.05558.

[58] A. H. Taub, *Relativistic rankine-hugoniot equations*, *Phys. Rev.* **74** (Aug, 1948) 328–334.

[59] L. Rezzolla and O. Zanotti, *Relativistic Hydrodynamics*. 2013.

[60] A. Buchel and C. Pagnutti, *Exotic Hairy Black Holes*, *Nucl. Phys.* **B824** (2010) 85–94, [arXiv:0904.1716].

[61] A. Buchel and C. Pagnutti, *Correlated stability conjecture revisited*, *Phys. Lett.* **B697** (2011) 168–172, [arXiv:1010.5748].

[62] T. Sakai and S. Sugimoto, *Low energy hadron physics in holographic QCD*, *Prog. Theor. Phys.* **113** (2005) 843–882, [hep-th/0412141].

[63] N. Jokela and A. V. Ramallo, *Universal properties of cold holographic matter*, *Phys. Rev.* **D92** (2015), no. 2 026004, [arXiv:1503.04327].

[64] G. Itsios, N. Jokela, and A. V. Ramallo, *Collective excitations of massive flavor branes*, *Nucl. Phys.* **B909** (2016) 677–724, [arXiv:1602.06106].

[65] M. Kulaxizi and A. Parnachev, *Holographic Responses of Fermion Matter*, *Nucl. Phys.* **B815** (2009) 125–141, [arXiv:0811.2262].

[66] C. Hoyos, B. S. Kim, and Y. Oz, *Ward Identities for Transport in 2+1 Dimensions*, *JHEP* **1503** (2015) 164, [arXiv:1501.05756].

[67] C. Hoyos, D. Rodríguez Fernández, N. Jokela, and A. Vuorinen, *Holographic quark matter and neutron stars*, *Phys. Rev. Lett.* **117** (2016), no. 3 032501, [arXiv:1603.02943].

[68] C. Ecker, C. Hoyos, N. Jokela, D. Rodríguez Fernández, and A. Vuorinen, *Stiff phases in strongly coupled gauge theories with holographic duals*, arXiv:1707.00521.

[69] C. Hoyos, N. Jokela, D. Rodríguez Fernández, and A. Vuorinen, *Breaking the sound barrier in AdS/CFT*, *Phys. Rev.* **D94** (2016), no. 10 106008, [arXiv:1609.03480].

[70] S. A. Hartnoll and P. Kovtun, *Hall conductivity from dyonic black holes*, *Phys. Rev.* **D76** (2007) 066001, [arXiv:0704.1160].

[71] S. A. Hartnoll, P. K. Kovtun, M. Muller, and S. Sachdev, *Theory of the Nernst effect near quantum phase transitions in condensed matter, and in dyonic black holes*, *Phys. Rev.* **B76** (2007) 144502, [arXiv:0706.3215].

[72] K. Goldstein, N. Iizuka, S. Kachru, S. Prakash, S. P. Trivedi, and A. Westphal, *Holography of Dyonic Dilaton Black Branes*, *JHEP* **10** (2010) 027, [arXiv:1007.2490].

[73] E. Gubankova, J. Brill, M. Cubrovic, K. Schalm, P. Schijven, and J. Zaanen, *Holographic fermions in external magnetic fields*, *Phys. Rev.* **D84** (2011) 106003, [arXiv:1011.4051].

[74] M. Lippert, R. Meyer, and A. Taliotis, *A holographic model for the fractional quantum Hall effect*, *JHEP* **01** (2015) 023, [arXiv:1409.1369].

[75] M. Fujita, W. Li, S. Ryu, and T. Takayanagi, *Fractional Quantum Hall Effect via Holography: Chern-Simons, Edge States, and Hierarchy*, *JHEP* **06** (2009) 066, [arXiv:0901.0924].

[76] O. Bergman, N. Jokela, G. Lifschytz, and M. Lippert, *Quantum Hall Effect in a Holographic Model*, *JHEP* **10** (2010) 063, [arXiv:1003.4965].

[77] N. Jokela, M. Jarvinen, and M. Lippert, *A holographic quantum Hall model at integer filling*, *JHEP* **05** (2011) 101, [arXiv:1101.3329].

[78] C. Kristjansen and G. W. Semenoff, *Giant D5 Brane Holographic Hall State*, *JHEP* **06** (2013) 048, [arXiv:1212.5609].

[79] Y. Bea, N. Jokela, M. Lippert, A. V. Ramallo, and D. Zoakos, *Flux and Hall states in ABJM with dynamical flavors*, *JHEP* **03** (2015) 009, [arXiv:1411.3335].

[80] E. Keski-Vakkuri and P. Kraus, *Quantum Hall Effect in AdS/CFT*, *JHEP* **09** (2008) 130, [arXiv:0805.4643].

[81] M. Fujita, M. Kaminski, and A. Karch, *SL(2,Z) Action on AdS/BCFT and Hall Conductivities*, *JHEP* **07** (2012) 150, [arXiv:1204.0012].

[82] O. Saremi and D. T. Son, *Hall viscosity from gauge/gravity duality*, *JHEP* **04** (2012) 091, [arXiv:1103.4851].

[83] D. T. Son and C. Wu, *Holographic Spontaneous Parity Breaking and Emergent Hall Viscosity and Angular Momentum*, *JHEP* **07** (2014) 076, [arXiv:1311.4882].

[84] C. Hoyos, B. S. Kim, and Y. Oz, *Odd Parity Transport In Non-Abelian Superfluids From Symmetry Locking*, *JHEP* **10** (2014) 127, [arXiv:1404.7507].

[85] S. Golkar and M. M. Roberts, *Viscosities and shift in a chiral superfluid: a holographic study*, arXiv:1502.07690.

[86] E. Annala, C. Ecker, C. Hoyos, N. Jokela, D. Rodríguez Fernández, and A. Vuorinen, *Holographic compact stars meet gravitational wave constraints*, arXiv:1711.06244.

[87] A. Anabalon, T. Andrade, D. Astefanesei, and R. Mann, *Universal Formula for the Holographic Speed of Sound*, arXiv:1702.00017.

[88] F. Bigazzi, A. L. Cotrone, J. Mas, D. Mayerson, and J. Tarrio, *D3-D7 Quark-Gluon Plasmas at Finite Baryon Density*, *JHEP* **04** (2011) 060, [arXiv:1101.3560].

[89] F. Bigazzi, A. L. Cotrone, and J. Tarrio, *Charged D3-D7 plasmas: novel solutions, extremality and stability issues*, *JHEP* **07** (2013) 074, [arXiv:1304.4802].

[90] A. F. Faedo, A. Kundu, D. Mateos, and J. Tarrio, *(Super)Yang-Mills at Finite Heavy-Quark Density*, *JHEP* **02** (2015) 010, [arXiv:1410.4466].

[91] A. F. Faedo, A. Kundu, D. Mateos, C. Pantelidou, and J. Tarrío, *Three-dimensional super Yang-Mills with compressible quark matter*, *JHEP* **03** (2016) 154, [arXiv:1511.05484].

[92] C. Hoyos-Badajoz and A. Karch, *Alternative large N(c) baryons and holography*, *Phys. Rev.* **D79** (2009) 125021, [arXiv:0904.0008].

3 Articles

The following papers constitute the body of the present thesis. All of them belong to international journals included in the Science Citation Index (SCI). Hyper-links to the on-line versions of the articles are also provided.

1. Carlos Hoyos, David Rodríguez Fernández, *Ward identities and relations between conductivities and viscosities in holography*, Journal of High Energy Physics, (2016)10.1007.013

2. Carlos Hoyos, David Rodríguez Fernández, Niko Jokela, Aleksi Vuorinen, *Holographic quark matter and neutron stars*, Physical Review Letters (2016), 10.1007.117.032501

3. Carlos Hoyos, Niko Jokela, David Rodríguez Fernández, Aleksi Vuorinen, *Breaking the sound barrier in holography*, Physical Review D (2016), 10.1103.94.106008

4. Christian Ecker, Carlos Hoyos, Niko Jokela, David Rodríguez Fernández, Aleksi Vuorinen, *Stiff phases in strongly coupled gauge theories with holographic duals*, Journal of High Energy Physics, (2017)10.1007.031

Published for SISSA by Springer

Received: November 13, 2015
Accepted: December 16, 2015
Published: January 4, 2016

JHEP01(2016)013

Ward identities and relations between conductivities and viscosities in holography

Carlos Hoyos and David Rodríguez Fernández

Department of Physics, Universidad de Oviedo,
Avda. Calvo Sotelo 18, 33007, Oviedo, Spain

E-mail: hoyoscarlos@uniovi.es, rodriguezferdavid@uniovi.es

Abstract: We derive relations between viscosities and momentum conductivity in $2+1$ dimensions by finding a generalization of holographic Ward identities for the energy-momentum tensor. The generalization is novel in the sense that it goes beyond the usual identities obtained from holographic renormalization. Our results are consistent with previous field theory analysis. The main tools we use are a constant 'probability current' in the gravity dual, that we are able to define for any system of linear ODEs, and parity symmetry.

Keywords: Gauge-gravity correspondence, Duality in Gauge Field Theories, AdS-CFT Correspondence, Holography and condensed matter physics (AdS/CMT)

ArXiv ePrint: 1511.01002

doi:10.1007/JHEP01(2016)013

Contents

JHEP01(2016)013

1 Introduction

Holography, in the sense of the AdS/CFT correspondence [1–3] and its generalizations, has been used as a tool to study strongly coupled systems that are otherwise intractable or notoriously difficult to deal with. An important aspect has been the derivation of fluid properties, in particular those associated to the transport of conserved currents such as energy, momentum or charge. Transport is characterized by transport coefficients, that can be defined from correlators of conserved currents through Kubo formulas, or in other

ways such as constitutive relations in hydrodynamics. In holography they have been computed both ways, following the seminal works [4, 5]. An alternative way to identify the coefficients is through the derivative expansion of the equilibrium partition function as in [6, 7], although dissipative coefficients are not captured with this method. One should bear in mind that those definitions are not always equivalent, when we discuss transport coefficients we will be referring to those derived from correlators.

Not all the transport coefficients one can possibly define are independent. For correlators of conserved currents there are Ward identities that impose relations among them, thus constraining some of the transport coefficients. In some cases these relations lead to interesting effects, an example is the relation between Hall conductivity and Hall viscosity found in [8] for Quantum Hall systems. Both coefficients are interesting from the point of view of the characterization of topological phases. For instance, in a Quantum Hall system the Hall conductivity is proportional to the filling fraction while the Hall viscosity depends on the shift [9–11], both of which take discrete values and remain fixed under small deformations. However, in order to determine the viscosity one in principle needs to deform the material and measure the resulting stress, while the conductivity can be determined by a much simpler measurement of an electric current. This situation is helped by the relation between the two. In the presence of an inhomogeneous electric field, the Hall current receives a correction, which to leading order in derivatives is

$$J_H^i \simeq \sigma_H^{(0)} E^i + \sigma_H^{(2)} \nabla^2 E^i \tag{1.1}$$

The coefficient $\sigma_H^{(2)}$ depends on the Hall viscosity and other quantities that can be determined independently. This in principle allows to measure the Hall viscosity via inhomogeneous electric fields, which may be easier to realize experimentally than a direct measurement of the viscosity. Originally the relation was obtained form an effective action approach, but later it was shown for Galilean invariant systems that the relation can be derived from Ward identities [12].

These relations were further generalized for any system with rotational invariance in [13]. For the general case (not Galilean invariant), the transport coefficients that are directly related are conductivities in the momentum current (or thermal conductivities) and viscosities. Charge conductivities also enter when the magnetic field is nonzero. In terms of retarded correlators of the energy-momentum tensor

$$\Gamma^{\mu\nu\alpha\beta}(x,\hat{x}) = \left\langle T^{\mu\nu}(x) T^{\alpha\beta}(\hat{x}) \right\rangle_R , \tag{1.2}$$

the relevant Ward identity is, in the absence of external sources ($i,j = 1,2$ label the spatial directions)

$$\partial_0 \hat{\partial}_0 \Gamma^{0i0j}(x,\hat{x}) + \partial_k \hat{\partial}_l \Gamma^{kilj}(x,\hat{x}) \simeq 0. \tag{1.3}$$

The right hand side might contain contact terms but otherwise it's zero because of the conservation of the energy-momentum tensor. The identity can be derived combining the two identities

$$\partial_\mu \Gamma^{\mu\nu\alpha\beta}(x,\hat{x}) \simeq 0, \quad \hat{\partial}_\alpha \Gamma^{\mu\nu\alpha\beta}(x,\hat{x}) \simeq 0. \tag{1.4}$$

JHEP01(2016)013

For readers familiar with the AdS/CFT correspondence it might seem that these identities have been derived already from the holographic renormalization procedure [14, 15], in particular the Ward identities for charged $2+1$ dimensional systems were studied in some detail in [16–18]. This is partially true, there is a set of Ward identities that hold for the correlators of the energy-momentum tensor with any other operators $\mathcal{O}_1, \ldots, \mathcal{O}_n$

$$\partial_\mu \langle T^{\mu\nu}(x)\mathcal{O}_1(x_1)\cdots\mathcal{O}_n(x_n)\rangle = 0. \tag{1.5}$$

In the case of asymptotically AdS spacetimes[1] this follows from 'kinematics', it is not necessary to know the full geometry but the identity follows from the asymptotic expansion and the equations of motion. However, the second identity in (1.4) does not follow directly from the asymptotic expansion, it requires further input.

So far the relations between viscosities and conductivities in holography could only be checked by direct computation of the correlators, but a general 'kinematic' argument should exist, since they follow from symmetries and will be valid in any field theory. In this paper we make a first step towards generalizing Ward identities for two-point functions of the energy-momentum in $2+1$ dimensions. We will establish the relation between the parity even components of the conductivities and the shear and bulk viscosities, our argument relies on constructing a quantity which is independent of the radial direction in the bulk geometry and taking advantage of parity symmetry. The radially independent quantity can be seen as a "probability current" for the solutions to the linear equations of motion. We give a general prescription on how to construct the probability current for any linear system of second order ordinary differential equations and apply it to a specific set of theories consisting of $3+1$-dimensional gravity coupled to a scalar field. In the context of scattering in black hole geometries, the probability current is the flux through a surface at a fixed value of the radial coordinate, in particular the flux through the horizon, so it determines the absorption by the black hole. In simple cases, such as a probe scalar field, one can see that the probability current is proportional to the spectral function of the dual operator. In more general cases it is still a combination of correlators, but we do not have a clean interpretation for it, we will use it as a mathematical device to derive the Ward identities.

The paper is organized as follows: in section 2 we derive the identities that relate shear viscosity and momentum conductivity in a conformal field theory (CFT). In section 3 we generalize our construction to theories with explicit breaking of conformal invariance via a relevant deformation and derive identities that relate bulk viscosity and momentum conductivity. In subsection 3.1 we present the general construction of the probability current. We discuss the results in section 4 and a possible application of the probability current to compute the spectrum of normalizable modes. We have gathered a collection of technical results in the appendices at the end of the paper.

2 Shear identity in a CFT

We will start by working out a simple example that will serve to illustrate the procedure we are proposing to derive generalized Ward identities, without the technical complications of more involved cases.

[1] Generalizations for other geometries have been discussed in [19–24].

JHEP01(2016)013

The simplest identity we can check using holography is the relation between shear viscosity and thermal conductivity in a CFT. We will restrict the analysis to (2+1)-dimensions, although it can be generalized to any number of dimensions. We will assume that the CFT has a gravity dual and that quantum and higher derivative corrections on the gravity side are small,[2] so it can be well approximated by classical Einstein gravity coupled to matter. For simplicity we will consider states where the CFT is at finite temperature but there are no other sources of breaking of conformal invariance (explicit or spontaneous). This implies that the effect of matter is simply to introduce a negative cosmological constant $\Lambda = -3/L^2$

$$S = \frac{1}{16\pi G_N}\int d^4x\,\sqrt{-g}\,(R - 2\Lambda)\,, \tag{2.1}$$

where G_N is the four-dimensional Newton's constant. The geometry dual to the thermal state of a CFT is the AdS_4 black brane

$$ds^2 = \frac{L^2}{z^2}\left(-f(z)dx_0^2 + dx_1^2 + dx_2^2 + \frac{dz^2}{f(z)}\right), \quad f(z) = 1 - \frac{z^3}{z_H^3}. \tag{2.2}$$

Where L is the AdS radius. The conformal AdS boundary is at $z = 0$, while $z = z_H$ is the position of the black brane horizon. We can set $z_H = 1$ by rescaling the coordinates

$$z \to z_H z, \quad x^\mu \to z_H x^\mu. \tag{2.3}$$

All dimensionful quantities will be given in units of z_H. Physical units can be restored by introducing z_H factors using dimensional analysis and then replacing the z_H dependence by a dependence on the temperature of the black brane

$$T = \frac{3}{4\pi z_H}\,. \tag{2.4}$$

Two-point retarded correlation functions of the energy-momentum tensor can be computed using AdS/CFT by solving for linearized fluctuations of the metric around the black brane background and imposing ingoing boundary conditions at the horizon [25]. We will work in the radial gauge where $\delta g_{Mz} = 0$[3] and we will expand in plane waves with momentum along the x_1 direction

$$\delta g_{\mu\nu} = -\frac{L^2}{z^2}\int \frac{d^3k}{(2\pi)^3} e^{ik_\mu x^\mu} h_{\mu\nu}(z). \tag{2.5}$$

For the calculation of the shear viscosity we only need to turn on the h_{12} and h_{02} components, and in the calculations we will fix the momentum to be $k^\mu = (\omega, k, 0)$ without loss of generality.

Varying the action (2.1) with respect to the metric g_{MN} yields Einstein's equations

$$R_{MN} - \frac{1}{2}g_{MN}R - \frac{3}{L^2}g_{MN} = 0. \tag{2.6}$$

[2] On the field theory side this means a large-N and strong coupling approximation.

[3] We will employ capital latin indexes for the bulk coordinates, greek indexes for the boundary coordinates. Latin lower case indexes will run for the spatial x_1, x_2 components.

JHEP01(2016)013

Expanding to linear order in the fluctuations, we find three equations, two dynamical and one constraint

$$\begin{aligned} 0 &= h_{12}'' - \left(\frac{2}{z} - \frac{f'}{f}\right) h_{12}' + \frac{\omega^2}{f^2} h_{12} + \frac{\omega k}{f^2} h_{02}, \\ 0 &= h_{02}'' - \frac{2}{z} h_{02}' - \frac{k^2}{f} h_{02} - \frac{\omega k}{f} h_{12}, \\ 0 &= \omega h_{02}' + k f h_{12}'. \end{aligned} \tag{2.7}$$

Where primes denote derivatives with respect to the radial direction z.

An important ingredient in our derivation is parity symmetry. The equations are invariant under the transformation

$$k \longrightarrow -k, \quad h_{12} \longrightarrow -h_{12}. \tag{2.8}$$

Therefore, for every solution h_{02}, h_{12} of the equations with frequency ω and momentum k, there is another solution for the opposite momentum with the same radial profile, up to the overall sign in h_{12}

$$\tilde{h}_{02}(\omega, -k, z) = h_{02}(\omega, k, z), \quad \tilde{h}_{12}(\omega, -k, z) = -h_{12}(\omega, k, z). \tag{2.9}$$

Note that generically introducing sources in the field theory will break parity, this will be reflected in the boundary conditions $h_{12}(\omega, k, z = 0) \neq -h_{12}(\omega, -k, z = 0)$ and $h_{02}(\omega, k, z = 0) \neq h_{02}(\omega, -k, z = 0)$. Nonetheless, the spectrum is determined by normalizable solutions $h_{12}(z = 0) = h_{02}(z = 0) = 0$, which will show parity invariance.

2.1 Probability current and parity

The equations of motion (2.7) can be cast in the form of coupled Schröedinger equations (plus a constraint) by changing to the following variables

$$h_{02} = z\psi_0, \quad h_{12} = \frac{z}{\sqrt{f}} \psi_1. \tag{2.10}$$

Then, the dynamical equations have the form

$$\begin{aligned} 0 &= \psi_1'' - \mathcal{V}_1 \psi_1 + \frac{\omega k}{f^{3/2}} \psi_0, \\ 0 &= \psi_0'' - \mathcal{V}_0 \psi_0 - \frac{\omega k}{f^{3/2}} \psi_1. \end{aligned} \tag{2.11}$$

Where

$$\mathcal{V}_1 = -\frac{\omega^2}{f^2} + \frac{f'}{fz} - \frac{(f')^2}{4f^2} + \frac{3}{fz^2} - \frac{1}{z^2}, \quad \mathcal{V}_0 = \frac{k^2}{f} + \frac{2}{z^2}. \tag{2.12}$$

For $k = 0$ the two modes decouple and one can naturally define probability currents for each of the fluctuations (bar denotes complex conjugation)

$$j_{0,1} = \overline{\psi}_{0,1} \psi_{0,1}{}' - \overline{\psi}_{0,1}{}' \psi_{0,1}. \tag{2.13}$$

JHEP01(2016)013

Since the potentials are real, these currents are independent of the radial coordinate

$$\frac{d}{dz}j_{0,1} = \overline{\psi}_{0,1}\psi_{0,1}'' - \overline{\psi}_{0,1}''\psi_{0,1} = \overline{\psi}_{0,1}(\mathcal{V}_{0,1}\psi_{0,1}) - (\mathcal{V}_{0,1}\overline{\psi}_{0,1})\psi_{0,1} = 0. \tag{2.14}$$

However, when the momentum is non-zero the currents j_0 and j_1 are not independent of the radial direction anymore. Instead, we find

$$\frac{d}{dz}j_1 = -\frac{\omega k}{f^{3/2}}(\overline{\psi}_1\psi_0 - \overline{\psi}_0\psi_1), \quad \frac{d}{dz}j_0 = \frac{\omega k}{f^{3/2}}(\overline{\psi}_0\psi_1 - \overline{\psi}_1\psi_0). \tag{2.15}$$

Even though separately the radial derivative of each current is non-zero we see that they are proportional to the same function. The combination $J = j_1 - j_0$ is actually independent of the radial direction. Note that J is invariant under the parity transformation (2.8), since it depends quadratically on h_{12} and the radial profile of the fluctuations does not change. We will use this fact to derive the generalized Ward identity by comparing the value of the current J at the horizon and at the boundary.

To leading order, the ingoing solutions near the horizon $z \to 1$ can be expanded as

$$\begin{aligned}\psi_1 &= (1-z)^{\frac{1}{2}-i\frac{\omega}{3}}\left(\mathcal{A}_1 + \cdots\right) + \sqrt{1-z}\left(-\frac{\sqrt{3}k}{\omega}\mathcal{B} + \cdots\right), \\ \psi_0 &= (1-z)^{1-i\frac{\omega}{3}}\left(\frac{i\sqrt{3}k}{3-i\omega}\mathcal{A}_1 + \cdots\right) + \mathcal{B}\left(1 + (1-z) + \cdots\right).\end{aligned} \tag{2.16}$$

The solution for ψ_0 when the momentum is zero and the two modes are decoupled is the one with coefficient $\mathcal{B}$. In that situation, there are no ingoing solutions for the vector mode. This solution actually does not contribute to the current, whose value at the horizon is

$$J_H = i\frac{2}{3}\omega\left|\mathcal{A}_1\right|^2. \tag{2.17}$$

Invariance of the current under parity implies that $J_H(-\mathcal{A}_1, -k) = J_H(\mathcal{A}_1, k)$. But

$$J_H(-\mathcal{A}_1, -k) = i\frac{2}{3}\omega\left|-\mathcal{A}_1(-k)\right|^2 = i\frac{2}{3}\omega\left|\mathcal{A}_1(-k)\right|^2 = J_H(\mathcal{A}_1, -k). \tag{2.18}$$

Therefore, $J_H(k) = J_H(-k)$ and since J is independent of the radial coordinate, we deduce that

$$J(k) = J(-k). \tag{2.19}$$

2.2 Ward identities

To leading order, the solutions near the boundary $z \to 0$ can be expanded as

$$\psi_{0,1} = \frac{1}{z}\left(H_{0,1}^{(0)} + H_{0,1}^{(2)}z^2 + \cdots\right) + z^2\left(T_{0,1}^{(0)} + \cdots\right). \tag{2.20}$$

The coefficients of the non-normalizable modes $H_{0,1}^{(0)}$ are proportional to the Fourier transform of the sources of the energy-momentum tensor, i.e. the boundary metric

$$g_{\mu\nu}^{(0)} = \eta_{\mu\nu} + \delta g_{\mu\nu}^{(0)}. \tag{2.21}$$

JHEP01(2016)013

The coefficients of the normalizable modes $T^{(0)}_{0,1}$ are related to the Fourier transform of the expectation value in the dual field theory

$$\langle T_{\mu\nu}\rangle = \langle T_{\mu\nu}\rangle_{\text{thermal}} + \delta\langle T_{\mu\nu}\rangle\,. \tag{2.22}$$

The exact relation follows from holographic renormalization [14]

$$\delta g^{(0)}_{a2} = -H^{(0)}_a,\ a=0,1.\quad \delta\langle T_{02}\rangle = -\frac{3L^2}{16\pi G_N}T^{(0)}_0,\qquad \delta\langle T_{12}\rangle = -\frac{3L^2}{16\pi G_N}\left[T^{(0)}_1+\frac{1}{2}H^{(0)}_1\right]. \tag{2.23}$$

The two-point correlation functions of the energy-momentum tensor can be computed by doing a variation of the expectation value with respect to the source

$$\Gamma_{a2b2} = \frac{\partial\langle T_{a2}\rangle}{\partial g^{b2}}\Big|_{\delta g_{\mu\nu}=0}. \tag{2.24}$$

Note that the normalizable solution is not independent, ingoing boundary conditions at the horizon impose a relation between the boundary normalizable and non-normalizable solutions, with some coefficients depending on the frequency and the momentum

$$\begin{aligned} T^{(0)}_1 &= C_{11}(\omega,k)H^{(0)}_1 + C_{10}(\omega,k)H^{(0)}_0,\\ T^{(0)}_0 &= C_{01}(\omega,k)H^{(0)}_1 + C_{00}(\omega,k)H^{(0)}_0. \end{aligned} \tag{2.25}$$

From (2.23) and (2.24), the correlation functions associated to the shear and transverse thermal conductivity are

$$\begin{aligned} \Gamma_{0202} &= -\frac{3L^2}{16\pi G_N}C_{00},\quad \Gamma_{1202} = -\frac{3L^2}{16\pi G_N}C_{10},\\ \Gamma_{0212} &= -\frac{3L^2}{16\pi G_N}C_{01},\quad \Gamma_{1212} = -\frac{3L^2}{16\pi G_N}\left[C_{11}+\frac{1}{2}\right]. \end{aligned} \tag{2.26}$$

The coefficients $H^{(2)}_{0,1}$ are fixed by the corresponding dynamical equations in (2.7). If we also take into account the constraint equation, we find the following conditions

$$\begin{aligned} H^{(2)}_1 &= \frac{\omega^2}{2}H^{(0)}_1 + \frac{\omega k}{2}H^{(0)}_0,\\ T^{(0)}_0 &= -\frac{k}{2\omega}H^{(0)}_1 - \frac{k}{\omega}T^{(0)}_1,\\ H^{(2)}_0 &= -\frac{k}{\omega}H^{(2)}_1 = -\frac{\omega k}{2}H^{(0)}_1 - \frac{k^2}{2}H^{(0)}_0. \end{aligned} \tag{2.27}$$

Using all these results, the probability current evaluated at the boundary has the following form

$$J_B = 3\left(\overline{H}^{(0)}_1 T^{(0)}_1 - H^{(0)}_1\overline{T}^{(0)}_1\right) + \frac{3k}{2\omega}\left(\overline{H}^{(0)}_0 H^{(0)}_1 - H^{(0)}_0\overline{H}^{(0)}_1\right) + \frac{3k}{\omega}\left(\overline{H}^{(0)}_0 T^{(0)}_1 - H^{(0)}_0\overline{T}^{(0)}_1\right). \tag{2.28}$$

JHEP01(2016)013

We see that indeed J_B is invariant under parity, since $J_B(-H_1,-T_1,-k)=J_B(H_1,T_1,k)$. However, in order for the condition (2.19) to hold, an additional constraint should be satisfied ("even" and "odd" is respect to $k\to -k$)

$$\omega\left(\overline{H}_1^{(0)}T_1^{(0)}-H_1^{(0)}\overline{T}_1^{(0)}\right)_{\rm odd}+\frac{k}{2}\left(\overline{H}_0^{(0)}H_1^{(0)}-H_0^{(0)}\overline{H}_1^{(0)}\right)+k\left(\overline{H}_0^{(0)}T_1^{(0)}-H_0^{(0)}\overline{T}_1^{(0)}\right)_{\rm even}=0. \tag{2.29}$$

We will use this relation to derive Ward identities for correlators in the dual field theory.

Using (2.27), we see that not all those coefficients are independent, but

$$\omega C_{01}(\omega,k)+kC_{11}(\omega,k)+\frac{k}{2}=0,\quad \omega C_{00}(\omega,k)+kC_{10}(\omega,k)=0. \tag{2.30}$$

This implies the following Ward identities

$$\omega\Gamma_{0212}+k\Gamma_{1212}=0,\quad \omega\Gamma_{0202}+k\Gamma_{1202}=0, \tag{2.31}$$

which correspond to the usual conservation of the energy-momentum tensor.

On the other hand, (2.29) for arbitrary sources leads to the conditions

$$\left(C_{11}-\overline{C}_{11}\right)_{\rm odd}=0, \tag{2.32}$$

$$\omega C_{10\,\rm odd}-\frac{k}{2}-k\,\overline{C}_{11,\rm even}=0. \tag{2.33}$$

This implies the following Ward identities

$$\left(\Gamma_{1212}-\overline{\Gamma}_{1212}\right)_{\rm odd}=0,\quad \omega\Gamma_{1202\,\rm odd}-k\overline{\Gamma}_{1212\,\rm even}=0. \tag{2.34}$$

Combining the two second identities in (2.31) and (2.34), we get

$$\left[\omega^2\Gamma_{0202}+k^2\overline{\Gamma}_{1212}\right]_{\rm even}=0. \tag{2.35}$$

From this expression we can derive the relation between shear viscosity and transverse thermal conductivity.

3 Bulk identity in a non-CFT

We would like now to study a more involved case, the relation between bulk viscosity and longitudinal thermal conductivity. Although the derivation is similar to the one we have used for the shear identity in a CFT, there are some features that cannot be easily generalized, in particular finding a constant probability current for a larger number of coupled fluctuations. We will show how this can be done using a particular example.

In a CFT the bulk viscosity is zero, so we should introduce a breaking of conformal invariance. This can be achieved by introducing additional couplings for relevant operators or giving them an expectation value. On the gravity side, this is translated into turning on scalar fields. In the simplest scenario there will be just one scalar coupled to Einstein gravity

$$S=\frac{1}{16\pi G_N}\int d^4x\,\sqrt{-g}\left(R-(\partial\phi)^2-2V(\phi)\right). \tag{3.1}$$

JHEP01(2016)013

The potential has a critical point at $\phi = 0$ corresponding to AdS with $\Lambda = V(0)$. In order for the dual operator $\mathcal{O}$ to be relevant, the mass of the scalar field should be negative $m^2L^2 = \partial^2 V(0) < 0$, so the critical point is a maximum of the potential. The mass of the field is related to the conformal dimension of the dual operator Δ as $m^2L^2 = \Delta(\Delta - 3)$.

The equations of motion are

$$\begin{aligned} R_{MN} - \frac{1}{2}R g_{MN} &= \partial_M\phi\partial_N\phi - \frac{1}{2}g_{MN}\left(\partial_K\phi\partial^K\phi + 2V(\phi)\right) , \\ 0 &= \Box\phi - \partial V(\phi) . \end{aligned} \tag{3.2}$$

We will consider a generic background black brane solution with the scalar field turned on

$$ds^2 = dr^2 + e^{2A(r)}\left(-e^{2B(r)}dx_0^2 + dx_1^2 + dx_2^2\right) , \quad \phi = \phi_0(r). \tag{3.3}$$

The boundary is at $r \to \infty$, where the solution is asymptotically AdS. Asymptotically close to the boundary the scalar field and the blackening function of the metric vanish $\phi_0, B \to 0$, while the warp factor becomes linear in the radial coordinate $A(r) \simeq \frac{r}{L}$. The horizon is at $r = r_H$, where the g_{00} component of the metric vanishes $B(r) \simeq \log(r - r_H)$. For convenience we will set $L = 1$ in the calculations, so all dimensionful quantities are given in units of the AdS radius. We will restore the dependence on L in the final expressions for one-point functions and correlators. To leading order,[4] the expansion of the solutions close to the boundary are

$$\begin{aligned} &A \sim r - \frac{\lambda^2}{8}e^{-2(3-\Delta)r} - \frac{1}{9}\left(3B_0 - \Delta(\Delta-3)\lambda v\right)e^{-3r} + \cdots , \\ &B \sim e^{-3r}B_0 + \cdots , \quad \phi_0 \sim \lambda e^{-(3-\Delta)r} + v e^{-\Delta r} + \cdots . \end{aligned} \tag{3.4}$$

The coefficients λ and v are proportional to the source and the expectation value of the dual scalar operator respectively. The coefficient B_0 is proportional to the thermal contribution to the energy density. We have computed the renormalized expectation values in appendix A using the holographic renormalization procedure. We find that the total energy density ε and pressure P are

$$\begin{aligned} \varepsilon = \langle T_{00}\rangle &= \frac{1}{8\pi G_N L}\left[-2B_0 - \frac{1}{3}(\Delta-3)(3-2\Delta)\lambda v\right] , \\ P = \langle T_{ii}\rangle &= \frac{1}{8\pi G_N L}\left[-B_0 + \frac{1}{3}(\Delta-3)(3-2\Delta)\lambda v\right] , \end{aligned} \tag{3.5}$$

while the expectation value of the dual scalar operator is

$$\langle\mathcal{O}\rangle = \frac{\mu^{\Delta-3}}{8\pi G_N L}(3-2\Delta)v. \tag{3.6}$$

Where μ is an arbitrary scale that enters in the definition of the source for the dual operator $\lambda = \mu^{\Delta-3}J^{(0)}$.

[4] We are presenting the expansions as if $3/2 < \Delta < 5/2$, but they are valid for any $1/2 < \Delta < 3$, except for special values, when $2\Delta - 3$ is an integer.

JHEP01(2016)013

The trace of the energy-momentum tensor satisfies the Ward identity

$$\left\langle T^{\mu}_{\mu} \right\rangle = \frac{1}{8\pi G_N L}(\Delta - 3)(3 - 2\Delta)\lambda v = (\Delta - 3) J^{(0)} \left\langle \mathcal{O} \right\rangle . \tag{3.7}$$

In order to compute correlation functions in the dual field theory we follow the usual analysis of linearized fluctuations of the metric and scalar field δg_{MN}, $\delta\phi$. We will work in the radial gauge $\delta g_{rM} = 0$ and expand in plane waves along the field theory directions

$$\delta g_{\mu\nu} = \int \frac{d^3k}{(2\pi)^3} e^{ik_\mu x^\mu} h_{\mu\nu}(r), \quad \delta\phi = e \int \frac{d^3k}{(2\pi)^3} e^{ik_\mu x^\mu} \varphi(r). \tag{3.8}$$

It is possible to repeat the derivation of the shear identity in this background by turning on only the h_{12} and h_{02} components of the metric. The structure of the equations is the same, with the only difference being that when the equations are written in the Schröedinger form the potentials depend on the background scalar.

For the present analysis we will turn on the minimal set of modes of the metric coupled to the scalar φ: h_{00}, h_{01}, h_{11} and h_{22} and we will fix the momentum to be $k^\mu = (\omega, k, 0)$ without loss of generality. It will be convenient to use a different basis of modes

$$\begin{aligned}
y_1 &= \frac{1}{2} e^{-\frac{A}{2}} \left(e^{-2B} h_{00} + h_{11} + h_{22} \right), \\
y_2 &= \frac{1}{2} e^{A} \left(-e^{-2B} h_{00} + h_{11} + h_{22} \right), \\
y_3 &= e^{\frac{3}{2}A} \varphi, \\
y_4 &= \frac{1}{2} e^{-\frac{A}{2}} \left(h_{11} - h_{22} \right), \\
y_5 &= e^{-\frac{A}{2} - 2B} h_{01}.
\end{aligned} \tag{3.9}$$

The dynamical equations of motion and the constraints are

$$y_i'' + a_{ij}\, y_j' + b_{ij}\, y_j = 0, \quad c_i^a\, y_i' + d_i^a\, y_i = 0, \ a = 1, 2, 3. \tag{3.10}$$

Where the coefficients are given in the appendix B.2. The structure is such that, for $i \neq 5$

$$a_{5i} = a_{i5} = 0, \quad b_{i5}, b_{5i} \propto k, \quad c_5^1, c_5^3, c_i^2 \propto k, \quad d_5^5, d_5^3, d_i^2 \propto k. \tag{3.11}$$

While all the other coefficients are proportional to even powers of k. One can easily check that the equations are invariant under the parity transformation

$$k \longrightarrow -k, \quad h_{01} \longrightarrow -h_{01} \quad (y_5 \longrightarrow -y_5). \tag{3.12}$$

3.1 Constructing a probability current

For the shear modes it was quite easy to construct a constant probability current. This was actually possible because the structure of the equations is quite special. The existence of a constant probability current was pointed out before in other simple cases, such as a probe scalar field in the BTZ black hole [25] and for longitudinal fluctuations of a gauge field in a charged asymptotically AdS_4 black hole [26]. In those cases it is roughly proportional to

JHEP01(2016)013

the on-shell action. As we will see, in the more complicated case of a scalar field coupled to the metric, the special structure of the vector modes is absent and in order to construct a constant current we need to introduce additional ingredients. Let us mention that it is possible to define in general a conserved 'symplectic current' w^μ [27, 28] that is useful to prove the conservation of Noether charges in the bulk and the first law of thermodynamics in holography (see [29, 30]). Similarly to the probability current, it is a bilinear functional of the fluctuations of the fields $w^\mu = w^\mu(\delta_1\Phi, \delta_2\Phi)$. However, in contrast to the probability current defined from the on-shell action, it vanishes for $\delta_1\Phi = \delta_2\Phi$. It would be interesting to see if the probability current we define below and the symplectic current are related.

Let us first consider zero momentum $k = 0$ with the background scalar field turned off $\phi_0 = 0$. The dynamical equations take a simpler form, with all the modes decoupled except for y_1 and y_2. For each of the decoupled modes the equations are

$$y_i'' + a_{ii}y_i' + b_{ii}y_i = 0, \;\; i = 3, 4, 5. \tag{3.13}$$

We can define new variables such that the equations take the form of Schröedinger equations. The new variables are

$$y_i(r) = e^{-\frac{1}{2}\int^r a_{ii}}\psi_i(r), \tag{3.14}$$

and the equations become

$$\psi_i'' - V_i\psi_i = 0, \quad V_i = -b_{ii} + \frac{1}{2}a_{ii}' - \frac{1}{4}a_{ii}^2. \tag{3.15}$$

Therefore, there is a constant probability current for each of these modes

$$j_i = \overline{\psi}_i{}'\psi_i - \overline{\psi}_i\psi_i{}'. \tag{3.16}$$

For the coupled modes, the coefficients of the dynamical equations are

$$a_{lm} = \begin{pmatrix} B' & e^{-\frac{3A}{2}}(A' - B') \\ 0 & 2B' \end{pmatrix}, \tag{3.17}$$

and

$$b_{lm} = \begin{pmatrix} -\frac{3}{4}A'(3A' + 4B') & -3e^{-\frac{3A}{2}}A'(A' - B') \\ e^{-\frac{A}{2}-2B}\omega^2 & e^{-2A-2B}\omega^2 - 9A'(A' + B') \end{pmatrix}, \quad l, m = 1, 2\,. \tag{3.18}$$

We can also put this equation in Schröedinger form by defining new variables

$$y_l = \Omega_{lm}\psi_m, \quad l, m = 1, 2. \tag{3.19}$$

The matrix Ω has to satisfy the differential equation

$$\Omega' = -\frac{a}{2}\Omega, \tag{3.20}$$

for which there is a formal solution

$$\Omega = \mathbb{1} + \sum_{n=1}^{\infty}\frac{(-1)^n}{2^n}\int^r dr_1\int^{r_1} dr_2\cdots\int^{r_{n-1}} dr_n\, a(r_1)a(r_2)\cdots a(r_n). \tag{3.21}$$

JHEP01(2016)013

The equations become, in matricial form

$$\psi'' - \mathcal{V}\psi = 0, \quad \mathcal{V} = \Omega^{-1}\left[\frac{a^2}{4} + \frac{a'}{2} - b\right]\Omega. \tag{3.22}$$

However, in this case we cannot construct a simple probability current. Naïvely the general form would be

$$J = \psi^{\dagger\prime} Q\psi - \psi^\dagger Q^\dagger \psi', \tag{3.23}$$

with Q a constant matrix. In order for the current to be constant it is necessary that the matrix Q satisfies the algebraic equations

$$\mathcal{V}^\dagger Q - Q^\dagger \mathcal{V} = 0, \quad Q = Q^\dagger. \tag{3.24}$$

For the shear mode this was the case because $\mathcal{V}$ can be expanded in Pauli matrices $\{\mathbb{1}, \sigma^3, i\sigma^2\}$ with real coefficents, so the algebraic relations are satisfied for $Q = \sigma^3$. However, for the scalar modes there is also a term in the potential proportional to σ^1, so the algebraic constraints cannot be satisfied in general.

A possible way to generalize the probability current would be to allow non-constant coefficients, and define the current as

$$J = \psi^{\dagger\prime}\mathcal{A}\psi' + \psi^{\dagger\prime}\mathcal{B}\psi - \psi^\dagger\mathcal{B}^\dagger\psi' + \psi^\dagger\mathcal{C}\psi, \tag{3.25}$$

with $\mathcal{A}^\dagger = -\mathcal{A}$, $\mathcal{C}^\dagger = -\mathcal{C}$. The condition that the current is constant $J' = 0$ together with the equations of motion (3.22) gives differential equations for the coefficents. A current of this form could also be defined for the original system of equations (even if $k \neq 0$ and $\phi_0 \neq 0$), without having to write the equations in Schröedinger form. The current would be

$$J = y^{\dagger\prime}\mathcal{A}y' + y^{\dagger\prime}\mathcal{B}y - y^\dagger\mathcal{B}^\dagger y' + y^\dagger\mathcal{C}y. \tag{3.26}$$

Rather than constructing J in this way and solving the differential equations for the coefficients, we will try a different approach. We will add additional fields so the probability current becomes a Noether current with known coefficients and then we will fix the boundary conditions of the auxiliary fields in terms of the boundary conditions of the original modes.

First let us introduce a matrix K such that the equations can be written in the form

$$K^{-1}\left(Ky'\right)' + by = 0, \quad K^{-1}K' = a \quad \Rightarrow \quad K' = Ka. \tag{3.27}$$

A formal solution is

$$K = \mathbb{1} + \sum_{n=1}^{\infty}\int^r dr_1 \int^{r_1} dr_2 \cdots \int^{r_{n-1}} dr_n\, a(r_n)\cdots a(r_2)\, a(r_1). \tag{3.28}$$

If we multiply by K on the left we get

$$\left(Ky'\right)' + Kby = 0. \tag{3.29}$$

JHEP01(2016)013

We can derive this from a Lagrangian by introducing new fields η. The number of auxiliary fields is the same as the number of original fluctuations and can be grouped in a vector of the same length. The Lagrangian that gives the equations for y is

$$\mathcal{L} = (\eta^\dagger)' K y' - \eta^\dagger K b y + (y^\dagger)' K^\dagger \eta' - y^\dagger b^\dagger K^\dagger \eta. \tag{3.30}$$

$$\left(K^\dagger \eta'\right)' + b^\dagger K^\dagger \eta = 0\,. \tag{3.31}$$

Note also that the equations are invariant under the parity transformation

$$k \longrightarrow -k, \quad \eta_5 \longrightarrow -\eta_5, \tag{3.32}$$

this will be important in the derivation of the new identities.

The equations for y and η become the same if $K = K^\dagger$ and $Kb = b^\dagger K$, in which case one can set $\eta = y$ and $\mathcal{L}$ can be used as a Lagrangian for the original system of equations.

The action of the extended system has a U(1) global symmetry

$$y \longrightarrow e^{i\alpha} y, \quad \eta \longrightarrow e^{i\alpha} \eta, \tag{3.33}$$

whose (anti-Hermitian) Noether current is

$$J = (\eta^\dagger)' K y - \eta^\dagger K y' + (y^\dagger)' K^\dagger \eta - y^\dagger K^\dagger \eta'. \tag{3.34}$$

The equations of motion imply that $J' = 0$. The current is invariant under the full parity symmetry acting on both y and η.

3.1.1 Current at the boundary

Our first goal is to compute the probability current at the boundary. For simplicity we will restrict to a quadratic potential for the scalar field $V(\phi) = \frac{1}{2} m^2 \phi^2$, with $m^2 < 0$ but above the Breitenlohner-Freedman bound, as is appropriate for a field dual to a relevant operator. For arbitrary potentials $V(\phi)$ with a maximum at $\phi = 0$ we have checked that there are no qualitative changes in the boundary expansions, although coefficients do depend on third and fourth derivatives of the potential.

The expansions of the background and the matrix K can be found in appendix C.1, and the one for the auxiliary fields in appendix C.4. Since the equations are second order, there are in principle two independent solutions for each of the y_i and η_i. One corresponds to the non-normalizable solution, which for the original fluctuations maps to the metric or to a source for the scalar operator in the dual field theory. The other solution is normalizable and for the original fluctuations maps to the expectation value of the energy-momentum tensor and the scalar operator. Let us compare the leading terms of each of the independent solutions in the expansions of the auxiliary fields to those of the original fluctuations.

$$\begin{aligned} y_1 &\sim e^{\frac{3}{2}r} y_1^{(0)} + e^{-\frac{3}{2}r} y_1^{(3)}, \\ \eta_1 &\sim e^{\frac{3}{2}r} \eta_1^{(0)} + e^{-\frac{3}{2}r} \eta_1^{(3)} - \frac{1}{8}(k^2 + 2\omega^2) e^{\frac{5}{2}r} \eta_2^{(0)} + \cdots, \end{aligned}$$

JHEP01(2016)013

$$
\begin{aligned}
y_2 &\sim e^{3r} y_2^{(0)} + e^{-3r} y_2^{(6)}, \\
\eta_2 &\sim e^{3r} \eta_2^{(0)} + e^{-3r} \eta_2^{(6)},
\end{aligned}
$$

$$
\begin{aligned}
y_3 &\sim e^{-(\frac{3}{2}-\Delta)r} y_3^{(3-\Delta)} + e^{(\frac{3}{2}-\Delta)r} y_3^{(\Delta)}, \\
\eta_3 &\sim e^{-(\frac{3}{2}-\Delta)r} \eta_3^{(3-\Delta)} + e^{(\frac{3}{2}-\Delta)r} \eta_3^{(\Delta)} + \frac{\Delta-3}{2} e^{(\frac{3}{2}+\Delta)r} \lambda \eta_2^{(0)} + \cdots,
\end{aligned}
$$

$$
\begin{aligned}
y_4 &\sim e^{\frac{3}{2}r} y_4^{(0)} + e^{-\frac{3}{2}r} y_4^{(3)}, \\
\eta_4 &\sim e^{\frac{3}{2}r} \eta_4^{(0)} + e^{-\frac{3}{2}r} \eta_4^{(3)} - \frac{k^2}{4} e^{\frac{5}{2}r} \eta_2^{(0)} + \cdots,
\end{aligned}
$$

$$
\begin{aligned}
y_5 &\sim e^{\frac{3}{2}r} y_5^{(0)} + e^{-\frac{3}{2}r} y_5^{(3)}, \\
\eta_5 &\sim e^{\frac{3}{2}r} \eta_5^{(0)} + e^{-\frac{3}{2}r} \eta_5^{(3)} - \frac{k\omega}{2} e^{\frac{5}{2}r} \eta_2^{(0)} + \cdots.
\end{aligned}
$$

The independent terms are the same, but the leading terms in the auxiliary fields start with a larger exponent due to the mixing with η_2. This can be understood as follows, close to the boundary the coefficients $a \to \mathbb{0}$, making $K \to \mathbb{1}$ and b becomes diagonal. If all the modes had the same asymptotics, then we will be in the case where we can set $\eta = y$. However, this is not exactly true because η_2 grows faster than the other modes and even though the off-diagonal components of b and a go to zero at the boundary, they do not decay fast enough to avoid the mixing. Nonetheless, while we cannot impose the condition $\eta = y$, we can fix some relation between the leading coefficients of the independent solutions. There is an ambiguity in this choice, since different combinations may be formed. The simplest option is simply to match the leading coefficients of each of the independent solutions for y with the leading coefficients of the independent solutions for η

$$
\begin{aligned}
&\eta_i^{(0)} = y_i^{(0)}, \qquad && \eta_i^{(3)} = y_i^{(3)}, \quad i = 1, 4, 5, \\
&\eta_2^{(0)} = y_2^{(0)}, \qquad && \eta_2^{(6)} = -y_2^{(6)}, \\
&\eta_3^{(3-\Delta)} = y_3^{(3-\Delta)}, \quad && \eta_3^{(\Delta)} = y_3^{(\Delta)}.
\end{aligned}
\tag{3.35}
$$

This fixes completely the auxiliary modes in terms of the original fluctuations.[5] We can group the non-normalizable coefficients in a vector H and the normalizable coefficients in another vector T,

$$
H^T = \begin{pmatrix} y_1^{(0)} & y_2^{(0)} & y_3^{(3-\Delta)} & y_4^{(0)} & y_5^{(0)} \end{pmatrix}, \; T^T = \begin{pmatrix} y_1^{(3)} & y_2^{(6)} & y_3^{(\Delta)} & y_4^{(3)} & y_5^{(3)} \end{pmatrix}. \tag{3.36}
$$

[5] The choice of sign for $\eta_2^{(6)}$ gives simpler expressions.

JHEP01(2016)013

In the following we will use the vector components H_i and T_i to refer to the normalizable and non-normalizable coefficients. The current evaluated at the boundary has the form

$$J_B = H^\dagger \mathcal{C} H + H^\dagger \mathcal{D} T - T^\dagger \mathcal{D}^\dagger H, \tag{3.37}$$

where $\mathcal{C}^\dagger = -\mathcal{C}$. The non-zero elements of $\mathcal{C}$ are

$$\mathcal{C}_{12} = -\mathcal{C}_{21},\ \mathcal{C}_{13} = -\mathcal{C}_{31},\ \mathcal{C}_{23} = -\mathcal{C}_{32},\ \mathcal{C}_{24} = -\mathcal{C}_{42},\ \mathcal{C}_{25} = -\mathcal{C}_{52}. \tag{3.38}$$

They have even powers of k except for $\mathcal{C}_{25}$, which is proportional to odd powers. The explicit value of the coefficients is given in appendix B.3. The non-zero elements of $\mathcal{D}$ are

$$\mathcal{D}_{11},\ \mathcal{D}_{22},\ \mathcal{D}_{33},\ \mathcal{D}_{44},\ \mathcal{D}_{55},\ \mathcal{D}_{13},\ \mathcal{D}_{21},\ \mathcal{D}_{23}, \tag{3.39}$$

all of which only have even powers of k. The explicit value is also in appendix B.3. One can easily check that current is explicitly invariant under the parity transformation

$$k \longrightarrow -k, \quad H_5 \longrightarrow -H_5, \quad T_5 \longrightarrow -T_5. \tag{3.40}$$

In order to compute correlators we impose ingoing boundary conditions at the horizon. At the boundary this means that the coefficients of the normalizable solutions are not independent, but they are proportional to the coefficients of the non-normalizable solutions:

$$T_i = C_{ij}(\omega, k) H_j, \tag{3.41}$$

or, in matrix notation, $T = CH$. Then, the current evaluated at the boundary can be written as

$$J_B = H^\dagger \mathcal{G} H, \quad \mathcal{G} = \mathcal{C} + \mathcal{D} C - C^\dagger \mathcal{D}^\dagger. \tag{3.42}$$

3.1.2 Current at the horizon

We now proceed to compute the probability current at the horizon. The background is taken to be regular at the horizon, with g_{00} having a simple zero at $r = r_H$.

$$A = A_H + O((r-r_H)^2)\,, B = \log(r-r_H) + B_H + O((r-r_H)^2)\,,\ \phi = \phi_H + O((r-r_H)^2). \tag{3.43}$$

To leading order, the matrix K close to the horizon takes the following form

$$K = (r-r_H) \begin{pmatrix} K^H_{11} & K^H_{12}(r-r_H) + e^{-\frac{3}{2}A_H} K^H_{11} & & & & \\ & K^H_{22}(r-r_H) & & & & \\ & K^H_{32}(r-r_H) & K^H_{33} & & & \\ & & & K^H_{44} & & \\ & & & & K^H_{55}(r-r_H)^2 & \end{pmatrix}. \tag{3.44}$$

The expansions of the background and the matrix K can be found in appendices C.2. The coefficients K^H_{ij} are not determined by the expansion close to the horizon. Their value can be determined by solving the differential equation for K imposing the condition at the boundary that $K \to \mathbb{1}$.

JHEP01(2016)013

Since the equations for the fluctuations are of second order, there are in principle two independent solutions for each of the y_i and η_i, generically of the form $\sim (r-r_H)^\alpha$. The exponent α can be complex. For the fluctuations y_i we impose regularity (if α is real) or ingoing boundary conditions (if α is complex). Since we have already imposed the conditions (3.35), there is no freedom left to fix the behavior of the auxiliary fields η_i at the horizon. The leading order terms of each of the independent solutions are

$$\begin{aligned}
&y_1 \sim y_1^H, \\
&\eta_1 \sim (r-r_H)^{-ic_H\,\omega}\eta_1^H + (r-r_H)^{ic_H\,\omega}\tilde{\eta}_1^H, \\
&\\
&y_2 \sim (r-r_H)^{-ic_H\,\omega} y_2^H, \\
&\eta_2 \sim \eta_2^H + \frac{\tilde{\eta}_2^H}{r-r_H}, \\
&\\
&y_3 \sim (r-r_H)^{-ic_H\,\omega} y_3^H, \\
&\eta_3 \sim (r-r_H)^{-ic_H\,\omega}\eta_3^H + (r-r_H)^{ic_H\,\omega}\tilde{\eta}_3^H, \\
&\\
&y_4 \sim (r-r_H)^{-ic_H\,\omega} y_4^H, \\
&\eta_4 \sim (r-r_H)^{-ic_H\,\omega}\eta_4^H + (r-r_H)^{ic_H\,\omega}\tilde{\eta}_4^H, \\
&\\
&y_5 \sim y_5^H \\
&\eta_5 \sim \eta_5^H + \frac{\tilde{\eta}_5^H}{(r-r_H)^2}.
\end{aligned}$$

Where we have defined $c_H = e^{-(A_H+B_H)}$. All the fluctuations are actually mixed, the expansion of the fluctuations and the auxiliary fields can be found in appendix C.5.

Let us group the coefficients of the solutions in the vectors y_H, η_H and $\tilde{\eta}_H$ with components

$$(y_H)_i = y_i^H, \quad (\eta_H)_i = \eta_i^H, \quad (\tilde{\eta}_H)_i = \tilde{\eta}_i^H. \tag{3.45}$$

The probability current evaluated at the horizon takes the form

$$J_H = \eta_H^\dagger \mathcal{M} y_H - y_H^\dagger \mathcal{M}^\dagger \eta_H + \tilde{\eta}_H^\dagger \mathcal{N} y_H - y_H^\dagger \mathcal{N}^\dagger \tilde{\eta}_H. \tag{3.46}$$

Where the non-zero entries of each matrix are

$$\begin{aligned}
&\mathcal{M}_{12} = 2e^{-\frac{3}{2}A_H}(ic_H\,\omega - 1)K_{11}^H, \quad \mathcal{M}_{33} = 2ic_H\,\omega K_{33}^H, \quad \mathcal{M}_{44} = 2ic_H\,\omega K_{44}^H, \\
&\mathcal{N}_{21} = e^{\frac{3}{2}A_H}K_{22}^H, \qquad\qquad\qquad \mathcal{N}_{55} = -2K_{55}^H.
\end{aligned} \tag{3.47}$$

When we solve the linear equations of motion, we can write a general solution in terms of the boundary values using a boundary-to-bulk propagator

$$y_i = G_{ij}(r,\omega,k)y_i^{(0)}, \quad \eta_i = \tilde{G}_{ij}(r,\omega,k)\eta_i^{(0)}. \tag{3.48}$$

JHEP01(2016)013

The parity symmetry of the equations of motion imply that the components $G_{5i}, G_{i5}, \tilde{G}_{5i}, \tilde{G}_{i5}$ for $i \neq 5$ are odd in momentum, while the rest of components are even. Since the elements $\mathcal{M}_{i5}$, $\mathcal{M}_{5i}$, $\mathcal{N}_{i5}$ and $\mathcal{N}_{5i}$ are all zero for $i \neq 5$, the current evaluated at the horizon will be even in momentum when the parity odd sources are zero $y_5^{(0)} = \eta_5^{(0)} = 0$ or when the parity even sources are zero $y_{i\neq 5}^{(0)} = \eta_{i\neq 5}^{(0)} = 0$. In these two cases the current should be invariant under $k \to -k$:

$$J(k) = J(-k). \tag{3.49}$$

However, if both parity even and parity odd sources are nonzero, in general the current will have contributions that are odd in momentum, in contrast to the case of the shear viscosity. We will denote the odd part of the horizon current as

$$[J_H]_{\text{odd}} = \frac{1}{2}\left(J_H(k) - J_H(-k)\right). \tag{3.50}$$

3.2 Boundary coefficients and correlators

The asymptotic expansion of metric and scalar fluctuations takes the form

$$h_{\mu\nu} = e^{2r}\left(h_{\mu\nu}^{(0)} + e^{-3r}G_{\mu\nu}^{T} + \cdots\right), \quad \delta\phi = e^{-(3-\Delta)r}\delta\lambda + e^{-\Delta r}G^{O} + \cdots. \tag{3.51}$$

We can identify $h_{\mu\nu}^{(0)}$ with a change of the metric in the dual field theory $g_{\mu\nu}^{(0)} = \eta_{\mu\nu} + h_{\mu\nu}^{(0)}$, that acts a as a source for the energy-momentum tensor. Similarly, $\delta\lambda = \mu^{\Delta-3}\delta J^{(0)}$ is a change of the coupling that acts as a source for the scalar operator. The changes in the expectation values of the energy-momentum tensor $\delta\langle T_{\mu\nu}\rangle$ and scalar $\delta\langle\mathcal{O}\rangle$ are proportional to the coefficients $G_{\mu\nu}^{T}$ and G^{O} respectively. We have used the holographic renormalization procedure to compute the change in the one-point functions relative to the background values given in (3.5) and (3.6)

$$\delta\langle\mathcal{O}\rangle = \frac{\mu^{\Delta-3}}{8\pi G_N L}(3-2\Delta)G^{O}, \tag{3.52}$$

$$\delta\langle T_{\mu\nu}\rangle = \frac{3}{16\pi G_N L}G_{\mu\nu}^{T} + \frac{(\Delta-3)(\Delta-1)}{2\Delta-3}\left[\langle\mathcal{O}\rangle\left(J^{(0)}h_{\mu\nu}^{(0)} + \delta J^{(0)}\eta_{\mu\nu}\right) + J^{(0)}\delta\langle\mathcal{O}\rangle\eta_{\mu\nu}\right].$$

The coefficients G are not independent, but they will be fixed in terms of the sources once regularity or ingoing boundary conditions are imposed on the solutions. In general they will have an expansion

$$\begin{aligned} G_{\mu\nu}^{T} &= G_{\mu\nu}^{TT\ \alpha\beta}h_{\alpha\beta}^{(0)} + G_{\mu\nu}^{TO}\delta\lambda, \\ G^{O} &= G^{OT\ \alpha\beta}h_{\alpha\beta}^{(0)} + G^{OO}\delta\lambda. \end{aligned} \tag{3.53}$$

Where the coefficients G^{TT}, G^{TO}, G^{OT} and G^{OO} are functions of the frequency and the momentum.

We can derive the correlators of the energy-momentum tensor and scalar by taking variations with respect to the one-point functions

$$\begin{aligned} \Gamma_{\mu\nu\alpha\beta}^{TT} &= -\eta_{\alpha\sigma}\eta_{\beta\rho}\frac{\delta\langle T_{\mu\nu}\rangle}{\delta h_{\sigma\rho}^{(0)}}, \quad \Gamma_{\mu\nu}^{TO} = \frac{\delta\langle T_{\mu\nu}\rangle}{\delta J^{(0)}}, \\ \Gamma_{\alpha\beta}^{OT} &= -\eta_{\alpha\sigma}\eta_{\beta\rho}\frac{\delta\langle\mathcal{O}\rangle}{\delta h_{\sigma\rho}^{(0)}}, \quad \Gamma^{OO} = \frac{\delta\langle\mathcal{O}\rangle}{\delta J^{(0)}}. \end{aligned} \tag{3.54}$$

JHEP01(2016)013

3.3 Ward identities

We have now all the ingredients to derive Ward identities. Let us start with the usual Ward identities for the conservation and the trace of the energy-momentum tensor. When we compute the solutions we find that not all the coefficients $G^T_{\mu\nu}$ are independent. They satisfy a linear relation, that in terms of the one-point functions becomes the trace Ward identity

$$\eta^{\mu\nu}\delta\langle T_{\mu\nu}\rangle - h^{(0)\,\mu\nu}\langle T_{\mu\nu}\rangle_T = (\Delta-3)\left[\delta J^{(0)}\langle\mathcal{O}\rangle + J^{(0)}\delta\langle\mathcal{O}\rangle\right]. \tag{3.55}$$

Where $\langle T_{\mu\nu}\rangle_T$ is the thermal energy-momentum tensor determined in (3.5).

The momentum constraint equations give two more Ward identities related to the conservation of the energy-momentum tensor

$$\begin{aligned} 0 &= \omega\delta\langle T_{00}\rangle + k\delta\langle T_{10}\rangle + \varepsilon(\omega h^{(0)}_{00} + k h^{(0)}_{01}) + \frac{\varepsilon+P}{2}\omega(h^{(0)}_{11}+h^{(0)}_{22}) - \omega\delta J^{(0)}\langle\mathcal{O}\rangle\,, \\ 0 &= \omega\delta\langle T_{01}\rangle + k\delta\langle T_{11}\rangle - P(\omega h^{(0)}_{01} + k h^{(0)}_{11}) - \frac{\varepsilon+P}{2}k h^{(0)}_{00} + k\delta J^{(0)}\langle\mathcal{O}\rangle\,. \end{aligned} \tag{3.56}$$

These are consistent with the covariant form of the Ward identity expanded to linear order

$$\partial_\mu\left(\delta\langle T^\mu_{\ \nu}\rangle - h^{(0)\,\mu\alpha}\langle T_{\alpha\nu}\rangle_T\right) + \Gamma^{(0)\,\mu}_{\mu\alpha}\langle T^\alpha_{\ \nu}\rangle_T - \Gamma^{(0)\,\alpha}_{\mu\nu}\langle T^\mu_{\ \alpha}\rangle_T = -\partial_\mu\delta J^{(0)}\langle\mathcal{O}\rangle\,. \tag{3.57}$$

In order to derive a generalized Ward identity for the scalar modes we can use the same argument we used for the shear modes. The current evaluated at the horizon has a contribution $[J_H]_{\rm odd}$ odd under $k\to -k$. Since the current is constant in the radial direction $J'=0$, the current evaluated at the boundary must have the same property. This gives the conditions

$$[\mathcal{G}]_{\rm odd} = \frac{\delta^2}{\delta H^\dagger \delta H}[J_H]_{\rm odd}. \tag{3.58}$$

Where $\mathcal{G}$ was defined in (3.42).

We use the basis of fluctuations y_i to compute the current, but then we change to the usual basis of metric and scalar fluctuations $h_{\mu\nu}$, $\delta\phi$ to extract $\mathcal{G}$ and derive the Ward identities. The map between the leading order terms is

$$\begin{aligned} y_1{}^{(0)} &= \frac{1}{2}\left(h^{(0)}_{11}+h^{(0)}_{22}+h^{(0)}_{00}\right), \quad y_2{}^{(0)} = \frac{1}{2}\left(h^{(0)}_{11}+h^{(0)}_{22}-h^{(0)}_{00}\right), \quad y_3{}^{(3-\Delta)} = \delta\lambda\,, \\ y_4{}^{(0)} &= \frac{1}{2}\left(h^{(0)}_{11}-h^{(0)}_{22}\right), \qquad\qquad y_5{}^{(0)} = h^{(0)}_{01}. \end{aligned} \tag{3.59}$$

If we turn on only the parity odd source $y_5{}^{(0)}$, then $[J_H]_{\rm odd}=0$ and the Ward identity is simply

$$\left[\Gamma^{TT}_{0101} - \overline{\Gamma}^{TT}_{0101}\right]_{\rm odd} = 0. \tag{3.60}$$

If we turn on only the parity even sources, we get a quite complicated expression. It becomes somewhat simpler if we impose on the source the tracelessness condition $\eta^{\mu\nu}h^{(0)}_{\mu\nu}=0 \Rightarrow y_2{}^{(0)}=0$ and set the source for the scalar field to zero $y_3{}^{(3-\Delta)}=0$, but it does not lead to any expression that relates to the Ward identity we are interested in.

JHEP01(2016)013

We have to allow for both parity odd an parity even sources. We find the following condition

$$\left[\Gamma^{TT}_{1101}+\overline{\Gamma}^{TT}_{0111}\right]_{\text{odd}}=-W_{\text{odd}}, \tag{3.61}$$

where the term that appears on the right hand side is schematically

$$W_{\text{odd}}=-\alpha_J\frac{\delta^2[J_H]_{\text{odd}}}{\delta\overline{h}^{(0)}_{01}\delta h^{(0)}_{11}}+\lambda\left[\alpha_{01}\Gamma^{OT}_{01}+\alpha_{00}\Gamma^{OT}_{00}\right]_{\text{odd}}+\alpha k\omega(\omega^2-k^2)^2. \tag{3.62}$$

α_{01} is a constant and α_{00} depends on the pressure and the expectation value of the scalar operator. The coefficients α_J and α are dimensionful constants determined by the overall factors that appear in the definition of the correlators Γ when we compute them using holographic renormalization.

If we multiply by k this equation and use the Ward identity (2.31) (with the source for the scalar fluctuation set to zero), such that $k\Gamma^{TT}_{1101}=-\omega\Gamma^{TT}_{0101}+\omega P$, then

$$\left[k\overline{\Gamma}^{TT}_{0111}-\omega\Gamma^{TT}_{0101}\right]_{\text{even}}=-\omega P-kW_{\text{odd}}\,. \tag{3.63}$$

Multiplying by ω and using (2.31), such that $\omega\overline{\Gamma}^{TT}_{0111}=-k\overline{\Gamma}^{TT}_{1111}+kP$, we obtain the expected form of the Ward identity

$$\left[\omega^2\Gamma^{TT}_{0101}+k^2\overline{\Gamma}^{TT}_{1111}\right]_{\text{even}}=(\omega^2+k^2)P+k\omega W_{\text{odd}}\,. \tag{3.64}$$

This establishes a relation between the momentum or thermal conductivity and the bulk viscosity. However, in contrast to the identity for the shear, we do not know how to completely determine the relation without first solving the equations for the fluctuations.

4 Discussion

In order to derive relations of the form (1.4) in holography we have constructed a probability current J from linear fluctuations of the metric and a scalar field in an asymptotically AdS spacetime. This current is independent of the radial coordinate and invariant under parity. Using these properties and comparing the value of the current at the AdS boundary and at the horizon, we found the Ward identities (2.35) and (3.64)

$$\left[\omega^2\Gamma_{0202}+k^2\overline{\Gamma}_{1212}\right]_{\text{even}}=0,\quad\left[\omega^2\Gamma^{TT}_{0101}+k^2\overline{\Gamma}^{TT}_{1111}\right]_{\text{even}}=(\omega^2+k^2)P+k\omega W_{\text{odd}}\,. \tag{4.1}$$

An expression for W_{odd} is given in (3.62). In order to derive the second identity we had to introduce auxiliary fields that allowed us to construct a constant probability current. This introduces an ambiguity, we can choose arbitrarily the boundary conditions of the auxiliary fields. We impose the same boundary conditions for the original fluctuations and the auxiliary fields at the AdS boundary, so the current is completely determined by the solutions to the original fluctuations.

JHEP01(2016)013

We can define the real part of the momentum conductivity κ and the shear and bulk viscosities η, ζ from the Kubo formulas[6]

$$\begin{aligned}\kappa_{ij} &= -\frac{1}{\omega}\,\mathrm{Im}\,\Gamma_{0i0j}(\omega,k),\\ \eta &= -\frac{1}{\omega}\,\mathrm{Im}\,\Gamma_{1212}(\omega,k),\\ \eta+\zeta &= -\frac{1}{\omega}\,\mathrm{Im}\,\Gamma_{1111}(\omega,k).\end{aligned} \tag{4.2}$$

For low momentum k, we can expand each of the transport coefficients in powers of k

$$\kappa_{ij} \simeq \kappa_{ij}^{(0)} + (k^2\delta^{ij} - k^i k^j)\kappa_T^{(2)} + k^i k^j \kappa_L^{(2)} + \cdots\,, \quad \eta = \eta^{(0)} + O(k^2), \quad \zeta = \zeta^{(0)} + O(k^2). \tag{4.3}$$

We can also expand $W_{\rm odd} \simeq k W_{\rm odd}^{(1)} + \cdots$. From the Ward identities we get the relations

$$\kappa_T^{(2)} = \frac{1}{\omega^2}\eta^{(0)}, \quad \kappa_L^{(2)} = \frac{1}{\omega^2}\left(\eta^{(0)} + \zeta^{(0)} - \mathrm{Im}\,W_{\rm odd}^{(1)}\right). \tag{4.4}$$

The first relation between the transverse component of the conductivity and the shear viscosity agree with field theory results. The second relation between the longitudinal conductivity and the bulk viscosity has the right structure, but we do not know from general arguments what is the contribution from $W_{\rm odd}$. In general, $W_{\rm odd}$ is an asymmetry in the mixed correlators of momentum and stress. From (3.61)

$$\mathrm{Im}\,W_{\rm odd} = \left[\mathrm{Im}\,\Gamma_{0111} - \mathrm{Im}\,\Gamma_{1101}\right]_{\rm odd}. \tag{4.5}$$

A naïve comparison with the Ward identity (2.23) at zero magnetic field in [13] would fix $\mathrm{Im}\,W_{\rm odd}^{(1)} = 0$. Although this probably holds in the holographic model, the correlators computed using holographic renormalization can differ by contact terms from the correlators that enter in the Ward identity in [13], so there might be additional contributions. It would be interesting to look for a general argument that fixes the asymmetry in holographic models.

In the calculation using the probability current $W_{\rm odd}$ contains two kind of contributions, one is coming from the evaluation of the probability current at the boundary and it is ambiguous because the probability current we have constructed depends on auxiliary fields whose boundary conditions can be fixed in different ways. The second kind of contribution depends on the value of the current at the horizon and it cannot be determined without explicitly solving the equations of motion. Since the correlators Γ are defined only in terms of the original fluctuations, the horizon and boundary ambiguities should cancel each other, but we cannot determine completely the Ward identity from parity invariance of the current alone. The situation is somewhat improved when only parity even or parity odd sources are turned on, in this case there are no spurious contributions from the horizon.

Even if we focus on the identity for the transverse component (2.35) our derivation of the Ward identity is not complete, it is restricted to terms that are even in momentum in the correlators. In principle we do not expect odd terms appearing in this identity when parity

[6] We expand the viscosity tensor as $\eta^{ijkl} = \eta(\delta^{ik}\delta^{jl} + \delta^{il}\delta^{jk} - \delta^{ij}\delta^{kl}) + \zeta\delta^{ij}\delta^{kl}$.

JHEP01(2016)013

is not broken, but the argument we used for the even terms does not apply to odd terms. This suggests that there must be a different, more general, derivation of the Ward identities.

A natural generalization of this work would be to derive similar Ward identities in holographic models with broken parity, in particular the relation between Hall viscosity and Hall conductivity. This is a direction that has not been explored much, even though there are a large variety of models that exhibit a non-zero Hall conductivity: dyonic black holes [18, 31–35], D-brane intersections of different types [36–40] and others [41, 42]. However, the value of the Hall viscosity has been determined in a different class of holographic models dual to parity breaking superfluids [43–46]. It would be interesting to check if and when the models that have a Hall conductivity also have a Hall viscosity, since this is mostly the case in Quantum Hall systems and other topological states in condensed matter.

Besides the use we have made of it, the probability current might prove to be useful for other tasks. A possible application is to compute the spectrum of normalizable modes, as are for instance quasinormal modes in a black hole geometry. Let us consider a system with n coupled fluctuations y_i, $i = 1, \ldots, n$ and the related auxiliary fields η_i. The expansion close to the AdS boundary will include the leading terms of the non-normalizable $y_i^{(d-\Delta_i)}$ (sources) and normalizable $y_i^{(\Delta_i)}$ (vev) solutions of the fluctuations, and similar terms appear in the auxiliary fields (even though the leading terms might be different due to mixing)

$$y_i \simeq y_i^{(d-\Delta_i)} e^{-(d-\Delta_i)r} + y_i^{(\Delta_i)} e^{-\Delta_i r}, \quad \eta_i \simeq \eta_i^{(d-\Delta_i)} e^{-(d-\Delta_i)r} + \eta_i^{(\Delta_i)} e^{-\Delta_i r} + \cdots . \tag{4.6}$$

If the sources are zero $y_i^{(d-\Delta_i)} = \eta_i^{(d-\Delta_i)} = 0$, the probability current will vanish. This will be independent of the value of the auxiliary fields at the horizon. The solutions for auxiliary fields can be computed by shooting from the AdS boundary with normalizable boundary conditions and do not have to satisfy any regularity conditions at the horizon. We will have n independent solutions that we can construct by imposing $\eta^{(\Delta_i)} = 0$ for all modes but one. Then, the condition that the probability current is zero at the horizon for each case will lead to n linear equations for the values of the fluctuations at the horizon y_i^H. In order to have a non-trivial solution the system must be degenerate, which will give a condition on the spectrum. This method is somewhat similar to the determinant method of [26], but there the system of linear equations is found by evaluating the solutions y_i with ingoing boundary conditions at a cutoff close to the boundary.

Acknowledgments

We would like to thank Ioannis Papadimitriou for useful comments. This work is partially supported by the Spanish grant MINECO-13-FPA2012-35043-C02-02. C.H. is supported by the Ramon y Cajal fellowship RYC-2012-10370. D.R.F. is supported by the GRUPIN 14-108 research grant from Principado de Asturias.

A Holographic renormalization

In order to compute expectation values and correlation functions of operators in the field theory dual, we follow the holographic renormalization prescription [14, 15]. We will write

JHEP01(2016)013

the metric as

$$ds^2 = dr^2 + g_{\mu\nu}dx^\mu dx^\nu. \tag{A.1}$$

The metric asymptotes an AdS space of radius L, $g_{\mu\nu} \sim e^{2r/L}$ when $r \to \infty$.

We can obtain the one-point functions of the scalar operator and the energy-momentum tensor by taking variation of the action with respect to the metric and the scalar field. Since the action is divergent we need to regularize it, this can be done by introducing a radial cutoff r_Λ. In order to have a well-defined variation with respect to the metric we have to add a Gibbons-Hawking term at the cutoff

$$S = \frac{1}{16\pi G_N}\int d^4x\sqrt{-g}\left(R - (\partial\phi)^2 - 2V(\phi)\right) + \frac{1}{8\pi G_N}\int_{r=r_\Lambda} d^3x\sqrt{-g}K. \tag{A.2}$$

Where $K = g^{\mu\nu}K_{\mu\nu}$ and $K_{\mu\nu}$ is the extrinsic curvature on radial slices

$$K_{\mu\nu} = \frac{1}{2}\partial_r g_{\mu\nu}. \tag{A.3}$$

The variation of the on-shell bulk action plus Gibbons-Hawking term is

$$\delta S_{\text{on-shell}} = \frac{1}{16\pi G_N}\int_{r=r_\Lambda} d^3x\,\sqrt{-g}\left[\left(K_{\mu\nu} - g_{\mu\nu}K\right)\delta g^{\mu\nu} - 2\partial_r\phi\delta\phi\right]. \tag{A.4}$$

The on-shell action has divergent terms when $r_\Lambda \to \infty$. They can be removed by adding a counterterm action at the cutoff

$$S_{c.t.} = \frac{L}{8\pi G_N}\int_{r=r_\Lambda} d^3x\,\sqrt{-g}\left(-\frac{2}{L^2} + \frac{\Delta-3}{2L^2}\phi^2 - \frac{1}{2}\hat{R}\right), \tag{A.5}$$

where $\hat{R}$ is the Ricci scalar of the induced metric on the radial slice. The variation of the sources for the dual operators $\delta g^{(0)\,\mu\nu}$, $\delta J^{(0)}$ are identified as

$$\delta g^{\mu\nu} = e^{-2r/L}\delta g^{(0)\,\mu\nu}, \quad \delta\phi = \mu^{\Delta-3}\delta J^{(0)}e^{-(3-\Delta)r/L}. \tag{A.6}$$

The one-point functions are computed from the variation of the action with respect to the sources

$$\langle T_{\mu\nu}\rangle = -\lim_{r_\Lambda\to\infty}\frac{2}{\sqrt{-g^{(0)}}}\frac{\delta S}{\delta g^{(0)\,\mu\nu}}, \quad \langle\mathcal{O}\rangle = -\lim_{r_\Lambda\to\infty}\frac{1}{\sqrt{-g^{(0)}}}\frac{\delta S}{\delta J^{(0)}}. \tag{A.7}$$

The finite one-point functions are defined as

$$\begin{aligned}\langle T_{\mu\nu}\rangle = &-\lim_{r_\Lambda\to\infty}\frac{1}{8\pi G_N}e^{-2r_\lambda/L}\frac{\sqrt{-g}}{\sqrt{-g^{(0)}}}\times \\ &\times\left[K_{\mu\nu} - g_{\mu\nu}K + \frac{1}{L}g_{\mu\nu}\left(2 - \frac{\Delta-3}{2}\phi^2\right) - L\left(\hat{R}_{\mu\nu} - \frac{1}{2}g_{\mu\nu}\hat{R}\right)\right]_{r=r_\Lambda}, \\ \langle\mathcal{O}\rangle = &\lim_{r_\Lambda\to\infty}\frac{\mu^{\Delta-3}}{8\pi G_N}e^{-(3-\Delta)r_\Lambda/L}\frac{\sqrt{-g}}{\sqrt{-g^{(0)}}}\left[\partial_r\phi - \frac{\Delta-3}{L}\phi\right]_{r=r_\Lambda}.\end{aligned}$$

JHEP01(2016)013

B Equations of motion

In this appendix, we write down the equations of motion derived from the action (2.1). In principle, we are not interested on the full solution of neither the metric functions $A\,, B$, nor of the scalar field ϕ, since the form of the asymptotic expansions suffices in this work. The same applies to the fluctuations $\{y_i\}, \{\eta_i\}\,, i = 1, \cdots, 5$.

B.1 Background equations

For the black brane background (3.3) plus scalar field $\phi = \phi_0(r)$ coupled to gravity, in absence of fluctuations the background equations of motion read (the r dependence is implicit)

$$0 = \phi_0' \left[3A' + B'\right] - V'\left(\phi_0\right) + \phi_0''\,, \tag{B.1}$$

$$0 = A'' - A'B' + \frac{1}{2}{\phi_0'}^2\,, \tag{B.2}$$

$$0 = B' \left[3A' + B'\right] + B''\,, \tag{B.3}$$

$$V\left(\phi_0\right) = \frac{1}{2}{\phi_0'}^2 - A' \left[2B' + 3A'\right]\,, \tag{B.4}$$

where the constraint was employed to set the potential as a function of the derivatives of $A\,, B$ and ϕ_0 alone.[7] Although we have freedom to choose the potential V, for the sake of simplicity we will restrict ourselves to a quadratic potential on the field ϕ, i.e., $V(\phi) \propto \phi^2$. This choice does not affect the results but simplifies somewhat the formulas.

B.2 Fluctuation equations

The equations of fluctuations are

$$y_i'' + a_{ij}\, y_j' + b_{ij}\, y_j = 0, \quad c_i^a\, y_i' + d_i^a\, y_i = 0,\ a = 1, 2, 3. \tag{B.5}$$

Where the coefficients of the dynamical equations are

$$a_{ij} = \begin{pmatrix} B' & e^{-\frac{3A}{2}}\left(A' - B'\right) & & & \\ & 2B' & & & \\ & e^{-\frac{3A}{2}}\phi_0' & B' & & \\ & & & B' & \\ & & & & 3B' \end{pmatrix}, \tag{B.6}$$

$$b_{12} = -e^{-\frac{7}{2}A}\left[\frac{k^2}{2} + 3e^{2A}A'\left(A' - B'\right)\right]\,, \qquad b_{13} = V'\left(\phi_0\right)\,,$$

$$b_{14} = e^{-2A}k^2\,, \qquad b_{21} = e^{-\frac{A}{2}}\left(\frac{k^2}{2} + e^{-2B}\omega^2\right)\,,$$

$$b_{23} = 3e^{\frac{3A}{2}}V'\left(\phi_0\right)\,, \qquad b_{24} = e^{-\frac{A}{2}}k^2\,,$$

[7] The prime will denote derivative with respect to the radial coordinate, except for the potential $V(\phi_0)$ where it denotes derivative with respect to the field ϕ_0.

JHEP01(2016)013

$$
\begin{aligned}
b_{25} &= 2e^{-\frac{A}{2}}k\omega\,, & b_{32} &= -3e^{-\frac{3A}{2}}A'\phi_0'\,,\\
b_{41} &= \frac{k^2}{2}e^{-2A}\,, & b_{42} &= -\frac{k^2}{2}e^{-\frac{7A}{2}}\,,\\
b_{45} &= e^{-2A}k\omega\,, & b_{51} &= \frac{1}{2}e^{-2(A+B)}k\omega\,,\\
b_{52} &= \frac{1}{2}e^{-\frac{7A}{2}-2B}k\omega\,, & b_{54} &= -e^{-2(A+B)}k\omega\,,
\end{aligned}
$$

$$
\begin{aligned}
b_{11} &= -\frac{1}{2}e^{-2A}k^2 + \frac{3}{4}\left[\phi_0'^{\,2} - A'\left(3A'+4B'\right)\right]\,,\\
b_{22} &= \frac{3}{2}\phi_0'^{\,2} + e^{-2A}\left(e^{-2B}\omega^2 - \frac{3k^2}{2}\right) - 9A'\left(A'+B'\right)\,,\\
b_{33} &= -3A'\left(B'+\frac{3}{4}A'\right) + \frac{3}{4}\phi_0'^{\,2} + e^{-2A}\left(e^{-2B}\omega^2 - k^2\right) - V''\left(\phi_0\right)\,,\\
b_{44} &= e^{-2(A+B)}\omega^2 + \frac{3}{4}\phi_0'^{\,2} - 3A'\left(B'+\frac{3}{4}A'\right)\,,\\
b_{55} &= \frac{3}{4}\left[\phi_0'^{\,2} - A'\left(3A'+8B'\right)\right]\,.
\end{aligned}
$$

The coefficients of the constraints are

$$
c_i^1 = -\frac{\omega}{2}\begin{pmatrix}1\\1\\0\\0\\\frac{k}{\omega}e^{2B(r)}\end{pmatrix},\ c_i^2 = -\frac{k}{4}\begin{pmatrix}1\\-3\\0\\2\\\frac{2\omega}{k}\end{pmatrix},\ c_i^3 = \begin{pmatrix}\frac{B'}{2}\\\frac{1}{2}\left(4A'+B'\right)\\-\phi_0'\\0\\0\end{pmatrix}, \tag{B.7}
$$

and

$$
d_i^1 = \frac{\omega}{2}\begin{pmatrix}B'(r)\\B'(r)\\-2\omega\phi_0'\\0\\0\end{pmatrix},\ d_i^2 = \frac{k}{2}\begin{pmatrix}-B'\\B'\\2\phi_0'\\0\\-\frac{2\omega}{k}B'\end{pmatrix},\ d_i^3 = 4e^{-2A}\begin{pmatrix}2\omega^2e^{-2B}+k^2\\2\omega^2e^{-2B}-3k^2\\4e^{2A}V'(\phi)\\2k^2\\k\omega\end{pmatrix}. \tag{B.8}
$$

B.3 Coefficients in the boundary current

The current evaluated at the boundary has the form

$$
J_B = H^\dagger\mathcal{C}H + H^\dagger\mathcal{D}T - T^\dagger\mathcal{D}^\dagger H, \tag{B.9}
$$

where $\mathcal{C}^\dagger = -\mathcal{C}$. The non-zero coefficients of $\mathcal{C}$ are

$$
\begin{aligned}
\mathcal{C}_{12} &= -\mathcal{C}_{21} = \frac{1}{64}(k^2+2\omega^2)(\omega^2-k^2)^2 + \frac{13}{6}B_0 - \frac{1}{2}\Delta(\Delta-3)\lambda v,\\
\mathcal{C}_{13} &= -\mathcal{C}_{31} = -\frac{1}{3}\Delta(\Delta-3)v,\\
\mathcal{C}_{23} &= -\mathcal{C}_{32} = -\frac{\Delta(2\Delta-9)}{2\Delta+3}v + \frac{3}{4}\Delta(2\Delta-7)B_0v - \frac{1}{32}(\Delta(2\Delta-3)^2-81)\lambda v^2,\\
\mathcal{C}_{24} &= -\mathcal{C}_{42} = -\frac{1}{32}k^2(\omega^2-k^2)^2,\\
\mathcal{C}_{25} &= -\mathcal{C}_{52} = -\frac{1}{16}k\omega(\omega^2-k^2)^2.
\end{aligned} \tag{B.10}
$$

JHEP01(2016)013

The non-zero components of $\mathcal{D}$ are

$$
\begin{aligned}
2\mathcal{D}_{11} &= \mathcal{D}_{22} = 2\mathcal{D}_{44} = 2\mathcal{D}_{55} = -4\mathcal{D}_{21} = 12, \\
\mathcal{D}_{33} &= 2(2\Delta - 3), \\
\mathcal{D}_{13} &= -\frac{1}{3}\Delta(\Delta-3)\lambda, \\
\mathcal{D}_{23} &= \frac{3}{4}(\Delta-3)(2\Delta+1)\lambda B_0 + \frac{(\Delta-3)(2\Delta+2)}{2\Delta-9}\lambda + \frac{1}{32}\left(\Delta(2\Delta-3)(2\Delta-9)+18(\Delta+3)\right)\lambda^2 v.
\end{aligned}
\tag{B.11}
$$

B.4 Coefficients in constraints

The components of $\mathcal{C}^a$ and $\mathcal{D}^a$ are

$$
\begin{aligned}
&\mathcal{C}_i^1 = -\omega\left\{\frac{1}{6}\left[3B_0 + (\Delta-3)\Delta\lambda v\right], B_0, -\frac{\Delta v}{3}(\Delta-1), 0, \frac{k}{6\omega}\left[(\Delta-3)\Delta\lambda v - 3B_0\right]\right\}, \\
&\mathcal{D}_i^1 = \left\{\omega, 0, \frac{1}{3}(\Delta-3)(\Delta-2)\lambda\omega, 0, k\right\}, \\
&\mathcal{C}_i^2 = -k\left\{\frac{1}{12}\left[(\Delta-3)\Delta\lambda v - 15B_0\right], B_0, \frac{1}{6}\Delta(3\Delta-5)v,\right. \\
&\left.\frac{1}{6}\left[(\Delta-3)\Delta\lambda v - 3B_0\right], \frac{\omega}{6k}\left[(\Delta-3)\Delta\lambda v - 15B_0\right]\right\}, \\
&\mathcal{D}_i^2 = \left\{\frac{k}{2}, 0, -\frac{1}{6}(\Delta-3)(3\Delta-4)k\lambda, k, \omega\right\}, \\
&\mathcal{C}_1^3 = B_0^2\left(k^2+\omega^2\right), \quad \mathcal{C}_4^3 = \frac{1}{6}B_0 k^2\left(3B_0 - (\Delta-3)\Delta\lambda v\right), \quad \mathcal{C}_5^3 = 2B_0^2 k\omega, \\
&\mathcal{C}_2^3 = \frac{B_0}{2(\Delta-3)\Delta\lambda v\left(k^2-2\omega^2\right)}\left[2 + \frac{3B_0\left(5\omega^2-4k^2\right)}{(\Delta-3)\Delta\lambda v\left(k^2-2\omega^2\right)} - \frac{(2(\Delta-3)\Delta+9)(8(\Delta-3)\Delta-9)\lambda v}{48B_0(\Delta-3)\Delta}\right], \\
&\mathcal{C}_3^3 = -\frac{v}{3}\left\{\frac{2B_0\Delta\left[(2\Delta-5)\omega^2+k^2\right]}{(k^2-2\omega^2)} + \frac{1}{72}(2(\Delta-3)\Delta+9)(8(\Delta-3)\Delta-9)\lambda v\right\}, \\
&\mathcal{D}_{1,5}^3 = 0, \quad \mathcal{D}_2^3 = \frac{4}{3}\left(k^2-2\omega^2\right), \quad \mathcal{D}_4^3 = B_0 k^2, \\
&\mathcal{D}_3^3 = \frac{1}{3}(\Delta-3)\lambda\left(k^2-2\omega^2\right)\left\{\frac{2B_0\left[(1-2\Delta)\omega^2+k^2\right]}{k^2-2\omega^2} - \frac{(2(\Delta-3)\Delta+9)(8(\Delta-3)\Delta-9)\lambda v}{72(\Delta-3)}\right\}.
\end{aligned}
$$

C Series expansions

In this appendix, we will detail the form of the on-shell series expansions which have been used in this work, both for the background functions and for the (original-auxiliary) fluctuations.

C.1 Background at the boundary

Since AdS is an asymptotic fixed point when $r \to \infty$, we must impose that at leading order $A \sim r\,, B \sim 0\,, \phi_0 \sim 0$ at the boundary. We express the subleading contribution as the sums

$$
\widetilde{A}(r) \sim \sum_{n,m} a_{(n,m)} e^{-(n+m\Delta)r}\,,
\tag{C.1}
$$

JHEP01(2016)013

$$B(r) \sim \sum_{n,m} b_{(n,m)} e^{-(n-\Delta)r}\,, \tag{C.2}$$

$$\phi_0(r) \sim \sum_{n,m} \phi_{(n,m)} e^{-(3n+\Delta m)r} \tag{C.3}$$

where $A(r) = r + \widetilde{A}(r)$. $a, b, \phi_{(n,m)}$ are real-valued coefficients and $\phi_{(1,-1)} = \lambda$, $\phi_{(0,1)} = v$, $b_{(1,0)} = B_0$. Combining (C.1)–(C.3) with (B.1)–(B.5) we find

$$\widetilde{A}(r) = a_{(2,-2)} e^{-2(3r-\Delta)r} + a_{(1,0)} e^{-3r} + a_{(0,2)} e^{-2\Delta r} + \cdots\,, \tag{C.4}$$

$$B(r) = B_0 e^{-3r} + b_{(3,-2)} e^{-(9-2\Delta)r} + b_{(2,0)} e^{-6r} + b_{(1,2)} e^{-(3+2\Delta)r} + \cdots\,, \tag{C.5}$$

$$\begin{aligned}\phi_0(r) = {} & \lambda e^{-(3-\Delta)r} + v e^{-\Delta r} + \phi_{(3,-3)} e^{-3(3-\Delta)r} + \phi_{(2,-1)} e^{-(6-\Delta)r} + \\ & + \phi_{(1,1)} e^{-(3+\Delta)r} + \phi_{(0,3)} e^{-3\Delta r} + \cdots\,,\end{aligned} \tag{C.6}$$

$$\begin{aligned}
a_{(2,-2)} &= -\frac{\lambda^2}{8}, & a_{(1,0)} &= \frac{1}{9}\left[(\Delta-3)\Delta\lambda v - 3B_0\right], \\
a_{(0,2)} &= -\frac{v^2}{8}\,, & b_{(3,-2)} &= \frac{9B_0\lambda^2}{72-16\Delta}\,, \\
b_{(2,0)} &= -\frac{1}{6}B_0(\Delta-3)\Delta\lambda v, & b_{(1,2)} &= \frac{9B_0 v^2}{8(2\Delta+3)}, \\
\phi_{(3,-3)} &= \frac{3(\Delta-3)\lambda^3}{8(4\Delta-9)}, & \phi_{(2,-1)} &= \frac{\Delta(4\Delta-15)\lambda^2 v}{24}\,, \\
\phi_{(1,1)} &= -\frac{\lambda v^2}{24}(\Delta-3)(4\Delta+3), & \phi_{(0,3)} &= \frac{3\Delta v^3}{8(4\Delta-3)}\,,
\end{aligned} \tag{C.7}$$

with $V(\phi) \sim \Delta(\Delta-3)\phi^2$.

C.2 Background at the horizon

As it was stated in section 3.1.2, we impose regularity of each of the background functions $A\,, \phi_0$ but B, which diverges logarithmically at the horizon

$$A(r) = \sum_{n=0} A_H^{(n)} (r-r_H)^n\,, \quad B(r) = \log(r-r_H) + \sum_{n=0} B_H^{(n)} (r-r_H)^n\,, \quad \phi_0(r) = \sum_{n=0} \phi_H^{(n)} (r-r_H)^n\,. \tag{C.8}$$

Plugging these expansions into the equations of motion,

$$A(r) = A_H + (r-r_H)^2 A_H^{(2)} + (r-r_H)^4 A_H^{(4)} + (r-r_H)^6 A_H^{(6)} + \cdots\,, \tag{C.9}$$

$$\begin{aligned}B(r) = {} & \log(r-r_H) + B_H + (r-r_H)^2 B_H^{(2)} + (r-r_H)^4 B_H^{(4)} + \\ & + (r-r_H)^6 B_H^{(6)} + \cdots\,,\end{aligned} \tag{C.10}$$

$$\phi_0(r) = \phi_H + (r-r_H)^2 \phi_H^{(2)} + (r-r_H)^4 \phi_H^{(4)} + (r-r_H)^6 \phi_H^{(6)} + \cdots\,, \tag{C.11}$$

up to $\mathcal{O}(r-r_H)^7$, $A_H^{(0)} = A_H$, $B_H^{(0)} = B_H$, $\phi_H^{(0)} = \phi_H$ in eq.(3.43) and

$$A^{(4)} = -\left(\frac{1}{2}A_H^{(2)2} + \frac{1}{64}V'(\phi_H)^2\right)\,, \quad A_H^{(6)} = \frac{3}{160}V'(\phi_H)^2 A_H^{(2)} + \frac{2}{5}A_H^{(2)3} - \frac{1}{768}V'(\phi_H)^2 V''(\phi_H)\,,$$

JHEP01(2016)013

$$B_H^{(2)} = -A_H^{(2)}\,, \qquad B_H^{(4)} = \frac{7}{10}A_H^{(2)2} + \frac{3}{320}V'(\phi_H)^2\,,$$
$$\phi_H^{(2)} = \frac{1}{4}V'(\phi_H)\,, \qquad \phi_H^{(4)} = \frac{1}{64}V'(\phi_H)\left(V''(\phi_H) - 8A_H^{(2)}\right),$$

$$\begin{aligned} B_H^{(6)} &= -\frac{3}{160}V'(\phi_H)^2 A_H{}^{(2)} - \frac{62}{105}A_H^{(2)3} + \frac{V'(\phi_H)^2 V''(\phi_H)}{1792}\,, \\ \phi_H^{(6)} &= V'(\phi_H)\left(\frac{1}{10}A_H{}^{(2)2} - \frac{1}{96}V''(\phi_H)A_H^{(2)} + \frac{1}{480}V'(\phi_H)^2 + \frac{V''(\phi_H)^2}{2304}\right). \end{aligned} \tag{C.12}$$

C.3 Matrix K

Near the horizon, since $e^B \sim (r - r_H)$, we take

$$K_{11,33,44} = \sum_{n=0} \widehat{K}^{(n)}_{11,33,44}(r-r_H)^{2n+1}, \quad K_{22} = \sum_{n=0} \widehat{K}^{(n)}_{22}(r-r_H)^{2n+2},$$
$$K_{55} = \sum_{n=0} \widehat{K}^{(n)}_{55}(r-r_H)^{2n+3}\,, \qquad K_{12} = \sum_{n=0} \widehat{K}^{(n)}_{12}(r-r_H)^{2n+1} + \widehat{K}^{(n,1)}_{12}(r-r_H)^{2n+2}\,,$$

$$K^H_{32} = \sum_{n=0} \widehat{K}^{(n)}_{32}(r-r_H)^{2n+2} + \widehat{K}^{(n,1)}_{32}(r-r_H)^{2n+3}\,,$$

Truncating these expansions at fair enough order,

$$\begin{aligned}
K_{11} &\sim (r-r_H)K^H_{11} + (r-r_H)^3\widehat{K}^{(1)}_{11} + (r-r_H)^5\widehat{K}^{(2)}_{11} + \cdots\,, \\
K_{12} &\sim (r-r_H)K^H_{12} + (r-r_H)^2\widehat{K}^{(0,1)}_{12} + (r-r_H)^3\widehat{K}^{(1)}_{12} + (r-r_H)^4\widehat{K}^{(1,1)}_{12} + (r-r_H)^6\widehat{K}^{(2,1)}_{12}\cdots\,, \\
K_{22} &\sim (r-r_H)^2K^H_{22} + (r-r_H)^4\widehat{K}^{(1)}_{22} + (r-r_H)^6\widehat{K}^{(2)}_{22} + \cdots\,, \\
K_{32} &\sim (r-r_H)^2K^H_{32} + (r-r_H)^3\widehat{K}^{(0,1)}_{32} + (r-r_H)^4\widehat{K}^{(1)}_{32} + (r-r_H)^5\widehat{K}^{(1,1)}_{32} + (r-r_H)^6\widehat{K}^{(2)}_{32}\cdots\,, \\
K_{33} &\sim (r-r_H)K^H_{33} + (r-r_H)^3\widehat{K}^{(1)}_{33} + (r-r_H)^5\widehat{K}^{(2)}_{33} + \cdots\,, \\
K_{44} &\sim (r-r_H)K^H_{44} + (r-r_H)^3\widehat{K}^{(1)}_{44} + (r-r_H)^5\widehat{K}^{(2)}_{44} + \cdots\,, \\
K_{55} &\sim (r-r_H)^3K^H_{55} + (r-r_H)^5\widehat{K}^{(2)}_{55} + \cdots\,,
\end{aligned}$$

with

$$\widehat{K}^{(1)}_{11} = -A^{(1)}_H K^H_{11}\,, \qquad \widehat{K}^{(1,1)}_{12} = -2A^{(1)}_H\widehat{K}^{(0,1)}_{12}\,,$$
$$\widehat{K}^{(1)}_{12} = \frac{5}{2}K^H_{11}e^{-\frac{3}{2}A^{(0)}_H}A^{(1)}_H\,, \qquad \widehat{K}^{(0,1)}_{12} = e^{-\frac{3}{2}A^{(0)}_H}K^H_{11}\,,$$
$$\widehat{K}^{(1)}_{22} = -2A^{(1)}_H K^H_{22}\,, \qquad \widehat{K}^{(1)}_{32} = -2A^{(1)}_H K^H_{32}\,,$$
$$\widehat{K}^{(0,1)}_{32} = \frac{1}{2}K^H_{33}V'(\phi_H)e^{-\frac{3}{2}A^{(0)}_H}\,, \qquad \widehat{K}^{(1)}_{33,44} = -A^{(1)}_H K^H_{33,44}\,,$$
$$\widehat{K}^{(1,1)}_{32} = \frac{K^H_{32}}{48}V'(\phi_H)\,e^{-\frac{3A^{(1)}_H}{2}}\left(V''(\phi_H) - 60A^{(2)}_H\right), \qquad \widehat{K}^{(2)}_{55} = -3A^{(1)}_H K^H_{55}\,,$$

$$\begin{aligned}
\frac{\widehat{K}^{(2)}_{22}}{K^H_{22}} &= \frac{\widehat{K}^{(2,1)}_{12}}{K^H_{12}} = \frac{\widehat{K}^{(2)}_{32}}{K^H_{32}} = \frac{1}{160}\left[544A_H^{(1)2} + 3V'(\phi_H)^2\right], \\
\frac{\widehat{K}^{(2)}_{ii}}{K^H_{ii}} &= \frac{3}{320}\left[128A_H^{(2)2} + V'(\phi_H)^2\right], \quad i = 1,3,4\,.
\end{aligned} \tag{C.13}$$

JHEP01(2016)013

up to $\mathcal{O}(r-r_H)^7$. On the other hand, near the boundary,

$$K^B_{ij} = \delta_{ij} + \sum_{n,m} \widetilde{K}^{(n,m)}_{ij} e^{-(3n+\Delta m)r}\,, \quad K^B_{12,32} = e^{-\frac{3r}{2}} \sum_{n,m} \widetilde{K}^{(n,m)}_{12,32} e^{-(3n+\Delta m)r}\,. \tag{C.14}$$

The on-shell series expansions read

$$\begin{aligned}
K^B_{11} &= 1 + e^{-3r}\widetilde{K}^{(1,0)}_{11} + e^{-(9r-2\Delta)r}\widetilde{K}^{(3,-2)}_{11} + e^{-6r}\widetilde{K}^{(2,0)}_{11} + e^{-(3r-2\Delta)r}\widetilde{K}^{(1,2)}_{11} + \cdots\,,\\
K^B_{12} &= e^{-\frac{3r}{2}}\left[\widetilde{K}^{(0,0)}_{12} + e^{-2(3-\Delta)r}\widetilde{K}^{(2,-2)}_{12} + e^{-3r}\widetilde{K}^{(1,0)}_{12} + e^{-2\Delta r}\widetilde{K}^{(0,2)}_{12} + \cdots\right]\,,\\
K^B_{22} &= 1 + e^{-3r}\widetilde{K}^{(1,0)}_{22} + \cdots\,,\\
K^B_{32} &= e^{-\frac{3r}{2}}\left[e^{-(3-\Delta)r}\widetilde{K}^{(1,-1)}_{32} + e^{-\Delta r}\widetilde{K}^{(0,1)}_{32} + \cdots\right]\,,\\
K^B_{ii} &= 1 + e^{-3r}\widetilde{K}^{(1,0)}_{ii} + \cdots\,, \quad i=3,4,5
\end{aligned}$$

with

$$\begin{aligned}
&\widetilde{K}^{(1,0)}_{11} = B_0\,, && \widetilde{K}^{(3,-2)}_{11} = \frac{9B_0\lambda^2}{8(9-2\Delta)}\,, && \widetilde{K}^{(2,0)}_{11} = \frac{1}{6}B_0\left[3B_0 - (\Delta-3)\Delta\lambda v\right]\,,\\
&\widetilde{K}^{(1,2)}_{11} = \frac{9B_0v^2}{8(2\Delta+3)}\,, && \widetilde{K}^{(0,0)}_{11} = -\frac{2}{3}\,, && \widetilde{K}^{(2,-2)}_{12} = -\frac{\lambda^2}{8}\,,\\
&\widetilde{K}^{(1,0)}_{12} = \frac{1}{9}\left[(\Delta-3)\Delta\lambda v - 19B_0\right]\,, && \widetilde{K}^{(0,2)}_{12} = -\frac{v^2}{8}\,, && \widetilde{K}^{(1,0)}_{22} = 2B_0\,,\\
&\widetilde{K}^{(1,-1)}_{32} = \frac{2(\Delta-3)\lambda}{2\Delta-9}\,, && \widetilde{K}^{(0,1)}_{32} = \frac{2\Delta v}{2\Delta+3}\,, && \widetilde{K}^{(1,0)}_{33} = \widetilde{K}^{(1,0)}_{44} = \frac{\widetilde{K}^{(1,0)}_{55}}{3} = B_0\,,
\end{aligned} \tag{C.15}$$

plus higher order terms.

C.4 Fluctuations at the boundary

The near boundary series expansion of the fluctuations is proposed analogously as for the background functions. However, in this case, in order to capture all possible contributions from backreaction and gravity, we will assume a more complex series expansion than the one considered for a CFT. This time,

$$y_{1,4,5}(r) = e^{\frac{3r}{2}} \sum_{n,m>0} \left(\sum_{l=1}^{4} y^{(n,m,-l)}_{1,4,5} e^{-l(3-\Delta)r} + \sum_{l=0}^{4} y^{(n,m,l)}_{1,4,5} e^{-l\Delta r}\right) e^{-\left(2n+\frac{3}{2}m\right)r}\,, \tag{C.16}$$

$$y_2(r) = e^{3r} \sum_{n,m>0} \left(y^{(n,m,-3)}_2 e^{-3(2-\Delta)r} + \sum_{l=1,2,4} y^{(n,m,-l)}_2 e^{-l(3-\Delta)r} + \sum_{l=0}^{4} y^{(n,m,l)}_2 e^{-l\Delta r}\right) e^{-\left(2n+\frac{3}{2}m\right)r}, \tag{C.17}$$

$$y_3(r) = e^{-\frac{3r}{2}} \sum_{n,m>0} \left(y^{(n,m,0)}_3 + e^{3r}\sum_{l=1}^{4} y^{(n,m,-l)}_3 e^{-l(3-\Delta)r} + y^{(n,m,l)}_3 e^{-l\Delta r}\right) e^{-\left(2n+\frac{3}{2}m\right)r}, \tag{C.18}$$

where the exponential pre-factors are due to the changes of variables (3.9). The non-normalizable modes are identified as $\{y^{(0,0,-1)}_3, y^{(0,0,0)}_{1,2,4,5}\}$, whereas the normalizable as $\{y^{(0,2,0)}_{1,4,5},\, y^{(0,4,0)}_2, y^{(0,0,1)}_3\}$. Up to the non-normalizable mode for each fluctuation,

$$\begin{aligned}
y_1 &= e^{\frac{3}{2}r}\left\{y^{(0)}_1 + y^{(1)}_1 e^{-2(3-\Delta)r} + y^{(2)}_1 e^{-2r} + y^{(3)}_1 e^{-3r} + \cdots\right\}\,,\\
y_2 &= e^{3r}\left\{y^{(0)}_2 + y^{(2)}_2 e^{-2r} + y^{(\Delta)}_2 e^{-2(3-\Delta)r} + y^{(3)}_2 e^{-3r} + y^{(2\Delta)}_2 e^{-2(4-\Delta)r} + y^{(3\Delta)}_2 e^{-2(1+\Delta)r} +\right.
\end{aligned}$$

JHEP01(2016)013

$$+y_2^{(5)}e^{-5r}+y_2^{(4\Delta)}e^{-4(3-\Delta)r}+y_2^{(5\Delta)}e^{-(9-2\Delta)r}+y_2^{(6)}e^{-6r}+\cdots\Big\}, \tag{C.19}$$

$$y_3=e^{-\frac{3}{2}r}\Big\{y_3^{(3-\Delta)}e^{\Delta r}+y_3^{(\Delta)}e^{-(\Delta-3)r}+\cdots\Big\},$$

$$y_{4,5}=e^{\frac{3}{2}r}\Big\{y_{4,5}^{(0)}+y_{4,5}^{(1)}e^{-2r}+y_{4,5}^{(2)}e^{-2(3-\Delta)r}+y_{4,5}^{(3)}e^{-3r}+\cdots\Big\},$$

where we have replaced the (n,m,l) numeration by other suited to the one employed along the work

$$\begin{aligned}
y_1^{(1)} &= -\frac{\lambda}{16}\left(3\lambda y_1^{(0)}+4y_3^{(3-\Delta)}\right),\\
y_1^{(2)} &= -\frac{1}{16}\left[4k\omega y_5^{(0)}+k^2\left(5y_1^{(0)}-6y_4^{(0)}+y_2^{(0)}\right)+2\omega^2\left(y_1^{(0)}+y_2^{(0)}\right)\right],\\
y_2^{(2)} &= \frac{1}{16}\left[4k\omega y_5^{(0)}+k^2\left(y_1^{(0)}+2y_4^{(0)}-3y_2^{(0)}\right)+2\omega^2\left(y_1^{(0)}+y_2^{(0)}\right)\right],\\
y_2^{(\Delta)} &= -\frac{3\lambda}{8}\left(2y_3^{(3-\Delta)}+\lambda y_2^{(0)}\right),\\
y_2^{(3)} &= \frac{1}{3}\Big\{(\Delta-3)\Delta\left[v\left(y_3^{(3-\Delta)}+\lambda y_2^{(0)}\right)+\lambda y_3^{(\Delta)}\right]-3B_0y_2^{(0)}\Big\},\\
y_2^{(2\Delta)} &= \frac{(10-3\Delta)\lambda}{128(\Delta-4)(2\Delta-5)}\Big\{4\lambda k\omega y_5^{(0)}+k^2\left[\lambda\left(y_1^{(0)}+2y_4^{(0)}-3y_2^{(0)}\right)-16y_3^{(3-\Delta)}\right]+\\
&\quad+2\omega^2\left[\lambda\left(y_1^{(0)}+y_2^{(0)}\right)+8y_3^{(3-\Delta)}\right]\Big\},\\
y_2^{(5)} &= \frac{-1}{720\mathcal{G}_1}\Bigg\{-3B_0\mathcal{G}_1\Big[k^2\left(13y_1^{(0)}-3y_2^{(0)}+26y_4^{(0)}\right)+52k\omega y_5^{(0)}-2\omega^2\left(35y_1^{(0)}+47y_2^{(0)}\right)\Big]+\\
&\quad+2\Big\{k^2\Big[(\Delta-3)\Delta\Big(3(16(\Delta-3)\Delta+47)\lambda v y_2^{(0)}+2\mathcal{G}_2\lambda v y_4^{(0)}+72(\Delta-1)(2\Delta-1)v y_3^{(3-\Delta)}+\\
&\quad+72(\Delta-2)(2\Delta-5)\lambda y_3^{(\Delta)}\Big)-36\mathcal{G}_1y_1^{(3)}-72\mathcal{G}_1y_4^{(3)}\Big]+4k\omega\Big[(\Delta-3)\Delta(\mathcal{G}_2)\lambda v y_5^{(0)}-36\mathcal{G}_1y_5^{(3)}\Big]+\\
&\quad+2\omega^2\Big[(\Delta-3)\Delta\Big(-6\left(8\Delta^2-6\Delta+1\right)v y_3^{(3-\Delta)}+(-16(\Delta-3)\Delta-47)\lambda v y_2^{(0)}\\
&\quad-6\left(8\Delta^2-42\Delta+55\right)\lambda y_3^{(\Delta)}\Big)-36\mathcal{G}_1y_1^{(3)}\Big]\Big\}+2(\Delta-3)\Delta\mathcal{G}_2\lambda v y_1^{(0)}\left(k^2+2\omega^2\right)\Bigg\},\\
\mathcal{G}_1 &= 4(\Delta-3)\Delta+5,\ \mathcal{G}_2=8(\Delta-3)\Delta-17,\\
y_2^{(3\Delta)} &= \frac{(3\Delta+1)v}{128\left(2\Delta^2+\Delta-1\right)}\Big\{k^2\left[v\left(y_1^{(0)}-3y_2^{(0)}+2y_4^{(0)}\right)-16y_3^{(\Delta)}\right]+4kv\omega y_5^{(0)}+\\
&\quad+2\omega^2\left[v\left(y_1^{(0)}+y_2^{(0)}\right)+8y_3^{(\Delta)}\right]\Big\},\\
y_2^{(4\Delta)} &= -\frac{3\lambda}{4(2\Delta-9)(4\Delta-9)}\Big\{B_0(9-4\Delta)\left[(2\Delta-9)y_3^{(3-\Delta)}+(\Delta-3)\lambda y_2^{(0)}\right]+\\
&\quad+\Delta(\Delta-3)^2\lambda\left(3vy_3^{(3-\Delta)}+\lambda vy_2^{(0)}+\lambda y_3^{(\Delta)}\right)\Big\},
\end{aligned}$$

$$\begin{aligned}
y_2^{(5\Delta)} &= \frac{9\Delta\lambda^3(4y_3^{(3-\Delta)}+\lambda y_2^{(0)})}{128(4\Delta-9)}, & y_4^{(1)} &= \frac{1}{4}\left[k^2\left(y_1^{(0)}-y_2^{(0)}\right)+2k\omega y_5^{(0)}+2\omega^2y_4^{(0)}\right],\\
y_{4,5}^{(2)} &= -\frac{3}{16}\lambda^2y_{4,5}^{(0)}, & y_5^{(1)} &= \frac{1}{4}k\omega\left(y_1^{(0)}+y_2^{(0)}-2y_4^{(0)}\right).
\end{aligned} \tag{C.20}$$

For the auxiliary fields $\{\eta_i\}$, we write

$$\begin{aligned}
\eta_{1,4,5} &= e^{\frac{5}{2}r}\sum_{n>0}\left(\sum_{l=0}^{4}e^{-l\Delta r}\eta_{1,4,5}^{(n,l)}+\sum_{l=1}^{4}e^{-l(3-\Delta)r}\eta_{1,4,5}^{(n,-l)}\right)e^{-\frac{n}{2}r},\\
\eta_2 &= e^{3r}\sum_{n>0}\left(\eta_2^{(n,-3)}e^{-3(2-\Delta)r}+\sum_{l=1,2,4}\eta_2^{(n,-l)}e^{-l(3-\Delta)r}+\sum_{l=0}^{4}e^{-l\Delta r}\eta_2^{(n,l)}\right)e^{-\frac{n}{2}r},
\end{aligned}$$

JHEP01(2016)013

$$\eta_3 = e^{\frac{3}{2}r}\sum_{n>0}\left(\eta_3^{(n,0)} + \sum_{l=1}^{4}\eta_3^{(n,-l)}e^{\Delta r}e^{-l(3r-\Delta r)} + \eta_3^{(n,m,l)}e^{-(l\Delta-3)r}\right)e^{-\frac{n}{2}r}\,, \tag{C.21}$$

with (after imposing the boundary conditions (3.35))

$$\begin{aligned}
\eta_1 &= e^{\frac{5}{2}r}\Big\{\eta_1^{(0,0)} + y_1^{(0)}e^{-r} + \eta_1^{(4,0)}e^{-2r} + \eta_1^{(0,-2)}e^{-2(3-\Delta)r} + \eta_1^{(6,0)}e^{-3r} + \eta_1^{(0,2)}e^{-2\Delta r} + \\
&\quad + \eta_1^{(2,-2)}e^{-(7-2\Delta)r} + y_1^{(3)}e^{-4r} + \cdots\Big\}\,, \\
\eta_2 &= e^{3r}\Big\{y_2^{(0)} + \eta_2^{(4,0)}e^{-2r} + \eta_2^{(0,-2)}e^{-2(3-\Delta)r} + \eta_2^{(6,0)}e^{-3r} + \eta_2^{(0,2)}e^{-2\Delta r} + \eta_2^{(8,0)}e^{-4r} + \\
&\quad + \eta_2^{(4,-2)}e^{-2(4-\Delta)r} + \eta_2^{(10,0)}e^{-5r} + \eta_2^{(4,2)}e^{-2(1+\Delta)r} + \eta_2^{(0,-4)}e^{-4(3-\Delta)r} + \\
&\quad + \eta_2^{(6,-2)}e^{-(9-2\Delta)r} + y_2^{(6)}e^{-6r} + \cdots\Big\}\,, \\
\eta_3 &= e^{\frac{3}{2}r}\Big\{y_3^{(3-\Delta)}e^{-(3-\Delta)r} + y_3^{(\Delta)}e^{-\Delta r} + \eta_2^{(0)}\frac{\Delta-3}{2}\lambda e^{\Delta r} + \cdots\Big\}, \\
\eta_{4,5} &= e^{\frac{5}{2}r}\Big\{\eta_{4,5}^{(0)} + y_{4,5}^{(0)}e^{-r} + \eta_{4,5}^{(4,0)}e^{-2r} + \eta_{4,5}^{(0,-2)}e^{-2(3-\Delta)r} + \eta_{4,5}^{(6,0)}e^{-3r} + \eta_{4,5}^{(0,2)}e^{-2\Delta r} + \\
&\quad + \eta_{4,5}^{(2,-2)}e^{-(7-2\Delta)r} + y_{4,5}^{(3)}e^{-4r} + \cdots\Big\}\,,
\end{aligned} \tag{C.22}$$

$$\eta_1^{(4,0)} = -\frac{1}{16}y_2^{(0)}\left(k^4 + k^2\omega^2 - 2\omega^4\right), \qquad \eta_1^{(0)} = -\frac{y_2^{(0)}}{8}\left(k^2 + 2\omega^2\right),$$

$$\eta_1^{(0,-2)} = \frac{(6\Delta-13)\lambda^2 y_2^{(0)}\left(k^2+2\omega^2\right)}{128(2\Delta-5)}, \qquad \eta_1^{(0,2)} = \frac{(6\Delta-5)v^2 y_2^{(0)}\left(k^2+2\omega^2\right)}{128(2\Delta-1)},$$

$$\eta_1^{(2,-2)} = -\frac{3}{16}\lambda^2 y_1^{(0)}, \qquad \eta_2^{(4,0)} = \frac{1}{24}y_2^{(0)}\left(2w^2 - 5k^2\right),$$

$$\eta_2^{(0,-2)} = \frac{\left(4\Delta^2-24\Delta+45\right)}{8(2\Delta-9)}\lambda^2 y_2^{(0)}, \qquad \eta_2^{(8,0)} = \frac{1}{48}y_2^{(0)}\left(k^4 - 5k^2\omega^2 + 4\omega^4\right),$$

$$\eta_2^{(0,2)} = -\frac{\left(4\Delta^2+9\right)}{8(2\Delta+3)}v^2 y_2^{(0)}, \qquad \eta_2^{(0,-4)} = \frac{3888 - \Delta\left\{4\Delta\left[\Delta(20\Delta-141)+207\right]+1701\right\}}{128(2\Delta-9)(2\Delta-7)(4\Delta-9)}\lambda^4 y_2^{(0)},$$

$$\eta_4^{(0,2)} = \frac{(6\Delta-5)}{64(2\Delta-1)}k^2v^2y_2^{(0)}, \qquad \eta_5^{(0,2)} = \frac{(6\Delta-5)}{32(2\Delta-1)}k\omega v^2 y_2^{(0)},$$

$$\eta_4^{(4,0)} = \frac{1}{8}k^2y_2^{(0)}\left(\omega^2-k^2\right), \qquad \eta_4^{(0,-2)} = \frac{(6\Delta-13)}{64(2\Delta-5)}k^2\lambda^2y_2^{(0)},$$

$$\eta_4^{(0)} = -\frac{1}{4}k^2y_2^{(0)}, \qquad \eta_4^{(2,-2)} = -\frac{3}{16}\lambda^2y_4^{(0)}, \qquad \eta_5^{(0)} = -\frac{1}{2}k\omega y_2^{(0)},$$

$$\eta_5^{(4,0)} = \frac{1}{4}k\omega y_2^{(0)}\left(\omega^2-k^2\right), \qquad \eta_5^{(0,-2)} = \frac{(6\Delta-13)}{32(2\Delta-5)}k\omega\lambda^2y_2^{(0)}, \qquad \eta_5^{(2,-2)} = -\frac{3}{16}\lambda^2y_5^{(0)},$$

$$\begin{aligned}
\eta_1^{(6,0)} &= \frac{1}{144}\Big\{\eta_2^{(0)}\left[B_0\left(33k^2-78\omega^2\right) - 2(\Delta-3)\Delta\lambda v\left(k^2+2\omega^2\right)\right] + \\
&\quad + 12\left[k^2(3y_4^{(0)} - 4y_1^{(0)} + 3k\omega y_5^{(0)} - 2\omega^2 y_2^{(0)}\right]\Big\}, \\
\eta_2^{(4,-2)} &= \frac{\lambda^2 y_2^{(0)}}{192\left(4\Delta^3-44\Delta^2+157\Delta-180\right)}\Big[2\left(48\Delta^4-600\Delta^3+2830\Delta^2-5959\Delta+4716\right)\omega^2 + \\
&\quad + \left(-96\Delta^4+1200\Delta^3-5654\Delta^2+11867\Delta-9324\right)k^2\Big], \\
\eta_2^{(6,0)} &= \frac{3y_2^{(0)}\left(B_0(27-4(\Delta-3)\Delta) - 12(\Delta-3)\Delta\lambda v\right)}{3(2\Delta-9)(2\Delta+3)} + \frac{y_1^{(0)}}{3}, \\
\eta_2^{(10,0)} &= \frac{1}{2160(2\Delta-9)(2\Delta+3)}\Big\{k^2\big[y_2^{(0)}\big[102B_0\left(4\Delta^2-12\Delta-27\right) +
\end{aligned}$$

JHEP01(2016)013

$$
\begin{aligned}
&+\Delta\left(532\Delta^3-3192\Delta^2+14157\Delta-28107\right)\lambda v\big]-336\left(4\Delta^2-12\Delta-27\right)y_1^{(0)}+\\
&+36\left(4\Delta^2-12\Delta-27\right)y_4^{(0)}\big]+2\omega^2\big\{y_2^{(0)}\big[\Delta\left(-236\Delta^3+1416\Delta^2-7011\Delta+14661\right)\lambda v\\
&-798B_0\left(4\Delta^2-12\Delta-27\right)\big]-156\left(4\Delta^2-12\Delta-27\right)y_1^{(0)}\big\}+468\left(4\Delta^2-12\Delta-27\right)k\omega y_5^{(0)}\Big\}\,,\\
\eta_2^{(4,2)} &= \frac{v^2y_2^{(0)}}{192\left(4\Delta^3+8\Delta^2+\Delta-3\right)}\Big[\left(96\Delta^4+48\Delta^3+38\Delta^2-25\Delta-15\right)k^2\\
&-2\left(48\Delta^4+24\Delta^3+22\Delta^2-5\Delta-3\right)\omega^2\Big]\,,\\
\eta_2^{(6,-2)} &= \frac{1}{96(2\Delta-15)(2\Delta-9)(2\Delta-7)(2\Delta+3)(4\Delta-9)}\Big\{(\Delta-3)\lambda\\
&\times\big[-\lambda y_2^{(0)}\big(24B_0(\Delta-3)(2\Delta-7)(2\Delta-3)(2\Delta+3)(4\Delta-9)+\\
&+\Delta\{8\Delta[2\Delta(\Delta\{\Delta[4\Delta(8\Delta-133)+3669]-11889\}+13500)+25839]-485757\}\lambda v\big)\\
&-96(2\Delta-15)(2\Delta-7)(2\Delta+3)(4\Delta-9)y_3^{(3-\Delta)}\big]\Big\}\,,\\
\eta_4^{(6,0)} &= \frac{1}{72}\left(k^2\big\{y_2^{(0)}\left[33B_0-2(\Delta-3)\Delta\lambda v\right]+24y_1^{(0)}\big\}-36k\omega y_5^{(0)}+36\omega^2y_4^{(0)}\right)\,,\\
\eta_5^{(6,0)} &= -\frac{1}{36}k\omega\Big\{y_2^{(0)}\left[2(\Delta-3)\Delta\lambda v-15B_0\right]+12y_1^{(0)}-18y_4^{(0)}\Big\}\,.
\end{aligned}
\tag{C.23}
$$

C.5 Fluctuations at the horizon

From the indicial polynomials of the dynamical equations for each fluctuation, we infer 3 roots,

$$
P_0=0\,,\quad P_\pm=\pm i\omega c_H\,,\quad c_H=e^{-(A_H+B_H)}\,. \tag{C.24}
$$

We demand regularity if the roots are real and ingoing condition if they are complex. Therefore, near the horizon, the original fluctuations may admit the general series expansion

$$
y_i=\sum_{n=0}y_i^{(0,n)}(r-r_H)^{2n}+(r-r_H)^{P_-}\sum_{n=0}y_i^{(1,n)}(r-r_H)^{2n}\,, \tag{C.25}
$$

with $i=1\,,\cdots,5$ and we have ruled out the P_+ root. As stated in section 3.1.2, the choice of the boundary conditions (3.35) fixes the series expansions of the auxiliary fields, regardless if the $\{y_i\}$ fields have a well defined near-horizon behavior. Therefore, we shall consider

$$
\begin{aligned}
\eta_i=\sum_n\Big[&\eta_i^{(0,n)}\left(r-r_H\right)^{n-2}+(r-r_H)^{P_-}\eta_i^{(1,n)}(r-r_H)^n+\\
&+(r-r_H)^{P_+}\eta_i^{(2,n)}(r-r_H)^n+\eta_i^{(2,n)}\log\left(r-r_H\right)\Big]\,.
\end{aligned}
\tag{C.26}
$$

The on-shell series expansions read

$$
\begin{aligned}
y_i&=y_i^{(0,0)}+y_i^{(0,1)}\left(r-r_H\right)^2+\left(r-r_H\right)^{P_-}\left[y_i^{(1,0)}+y_i^{(1,1)}\left(r-r_H\right)^2\right]+\cdots\,,\quad i\neq3,4\\
y_3&=\left(r-r_H\right)^{P_-}\left[y_3^{(1,0)}+y_3^{(1,1)}\left(r-r_H\right)^2\right]+\cdots\,,\\
y_4&=y_4^{(0,1)}\left(r-r_H\right)^2+\left(r-r_H\right)^{P_-}\left[y_i^{(1,0)}+y_i^{(1,1)}\left(r-r_H\right)^2\right]+\cdots\,,
\end{aligned}
\tag{C.27}
$$

$$
\eta_1=\eta_1^{(0,2)}+\eta_1^{(1,0)}(r-r_H)^{P_-}+\eta_1^{(2,0)}(r-r_H)^{P_+}+\eta_1^{(0,3)}(r-r_H)+\cdots\,,
$$

JHEP01(2016)013

$$
\begin{aligned}
\eta_2 &= \frac{\eta_2^{(0,1)}}{r-r_H} + \eta_2^{(0,2)} + \eta_2^{(1,0)}(r-r_H)^{P_-} + \eta_2^{(2,0)}(r-r_H)^{P_+} + \\
&\quad +(r-r_H)\left[\eta_2^{(0,3)} + \eta_2^{(1,2)}(r-r_H)^{P_-} + \eta_2^{(2,2)}(r-r_H)^{P_+}\right] + \cdots , \\
\eta_3 &= \eta_3^{(1,0)}(r-r_H)^{P_-} + \eta_3^{(2,0)}(r-r_H)^{P_+} + \cdots , \\
\eta_4 &= \eta_4^{(0,2)} + \eta_4^{(1,0)}(r-r_H)^{P_-} + \eta_4^{(2,0)}(r-r_H)^{P_+} + \cdots , \\
\eta_5 &= \frac{\eta_5^{(0,0)}}{(r-r_H)^2} + \eta_5^{(0,2)} + \eta_5^{(1,0)}(r-r_H)^{P_-} + \eta_5^{(2,0)}(r-r_H)^{P_+} + \cdots ,
\end{aligned}
\tag{C.28}
$$

where most of the coefficients are not independent from each other. For the main fluctuations,

$$
\begin{aligned}
{y_1}^{(0,1)} &= \frac{1}{6\left(\frac{4}{c_H^2}+\omega^2\right)}\left\{{y_1}^{(0,0)}\left[9{A_H}^{(1)}\left(\frac{4}{c_H^2}+\omega^2\right) - 4k^2e^{2B_H}\right] - 4k\omega{y_5}^{(0,0)}e^{2B_H}\right\}, \\
{y_1}^{(1,0)} &= \frac{i}{\omega}{y_2}^{(1,0)}e^{B_H-\frac{A_H}{2}} , \\
{y_1}^{(1,1)} &= \frac{e^{B_H-\frac{3A_H}{2}}}{4\omega\left(\frac{1}{c_H}-i\omega\right)\left(\frac{2}{c_H}-i\omega\right)\left(\frac{3}{c_H}-i\omega\right)}\left\{{y_2}^{(1,0)}\left[2e^{A_H}A_H^{(1)}\left(\frac{12i\omega^2}{c_H}+\frac{21\omega}{c_H^2}+\frac{18i}{c_H^3}+11\omega^3\right)+\right.\right. \\
&\quad \left. +k^2e^{B_H}\left(\frac{1}{c_H}-3i\omega\right)\left(\omega+\frac{2i}{c_H}\right)\right] - 4\omega e^{\frac{3A_H}{2}+B_H}\left[k^2{y_4}^{(1,0)}\left(\frac{2}{c_H}-i\omega\right)+\right. \\
&\quad \left.\left. +{y_3}^{(1,0)}V'(\phi_H)e^{2A_H}\left(\frac{3}{c_H}-2i\omega\right)\right]\right\}, \\
{y_2}^{(0,0)} &= -{y_1}^{(0,0)}e^{\frac{3A_H}{2}} , \\
{y_2}^{(0,1)} &= -\frac{1}{3}e^{\frac{3A_H}{2}}\left[9{y_1}^{(0,0)}{A_H}^{(1)} + \frac{4ke^{2B_H}c_H\left(k{y_1}^{(0,0)}+\omega{y_5}^{(0,0)}\right)}{\omega^2c_H+4}\right] , \\
{y_2}^{(1,1)} &= \frac{e^{B_H-A_H}}{4\omega\left(\frac{2}{c_H}-i\omega\right)\left(\frac{3}{{c_H}^2}-\frac{4i\omega}{c_H}-\omega^2\right)}\left\{{y_2}^{(1,0)}\left[-\frac{100i\omega^2}{c_H}{A_H}^{(1)}e^{2A_H}+\frac{72\omega}{c_H^2}A_H^{(1)}e^{2A_H}\right.\right. \\
&\quad \left. -36\omega^3e^{2A_H}A_H^{(1)} - \frac{2ik^2}{c_H^3}+\frac{2k^2\omega}{{c_H}^2}-\frac{3ik^2\omega^2}{c_H}-k^2\omega^3\right] \\
&\quad \left. -\frac{4k^2\omega}{c_H^2}{y_4}^{(1,0)}e^{\frac{A_H}{2}} - 4\omega{y_3}^{(1,0)}V'(\phi_H)e^{\frac{7A_H}{2}}\left(\frac{3}{{c_H}^2}-\frac{3i\omega}{c_H}-\omega^2\right)\right\}, \\
{y_3}^{(1,1)} &= \frac{1}{8\left(\frac{1}{c_H}-i\omega\right)}\left[2{y_3}^{(1,0)}\left(k^2e^{B_H-A_H}+\frac{6{A_H}^{(1)}}{c_H}-2i\omega{A_H}^{(1)}+\frac{V''(\phi_H)}{c_H}\right)+\right. \\
&\quad \left. +i\omega{y_2}^{(1,0)}V'(\phi_H)e^{-\frac{3A_H}{2}}\right], \\
y_4^{(0,1)} &= -\frac{ke^{2B_H}\left(k{y_1}^{(0,0)}+\omega{y_5}^{(0,0)}\right)}{\frac{4}{c_H^2}+\omega^2} , \\
{y_4}^{(1,1)} &= \frac{1}{\frac{8\omega}{c_H}-8i\omega^2}\left[{y_2}^{(1,0)}k^2e^{B_H-\frac{3A_H}{2}}\left(-\omega e^{-A_H}+ie^{B_H}\right)+2k\omega^2{y_5}^{(1,0)}e^{B_H-A_H}+\right. \\
&\quad \left. +{y_4}^{(1,0)}\left(\frac{12\omega{A_H}^{(1)}}{c_H}-4i\omega^2{A_H}^{(1)}\right)\right], \\
y_5^{(0,1)} &= \frac{3}{2}{y_5}^{(0,0)}{A_H}^{(1)} , \\
{y_5}^{(1,0)} &= \frac{k}{2\omega\left(\omega+\frac{2i}{c_H}\right)}\left[{y_2}^{(1,0)}e^{-\frac{A_H}{2}}\left(\omega e^{-A_H}+ie^{B_H}\right)-2\omega{y_4}^{(1,0)}\right] ,
\end{aligned}
\tag{C.29}
$$

JHEP01(2016)013

whilst for the auxiliary fluctuations,

$$
\begin{aligned}
\eta_1^{(0,2)} &= -\frac{k\tilde{\eta}_5^H K_{55}^{\rm H} + 2\omega e^{\frac{3A_H}{2}}\tilde{\eta}_2^H K_{22}^{\rm H}}{2\omega K_{11}^{\rm H}}\,,\\
\eta_1^{(0,3)} &= \frac{\omega e^{\frac{3A_H}{2}}}{2\left(\frac{1}{c_H^2}+\omega^2\right)(K_{11}^{\rm H})^2}\left[k\tilde{\eta}_5^H K_{12}^{\rm H}K_{55}^{\rm H} + 2\omega K_{22}^{\rm H}\left(e^{\frac{3A_H}{2}}\tilde{\eta}_2^H K_{12}^{\rm H} - \eta_2^H K_{11}^{\rm H}\right)\right]\,,\\
\eta_2^{(1,0)} &= -\frac{\eta_1^H K_{12}^{\rm H} + \eta_3^H K_{32}^{\rm H}}{K_{22}^{\rm H}}\,,\\
\eta_2^{(2,0)} &= -\frac{\tilde{\eta}_1^H K_{12}^{\rm H} + \tilde{\eta}_3^H K_{32}^{\rm H}}{K_{22}^{\rm H}}\,,\\
\eta_2^{(0,3)} &= \frac{e^{-\frac{3A_H}{2}}}{2\omega K_{22}^{\rm H}}\Bigg\{A_H{}^{(1)}\left(8\omega e^{\frac{3A_H}{2}}\tilde{\eta}_2^H K_{22}^{\rm H} - 3k\tilde{\eta}_5^H K_{55}^{\rm H}\right)\\
&\quad - \frac{\omega^2 e^{3A_H}K_{12}^{\rm H}\left[K_{12}^{\rm H}\left(k\tilde{\eta}_5^H K_{55}^{\rm H} + 2\omega e^{\frac{3A_H}{2}}\tilde{\eta}_2^H K_{22}^{\rm H}\right) - 2\omega\eta_2^H K_{11}{}^{\rm H}K_{22}^{\rm H}\right]}{(K_{11}^{\rm H})^2\left(\frac{1}{c_H^2}+\omega^2\right)}\Bigg\}\,,\\
\eta_2^{(1,2)} &= \frac{e^{-\frac{3A_H}{2}}}{2K_{22}^H\left(-\frac{3i\omega}{c_H}+\frac{2}{c_H^2}-\omega^2\right)}\Big\{2\eta_1^H K_{11}^H\Big[2k^2e^{2B_H} + A_H{}^{(1)}\left(\frac{7i\omega}{c_H}+\frac{6}{c_H^2}+5\omega^2\right)\Big] +\\
&\quad +\eta_3^H\omega K_{33}^H V'(\phi_H)\left(\omega+\frac{2i}{c_H}\right) + 2k^2\eta_4^H K_{44}^H e^{2B_H}\Big\},\\
\eta_2^{(2,2)} &= \frac{e^{-\frac{3A_H}{2}}}{2K_{22}^{\rm H}\left(3i\frac{\omega}{c_H}+\frac{2}{c_H^2}-\omega^2\right)}\Bigg\{2\tilde{\eta}_1^H K_{11}^{\rm H}\left[2k^2e^{2B_H} + A_H{}^{(1)}\left(-7i\frac{\omega}{c_H}+\frac{6}{c_H^2}+5\omega^2\right)\right] +\\
&\quad +\omega\tilde{\eta}_3^H K_{33}^{\rm H}V'(\phi_H)\left(\omega - 2ie^{A_H+B_H}\right) + 2k^2e^{2B_H}\tilde{\eta}_4^H K_{44}^{\rm H}\Bigg\}\,,\\
\eta_4^{(0,2)} &= \frac{k\tilde{\eta}_5^H K_{55}^{\rm H}}{\omega K_{44}^{\rm H}}\,,\\
\eta_5^{(1,0)} &= -\frac{ike^{2B_H}\left(2\eta_1^H K_{11}^{\rm H} + \eta_4^H K_{44}^{\rm H}\right)}{K_{55}^{\rm H}\left(\frac{2}{c_H}-i\omega\right)}\,,\\
\eta_5^{(2,0)} &= \frac{ike^{2B_H}\left(2\tilde{\eta}_1^H K_{11}^{\rm H} + \tilde{\eta}_4^H K_{44}^{\rm H}\right)}{\left(\frac{2}{c_H}+i\omega\right)K_{55}^{\rm H}}\,,
\end{aligned}
\tag{C.30}
$$

plus higher order terms. $\eta_{1,3,4}^{(1,0)} = \eta_{1,3,4}^H$, $\eta_{1,3,4}^{(2,0)} = \tilde{\eta}_{1,3,4}^H$, $\eta_2^{(0,2)} = \eta_2^H$, $\eta_2^{(0,1)} = \tilde{\eta}_2^H$, $\eta_5^{(0,2)} = \eta_5^H$ and $\eta_5^{(0,0)} = \tilde{\eta_5}^H$, as it appears in section 3.1.2.

References

[1] J.M. Maldacena, *The large-N limit of superconformal field theories and supergravity*, *Int. J. Theor. Phys.* **38** (1999) 1113 [hep-th/9711200] [INSPIRE].

[2] S.S. Gubser, I.R. Klebanov and A.M. Polyakov, *Gauge theory correlators from noncritical string theory*, *Phys. Lett.* **B 428** (1998) 105 [hep-th/9802109] [INSPIRE].

[3] E. Witten, *Anti-de Sitter space and holography*, *Adv. Theor. Math. Phys.* **2** (1998) 253 [hep-th/9802150] [INSPIRE].

JHEP01(2016)013

[4] G. Policastro, D.T. Son and A.O. Starinets, *The shear viscosity of strongly coupled $N = 4$ supersymmetric Yang-Mills plasma*, *Phys. Rev. Lett.* **87** (2001) 081601 [hep-th/0104066] [INSPIRE].

[5] S. Bhattacharyya, V.E. Hubeny, S. Minwalla and M. Rangamani, *Nonlinear fluid dynamics from gravity*, *JHEP* **02** (2008) 045 [arXiv:0712.2456] [INSPIRE].

[6] N. Banerjee, J. Bhattacharya, S. Bhattacharyya, S. Jain, S. Minwalla and T. Sharma, *Constraints on fluid dynamics from equilibrium partition functions*, *JHEP* **09** (2012) 046 [arXiv:1203.3544] [INSPIRE].

[7] K. Jensen, M. Kaminski, P. Kovtun, R. Meyer, A. Ritz and A. Yarom, *Towards hydrodynamics without an entropy current*, *Phys. Rev. Lett.* **109** (2012) 101601 [arXiv:1203.3556] [INSPIRE].

[8] C. Hoyos and D.T. Son, *Hall viscosity and electromagnetic response*, *Phys. Rev. Lett.* **108** (2012) 066805 [arXiv:1109.2651] [INSPIRE].

[9] X.G. Wen and A. Zee, *Shift and spin vector: new topological quantum numbers for the Hall fluids*, *Phys. Rev. Lett.* **69** (1992) 953 [*Erratum ibid.* **69** (1992) 3000] [INSPIRE].

[10] N. Read, *Non-Abelian adiabatic statistics and Hall viscosity in quantum Hall states and $p_x + ip_y$ paired superfluids*, *Phys. Rev.* **B 79** (2009) 045308 [arXiv:0805.2507] [INSPIRE].

[11] N. Read and E.H. Rezayi, *Hall viscosity, orbital spin and geometry: paired superfluids and quantum Hall systems*, *Phys. Rev.* **B 84** (2011) 085316 [arXiv:1008.0210] [INSPIRE].

[12] B. Bradlyn, M. Goldstein and N. Read, *Kubo formulas for viscosity: hall viscosity, Ward identities and the relation with conductivity*, *Phys. Rev.* **B 86** (2012) 245309 [arXiv:1207.7021] [INSPIRE].

[13] C. Hoyos, B.S. Kim and Y. Oz, *Ward identities for transport in $2 + 1$ dimensions*, *JHEP* **03** (2015) 164 [arXiv:1501.05756] [INSPIRE].

[14] S. de Haro, S.N. Solodukhin and K. Skenderis, *Holographic reconstruction of space-time and renormalization in the AdS/CFT correspondence*, *Commun. Math. Phys.* **217** (2001) 595 [hep-th/0002230] [INSPIRE].

[15] I. Papadimitriou and K. Skenderis, *Correlation functions in holographic RG flows*, *JHEP* **10** (2004) 075 [hep-th/0407071] [INSPIRE].

[16] S.A. Hartnoll and C.P. Herzog, *Ohm's law at strong coupling: S duality and the cyclotron resonance*, *Phys. Rev.* **D 76** (2007) 106012 [arXiv:0706.3228] [INSPIRE].

[17] C.P. Herzog, *Lectures on holographic superfluidity and superconductivity*, *J. Phys.* **A 42** (2009) 343001 [arXiv:0904.1975] [INSPIRE].

[18] J. Lindgren, I. Papadimitriou, A. Taliotis and J. Vanhoof, *Holographic Hall conductivities from dyonic backgrounds*, *JHEP* **07** (2015) 094 [arXiv:1505.04131] [INSPIRE].

[19] I. Kanitscheider, K. Skenderis and M. Taylor, *Precision holography for non-conformal branes*, *JHEP* **09** (2008) 094 [arXiv:0807.3324] [INSPIRE].

[20] I. Papadimitriou, *Holographic renormalization of general dilaton-axion gravity*, *JHEP* **08** (2011) 119 [arXiv:1106.4826] [INSPIRE].

[21] B. Gouteraux, J. Smolic, M. Smolic, K. Skenderis and M. Taylor, *Holography for Einstein-Maxwell-dilaton theories from generalized dimensional reduction*, *JHEP* **01** (2012) 089 [arXiv:1110.2320] [INSPIRE].

JHEP01(2016)013

[22] M.M. Caldarelli, J. Camps, B. Goutéraux and K. Skenderis, *AdS/Ricci-flat correspondence*, *JHEP* **04** (2014) 071 [arXiv:1312.7874] [INSPIRE].

[23] W. Chemissany and I. Papadimitriou, *Lifshitz holography: the whole shebang*, *JHEP* **01** (2015) 052 [arXiv:1408.0795] [INSPIRE].

[24] J. Hartong, E. Kiritsis and N.A. Obers, *Lifshitz space-times for Schrödinger holography*, *Phys. Lett.* **B 746** (2015) 318 [arXiv:1409.1519] [INSPIRE].

[25] D.T. Son and A.O. Starinets, *Minkowski space correlators in AdS/CFT correspondence: recipe and applications*, *JHEP* **09** (2002) 042 [hep-th/0205051] [INSPIRE].

[26] I. Amado, M. Kaminski and K. Landsteiner, *Hydrodynamics of holographic superconductors*, *JHEP* **05** (2009) 021 [arXiv:0903.2209] [INSPIRE].

[27] J. Lee and R.M. Wald, *Local symmetries and constraints*, *J. Math. Phys.* **31** (1990) 725 [INSPIRE].

[28] R.M. Wald and A. Zoupas, *A general definition of 'conserved quantities' in general relativity and other theories of gravity*, *Phys. Rev.* **D 61** (2000) 084027 [gr-qc/9911095] [INSPIRE].

[29] I. Papadimitriou and K. Skenderis, *Thermodynamics of asymptotically locally AdS spacetimes*, *JHEP* **08** (2005) 004 [hep-th/0505190] [INSPIRE].

[30] I. Papadimitriou, *Holographic renormalization as a canonical transformation*, *JHEP* **11** (2010) 014 [arXiv:1007.4592] [INSPIRE].

[31] S.A. Hartnoll and P. Kovtun, *Hall conductivity from dyonic black holes*, *Phys. Rev.* **D 76** (2007) 066001 [arXiv:0704.1160] [INSPIRE].

[32] S.A. Hartnoll, P.K. Kovtun, M. Muller and S. Sachdev, *Theory of the Nernst effect near quantum phase transitions in condensed matter and in dyonic black holes*, *Phys. Rev.* **B 76** (2007) 144502 [arXiv:0706.3215] [INSPIRE].

[33] K. Goldstein, N. Iizuka, S. Kachru, S. Prakash, S.P. Trivedi and A. Westphal, *Holography of dyonic dilaton black branes*, *JHEP* **10** (2010) 027 [arXiv:1007.2490] [INSPIRE].

[34] E. Gubankova, J. Brill, M. Cubrovic, K. Schalm, P. Schijven and J. Zaanen, *Holographic fermions in external magnetic fields*, *Phys. Rev.* **D 84** (2011) 106003 [arXiv:1011.4051] [INSPIRE].

[35] M. Lippert, R. Meyer and A. Taliotis, *A holographic model for the fractional quantum Hall effect*, *JHEP* **01** (2015) 023 [arXiv:1409.1369] [INSPIRE].

[36] M. Fujita, W. Li, S. Ryu and T. Takayanagi, *Fractional quantum Hall effect via holography: Chern-Simons, edge states and hierarchy*, *JHEP* **06** (2009) 066 [arXiv:0901.0924] [INSPIRE].

[37] O. Bergman, N. Jokela, G. Lifschytz and M. Lippert, *Quantum Hall effect in a holographic model*, *JHEP* **10** (2010) 063 [arXiv:1003.4965] [INSPIRE].

[38] N. Jokela, M. Jarvinen and M. Lippert, *A holographic quantum Hall model at integer filling*, *JHEP* **05** (2011) 101 [arXiv:1101.3329] [INSPIRE].

[39] C. Kristjansen and G.W. Semenoff, *Giant D5 brane holographic Hall state*, *JHEP* **06** (2013) 048 [arXiv:1212.5609] [INSPIRE].

[40] Y. Bea, N. Jokela, M. Lippert, A.V. Ramallo and D. Zoakos, *Flux and Hall states in ABJM with dynamical flavors*, *JHEP* **03** (2015) 009 [arXiv:1411.3335] [INSPIRE].

JHEP01(2016)013

[41] E. Keski-Vakkuri and P. Kraus, *Quantum Hall effect in AdS/CFT*, *JHEP* **09** (2008) 130 [arXiv:0805.4643] [INSPIRE].

[42] M. Fujita, M. Kaminski and A. Karch, SL$(2, Z)$ *action on AdS/BCFT and Hall conductivities*, *JHEP* **07** (2012) 150 [arXiv:1204.0012] [INSPIRE].

[43] O. Saremi and D.T. Son, *Hall viscosity from gauge/gravity duality*, *JHEP* **04** (2012) 091 [arXiv:1103.4851] [INSPIRE].

[44] D.T. Son and C. Wu, *Holographic spontaneous parity breaking and emergent Hall viscosity and angular momentum*, *JHEP* **07** (2014) 076 [arXiv:1311.4882] [INSPIRE].

[45] C. Hoyos, B.S. Kim and Y. Oz, *Odd parity transport in non-Abelian superfluids from symmetry locking*, *JHEP* **10** (2014) 127 [arXiv:1404.7507] [INSPIRE].

[46] S. Golkar and M.M. Roberts, *Viscosities and shift in a chiral superfluid: a holographic study*, arXiv:1502.07690 [INSPIRE].

JHEP01(2016)013

Holographic Quark Matter and Neutron Stars

Carlos Hoyos,[1,*] Niko Jokela,[2,†] David Rodríguez Fernández,[1,‡] and Aleksi Vuorinen[2,§]
[1]Department of Physics, Universidad de Oviedo, Avenida Calvo Sotelo 18, ES-33007 Oviedo, Spain
[2]Department of Physics and Helsinki Institute of Physics, University of Helsinki, P.O. Box 64, Helsinki FI-00014, Finland
(Received 15 March 2016; revised manuscript received 10 May 2016; published 12 July 2016)

We use a top-down holographic model for strongly interacting quark matter to study the properties of neutron stars. When the corresponding equation of state (EOS) is matched with state-of-the-art results for dense nuclear matter, we consistently observe a first-order phase transition at densities between 2 and 7 times the nuclear saturation density. Solving the Tolman-Oppenheimer-Volkov equations with the resulting hybrid EOSs, we find maximal stellar masses in excess of two solar masses, albeit somewhat smaller than those obtained with simple extrapolations of the nuclear matter EOSs. Our calculation predicts that no quark matter exists inside neutron stars.

DOI: 10.1103/PhysRevLett.117.032501

Quantitatively predicting the thermodynamic properties of dense nuclear and quark matter is one of the main challenges of modern nuclear theory. The complexity of the task originates from the need to nonperturbatively solve the theory of strong interactions, QCD, at finite baryon chemical potential μ_B. This combination of requirements is problematic, as it makes all the usual first-principles tools fail: Lattice simulations suffer from the infamous sign problem at a finite baryon chemical potential [1], while perturbative QCD is invalidated by the sizable value of the gauge coupling at moderate densities [2]. At present, the equation of state (EOS) of cold strongly interacting matter is under quantitative control at baryon densities below the nuclear saturation limit, $n_B \leq n_s \approx 0.16/\mathrm{fm}^3$, where the chiral effective theory (CET) works [3,4], as well as at a baryon chemical potential above roughly 2.5 GeV, where the perturbative EOS converges [5–8]. These limits unfortunately exclude the densities $n_s \leq n_B \leq 10 n_s$, where a deconfining phase transition to quark matter is expected to occur [9].

Remarkably, baryon densities well beyond the saturation limit are realized inside the most massive neutron stars [10]. Because of the difficulties alluded to above, a microscopic description of these objects necessitates bold extrapolations of the CET results, typically relying on a systematic use of so-called polytropic EOSs [11]. The polytropic EOSs have as such no physical content but simply parameterize our current ignorance of the high-density EOS in a way that allows constraining from both the low- and high-density sides [12]. The fact that no first-principles results are available for ultradense nuclear matter or strongly coupled quark matter makes progress towards a quantitatively reliable neutron star matter EOS excruciatingly slow.

Clearly, there is a need for fundamentally new approaches to the physics of strongly coupled quark matter—a challenge not unlike understanding the dynamics of hot quark-gluon plasma [13]. In this context, a very promising approach has turned out to be to apply the holographic duality [14–16]. It has been successfully used to study the deconfined phases of QCD matter [17,18] and to probe very nontrivial equilibration dynamics [19–21], teaching the heavy ion community many qualitative and even quantitative lessons about the behavior of strongly coupled QCD matter.

So far, holography has been used to study the cold and dense part of the QCD phase diagram only to a limited extent (see, however, [22–26]). The reason for this is that, in its best understood limit, the duality deals with supersymmetric conformal field theories, which are fundamentally different than QCD. In particular, they typically contain only adjoint representation fields and have therefore no analog of the fundamental representation quarks that dominate the properties of cold and dense QCD matter.

Despite the above issues, the situation is not hopeless: In the 't Hooft limit of $\lambda_{\mathrm{YM}} \equiv g^2_{\mathrm{YM}} N_c \gg 1$ and $N_c \gg N_f$, the dynamics of fundamental flavors can be captured by degrees of freedom carried by probe D-branes, while the gluon sector continues to be described by classical supergravity (SUGRA) [27]. States with finite baryon density in the gauge theory correspond to gravity configurations with a gauge field turned on in the D-brane worldvolume. The free energy can then be computed by evaluating the classical on-shell action of SUGRA together with the D-brane action. Given the relative simplicity of the calculations involved, the duality thus bestows us with a powerful tool to explore strongly coupled quark matter even at high density.

Our goal in this Letter is to take the logical step from the $D3$-$D7$ construction of Ref. [27] to phenomenological neutron star physics by investigating the implications of using a holographic EOS for cold quark matter just above the deconfinement transition. Because of technical restrictions discussed in the following section, completing this task requires some bold extrapolations. It will, however, lead us to results in excellent accordance with current phenomenological expectations, with only one parameter fitted to experiments.

The Letter is organized as follows: Our construction is thoroughly explained in the second section, while the resulting EOS and its relation to that of nuclear matter is analyzed in the third section. The implications of the hybrid EOS for the properties of neutron stars are then displayed in the fourth section, while conclusions are drawn and an outlook presented in the fifth section.

Holographic model.—In order to describe quark matter at nonzero density, let us consider a $D3$-$D7$ brane intersection. The field theory is then the $\mathcal{N}=2$ super Yang-Mills (SYM) theory with the matter content of the $\mathcal{N}=4$ $SU(N_c)$ SYM theory in the adjoint sector and N_f matter hypermultiplets in the fundamental representation. Thus, in addition to the QCD quarks and gluons, there are squarks and several species of adjoint fermions and scalars. The theory has a global $U(N_f) \sim U(1)_B \times SU(N_f)$ flavor symmetry, the $U(1)_B$ part of which we identify as the baryon symmetry. For two flavors, i.e., $N_f = 2$, isospin is the Abelian subgroup $U(1)_I \subset SU(2)$. Note that both quarks and squarks are charged under the flavor symmetry, so a typical state will have a finite density of both types of particles. Also, we do not expect our model to capture the correct gluon dynamics, as it has exact superconformal invariance.

In the large-N_c limit and at strong 't Hooft coupling, the $\mathcal{N}=4$ SYM theory has a holographic description in terms of classical type IIB SUGRA in an $AdS_5 \times S^5$ geometry [14]. In the 't Hooft limit $N_f \ll N_c$, the flavor sector can be introduced as N_f probe $D7$-branes extended along the AdS_5 directions and wrapping an $S^3 \subset S^5$ [27]. The thermodynamic properties of the model have been studied in great detail at nonzero temperature and charge density [28–40]. The free energy can be split into the contributions of adjoint and flavor fields:

$$F = F_{\mathcal{N}=4} + F_{\text{flavor}}, \tag{1}$$

where the first term is independent of the charge density and does not play a very important role for us.

We work in the grand canonical ensemble, so that the free energy is a function of the temperature T as well as chemical potentials corresponding to the conserved charges. Barring the presence of a mixture of two phases, possible in a first-order transition, the matter inside neutron stars is typically taken to be locally charge neutral and in beta equilibrium. This can be realized by taking the chemical potentials and densities of the u, d, and s quarks to agree [41], which implies neglecting the differences in their bare masses and setting both the isospin chemical potential and electron density to zero. In the zero-temperature limit, relevant for quiescent neutron stars, the EOS can then be parameterized by the baryon chemical potential $\mu_B = N_c \mu_q$ alone. In this case, the holographic setup simplifies somewhat, as there is no spontaneous breaking of flavor symmetry in the 't Hooft limit [35–39].

In the limit explained above, the flavor contribution to the grand canonical free energy density reads [31,42–45]

$$\mathcal{F}_{\text{flavor}} = -\frac{N_c N_f}{4\gamma^3 \lambda_{\text{YM}}} (\mu_q^2 - m^2)^2 + \mathcal{O}(\mu_q^3 T, T^4), \tag{2}$$

where $\gamma \equiv \Gamma(7/6)\Gamma(1/3)/\sqrt{\pi}$ and m is a mass parameter associated with the fermions. The model has thus four parameters: the number of colors N_c, the number of flavors N_f, the 't Hooft coupling λ_{YM}, and the mass m appearing in the dimensionless ratio μ_q/m. We choose them according to the properties of deconfined QCD matter at the relevant densities, which implies setting $N_c = N_f = 3$. The contribution of the adjoint sector to the free energy $\mathcal{F}_{\mathcal{N}=4} \sim N_c^2 T^4$ becomes of the same order as the $\mathcal{O}(T^4)$ corrections to the flavor free energy and can thereby be neglected.

Upon choosing the above values for N_c and N_f, we are extrapolating our model to a regime where finite N_c and N_f/N_c corrections are expected to become important [46–50]. For practical reasons, we however neglect them in the following, which implies that we treat the model as phenomenologically motivated by the original string theory construction. We also allow λ_{YM} and m to take values appropriate for the physical system under consideration, expecting them to lie in a region where the holographic approach remains at least qualitatively valid (for a recent discussion of the convergence of strong coupling expansions, see [51]).

With the above reservations, we proceed to note that, in the limit of large chemical potentials, the free energy density of our model approaches the value

$$\mathcal{F}_{\text{flavor}} \to -\frac{N_c N_f}{4\gamma^3 \lambda_{\text{YM}}} \mu_q^4, \tag{3}$$

the form of which is fixed by conformal invariance in the UV. In QCD, the corresponding quantity is known to approach the Stefan-Boltzmann value [5]

$$\mathcal{F}_{\text{QCD}} \to -\frac{N_c N_f}{12\pi^2} \mu_q^4, \tag{4}$$

so imposing the requirement that our model has the correct limiting behavior at large density fixes the value of the 't Hooft coupling as $\lambda_{\text{YM}} = 3\pi^2/\gamma^3 \simeq 10.74$. With this choice, our model can be seen to match the perturbative EOS of Ref. [7] already at moderate densities.

Finally, we discuss the choice of the mass parameter m. We expect that in the strongly coupled region the effective masses of the quarks receive large nonperturbative corrections, so relating this last remaining parameter of our model to the (differing) bare masses of the u, d, and s quarks would be largely nonsensical. Rather, we fix m through the value of μ_q, where the pressure of our model vanishes, requiring it to agree with the value obtained from the EOS

of nuclear matter [52]. This gives $m \approx 308.55$ MeV, just below one-third of the nucleon mass.

As argued above, at large densities and vanishing temperature, the pressure p and the energy density ε of our model can be determined from Eq. (2) as $p = -\mathcal{F}_{\text{flavor}}$ and $\varepsilon = \mu_q(\partial p/\partial \mu_q) - p$, respectively. The EOS thus takes the simple form

$$\varepsilon = 3p + m^2\sqrt{\frac{N_c N_f}{4\gamma^3 \lambda_{\text{YM}}}\,p} = 3p + \frac{\sqrt{3}m^2}{2\pi}\sqrt{p}, \qquad (5)$$

while the speed of sound squared reads $c_s^2 = (\partial p/\partial \varepsilon)$. From (5), c_s^2 always resides below the conformal value of $1/3$, making our EOS comparatively soft, seemingly at odds with the conclusions of Ref. [53]. It should, however, be noted that in Ref. [53] the transition between the nuclear and quark matter phases was fixed to occur at twice the nuclear saturation density. In our case, this parameter is one of the predictions of the model, and its value turns out to be always somewhat larger than $2n_s$.

Matching to nuclear matter.—Having obtained a candidate EOS for strongly coupled dense quark matter, the natural question arises, how to best use it in applications within neutron star physics. At low densities, we expect the matter to reside in the confined phase and, as the density is increased, find a transition to deconfined matter. This transition cannot be realized purely within the $D3$-$D7$ model, because at nonzero baryon density quarks are always in a deconfined phase, at least in the large-N_c limit [54]. The most natural strategy is therefore to describe the low-density phase using state-of-the-art results from the CET of nuclear interactions below the saturation density, extrapolated to higher densities with polytropic EOSs [11]. We then compare the corresponding pressure, i.e., minus the free energy density, to that of our holographic system, thereby determining the dominant phase at each quark chemical potential. Because of the uncertainty related to the low-density result, the matching should not be performed using a single confining EOS; instead, we apply the three EOSs given in Table 5 of Ref. [11], dubbed "soft," "intermediate," and "stiff," to represent different possible behaviors of the nuclear matter EOS. Of the three, the soft and stiff EOSs correspond to extreme cases, while the intermediate one can be considered a typical low-density EOS.

Our detailed construction is shown in Fig. 1, where on the left side we display the three low-density EOSs together with our quark matter EOS in the form of pressure vs quark chemical potential. As can be seen from here, there is a critical chemical potential μ_{crit} for each of the three low-density EOSs, at which a phase transition to deconfined quark matter occurs. In all cases, the transition is of first order, which can be verified from the right figure that displays the hybrid EOSs on a logarithmic pressure vs energy density plane. Notice that the holographic quark matter EOS smoothly connects to the perturbative one of Ref. [7] at high density.

It is interesting to note that the densities, at which the first-order phase transitions occur, are consistently in a phenomenologically viable region: For the soft nuclear matter EOS we get $n_{\text{crit}} = 6.92n_s$, for the intermediate one $n_{\text{crit}} = 3.79n_s$, and for the stiff case $n_{\text{crit}} = 2.37n_s$. This strengthens our conclusion that the holographic description is consistent with the expected properties of strongly coupled quark matter at least on a qualitative level. The order of the transition is, however, highly sensitive to the details of the EOS near the transition and may, therefore, be smoother than we predict.

Neutron star structure.—The EOS of strongly interacting matter is in a one-to-one correspondence with the mass-radius relation of neutron stars. This link is provided by the Tolman-Oppenheimer-Volkov (TOV) equations that govern hydrostatic equilibrium inside the stars. The equations take as input the relation between the energy density ε and pressure P of the matter, i.e., its EOS, as well as the central

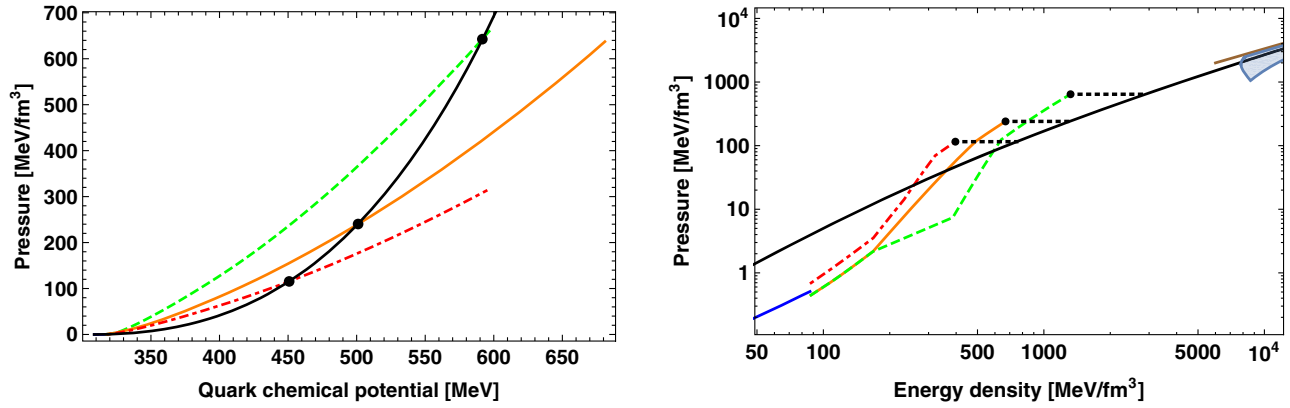

FIG. 1. (Left) The holographic quark matter EOS (black curve) together with the nuclear matter EOSs of Ref. [11]: soft (green line), intermediate (orange line), and stiff (red line). (Right) The matching procedure from the low-energy EOSs to the quark matter one, with the dashed black lines showing the jump in the energy density, characteristic of a first-order transition. Shown are also the CET results of Refs. [3,4] (blue curve), the conformal limit (brown curve), and the perturbative result of Ref. [7] (light blue band, generated by varying the renormalization scale).

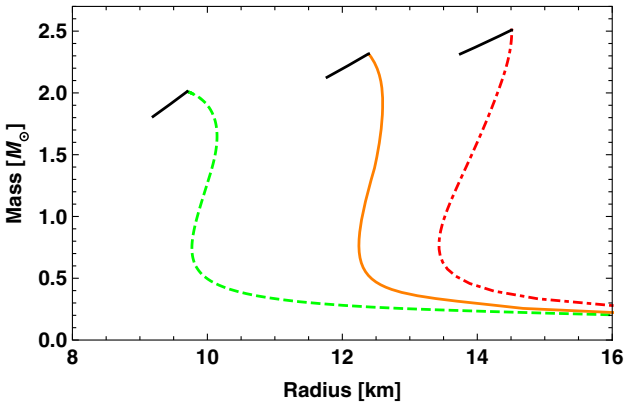

FIG. 2. The mass-radius relations corresponding to the three matched EOSs of Fig. 1 (right). The black lines correspond to an unstable branch of stars containing quark matter. The forms of the M-R relations are fairly generic; see, e.g., [41].

energy density $\varepsilon(r=0)$, and produce the mass and radius of the corresponding star. Varying $\varepsilon(r=0)$, we then obtain a well-defined curve on the MR plane.

A subtlety related to systems where a first-order phase transition occurs is the possible existence of mixed phases. This, however, strongly depends on the value of the microscopic surface tension between the nuclear and quark matter phases. As this parameter is beyond the validity of our description, and only crude estimates for the quantity exist in QCD, we have chosen to neglect this scenario and consider only stars made of pure phases.

Plugging the three EOSs of Fig. 1 into the TOV equations, we obtain the mass-radius curves displayed in Fig. 2. They follow the corresponding curves of Ref. [11] until they abruptly come to an end at points that mark the densities of our first-order phase transition. Here, the solutions to the TOV equation take a sharp turn towards smaller masses and radii, signaling an instability with respect to radial oscillations [41]. This behavior follows from the sizable latent heat $\Delta Q = \mu_{\rm crit}\Delta n$ at our first-order transition, i.e., the fact that the transitions are relatively strong for all three nuclear matter EOSs due to the softness of the holographic EOS (cf. [12] and Fig. 6 therein). The values we find for ΔQ are $(331\ \mathrm{MeV})^4$ (soft), $(265\ \mathrm{MeV})^4$ (intermediate), and $(229\ \mathrm{MeV})^4$ (stiff).

The main conclusion to be drawn from our results is that, with quark matter following a holographic EOS, it is unlikely that any deconfined matter could be found inside neutron stars. The maximal masses of the stars are dictated by the densities at which a phase transition from nuclear to quark matter occurs, with the most massive star having a central density at exactly this value. For the three nuclear matter EOSs of Ref. [11], we find maximal masses of 2.01, 2.32, and 2.50 times the solar mass $M_\odot$, corresponding to radii of 9.7, 12.4, and 14.5 km.

Conclusions and outlook.—Neutron stars provide a unique laboratory for the study of cold ultradense nuclear matter—and possibly even deconfined quark matter. Recent years have witnessed remarkable progress in their observational study, with the detection of the first two solar mass stars already ruling out several models of dense nuclear matter [64] and the recent discovery of gravitational waves by the LIGO and Virgo Collaborations raising hopes of a dramatic improvement in the accuracy of radius measurements [65]. This poses a prominent challenge for the theory community and highlights the need to understand the properties of dense nuclear and quark matter from first principles.

In this Letter, we have taken first steps towards the goal of building a phenomenological description for real world quark matter using holography. Under the usual large-N_c and strong coupling assumptions, it is possible to find a simple analytic expression for the EOS, which we, however, need to extrapolate to a regime where sizable corrections are to be expected. An important additional caveat is that the phase diagram of the theory may possess nontrivial structure; for instance, it was argued in Ref. [66] that at low temperatures squarks may condense and the system resides in a Higgs phase. No other instabilities have been found [50], but the appearance of spatially modulated phases is not ruled out [67–70].

Despite the above limitations, the predictions of our model display remarkably good agreement with those of complementary approaches (see, e.g., [11,12], and references therein). After fixing the parameters of our setup in a simple way, we obtained results that consistently indicate the presence of a strong first-order deconfinement transition between the nuclear and quark matter phases at baryon densities between roughly 2 and 7 times the nuclear saturation density. Because of the sizable latent heat associated with the transition, we predict that no stars with quark matter cores exist: As soon as there is even a small amount of quark matter in the center of a neutron star, it becomes unstable with respect to radial oscillations.

There exist a number of directions in which our current work can be generalized. The obvious extension would be to allow a mixed phase of nuclear and quark matter, assuming a given value for the surface tension between the two phases [71]. In addition, one may consider corrections due to the different bare masses of the quark flavors, as well as to nonzero temperature or background magnetic fields. With moderate effort, one may also consider the effects of finite N_c and $\lambda_{\rm YM}$ corrections on the EOS, utilizing existing results at the next-to-leading-order level. Finally, an important strength of holography lies, of course, in its applicability to the determination of quantities that are very challenging for traditional field theory techniques. These include, e.g., transport constants and emission rates, which could both be considered within our present model.

An interesting, albeit also challenging, direction to pursue would be to consider more refined top-down holographic models of QCD. One of the most appealing candidates is the Sakai-Sugimoto model [55], which has the same matter

content as QCD at low energies and furthermore realizes confinement and chiral symmetry breaking in a natural way. As there are indications that this model exhibits a phase transition between baryonic and deconfined matter [26], it might enable performing the matching to the CET EOS at much lower densities where the uncertainty of the latter result is smaller. In the deconfined phase, the corresponding EOS is, in addition, significantly stiffer that of a conformal theory [72,73], which may lead to the existence of stable stars with quark matter cores. A potential drawback of this approach is, however, that at very large densities it deviates from QCD due to the lack of a UV fixed point.

We thank Aleksi Kurkela, Joonas Nättilä, and Alfonso V. Ramallo for useful discussions. N. J. and A. V. have been supported by the Academy of Finland Grants No. 273545 and No. 1268023, while C. H. and D. R. F. are partially supported by the Spanish Grant No. MINECO-13-FPA2012-35043-C02-02. C. H. is, in addition, supported by the Ramon y Cajal fellowship RYC-2012-10370 and D. R. F. by the GRUPIN 14-108 research grant from Principado de Asturias.

[*]hoyoscarlos@uniovi.es
[‡]niko.jokela@helsinki.fi
[†]rodriguezferdavid@uniovi.es
[§]aleksi.vuorinen@helsinki.fi

[1] M. Cristoforetti, F. Di Renzo, and L. Scorzato (AuroraScience Collaboration), Phys. Rev. D **86**, 074506 (2012).
[2] U. Kraemmer and A. Rebhan, Rep. Prog. Phys. **67**, 351 (2004).
[3] I. Tews, T. Kruger, K. Hebeler, and A. Schwenk, Phys. Rev. Lett. **110**, 032504 (2013).
[4] A. Gezerlis, I. Tews, E. Epelbaum, S. Gandolfi, K. Hebeler, A. Nogga, and A. Schwenk, Phys. Rev. Lett. **111**, 032501 (2013).
[5] B. A. Freedman and L. D. McLerran, Phys. Rev. D **16**, 1169 (1977).
[6] A. Vuorinen, Phys. Rev. D **68**, 054017 (2003).
[7] A. Kurkela, P. Romatschke, and A. Vuorinen, Phys. Rev. D **81**, 105021 (2010).
[8] A. Kurkela and A. Vuorinen, arXiv:1603.00750 [Phys. Rev. Lett. (to be published)].
[9] K. Fukushima and C. Sasaki, Prog. Part. Nucl. Phys. **72**, 99 (2013).
[10] H. Heiselberg and M. Hjorth-Jensen, Phys. Rep. **328**, 237 (2000).
[11] K. Hebeler, J. M. Lattimer, C. J. Pethick, and A. Schwenk, Astrophys. J. **773**, 11 (2013).
[12] A. Kurkela, E. S. Fraga, J. Schaffner-Bielich, and A. Vuorinen, Astrophys. J. **789**, 127 (2014).
[13] N. Brambilla *et al.*, Eur. Phys. J. C **74**, 2981 (2014).
[14] J. M. Maldacena, Adv. Theor. Math. Phys. **2**, 231 (1998).
[15] S. S. Gubser, I. R. Klebanov, and A. M. Polyakov, Phys. Lett. B **428**, 105 (1998).
[16] E. Witten, Adv. Theor. Math. Phys. **2**, 253 (1998).
[17] J. Erdmenger, N. Evans, I. Kirsch, and E. Threlfall, Eur. Phys. J. A **35**, 81 (2008).
[18] A. Adams, L. D. Carr, T. Schäfer, P. Steinberg, and J. E. Thomas, New J. Phys. **14**, 115009 (2012).
[19] J. Casalderrey-Solana, M. P. Heller, D. Mateos, and W. van der Schee, Phys. Rev. Lett. **111**, 181601 (2013).
[20] H. Bantilan and P. Romatschke, Phys. Rev. Lett. **114**, 081601 (2015).
[21] P. M. Chesler and L. G. Yaffe, J. High Energy Phys. 10 (2015) 070.
[22] O. Bergman, G. Lifschytz, and M. Lippert, J. High Energy Phys. 11 (2007) 056.
[23] M. Rozali, H.-H. Shieh, M. Van Raamsdonk, and J. Wu, J. High Energy Phys. 01 (2008) 053.
[24] K.-Y. Kim, S.-J. Sin, and I. Zahed, J. High Energy Phys. 09 (2008) 001.
[25] V. Kaplunovsky, D. Melnikov, and J. Sonnenschein, J. High Energy Phys. 11 (2012) 047.
[26] S.-w. Li, A. Schmitt, and Q. Wang, Phys. Rev. D **92**, 026006 (2015).
[27] A. Karch and E. Katz, J. High Energy Phys. 06 (2002) 043.
[28] D. Mateos, R. C. Myers, and R. M. Thomson, Phys. Rev. Lett. **97**, 091601 (2006).
[29] S. Kobayashi, D. Mateos, S. Matsuura, R. C. Myers, and R. M. Thomson, J. High Energy Phys. 02 (2007) 016.
[30] D. Mateos, R. C. Myers, and R. M. Thomson, J. High Energy Phys. 05 (2007) 067.
[31] A. Karch and A. O'Bannon, J. High Energy Phys. 11 (2007) 074.
[32] S. Nakamura, Y. Seo, S.-J. Sin, and K. P. Yogendran, Prog. Theor. Phys. **120**, 51 (2008).
[33] K. Ghoroku, M. Ishihara, and A. Nakamura, Phys. Rev. D **76**, 124006 (2007).
[34] D. Mateos, S. Matsuura, R. C. Myers, and R. M. Thomson, J. High Energy Phys. 11 (2007) 085.
[35] J. Erdmenger, M. Kaminski, P. Kerner, and F. Rust, J. High Energy Phys. 11 (2008) 031.
[36] M. Ammon, J. Erdmenger, M. Kaminski, and P. Kerner, Phys. Lett. B **680**, 516 (2009).
[37] P. Basu, J. He, A. Mukherjee, and H.-H. Shieh, J. High Energy Phys. 11 (2009) 070.
[38] T. Faulkner and H. Liu, arXiv:0812.4278.
[39] M. Ammon, J. Erdmenger, M. Kaminski, and P. Kerner, J. High Energy Phys. 10 (2009) 067.
[40] J. Erdmenger, V. Grass, P. Kerner, and T. H. Ngo, J. High Energy Phys. 08 (2011) 037.
[41] N. Glendenning, *Compact Stars. Nuclear Physics, Particle Physics and General Relativity* (Springer-Verlag, New York, 1996), p. 90.
[42] A. Karch, D. T. Son, and A. O. Starinets, Phys. Rev. Lett. **102**, 051602 (2009).
[43] A. Karch, M. Kulaxizi, and A. Parnachev, J. High Energy Phys. 11 (2009) 017.
[44] M. Ammon, M. Kaminski, and A. Karch, J. High Energy Phys. 11 (2012) 028.
[45] G. Itsios, N. Jokela, and A. V. Ramallo, arXiv:1602.06106.
[46] S. S. Gubser, I. R. Klebanov, and A. A. Tseytlin, Nucl. Phys. **B534**, 202 (1998).

[47] F. Bigazzi, A. L. Cotrone, J. Mas, A. Paredes, A. V. Ramallo, and J. Tarrio, J. High Energy Phys. 11 (2009) 117.
[48] C. Nunez, A. Paredes, and A. V. Ramallo, Adv. High Energy Phys. **2010**, 196714 (2010).
[49] F. Bigazzi, A. L. Cotrone, J. Mas, D. Mayerson, and J. Tarrio, J. High Energy Phys. 04 (2011) 060.
[50] F. Bigazzi, A. L. Cotrone, and J. Tarrio, J. High Energy Phys. 07 (2013) 074.
[51] S. Waeber, A. Schäfer, A. Vuorinen, and L. G. Yaffe, J. High Energy Phys. 11 (2015) 087.
[52] J. W. Negele and D. Vautherin, Nucl. Phys. **A207**, 298 (1973).
[53] P. Bedaque and A. W. Steiner, Phys. Rev. Lett. **114**, 031103 (2015).
[54] This is not the case for other holographic models, such as the Sakai-Sugimoto one [55]; cf. [22–26,56–59]. Attempts in this direction have, however, led to either unstable or unrealistic stars [60–63].
[55] T. Sakai and S. Sugimoto, Prog. Theor. Phys. **113**, 843 (2005).
[56] K.-Y. Kim, S.-J. Sin, and I. Zahed, J. Korean Phys. Soc. **63**, 1515 (2013).
[57] M. Rho, S.-J. Sin, and I. Zahed, Phys. Lett. B **689**, 23 (2010).
[58] V. Kaplunovsky and J. Sonnenschein, J. High Energy Phys. 04 (2014) 022.
[59] V. Kaplunovsky, D. Melnikov, and J. Sonnenschein, Mod. Phys. Lett. B **29**, 1540052 (2015).
[60] P. Burikham, E. Hirunsirisawat, and S. Pinkanjanarod, J. High Energy Phys. 06 (2010) 040.
[61] Y. Kim, C.-H. Lee, I. J. Shin, and M.-B. Wan, J. High Energy Phys. 10 (2011) 111.
[62] K. Ghoroku, K. Kubo, M. Tachibana, and F. Toyoda, Int. J. Mod. Phys. A **29**, 1450060 (2014).
[63] Y. Kim, I. J. Shin, C.-H. Lee, and M.-B. Wan, J. Korean Phys. Soc. **66**, 578 (2015).
[64] P. Demorest, T. Pennucci, S. Ransom, M. Roberts, and J. Hessels, Nature (London) **467**, 1081 (2010).
[65] B. P. Abbott *et al.* (Virgo and LIGO Scientific Collaborations), Phys. Rev. Lett. **116**, 061102 (2016).
[66] H.-Y. Chen, K. Hashimoto, and S. Matsuura, J. High Energy Phys. 02 (2010) 104.
[67] S. K. Domokos and J. A. Harvey, Phys. Rev. Lett. **99**, 141602 (2007).
[68] S. Nakamura, H. Ooguri, and C.-S. Park, Phys. Rev. D **81**, 044018 (2010).
[69] A. Donos and J. P. Gauntlett, J. High Energy Phys. 08 (2011) 140.
[70] O. Bergman, N. Jokela, G. Lifschytz, and M. Lippert, J. High Energy Phys. 10 (2011) 034.
[71] L. F. Palhares and E. S. Fraga, Phys. Rev. D **82**, 125018 (2010).
[72] M. Kulaxizi and A. Parnachev, Nucl. Phys. **B815**, 125 (2009).
[73] N. Jokela and A. V. Ramallo, Phys. Rev. D **92**, 026004 (2015).

PHYSICAL REVIEW D **94,** 106008 (2016)

Breaking the sound barrier in holography

Carlos Hoyos,[1,*] Niko Jokela,[2,†] David Rodríguez Fernández,[1,‡] and Aleksi Vuorinen[2,§]

[1]*Department of Physics, Universidad de Oviedo, Avda. Calvo Sotelo 18, ES-33007 Oviedo, Spain*

[2]*Department of Physics and Helsinki Institute of Physics, P.O. Box 64, FI-00014 University of Helsinki, Finland*

(Received 20 September 2016; published 15 November 2016)

It has been conjectured that the speed of sound in holographic models with UV fixed points has an upper bound set by the value of the quantity in conformal field theory. If true, this would set stringent constraints for the presence of strongly coupled quark matter in the cores of physical neutron stars, as the existence of two-solar-mass stars appears to demand a very stiff equation of state. In this article, we present a family of counterexamples to the speed of sound conjecture, consisting of strongly coupled theories at finite density. The theories we consider include $\mathcal{N}=4$ super Yang-Mills at finite R-charge density and nonzero gaugino masses, while the holographic duals are Einstein-Maxwell theories with a minimally coupled scalar in a charged black hole geometry. We show that for a small breaking of conformal invariance, the speed of sound approaches the conformal value from above at large chemical potentials.

DOI: 10.1103/PhysRevD.94.106008

I. INTRODUCTION

Quantitatively understanding the properties of strongly interacting matter in the cold and extremely dense region realized in the cores of neutron stars constitutes a long-standing problem in nuclear physics [1,2]. The situation is complicated by a lack of first principles field theory tools; perturbative QCD is only applicable at extremely high densities [3,4], while lattice Monte Carlo simulations are altogether prohibited due to the sign problem [5]. Add to this the fact that robust nuclear physics methods—including their modern formulations, such as the Chiral Effective Theory [6]—are only reliable below the nuclear saturation density $n_s \approx 0.16/\mathrm{fm}^3$ [7]. It becomes clear that fundamentally new approaches to the problem are urgently needed. In this context, a highly promising avenue is the application of the holographic duality [8], which has indeed been lately applied to the description of both the nuclear [9–16] and quark matter [17–19] phases inside a neutron star.

The most fundamental quantity that governs the thermodynamic behavior of neutron star matter is its equation of state (EoS), i.e. the functional dependence of its energy density ε on the pressure p. Oftentimes, it is, however, more illuminating to inspect the derivative $\partial p/\partial\varepsilon$, which equals the speed of sound squared in the system, v_s^2. This quantity namely describes the stiffness of the matter—a property needed to build massive stars capable of resisting gravitational collapse into a black hole. Causality restricts this parameter to obey the relation $v_s^2 < 1$ (and thermodynamic stability guarantees that $v_s^2 > 0$), but it has been widely speculated that a more restrictive bound might exist as well. In particular, the lack of known physical systems in a deconfined phase with a speed of sound exceeding the conformal value $v_s^2 = 1/3$ has prompted a conjecture that this might represent a theoretical upper limit for the quantity [20,21] in the same spirit that $\eta/s = 1/(4\pi)$ was initially thought to represent a lower limit for the shear viscosity to entropy ratio in any strongly coupled fluid [22]. Some support for this argument comes from the fact that both the inclusion of a nonzero mass to a conformal system as well as the introduction of perturbatively weak interactions in an asymptotically free theory are known to lead to a speed of sound below the conformal limit.

The speed of sound conjecture has been widely discussed in the context of neutron star physics, and it has been shown to be in rather strong tension with the known existence of two-solar-mass neutron stars [23,24], which requires a very stiff EoS [25]. This points toward a highly nontrivial behavior of v_s as a function of the baryon chemical potential. Namely, at low densities, the speed of sound is known to have a very small value, while its behavior at asymptotically large μ_B is a logarithmic *rise* toward $v_s^2 = 1/3$. This implies that, should the speed of sound bound be violated somewhere, v_s needs to possess at least two extrema, a maximum and a minimum, between which the quantity may either behave continuously or jump from the maximum to the minimum value.

Recalling the success of holographic methods in the description of strongly coupled quark gluon plasma produced in heavy ion collisions [2,26], it is clearly worthwhile to study the behavior of the speed of sound in holographic models of quark matter. Here, one, however, quickly realizes that the speed of sound bound is not easily

*hoyoscarlos@uniovi.es
†niko.jokela@helsinki.fi
‡rodriguezferdavid@uniovi.es
§aleksi.vuorinen@helsinki.fi

violated; all known examples of asymptotically five-dimensional Anti-de Sitter spacetime (AdS_5) geometries predict $v_s^2 \leq 1/3$ [21].[1] The known violations of the bound occur in theories that do not flow to a four-dimensional conformal field theory (CFT) in the UV and thus do not correspond to ordinary renormalizable field theories in four dimensions. Such examples include the $3+1$-dimensional brane intersections $D4-D6$, $D5-D5$, and $D4-D8$ (the Sakai-Sugimoto model [29]), corresponding to the respective speeds of sound $v_s^2 = 1/2, 1, 2/5$ [30–32]. It is well known that, even after a compactification to $3+1$ dimensions, it is not possible to disentangle four-dimensional dynamics from the additional degrees of freedom that live on the higher-dimensional color branes, and thus the thermodynamic properties may be very different from a bona fide four-dimensional theory. Another class of examples that violate the bound are nonrelativistic geometries, such as the Lifshitz ones [33–36], for which a scaling symmetry fixes $\partial p/\partial \varepsilon = z/3$, with z the dynamical exponent of the dual nonrelativistic theory. For any $z > 1$, the EoS of the nonrelativistic theory is stiffer than the conformal one. In this case, the violation of the bound is in some sense trivial, since the dual theory is nonrelativistic.

For the reasons listed above, it is very challenging to build a holographic description for dense strongly interacting quark matter that would allow for the existence of deconfined matter inside even the heaviest neutron stars observed. Indeed, in a recent study of hybrid neutron stars by the present authors [19], where a holographic EoS was constructed for the quark matter phase, it was discovered that the stars became unstable as soon as even a microscopic amount of quark matter was present in their cores. This was attributed to a very strong first order deconfining phase transition in the model, which was ultimately due to the relatively low stiffness of the conformal quark matter EoS, corresponding to $v_s^2 = 1/3$. These findings are in line with the analysis of Ref. [37], where it was seen that large speeds of sound were necessary to obtain stars containing nonzero amounts of quark matter in their cores.

One possible resolution to the speed of sound puzzle is clearly that the quantity rises to a value $v_s > 1/\sqrt{3}$ in the nuclear matter phase, then discontinuously jumps to a low value at a first order deconfinement phase transition, and finally slowly rises toward the conformal limit in the deconfined phase. In the paper at hand, we propose another viable scenario, involving a violation of the speed of sound bound in the deconfined phase and thereby paving the way to the existence of quark matter in neutron star cores. We do this by constructing a holographic EoS for dense deconfined matter that not only exhibits a speed of sound above the conformal limit but in addition involves an asymptotically anti-de Sitter (AdS) spacetime. This provides an explicit counterexample to the common lore that asymptotically AdS spacetimes necessitate $v_s < 1/\sqrt{3}$,[2] and suggests that there may exist a large class of realistic holographic models for dense deconfined QCD matter that involve speeds of sound significantly above this bound.

Our paper is organized as follows. In Sec. II, we consider a class of models involving an Einstein-Maxwell action with a minimally coupled charged bulk scalar and show that the speed of sound bound is violated in it for different values of the charge and the mass of the scalar. In Sec. III, we consider a top-down string theory setup in this class, dual to $\mathcal{N}=4$ super–Yang-Mills theory at nonzero R-charge density and confirm that the speed of sound is larger than the conformal value before the system becomes unstable toward the formation of a homogeneous condensate. In Sec. IV, we finally discuss the implications of our findings, while Appendixes A, B, and C are devoted to a closer look at some technical details of our computation.

II. SPEED OF SOUND AT FINITE DENSITY

In order to construct a holographic model for a finite density system, in which the speed of sound bound might be violated, we should clearly incorporate both a nonzero charge density and a breaking of conformal invariance. The simplest such model is Einstein-Maxwell gravity minimally coupled to a scalar field (charged or not), for which the action reads

$$S = \frac{1}{16\pi G_5}\int d^5x[R - L^2F^2 - |D\phi|^2 - V(|\phi|^2)], \qquad (2.1)$$

where L will be fixed to be equal to the AdS radius. The field ϕ appearing here is a complex scalar with charge q, such that the covariant derivative acting on it reads

$$D_\mu\phi = \partial_\mu\phi - iqA_\mu\phi. \qquad (2.2)$$

The potential V can, on the other hand, be expanded to quadratic order as

$$V(|\phi|^2) \simeq -\frac{12}{L^2} + m^2|\phi|^2, \qquad m^2L^2 = \Delta(\Delta-4). \qquad (2.3)$$

Following the usual AdS/CFT dictionary, we take the scalar field to be dual to a relevant operator of dimension $1 < \Delta < 4$, while the gauge field A_μ is dual to a $U(1)$ conserved current. The equations of motion following from this action are

[1] For two exceptions to this that are, however, dynamically unstable, see Refs. [27,28].

[2] Note, however, that there is no apparent reason on the field theory side to suspect that the speeds of sound in theories that are UV complete would exhibit a universal upper bound.

$$
\begin{aligned}
&D_M(\sqrt{-g}g^{MN}D_N\phi) - m^2\sqrt{-g}\phi = 0\\
&4L^2\partial_M(\sqrt{-g}F^{MN}) = iq\sqrt{-g}g^{MN}[\phi^*(D_M\phi) - (D_M\phi)^*\phi]\\
&T^{(A)}_{MN} + T^{(\phi)}_{MN} = R_{MN} - \frac{1}{2}Rg_{MN}\\
&T^{(A)}_{MN} = 2L^2\left(F_{MA}F_N{}^A - \frac{1}{4}F^2 g_{MN}\right)\\
&T^{\phi}_{MN} = \frac{1}{2}[(D_M\phi)^*D_N\phi + (D_N\phi)^*D_M\phi\\
&\qquad - (|D\phi|^2 + V)g_{MN}].
\end{aligned}
\tag{2.4}
$$

If the scalar field is turned off, i.e. $\phi = 0$, a homogeneous and isotropic charged state in the field theory has a gravity dual description given by the AdS Reissner-Nordström (AdSRN) metric

$$
\begin{aligned}
&ds^2 = L^2\frac{dr^2}{r^2 f(r)} + \frac{r^2}{L^2}[-f(r)dt^2 + d\vec{x}^2],\\
&f(r) = 1 + \frac{Q^2}{r^6} - \frac{M}{r^4}.
\end{aligned}
\tag{2.5}
$$

The gauge potential in the AdSRN solution is

$$
A_0 = \mu\left[1 - \left(\frac{r_H}{r}\right)^2\right], \tag{2.6}
$$

where r_H is the position of the black hole horizon and

$$
M = r_H^4 + \frac{Q^2}{r_H^2}, \qquad \mu = \sqrt{3}\frac{Q}{2L^2 r_H^2}. \tag{2.7}
$$

The Hawking temperature is then

$$
T = \frac{r_H}{2\pi L^2}(2 - r_H^{-6}Q^2). \tag{2.8}
$$

At the critical value $Q_c = \sqrt{2}r_H^3$, the solution becomes extremal ($T = 0$). The horizon radius can be determined by the temperature and the chemical potential to be

$$
\frac{r_H}{L^2} = \frac{T}{6}\left(3\pi + \sqrt{9\pi^2 + \frac{24\mu^2}{T^2}}\right). \tag{2.9}
$$

The AdSRN solution is dual to a charged state in a CFT, and therefore the speed of sound is fixed to the conformal value $v_s^2 = 1/3$. In order to deviate from this value, we need to break conformal invariance. For this, we will consider a nonvanishing scalar field $\phi \neq 0$. The asymptotic expansion of the scalar close to the AdS boundary is

$$
\phi \simeq \left(\frac{L}{r}\right)^{4-\Delta} L^{4-\Delta}\tilde{\phi}_{(0,0)} + \left(\frac{L}{r}\right)^{\Delta} L^{\Delta}\phi_{(0,0)}. \tag{2.10}
$$

In this expansion, the first term has the interpretation as a deformation of the CFT by the relevant operator with a coupling $J \equiv \tilde{\phi}_{(0,0)}$, while $\phi_{(0,0)}$ determines the expectation value of the dual operator. An explicit breaking of conformal invariance then corresponds to solutions for which $J \neq 0$.

In order to simplify the analysis, we will restrict to a small breaking of conformal invariance $J/\mu^{4-\Delta} \ll 1$ and/or $J/T^{4-\Delta} \ll 1$. In this case, the amplitude of the scalar field will be small and can be treated as a probe in the AdSRN geometry. Furthermore, we can approximate the potential by the quadratic and constant term, as in (2.3), and reduce the problem to solving the linearized equations of motion for the scalar field

$$
\begin{aligned}
&\frac{1}{\sqrt{-g}}\partial_M(\sqrt{-g}g^{MN}(\partial_N\phi - iqA_N\phi))\\
&\quad - iqA_M g^{MN}(\partial_N\phi - iqA_N\phi) - m^2\phi = 0.
\end{aligned}
\tag{2.11}
$$

Taking $\phi = \phi(r)$ and defining $\Delta = 2 + \nu$, the equation of motion in the AdSRN background reduces to

$$
\phi'' + \left(\frac{5}{r} + \frac{f'}{f}\right)\phi' + \left(\frac{4 - \nu^2}{r^2 f} + \frac{q^2 L^4}{r^4 f^2}A_0^2\right)\phi = 0. \tag{2.12}
$$

For computational purposes, it will be convenient to work with a different radial coordinate $u = r_H^2/r^2$ and introduce a parameter $\mathcal{Q}$ such that $Q = r_H^3\mathcal{Q}$. In this coordinate, the equation of motion takes the form

$$
0 = \phi'' + \frac{\zeta_1(u)}{u}\phi' + \frac{\zeta_2(u)}{u^2}\phi, \tag{2.13}
$$

where

$$
\begin{aligned}
\zeta_1 &= \frac{u+2}{\mathcal{Q}^2u^2 - u - 1} + \frac{1}{u-1} + 2\\
\zeta_2 &= \frac{u[3q^2\mathcal{Q}^2(u-1) - 4(\nu^2-4)(\mathcal{Q}^2u - 1)] + 4(\nu^2-4)}{16(u-1)(\mathcal{Q}^2u^2 - u - 1)^2}.
\end{aligned}
\tag{2.14}
$$

In these coordinates, the horizon is at $u = 1$, while the asymptotic AdS boundary is at $u = 0$. The expansion close to the boundary is

$$
\phi \simeq \alpha_- u^{1-\frac{\nu}{2}} + \alpha_+ u^{1+\frac{\nu}{2}}, \tag{2.15}
$$

where α_- and α_+ are the coefficients of the non-normalizable and normalizable modes, respectively. They are related to the coefficients in the expansion (2.10) as

$$
J = \tilde{\phi}_{(0,0)} = \alpha_-\left(\frac{r_H}{L^2}\right)^{2-\nu}, \quad \phi_{(0,0)} = \alpha_+\left(\frac{r_H}{L^2}\right)^{2+\nu}. \tag{2.16}
$$

A. Near-extremal solutions

Our first goal will be to determine the behavior of the speed of sound in the limit of large densities $\mu \gg T$. The AdSRN geometry will be very close to the extremal solution, and it will deviate only in the neighborhood of the black hole horizon, where in the extremal case the geometry becomes $AdS_2 \times \mathbb{R}^3$ while in the nonextremal case there is an ordinary black hole horizon.

Let us introduce a small parameter $\epsilon \ll 1$, such that the solution becomes extremal when $\epsilon \to 0$:

$$\mathcal{Q} = \sqrt{2}(1-\epsilon). \tag{2.17}$$

In the region away from the horizon, $1-u \gg \epsilon$, we can simply set $\epsilon = 0$ to leading order and solve the equations of motion. Deviations from the extremal limit can be computed in a systematic way by means of a perturbative expansion in ϵ.

In the region close to the horizon $1-u \sim \epsilon$ the naive expansion in ϵ breaks down, since the geometry deviates from the extremal AdSRN. Instead, one can take a near-horizon expansion by introducing a new radial coordinate v defined as

$$u = 1 - \frac{4}{3}\epsilon v \tag{2.18}$$

and expanding the equations to leading order in ϵ. The resulting solution will be a good approximation in the near-horizon region $1 \gg 1-u$. We impose the condition that the solution is regular at the horizon, which completely determines it up to an overall constant.

A full solution valid throughout the full geometry can be constructed by matching both kinds of expansions in the overlapping region $1 \gg 1-u \gg \epsilon$. We give the full details of the calculation and the matching in Appendix A 1. The ratio between the coefficients of the normalizable and non-normalizable modes in the boundary expansion (2.15) is given in (A11), reading schematically

$$\frac{\alpha_+}{\alpha_-} = Z_{\nu,q}\frac{1+\beta_1\left(\frac{4\epsilon}{9}\right)^{\lambda/\sqrt{3}}}{1+\beta_2\left(\frac{4\epsilon}{9}\right)^{\lambda/\sqrt{3}}}, \tag{2.19}$$

where

$$\lambda = \sqrt{\nu^2 - \frac{q^2}{2} - 1}. \tag{2.20}$$

We see that, depending on whether λ is real or imaginary, there can be two qualitatively different behaviors. For imaginary λ, the ratio will have an oscillatory behavior with a period that depends logarithmically on ϵ. On the other hand, if λ is real, the terms depending on ϵ can be neglected in a first approximation. For the rest of this section, we will take λ to be real, which imposes a lower bound on the conformal dimension of the scalar,

$$\nu^2 > 1 + \frac{q^2}{2} \Rightarrow \Delta > 2 + \sqrt{1+\frac{q^2}{2}} \geq 3. \tag{2.21}$$

This agrees with the condition that the effective mass of the scalar field is above the Breitenlohner-Freedman bound in the two-dimensional Anti-de Sitter spacetime (AdS_2) region of the extremal black hole [38,39]:

$$m_{\text{eff}}^2 R_{AdS_2}^2 \geq -\frac{1}{4}, \qquad R_{AdS_2}^2 = \frac{R^2}{12}, \qquad m_{\text{eff}}^2 = m^2 - \frac{q^2}{2R^2}. \tag{2.22}$$

Assuming the bound is satisfied, the ratio between the two coefficients is, to leading order in ϵ,

$$\frac{\alpha_+}{\alpha_-} = -3^\nu \frac{\Gamma(1-\nu)\Gamma\left(\frac{1+\nu}{2}+\frac{\lambda+q}{2\sqrt{3}}\right)\Gamma\left(\frac{1+\nu}{2}+\frac{\lambda-q}{2\sqrt{3}}\right)}{\Gamma(1+\nu)\Gamma\left(\frac{1-\nu}{2}+\frac{\lambda+q}{2\sqrt{3}}\right)\Gamma\left(\frac{1-\nu}{2}+\frac{\lambda-q}{2\sqrt{3}}\right)}. \tag{2.23}$$

B. Nonextremal solutions

If the bound of the speed of sound is violated at large densities, it will approach the conformal value from *above*. At zero density, the results of Refs. [20,21] tell us that at zero density and large temperatures the conformal value is approached from *below*. Therefore, one expects an interpolation between the two behaviors as the ratio μ/T is varied from infinity to zero, and in particular there should be a maximal value of the speed of sound at some intermediate value. In order to study this behavior, we need to go beyond the near-extremal limit. Another important reason to do it is that it will allow us to study the stability of the solutions against a condensation of the scalar.

In order to construct the nonextremal solutions, we will resort to numerics to solve the equation (2.13). We impose regularity of the scalar field at the horizon and shoot toward the boundary, where we read the values of the coefficients for the normalizable and non-normalizable modes. The parameters of the numerical calculation that we can vary are $\mathcal{Q}$ in the equations (2.13) and the amplitude of the scalar solution, α_-, in the boundary expansion (2.15). They can be used to determine the value of the chemical potential and the temperature normalized by the coupling of the relevant deformation,

$$\begin{aligned} \mu_r &\equiv \frac{\mu}{J^{\frac{1}{4-\Delta}}} = \frac{\sqrt{3}}{2}\mathcal{Q}\alpha_-^{\frac{1}{\nu-2}}, \\ t_r &\equiv \frac{T}{J^{\frac{1}{4-\Delta}}} = \frac{2-\mathcal{Q}^2}{2\pi}\alpha_-^{\frac{1}{\nu-2}}. \end{aligned} \tag{2.24}$$

The value of the normalizable coefficient α_+ is extracted from the numerical solution and can be used to determine the expectation value of the dual operator and the components of the energy-momentum tensor.

The way we proceed is the following. We first expand close to the horizon $u = 1$ and impose regularity. The scalar field has a Taylor expansion that we truncate at, say, the fifth order,

$$\phi_h(u) = \sum_{n=0}^{5} \phi^H_{(n)}(1-u)^n. \tag{2.25}$$

The coefficients $\phi^H_{(n)}$ for $n > 0$ are determined by $\phi^H_{(0)}$ and ν, q, and $\mathcal{Q}$ in (2.14). We fix $\phi^H_{(0)} = 1$ and use the truncated expansion to give initial conditions for the numerical calculation

$$\begin{aligned} \phi_n(1-\epsilon_0) &= \phi_h(1-\epsilon_0), \\ \phi'_n(1-\epsilon_0) &= \phi'_h(1-\epsilon_0), \end{aligned} \tag{2.26}$$

where ϕ_n is the numerical solution and we take $\epsilon_0 = 10^{-5}$ as the cutoff in the radial direction. We shoot toward the boundary using NDSolve in Mathematica 10 and find a numerical solution ϕ_n defined in the interval $\epsilon_0 \le u \le 1-\epsilon_0$. We do this for $\nu = 1$, $q = 10^{-5}$ to study the speed of sound and for $\nu = 1, 1.1, 1.3, 1.6$ and $q = 0.5, 1, 4, 5$ and the critical values $q^* = 1.47, 1.64, 1.97, 2.44$ for the stability analysis. In all cases, we vary $\mathcal{Q}$ starting at $\mathcal{Q} = 10^{-5}$ with a step $\Delta\mathcal{Q} = 0.005$ and keeping $\mathcal{Q} < \sqrt{2}$.

Once we have obtained the numerical solution, we extract the values of the coefficients of the normalizable and non-normalizable modes by evaluating the solution at the boundary cutoff $u = \epsilon_0$. For $\nu > 1$, we define the numerical values as

$$(\alpha_-)_n = u^{\frac{\nu}{2}-1}\phi_n(u)|_{u=\epsilon_0} \tag{2.27}$$

$$(\alpha_+)_n = \frac{1}{\nu} u^{1-\nu}\partial_u[u^{\frac{\nu}{2}-1}\phi_n(u)]\big|_{u=\epsilon_0}. \tag{2.28}$$

These values are determined by $\mathcal{Q}$, ν, and q. In the numerical calculation, we have fixed the amplitude of the scalar field. Since the equations of motion are linear, we can generate a full set of values by doing a trivial rescaling,

$$\alpha_- = a(\alpha_-)_n, \qquad \alpha_+ = a(\alpha_+)_n, \tag{2.29}$$

for some real number a. We determine the value of a by fixing the temperature in units of the relevant coupling (2.24) for each value of $\mathcal{Q}$.

C. Thermodynamics

Following the usual AdS/CFT dictionary, the free energy (grand canonical potential) is proportional to the renormalized on-shell action in Euclidean signature $F = TS^E_{\text{ren}}$. Since there is a nonzero chemical potential, it will be convenient to work in Lorentzian signature, such that the renormalized on-shell action reads

$$S_{\text{ren}} = \int dt L_{\text{ren}} = V_3 \int dt \mathcal{L}_{\text{ren}}. \tag{2.30}$$

In (2.30), we have used the fact that the backgrounds we study are homogeneous, and V_3 is the corresponding spatial volume along the boundary directions. The free energy density becomes then

$$\mathcal{F} = -\mathcal{L}_{\text{ren}}, \tag{2.31}$$

which we have computed in (C4) in terms of the coefficients of the asymptotic expansions given in (B8). Comparing with the pressure $p = \langle T^{ii}\rangle$, given in (C9), we see that the free energy is equal to minus the pressure $\mathcal{F} = -p$. The expressions for the energy density $\varepsilon = \langle T^{00}\rangle$ and the charge density $n = \langle J^0\rangle$ can be found in (C8) and (C11), respectively. Using these expressions as well as (B45) and (B43), one finds the usual thermodynamic relation

$$\varepsilon + p = \mu n + Ts. \tag{2.32}$$

It will be convenient to use dimensionless quantities given in units of the scale introduced by the coupling for the scalar operator J. We will also omit a common factor that depends on the AdS radius L.[3] We then define the reduced quantities:

$$\begin{aligned} \varepsilon_r &= \frac{\varepsilon}{\frac{L^3}{16\pi G_5} J^{\frac{4}{2-\nu}}}, & p_r &= \frac{p}{\frac{L^3}{16\pi G_5} J^{\frac{4}{2-\nu}}}, \\ v_r &= \frac{\langle \mathcal{O}\rangle}{\frac{L^3}{16\pi G_5} J^{\frac{2+\nu}{2-\nu}}}, & n_r &= \frac{n}{\frac{L^3}{16\pi G_5} J^{\frac{3}{2-\nu}}}. \end{aligned} \tag{2.33}$$

The energy density and pressure depend on the enthalpy $w = \varepsilon + p$ and the expectation value of the scalar operator as

$$\varepsilon_r = \frac{3}{4} w_r + \frac{1}{2}(2-\nu) v_r \tag{2.34}$$

$$p_r = \frac{1}{4} w_r - \frac{1}{2}(2-\nu) v_r \tag{2.35}$$

$$v_r = -2\nu \frac{\alpha_+}{\alpha_-} \alpha_-^{\frac{2\nu}{\nu-2}}. \tag{2.36}$$

Note that in the linearized approximation the ratio α_+/α_- is independent of α_-.

Comparing the Reissner-Nordström solution for the background metric (2.5) with the expansions (B8) and renormalized values (C8), (C9), one can write the enthalpy as

[3] $L^3/G_5 \propto N_c^2$ following the usual AdS/CFT dictionary, so this just amounts to omitting a constant factor proportional to the number of degrees of freedom of the theory.

$$w_r = \frac{4M}{J^{\frac{4}{2-\nu}}L^8} = \frac{4r_H^4}{J^{\frac{4}{2-\nu}}L^8}(1+\mathcal{Q}^2) + O\left(\frac{J^2}{J^{\frac{4}{2-\nu}}}\right). \tag{2.37}$$

Neglecting the subleading terms and using (2.24), this can be written as

$$w_r \simeq 4\alpha_-^{\frac{4}{\nu-2}}(1+\mathcal{Q}^2). \tag{2.38}$$

D. Speed of sound

There are several possible definitions of the speed of sound in a charged system, depending on which thermodynamic quantities are held fixed. The speed of the sound waves is usually associated with a quantity called the adiabatic speed of sound, but for us it will be easier to compute the isothermal speed of sound. The difference between the two is proportional to the ratio T/μ, so the distinction is unimportant for large values of the chemical potential. In our calculation, we can vary the relative values of the temperature and chemical potential with respect to the scale fixed by the symmetry breaking coupling J. Through (2.24), those can be parametrized by variations of α_- and $\mathcal{Q}$. An isothermal variation $t_r =$ constant will satisfy

$$\alpha_-(\mathcal{Q}) = (\pi t_r)^{\nu-2}\left(1-\frac{\mathcal{Q}^2}{2}\right)^{2-\nu}. \tag{2.39}$$

The changes in the enthalpy and the vacuum expectation value (VEV) for large values of the chemical potential are

$$dw_r \simeq 24\alpha_-^{\frac{4}{\nu-2}}\mathcal{Q}\frac{2+\mathcal{Q}^2}{2-\mathcal{Q}^2}d\mathcal{Q} \tag{2.40}$$

$$dv_r \simeq -2\nu\alpha_-^{\frac{2\nu}{\nu-2}}\left[4\nu\frac{\mathcal{Q}}{2-\mathcal{Q}^2}\frac{\alpha_+}{\alpha_-}+\frac{d}{d\mathcal{Q}}\left(\frac{\alpha_+}{\alpha_-}\right)\right]d\mathcal{Q}, \tag{2.41}$$

leading to the ratio

$$\frac{dv_r}{dw_r} = -\frac{\nu}{3(2+\mathcal{Q}^2)}\alpha_-^2\left[\nu\frac{\alpha_+}{\alpha_-}+\frac{2-\mathcal{Q}^2}{4\mathcal{Q}}\frac{d}{d\mathcal{Q}}\left(\frac{\alpha_+}{\alpha_-}\right)\right]. \tag{2.42}$$

The isothermal speed of sound becomes in turn

$$v_s^2 = \left(\frac{\partial p_r}{\partial \epsilon_r}\right)_{t_r} = \frac{1}{3}\frac{1-2(2-\nu)\frac{dv_r}{dw_r}}{1+\frac{2}{3}(2-\nu)\frac{dv_r}{dw_r}} \simeq \frac{1}{3}\left(1-\frac{8}{3}(2-\nu)\frac{dv_r}{dw_r}\right). \tag{2.43}$$

At large values of the chemical potential, the solution is near extremal, $\mathcal{Q} \simeq \sqrt{2}$, and

$$\alpha_-^2 \simeq \left(\sqrt{\frac{2}{3}}\mu_r\right)^{2\nu-4} \ll 1, \tag{2.44}$$

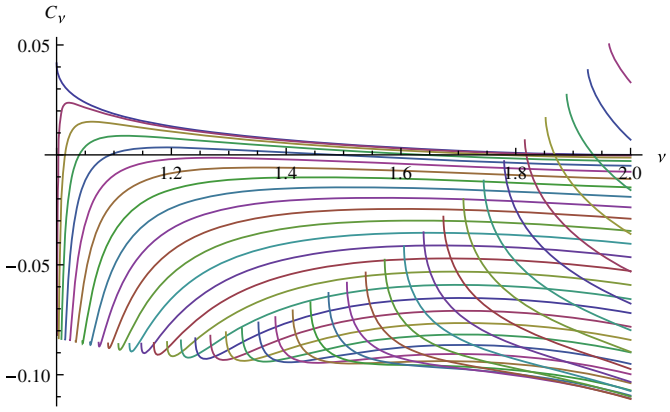

FIG. 1. C_ν vs ν $(1 \le \nu \le 2)$ for different values of $0 \le q < \sqrt{6}$. For $q = 0$ (the upper curve), $C_\nu > 0\ \forall\nu$, but as q increases, a range of values of ν exists for which $C_\nu < 0$. If q is close to $\sqrt{6}$, then C_ν becomes positive again.

while the speed of sound becomes

$$v_s^2 \simeq \frac{1}{3}(1+4C_\nu\mu_r^{2\nu-4}). \tag{2.45}$$

The coefficient that appears in the correction to the conformal value is

$$C_\nu = \frac{1}{8}\left(\frac{2}{3}\right)^\nu\nu^2(2-\nu)\frac{\alpha_+}{\alpha_-}, \tag{2.46}$$

where the value of the ratio α_+/α_- is given in (2.23). The sign of C_ν determines whether the speed of sound is above the conformal value (positive C_ν) or below (negative). As one can see in Fig. 1, there are values of ν and q for which $C_\nu > 0$ is possible. In particular, for $q = 0$ the speed of sound is above the conformal value for any ν.

We have determined the asymptotic form of the speed of sound at very large densities. When μ_r/t_r is finite, there will be temperature-dependent corrections, and eventually, for $\mu_r/t_r \ll 1$, one should recover the results of Refs. [20,21] and find that the speed of sound is always below the conformal value. Using our numerical solutions, we plot the speed of sound as a function of the chemical potential for fixed values of the temperature in Fig. 2. We have chosen q and Δ in such a way that the near-extremal analysis predicts an asymptotic speed of sound above the conformal value, which can be appreciated in the large-μ_r part of the plot. For small values of μ_r, we observe that indeed the speed of sound falls below the conformal value. One also notices that as t_r is increased, the speed of sound becomes globally closer to the conformal value, as expected. The position of the maximum in the speed of sound depends strongly on the temperature, and, not surprisingly, it gets pushed to larger values of the chemical potential as the temperature is increased. The maximum amplitude seems to become steeper as the temperature is

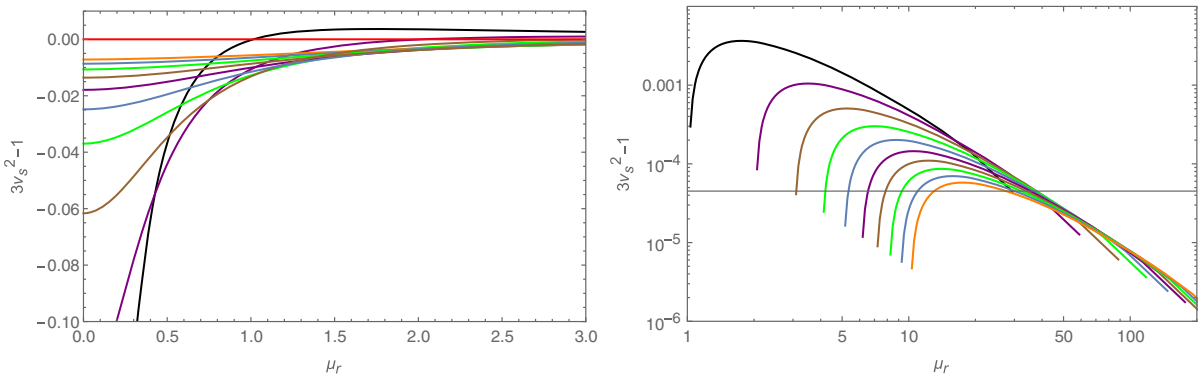

FIG. 2. Left figure: $3v_s^2 - 1$ as a function of chemical potential for fixed values of the temperature. The black curve (lowest at $\mu_r = 0$) is for $t_r = 0.1$, and the orange curve (highest at $\mu_r = 0$) is for $t_r = 1$. Curves in between have intermediate values separated by $\Delta t_r = 0.1$ steps. We have taken $q \approx 10^{-5}$, $\nu = 1.1$. Right figure: the same plot in logarithmic scale, from where one can see the maximum more clearly.

lowered, which suggests that the stiffest equations of state would be realized at very low temperatures and chemical potentials of order of the scale set by the relevant coupling.

E. Stability

We have confirmed the existence of finite density states for which the bound on the speed of sound is violated in holographic models with a UV fixed point. Note that violations were also observed in Ref. [27] at zero density, but the states for which this happened are unstable [28], so they may be discarded as unphysical. In principle, the same could happen for the states we are considering here, so it is important to check the stability of our solutions. A full-fledged analysis would require a study of the full spectrum of quasinormal modes at finite frequency and momentum. This is beyond the scope of the present paper, but we will analyze stability against the formation of a homogeneous condensate, which is usually the first kind of instability one encounters as the density is increased. This implies that we will restrict the discussion to zero momentum modes. Other instabilities may occur for nonzero momentum that would involve the breaking of translational and/or rotational symmetries; see e.g. Refs. [40–42].

At zero chemical potential and finite temperature, the state will be dual to a thermal state of a CFT. If the relevant coupling is zero, $J = 0$, the expectation value of the scalar operator will vanish. Technically, there is no solution to the equations of motion for the scalar such that one has a solution which is both normalizable and regular at the black hole horizon at zero frequency (we should remark that we are discussing configurations for which the scalar is close to the critical point of the potential, $\phi = 0$). There are normalizable and regular solutions that correspond to the quasinormal modes of the scalar field for complex values of the frequency. Stability of the large temperature state implies that those modes are located on the lower complex frequency plane.

If we turn on the chemical potential and start increasing its value, eventually there could be a point where a zero frequency normalizable and regular solution exists for the scalar. This can be seen as having a quasinormal mode that moves on the complex frequency plane as the chemical potential is varied and reaches the origin. Further increasing the chemical potential typically makes the quasinormal mode migrate to the upper complex frequency plane, thus becoming an instability. Therefore, one can determine the onset of the instability as the point where a regular and normalizable solution appears for the first time. From the field theory perspective, this is the critical point that marks the onset of spontaneous symmetry breaking and the formation of a condensate.

The form of the near-extremal solutions suggests that if the bound (2.21) is not satisfied, the oscillatory behavior of the coefficients will probably lead to the appearance of zero frequency quasinormal modes and hence instabilities, so this puts a bound on the charge of the scalar relative to its dimension. However, this does not show whether an instability appeared before the near-extremal regime was reached, and so we need to resort to the numerical solutions to shed some light on this issue. In Fig. 3, we plot the dimensionless ratio of the expectation value and the relevant coupling, in terms of the normalizable and non-normalizable coefficients of the numerical solutions, for different values of $\mathcal{Q} \propto \mu_r/t_r$. At the points where the ratio becomes zero, there is a zero frequency quasinormal mode, and most likely there will be an instability at larger values of $\mathcal{Q}$. In all cases, the plots show that the onset of the instability ventures into the nonextremal region only for values of the charge of the scalar q that are above the bound (2.21). Therefore, as long as the values of the dimension and the charge are such that the near-extremal solution is stable, we do not expect the solution to be unstable against condensation. Keeping in mind the possibility of having other instabilities, we conclude that the speed of sound bound can be violated in physical states at large densities.

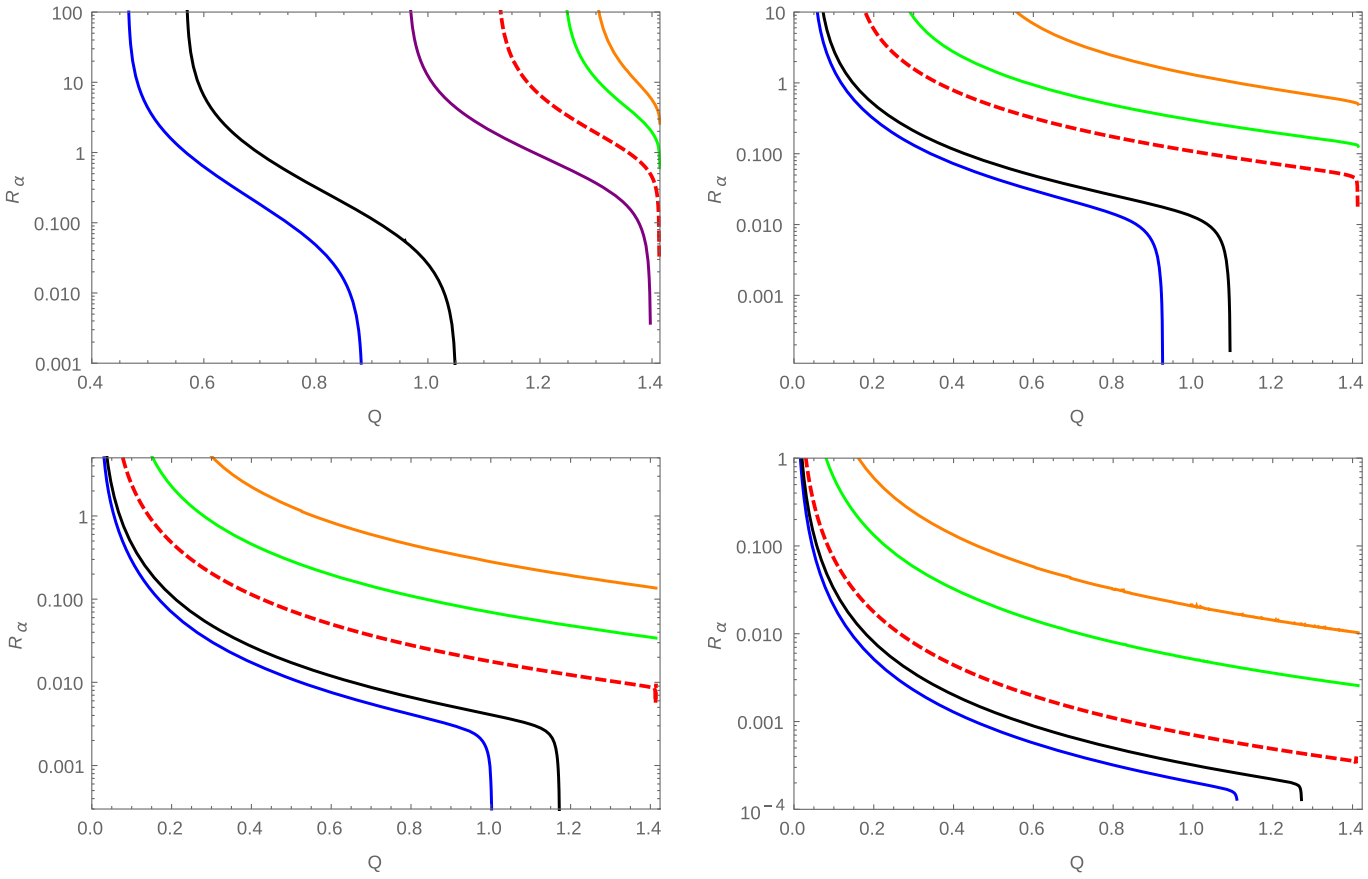

FIG. 3. Ratio of non-normalizable over normalizable coefficients of zero frequency regular solutions $R_\alpha = \alpha_-/\alpha_+$ as a function of $\mathcal{Q} \propto \mu_r/t_r$. The curves represent different values of the charge of the scalar: $q = 0.5$ (orange), $q = 1$ (green), $q = 4$ (black), and $q = 5$ (blue). For $\nu = 1$, we have plotted in addition the curve for $q = 2$ (purple), corresponding to the string theory model introduced in Sec. III. The red dashed curve denotes the approximate value of the charge q^* at which the first instability appears at $\mathcal{Q} = \sqrt{2} - 10^{-3}$. Each plot corresponds to a different value of the conformal dimensions of the scalar. From left to right and top to bottom: $\nu = 1$, $q^* \simeq 1.47$; $\nu = 1.1$, $q^* \simeq 1.64$; $\nu = 1.3$, $q^* \simeq 1.97$; and $\nu = 1.6$, $q^* \simeq 2.44$. As the conformal dimension is increased, the onset of the instability for a fixed q happens at larger values of μ_r/t_r.

III. SPEED OF SOUND IN *R*-CHARGED STATES

In the previous section, we found a family of models for which the bound on the speed of sound was violated. Our approach in this was bottom up; we considered a generic Einstein-Maxwell action with a minimally coupled charged scalar, but we did not try to embed it in any string theory construction. A natural concern is whether the results we obtained also apply in a bona fide gravity dual or whether the additional structures in string theory will always restrict parameters in such a way that the bound is preserved.

In order to answer this question, we will study a closely related string theory model. The field theory is $\mathcal{N} = 4$ $SU(N_c)$ super–Yang-Mills at nonzero R-charge density. There are a variety of charged states that have a holographic dual description in terms of rotating branes and giant gravitons [43–45] in an asymptotically $AdS_5 \times S^5$ space. A subclass is captured by the consistent truncation of five-dimensional $\mathcal{N} = 8$ SUGRA found in Ref. [46] (the truncation is nicely presented in Ref. [47], which we follow closely). There are three $U(1)$ gauge fields $A_\mu^{(I)}$, $I = 1, 2, 3$ corresponding to the three commuting R-charges in the Cartan subgroup of the $SU(4)$ R-symmetry group. There are also four complex scalars $\zeta_i = \tanh(\varphi_i)e^{i\theta_i}$, $i = 1, 2, 3, 4$ dual to the gaugino bilinears

$$\varphi_i \leftrightarrow \mathrm{tr}\lambda_i\lambda_i + \mathrm{H.c.}, \tag{3.1}$$

and two real scalars α, β dual to the $\mathcal{N} = 4$ scalar bilinears

$$\begin{aligned}\alpha &\leftrightarrow \mathrm{tr}(X_1^2 + X_2^2 + X_3^2 + X_4^4 - 2X_5^2 - 2X_6^2),\\ \beta &\leftrightarrow \mathrm{tr}(X_1^2 + X_2^2 - X_3^2 - X_4^2).\end{aligned} \tag{3.2}$$

For convenience, we define $\rho = e^\alpha$ and $\nu = e^\beta$, whereby the Lagrangian density becomes

$$e^{-1}\mathcal{L} = \frac{1}{4}R - \frac{1}{4g^2}[\rho^4\nu^{-4}F^{(1)}_{\mu\nu}F^{(1)\mu\nu} + \rho^4\nu^4F^{(2)}_{\mu\nu}F^{(2)\mu\nu} + \rho^{-8}F^{(3)}_{\mu\nu}F^{(3)\mu\nu}] + \frac{1}{2}\sum_{i=1}^{4}(\partial_\mu\varphi_i)^2 + 3(\partial_\mu\alpha)^2 + (\partial_\mu\beta)^2 + \frac{1}{8}\sum_i \sinh^2(2\varphi_i)(\partial_\mu\theta_i + c_{iI}A^{(I)}_\mu)^2 - V, \tag{3.3}$$

where

$$c_{iI} = \begin{pmatrix} 1 & 1 & -1 \\ 1 & -1 & 1 \\ -1 & 1 & 1 \\ -1 & -1 & -1 \end{pmatrix}. \tag{3.4}$$

The scalar potential is determined by a superpotential W as follows [48],

$$V = \frac{g^2}{8}\left[\frac{1}{6}\left(\frac{\partial W}{\partial\alpha}\right)^2 + \frac{1}{2}\left(\frac{\partial W}{\partial\beta}\right)^2 + \sum_{i=1}^{4}\left(\frac{\partial W}{\partial\varphi_i}\right)^2\right] - \frac{g^2}{3}W^2, \tag{3.5}$$

where

$$W = -\frac{1}{4\rho^2\nu^2}[(1+\nu^4-\nu^2\rho^6)\cosh(2\varphi_1) + (-1+\nu^4+\nu^2\rho^6)\cosh(2\varphi_2) + (1-\nu^4\nu^2\rho^6)\cos(2\varphi_3) + (1+\nu^4+\nu^2\rho^6)\cos(2\varphi_4)]. \tag{3.6}$$

When the three charges are equal, $A^{(I)}_\mu = 2A_\mu/\sqrt{3}$, and the scalars are turned off, the SUGRA action reduces to Einstein-Maxwell with a cosmological constant, and AdS Reissner-Nordström is a solution to the equations of motion [49,50] (see also Ref. [47] for more general charged black hole solutions).

If we take the scalars into account but remain in the equal charge case, then it is consistent with the equations of motion to set $\alpha = \beta = 0$. By setting $\varphi_i = \varphi/(2\sqrt{2})$ and

$$\theta_1 = \theta_2 = \theta_3 = -\theta/\sqrt{3}, \qquad \theta_4 = \sqrt{3}\theta, \tag{3.7}$$

the action becomes

$$e^{-1}\mathcal{L} = \frac{1}{4}R - \frac{1}{g^2}F_{\mu\nu}F^{\mu\nu} + \frac{1}{4}(\partial_\mu\varphi)^2 + \frac{1}{2}\sinh^2\left(\frac{\varphi}{\sqrt{2}}\right)(\partial_\mu\theta - 2A_\mu)^2 - V_\varphi, \tag{3.8}$$

where

$$V_\varphi = -\frac{3g^2}{16}(3+\cosh(\sqrt{2}\varphi)). \tag{3.9}$$

The coupling constant g is related to the AdS radius as $g = 2/L$. If we expand to quadratic order in φ, we get that the scalar terms of the action are

$$e^{-1}\mathcal{L}_\varphi \simeq \frac{1}{4}\left[(\partial_\mu\varphi)^2 + \varphi^2(\partial_\mu\theta - 2A_\mu)^2 - \frac{12}{L^2} - \frac{3}{L^2}\varphi^2\right] = \frac{1}{4}\left[|D_\mu\phi|^2 - \frac{12}{L^2} - \frac{3}{L^2}|\phi|^2\right]. \tag{3.10}$$

In this Lagrangian, we have defined the complex scalar field $\phi = \varphi e^{i\theta}$ and the covariant derivative $D_\mu\phi = \partial_\mu\phi - 2iA_\mu\phi$. Therefore, for a small amplitude of the scalar field, the dynamics reduce to those of a field of charge $q = 2$ and mass $m^2L^2 = -3$, dual to a $\Delta = 3$ scalar operator which is a combination of components of the gaugino bilinears. The coefficient of the quartic term as in (B11) is $V_4 = -1$. This is within the class of models we are considering, but the dimension is integer, and the relation between the dimension and the charge does not satisfy the bound (2.21). This introduces some technical complications, as the asymptotic expansion of the scalar close to the AdS boundary is modified by the introduction of logarithmic terms

$$\phi \simeq \frac{L^2}{r}\tilde{\phi}_{(0,0)} + \frac{L^6}{r^3}\tilde{\phi}_{(2,1)}\log\frac{r}{L} + \left(\frac{L}{r}\right)^3 L^3\phi_{(0,0)}. \tag{3.11}$$

We will redo the analysis for this special case in the following.

A. Solutions

The equations of motion for the scalar field can be obtained from (2.13) by setting $\nu = 1$ in (2.14). The leading terms in the expansion close to the AdS boundary are

$$\phi \simeq \alpha_- u^{1/2} + \tilde{\alpha}_+ u^{3/2}\log u + \alpha_+ u^{3/2}, \tag{3.12}$$

where $\tilde{\alpha}_+$ is determined by α_-. We can find an analytic near-extremal solution following the same procedure discussed in the previous section, although the details are slightly different because the dimension of the scalar operator is an integer number. The full calculation can be found in Appendix A 2. The ratio between normalizable and non-normalizable coefficients takes the same form as in the previous examples (2.19), but in this case $\lambda = i/\sqrt{2}$ is complex [the bound (2.21) is not satisfied]. To go beyond the near-extremal limit, we use numerics, and the solutions are computed in the same way as in the previous section.

Once we have obtained the numerical solution, we extract the values of the coefficients of the normalizable and non-normalizable modes by evaluating the solution at

the boundary cutoff $u=\epsilon_0$. For $\nu=1$, we define the numerical values as

$$(\alpha_-)_n = u^{-1/2}\phi_n(u)|_{u=\epsilon_0} \tag{3.13}$$

$$(\tilde{\alpha}_+)_n = u\partial_u^2[u^{-1/2}\phi_n(u)]|_{u=\epsilon_0} \tag{3.14}$$

$$(\alpha_+)_n = \partial_u[u^{-1/2}\phi_n(u)] - (\tilde{\alpha}_+)_n(\log u+1)|_{u=\epsilon_0}. \tag{3.15}$$

These values are determined by $\mathcal{Q}$ and q. In the numerical calculation, we have fixed the amplitude of the scalar field. Since the equations of motion are linear, we can again generate a full set of values by doing a trivial rescaling,

$$\alpha_- = a(\alpha_-)_n, \quad \tilde{\alpha}_+ = a(\tilde{\alpha}_+)_n, \quad \alpha_+ = a(\alpha_+)_n, \tag{3.16}$$

for some real number a. We determine the value of a by fixing the temperature in units of the relevant coupling (3.18) for each value of $\mathcal{Q}$.

B. Thermodynamics

We have computed the free energy density in (C14), in terms of the coefficients of the asymptotic expansions given in (B12). Comparing with the pressure $p=\langle T^{ii}\rangle$, given in (C16), we see that it is equal to minus the pressure $\mathcal{F}=-p$. The expressions for the energy density $\varepsilon=\langle T^{00}\rangle$ and the charge density $n=\langle J^0\rangle$ can be found in (C15) and (C18), respectively. Using these expressions as well as (B48) and (B43), one finds the usual thermodynamic relation

$$\varepsilon + p = \mu n + Ts. \tag{3.17}$$

We again introduce the reduced quantities (2.24) and (2.33) with $\nu=1$; in particular, the reduced temperature and chemical potential read

$$\mu_r \equiv \frac{\mu}{J} = \frac{\sqrt{3}}{2}\frac{\mathcal{Q}}{\alpha_-}, \qquad t_r \equiv \frac{T}{J} = \frac{2-\mathcal{Q}^2}{2\pi\alpha_-}. \tag{3.18}$$

The energy density and pressure depend on the enthalpy $w=\varepsilon+p$ and the expectation value of the scalar operator as

$$\varepsilon_r = \frac{3}{4}w_r + \frac{1}{2}\tilde{v}_r \tag{3.19}$$

$$p_r = \frac{1}{4}w_r - \frac{1}{2}\tilde{v}_r \tag{3.20}$$

$$\tilde{v}_r = v_r - \frac{1}{2}q^2\mu_r^2 + \left(\frac{1}{6}+\frac{V_4}{4}\right). \tag{3.21}$$

Comparing with the Reissner-Nordström solution for the background metric (2.5) with the expansions (B12) and using the expressions for the renormalized values (C22) and (C23) and the relation with the coefficients in the u expansion (B22), the leading order contributions are

$$w_r = 4\frac{1}{\alpha_-^4}(1+\mathcal{Q}^2) + O\left(\frac{\log\alpha_-}{\alpha_-^2}\right) \tag{3.22}$$

$$\tilde{v}_r = -2\frac{\alpha_+}{\alpha_-}\frac{1}{\alpha_-^2} + q^2\mu_r^2\log\alpha_- + \kappa_1 q^2\mu_r^2 + O(\log\alpha_-). \tag{3.23}$$

C. Speed of sound and stability

Through (3.18), an isothermal variation will satisfy

$$\alpha_-(\mathcal{Q}) = \frac{1}{\pi t_r}\left(1-\frac{\mathcal{Q}^2}{2}\right). \tag{3.24}$$

For asymptotically large values of the chemical potential, the changes in enthalpy and the term associated to the breaking of conformal invariance are, to leading order,

$$dw_r \simeq 24\frac{\mathcal{Q}}{\alpha_-^4}\frac{2+\mathcal{Q}^2}{2-\mathcal{Q}^2}d\mathcal{Q} \tag{3.25}$$

$$d\tilde{v}_r \simeq \frac{3}{2}q^2\mathcal{Q}\frac{2+\mathcal{Q}^2}{2-\mathcal{Q}^2}\frac{\log\alpha_-}{\alpha_-^2}d\mathcal{Q}, \tag{3.26}$$

giving

$$\frac{dv_r}{dw_r} \simeq \frac{q^2}{16}\alpha_-^2\log\alpha_-. \tag{3.27}$$

Similarly, the isothermal speed of sound is

$$v_s^2 = \left(\frac{\partial p_r}{\partial\epsilon_r}\right)_{t_r} \simeq \frac{1}{3}\left(1-\frac{8}{3}\frac{dv_r}{dw_r}\right). \tag{3.28}$$

At large values of the chemical potential, the solution is near-extremal $\mathcal{Q}\simeq\sqrt{2}$ and

$$\alpha_-^2 \simeq \frac{3}{2\mu_r^2} \ll 1, \tag{3.29}$$

while the speed of sound becomes

$$v_s^2 \simeq \frac{1}{3}\left(1+\frac{1}{4}q^2\frac{\log\mu_r}{\mu_r^2}\right). \tag{3.30}$$

The speed of sound will approach the conformal value from above at asymptotically large densities. However, we expect to have instabilities in the extremal limit, and in order to go beyond this limit, we will resort to numerics. The result will depend on the choice of a finite counterterm κ_1 that is shown explicitly in (C22) and (C23). We will set

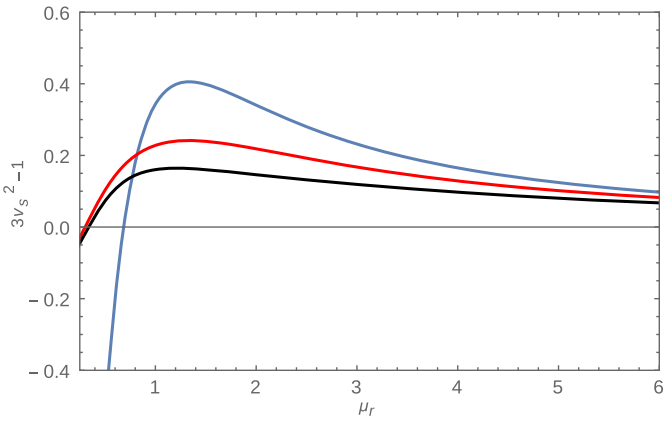

FIG. 4. $3v_s^2 - 1$ as a function of the chemical potential for different values of the temperature: $t_r = 0.1$ (blue), $t_r = 0.5$ (red), and $t_r = 1$ (black). Notice that for all values of the temperature, the curves approach the conformal value at large values of the chemical potential.

$\kappa_1 = 0$, noting that as long as this parameter is not large, it will not qualitatively affect to the results. We present the deviation of the isothermal speed of sound from the conformal value, $3v_s^2 - 1$, in Fig. 4 for different values of the temperature. We see that the speed of sound remains above the conformal value until relatively low values of the chemical potential. The value $\mu_r = 1$ corresponds to $\mathcal{Q} \simeq 0.83\sqrt{2}, 0.43\sqrt{2}, 0.24\sqrt{2}$ for $t_r = 0.1$, 0.5, 1, respectively.

As we found in the previous section (see Fig. 3 for $\nu = 1$), we expect the instability that will trigger the formation of a homogeneous condensate to appear close to the near-extremal regime, since we found a critical charge of $q^* \simeq 1.47$ for $\mathcal{Q} = \sqrt{2} - 10^{-3}$, which is close to the value we have in the R-charged solution $q = 2$. For $q = 2$, we find that the instability appears at $\mathcal{Q}^* \simeq 1.396$ (purple curve in Fig. 3). This corresponds to values of the chemical potential $\mu_r \simeq 14.8, 74.2, 148.4$ for $t_r = 0.1$, 0.5, 1, respectively. We have thus shown that the speed of sound can be violated in the R-charged state with no obvious instabilities.

IV. CONCLUSIONS AND OUTLOOK

According to current understanding, it appears likely that the speed of sound in neutron star matter exceeds the conformal value $v_s = 1/\sqrt{3}$ in the dense nuclear matter phase [25]. Knowing that for ultradense quark matter, the speed of sound approaches this value from below, we are in practice left with two possibilities: either the quantity exhibits a discontinuous jump in a first order phase transition or it must continuously first decrease and then increase its value in the quark matter phase. The latter scenario has, however, been disfavored due to the lack of first principles calculations exhibiting speeds of sound larger than the conformal value in deconfined matter. In addition to perturbative calculations, this statement holds true for all known holographic setups that flow to a four-dimensional CFT in the UV, which has prompted speculation of a more fundamental speed of sound bound [20,21].

In the paper at hand, we have shown that the conjectured bound on the speed of sound in holographic models with UV fixed points is violated for a simple class of models involving RG flows triggered by relevant scalar operators charged under a global Abelian symmetry. Within this class, we were able to find a string theory example: a charged black hole dual to $\mathcal{N} = 4$ theory at finite R-charge density, deformed by a gaugino mass term. Since at very large densities an instability toward the formation of a homogeneous condensate will develop, we made sure that the violation occurs in the stable regime. We may conclude that there is no universal bound for the speed of sound in holographic models dual to ordinary four-dimensional relativistic field theories. This comes as good news for everyone wishing to build realistic holographic models for high-density nuclear or quark matter.

A natural extension of our work is clearly to go beyond the approximation of a small breaking of conformal invariance and study how high values the speed of sound can be maximally obtained. Of particular interest is to investigate whether large enough speeds can be obtained that would allow the building of stable hybrid stars with holographic quark matter in their cores. Continuing along these lines, it might be interesting to study the behavior of bottom-up models designed to match the properties of QCD at zero [51–55] and finite density [56] and to see if they give phenomenologically sensible results at very small temperatures.

A different but equally interesting challenge to pursue would be to find a top-down model with finite baryon (rather than R-charge) density. Quark matter is typically introduced by embedding probe branes in the geometry, and in the known examples where the theory is truly $(3 + 1)$-dimensional, the bound is satisfied even at finite density. This might change upon considering the backreaction of the branes. Solutions with backreacted flavors at finite density have been recently constructed in Refs. [57–60]. Another possibility is to take an alternative large-N limit where (anti)fundamental fields are extrapolated to two-index antisymmetric representations [61] and where operators with baryon charge map to gravitational modes. We leave these investigations for future work.

ACKNOWLEDGMENTS

N. J. and A. V. are supported by the Academy of Finland Grants No. 1273545, No. 1297472, and No. 1303622, while C. H. and D. R. F. are partially supported by the Spanish Grant No. MINECO-16-FPA2015-63667-P. C. H. is in addition supported by the Ramon y Cajal fellowship RYC-2012-10370, and D. R. F. is supported by the FC-15-GRUPIN-14-108 research grant from Principado

de Asturias. N. J. wishes to thank Long Island University and Stony Brook University for warm hospitality as well as the Nordita program on Black Holes and Emergent Spacetime and the Heraklion Workshop on Theoretical Physics for providing prolific environments during a time when this work was being finished.

APPENDIX A: NEAR-EXTREMAL SOLUTIONS

1. Noninteger Δ

a. Near-horizon solution

First, we expand (2.13) in the region close to the horizon. It is convenient to introduce a new radial coordinate v, defined as

$$u = 1 - \frac{4}{3}\epsilon v. \tag{A1}$$

We then expand (2.13) to leading order in ϵ. In this new coordinate, the horizon is located at $v = 0$, and the asymptotic region gets pushed to $v > 1/\epsilon \to \infty$. The solution to the equation of motion that is regular as $v \to 0$ is

$$\phi = \phi_H (1+v)^{-i\frac{q}{2\sqrt{6}}} {}_2F_1\left[\frac{1}{2} - i\frac{q}{2\sqrt{6}} - \frac{\lambda}{2\sqrt{3}}, \frac{1}{2} - i\frac{q}{2\sqrt{6}} + \frac{\lambda}{2\sqrt{3}}, 1, -v\right] + \text{c.c.}, \tag{A2}$$

where we have defined $\lambda = \sqrt{\nu^2 - \frac{q^2}{2} - 1}$ and where $\phi(0) = \phi_H$ is the value of the scalar field at the horizon. The expansion as $v \to \infty$ gives, to leading order,

$$\phi \sim \phi_H \left(C_- v^{-\frac{1}{2} - \frac{\lambda}{2\sqrt{3}}} + C_+ v^{-\frac{1}{2} + \frac{\lambda}{2\sqrt{3}}}\right), \tag{A3}$$

where

$$C_\pm = \frac{\Gamma\left(\pm\frac{\lambda}{\sqrt{3}}\right)}{\left|\Gamma\left(\frac{1}{2} - i\frac{q}{2\sqrt{6}} \pm \frac{\lambda}{2\sqrt{3}}\right)\right|^2}. \tag{A4}$$

b. Asymptotic solution

We can find the leading order solution simply setting $\epsilon \to 0$ in the equation, giving the solution in the extremal Reissner-Nordström geometry

$$\phi = \alpha_+ \varphi_+ + \alpha_- \varphi_-, \tag{A5}$$

where $\alpha_\pm$ are arbitrary coefficients and

$$\varphi_\pm = u^{1\pm\frac{\nu}{2}} (1-u)^{-\frac{1}{2} - \frac{|q-\lambda|}{q-\eta}\frac{\lambda}{2\sqrt{3}}} (1+2u)^{-\frac{1\pm\nu}{2} + \frac{|q-\lambda|}{q-\lambda}\frac{\lambda}{2\sqrt{3}}} \times {}_2F_1\left[\frac{1\pm\nu}{2} + \frac{|q-\lambda|}{2\sqrt{3}}, \frac{1\pm\nu}{2} - \frac{q+\lambda}{q-\lambda}\frac{|q-\lambda|}{2\sqrt{3}}, 1\pm\nu, \frac{3u}{1+2u}\right]. \tag{A6, A7}$$

Expanding close to the boundary $u \to 0$, the coefficients behave as

$$\varphi_\pm \sim u^{1\pm\frac{\nu}{2}}. \tag{A8}$$

Therefore, φ_+ is the normalizable mode, and φ_- is the non-normalizable mode. We now evaluate the solution at $u = 1 - \frac{4}{3}\epsilon v$ and expand for $\epsilon \to 0$. The expansion takes the same form as for the near-horizon solution

$$\varphi_\pm \sim \left(D_{\pm-} v^{-\frac{1}{2} - \frac{\lambda}{2\sqrt{3}}} + D_{\pm+} v^{-\frac{1}{2} + \frac{\lambda}{2\sqrt{3}}}\right). \tag{A9}$$

The coefficients and exponents depend on the sign of $q - \lambda$, but the final result is the same for both $q > \lambda$ and $\lambda < q$.

c. Matching

We have to match the coefficients of the near-horizon and asymptotic solutions in such a way that the leading order terms in the overlapping region (A3) and (A9) are the same. This gives the conditions

$$\alpha_+ D_{\pm+} + \alpha_- D_{\pm-} = \phi_H C_\pm, \tag{A10}$$

thus fixing α_+ and α_- in terms of ϕ_H and the coefficients of the expansion. In the end, we should fix the coefficient of the non-normalizable mode to be equal to the source of the dual operator. That fixes the value of the scalar at the horizon and the coefficient of the normalizable mode, both of which are also proportional to the source. The proportionality coefficient of the normalizable mode that determines the VEV of the dual operator is proportional to

$$\frac{\alpha_+}{\alpha_-} = -3^\nu \frac{\Gamma(1-\nu)\Gamma\left(\frac{1+\nu}{2} + \frac{\lambda+q}{2\sqrt{3}}\right)\Gamma\left(\frac{1+\nu}{2} + \frac{\lambda-q}{2\sqrt{3}}\right)}{\Gamma(1+\nu)\Gamma\left(\frac{1-\nu}{2} + \frac{\lambda+q}{2\sqrt{3}}\right)\Gamma\left(\frac{1-\nu}{2} + \frac{\lambda-q}{2\sqrt{3}}\right)} \times \frac{1 + \beta_1 \left(\frac{4\epsilon}{9}\right)^{\lambda/\sqrt{3}}}{1 + \beta_2 \left(\frac{4\epsilon}{9}\right)^{\lambda/\sqrt{3}}}, \tag{A11}$$

where

$$\beta_1 = \frac{\Gamma\left(-\frac{\lambda}{\sqrt{3}}\right)\Gamma\left(1 - \frac{\lambda}{\sqrt{3}}\right)}{\Gamma\left(\frac{\lambda}{\sqrt{3}}\right)\Gamma\left(1 + \frac{\lambda}{\sqrt{3}}\right)} \frac{\Gamma\left(\frac{1}{2} - i\frac{q}{2\sqrt{6}} + \frac{\lambda}{2\sqrt{3}}\right)\Gamma\left(\frac{1}{2} + i\frac{q}{2\sqrt{6}} + \frac{\lambda}{2\sqrt{3}}\right)}{\Gamma\left(\frac{1}{2} - i\frac{q}{2\sqrt{6}} - \frac{\lambda}{2\sqrt{3}}\right)\Gamma\left(\frac{1}{2} + i\frac{q}{2\sqrt{6}} - \frac{\lambda}{2\sqrt{3}}\right)} \times \frac{\Gamma\left(\frac{1-\nu}{2} + \frac{\lambda+q}{2\sqrt{3}}\right)\Gamma\left(\frac{1-\nu}{2} + \frac{\lambda-q}{2\sqrt{3}}\right)}{\Gamma\left(\frac{1-\nu}{2} - \frac{\lambda+q}{2\sqrt{3}}\right)\Gamma\left(\frac{1-\nu}{2} - \frac{\lambda-q}{2\sqrt{3}}\right)} \tag{A12}$$

and

$$\beta_2 = \frac{\cos\left(\frac{q\pi}{\sqrt{3}}\right) + \cos\left[\pi\left(\frac{\lambda}{\sqrt{3}} - \nu\right)\right]}{\cos\left(\frac{q\pi}{\sqrt{3}}\right) + \cos\left[\pi\left(\frac{\lambda}{\sqrt{3}} + \nu\right)\right]}\beta_1. \tag{A13}$$

The terms that go as $\sim\epsilon^{\lambda/\sqrt{3}}$ can be neglected only if $\lambda > 0$. This requires

$$\nu^2 > 1 + \frac{q^2}{2} \Rightarrow \Delta > 2 + \sqrt{1 + \frac{q^2}{2}}. \tag{A14}$$

If $q^2 \geq 6$, this is not possible for $\Delta < 4$.

2. Solutions for $\Delta = 3$

We can set $\nu = 1$ in Eq. (2.14) and follow the same procedure.

a. Near-horizon solution

We can convert the equation of motion in a hypergeometric equation by extracting a factor from the scalar field $\phi = (1+v)^{-i\frac{q}{2\sqrt{6}}}X$. The resulting equation is (we keep q as a parameter)

$$v(1+v)X'' + \left(1 + \left(2 - i\frac{q}{\sqrt{6}}\right)v\right)X' + \left(\frac{1}{4} - i\frac{q}{2\sqrt{6}}\right)X = 0. \tag{A15}$$

The regular solution is

$$X = {}_2F_1\left(\frac{1}{2}, \frac{1}{2} - i\frac{q}{\sqrt{6}}, 1, -v\right). \tag{A16}$$

In order to make the solution real, we combine it with the complex conjugate:

$$\phi = \frac{\phi_H}{2}\left[(1+v)^{-i\frac{q}{2\sqrt{6}}}{}_2F_1\left(\frac{1}{2}, \frac{1}{2} - i\frac{q}{\sqrt{6}}, 1, -v\right) + (1+v)^{i\frac{q}{2\sqrt{6}}}{}_2F_1\left(\frac{1}{2}, \frac{1}{2} + i\frac{q}{\sqrt{6}}, 1, -v\right)\right]. \tag{A17}$$

The expansion as $v \to \infty$ is

$$\phi \sim \frac{\phi_H}{2}\left(C_- v^{-\frac{1}{2} - i\frac{q}{2\sqrt{6}}} + C_+ v^{-\frac{1}{2} + i\frac{q}{2\sqrt{6}}}\right), \tag{A18}$$

where

$$C_\pm = \frac{\Gamma\left(\pm i\frac{q}{\sqrt{6}}\right)}{\sqrt{\pi}\Gamma\left(\frac{1}{2} \pm i\frac{q}{\sqrt{6}}\right)}. \tag{A19}$$

b. Asymptotic solution

We can find the leading order solution simply setting $\epsilon \to 0$ in (2.13):

$$\phi'' - \frac{1 + u + 4u^2}{u(1-u)(2u+1)}\phi' + \frac{3}{8}\frac{2 + (4+q^2)u}{u^2(1-u)^2(1+2u)^2}\phi = 0. \tag{A20}$$

We can convert this in a hypergeometric equation by defining

$$\hat{\varphi}_\mp = (2u+1)^{\pm i\frac{q}{2\sqrt{6}}}(1-u)^{-\frac{1}{2}\mp i\frac{q}{2\sqrt{6}}}u^{\frac{1}{2}}X_\mp\left[\frac{3u}{2u+1}\right] \tag{A21}$$

and changing variables to

$$z = \frac{3u}{2u+1}, \qquad u = \frac{z}{2z-3}. \tag{A22}$$

Equation (A20) becomes

$$z(1-z)X_\mp'' + \left(\pm i\frac{q}{\sqrt{6}}\right)zX_\mp' + \frac{q^2}{8}X_\mp = 0. \tag{A23}$$

The two independent solutions are

$$X_\mp = {}_2F_1\left(\frac{q}{2\sqrt{3}}\left(1 \mp \frac{i}{\sqrt{2}}\right), -\frac{q}{2\sqrt{3}}\left(1 \pm \frac{i}{\sqrt{2}}\right), 1 \mp i\frac{q}{\sqrt{6}}, 1 - z\right). \tag{A24}$$

The general scalar solution is thus

$$\phi = \hat{\alpha}_+\hat{\varphi}_+ + \hat{\alpha}_-\hat{\varphi}_-, \tag{A25}$$

where $\hat{\alpha}_\pm$ are arbitrary coefficients.

Expanding close to the boundary $u \to 0$,

$$\hat{\varphi}_\mp \sim A_\mp u^{1/2} + B_\mp u^{3/2}. \tag{A26}$$

The coefficients $A_\mp$ correspond to the non-normalizable mode, and the coefficients $B_\mp$ correspond to the normalizable mode. We define the non-normalizable φ_- and normalizable φ_+ modes as

$$\varphi_- = \frac{B_-\hat{\varphi}_+ - B_+\hat{\varphi}_-}{B_-A_+ - B_+A_-} \tag{A27}$$

$$\varphi_+ = \frac{A_-\hat{\varphi}_+ - A_+\hat{\varphi}_-}{A_-B_+ - A_+B_-}. \tag{A28}$$

The general solution is

$$\varphi = \alpha_+\varphi_+ + \alpha_-\varphi_-. \tag{A29}$$

We now evaluate the solution at $u = 1 - \frac{4}{3}\epsilon v$ and expand for $\epsilon \to 0$. The expansion takes the same form as for the near-horizon solution

$$\varphi_\pm \sim \left(D_{\pm-} v^{-\frac{1}{2}-i\frac{q}{2\sqrt{6}}} + D_{\pm+} v^{-\frac{1}{2}+i\frac{q}{2\sqrt{6}}}\right). \tag{A30}$$

c. Matching

We have to match the coefficients of the near-horizon and asymptotic solutions in such a way that the leading order terms in the overlapping region (A18) and (A30) are the same. This gives the conditions

$$\alpha_- D_{\pm-} + \alpha_+ D_{\pm+} = \phi_H C_\pm. \tag{A31}$$

This fixes α_- and α_+ in terms of ϕ_H and the coefficients of the expansion. In the end, we should fix the coefficient of the non-normalizable mode to be equal to the source of the dual operator. That fixes the value of the scalar at the horizon and the coefficient of the normalizable mode, both of which are also proportional to the source. The proportionality coefficient of the normalizable mode that determines the VEV of the dual operator is proportional to

$$\frac{\alpha_+}{\alpha_-} = \left[\frac{1}{2} - i\frac{\sqrt{6}q}{4} - \frac{3}{8}q^2\left(H_{\frac{2+i\sqrt{2}}{4\sqrt{3}}q} + H_{\frac{-2+i\sqrt{2}}{4\sqrt{3}}q} + \log 3\right)\right] \times \frac{1+\beta_1\left(\frac{4\epsilon}{9}\right)^{iq/\sqrt{6}}}{1+\beta_2\left(\frac{4\epsilon}{9}\right)^{iq/\sqrt{6}}}, \tag{A32}$$

where

$$\beta_2 = \frac{-3+i\sqrt{6}q}{q^2\Gamma(qc)}\left[\frac{\Gamma(1-i\frac{q}{\sqrt{6}})}{\Gamma(i\frac{q}{\sqrt{6}})}\right]^2 \times \frac{\Gamma\left(-\frac{1}{2}+i\frac{q}{\sqrt{6}}\right)}{\Gamma\left(\frac{1}{2}-i\frac{q}{\sqrt{6}}\right)}\frac{\Gamma\left(\frac{2+i\sqrt{2}}{4\sqrt{3}}q\right)\Gamma\left(\frac{-2+i\sqrt{2}}{4\sqrt{3}}q\right)}{\Gamma\left(\frac{2-i\sqrt{2}}{4\sqrt{3}}q\right)}. \tag{A33}$$

Here,

$$c = -\frac{\sqrt{1+i2\sqrt{2}}}{2\sqrt{6}} \simeq -0.29 - 0.2i. \tag{A34}$$

The other coefficient is

$$\beta_1 = \frac{1+i\sqrt{\frac{3}{2}}q - \frac{3}{4}q^2\left(-1+H_{\frac{2-i\sqrt{2}}{4\sqrt{3}}q} + H_{cq} + \log 3\right)}{1-i\sqrt{\frac{3}{2}}q - \frac{3}{4}q^2\left(-1+H_{\frac{2+i\sqrt{2}}{4\sqrt{3}}q} + H_{\frac{-2+i\sqrt{2}}{4\sqrt{3}}q} + \log 3\right)}\beta_2. \tag{A35}$$

Note that the terms that go as $\sim\epsilon^{iq/\sqrt{6}}$ cannot be neglected.

APPENDIX B: USEFUL FORMULAS

1. Equations of motion and boundary expansions

In the presence of a nonzero scalar $\phi(r)$ and gauge field $A_0(r)$, we consider an ansatz for the metric of the form

$$ds^2 = \frac{L^2}{r^2 f(r)}dr^2 + \frac{r^2}{L^2}e^{2A(r)}(-f(r)dt^2 + dx^2). \tag{B1}$$

The equations of motion (2.4) become

$$0 = f'' + \left(4A' + \frac{5}{r}\right)f' - L^4 e^{-2A}\left[\frac{4}{r^2}A_0'^2 + \frac{2q^2}{r^4 f}A_0^2\phi^2\right] \tag{B2}$$

$$0 = A_0'' + \left(2A' + \frac{3}{r}\right)A_0' - q^2\frac{\phi^2}{2r^2 f}A_0 \tag{B3}$$

$$0 = A'' + \frac{1}{r}A' + \frac{1}{3}\left(\phi'^2 + L^4 q^2 e^{-2A}\frac{A_0^2\phi^2}{r^4 f^2}\right) \tag{B4}$$

$$0 = \phi'' + \left(4A' + \frac{f'}{f} + \frac{5}{r}\right)\phi' + \left[L^4 q^2 e^{-2A}\frac{A_0^2}{r^4 f^2} - \frac{\Delta(\Delta-4)}{r^2 f}\right]\phi \tag{B5}$$

$$0 = L^4 e^{-2A}\frac{A_0'^2}{r^2 f} + A'\left(\frac{12}{r} + \frac{3}{2}\frac{f'}{f} + 6A'\right) + \frac{6}{r^2}\left(1-\frac{1}{f}\right) + \frac{3f'}{2rf} - \frac{1}{2}\phi'^2 + \phi^2\left[\frac{\Delta(\Delta-4)}{2r^2 f} - L^4 q^2 e^{-2A}\frac{A_0^2}{2r^4 f^2}\right]. \tag{B6}$$

Assuming the mass of the scalar is such that there are no logarithmic terms (noninteger Δ), the gravity solution admits the series expansion

$$f = 1 + \sum_{n,m}\frac{f_{(n,m)}}{r^{n+m\Delta}}, \qquad A_0 = \mu + \sum_{n,m}\frac{A_{0(n,m)}}{r^{n+m\Delta}},$$
$$A = \sum_{m,n}\frac{A_{(n,m)}}{r^{n+m\Delta}}$$
$$\phi = \frac{L^{2(4-\Delta)}}{r^{4-\Delta}}\sum_{n,m}\frac{\tilde{\phi}_{(n,m)}}{r^{n+m\Delta}} + \frac{L^{2\Delta}}{r^\Delta}\sum_{n,m}\frac{\phi_{(n,m)}}{r^{n+m\Delta}}, \tag{B7}$$

where we will identify $\tilde{\phi}_{(0,0)}$ as the source and $\phi_{(0,0)}$ as the VEV, with dimensions $4-\Delta$ and Δ, respectively. Using the equations of motion, we fix the leading coefficients to be

$$\begin{aligned}
\phi &\sim \frac{L^{2(4-\Delta)}}{r^{4-\Delta}}\tilde{\phi}_{(0,0)} + \frac{L^{2\Delta}}{r^{\Delta}}\phi_{(0,0)} + \frac{L^{6(4-\Delta)}}{r^{3(4-\Delta)}}\frac{\Delta-4}{12(\Delta-3)}\tilde{\phi}^3_{(0,0)} + \frac{L^{2(6-\Delta)}}{r^{6-\Delta}}\frac{\mu^2 q^2}{4(\Delta-3)}\tilde{\phi}_{(0,0)} + \cdots \\
A &\sim -\frac{1}{12}\frac{L^{4(4-\Delta)}}{r^{2(4-\Delta)}}\tilde{\phi}^2_{(0,0)} - \frac{L^{8(4-\Delta)}}{r^{4(4-\Delta)}}\frac{\Delta-4}{96(\Delta-3)}\tilde{\phi}^4_{(0,0)} - \frac{L^{5(4-\Delta)}}{r^{2(5-\Delta)}}\frac{\mu^2 q^2(\Delta^2-8\Delta+18)}{24(\Delta-3)(\Delta-5)^2}\tilde{\phi}^2_{(0,0)} + \frac{L^8}{r^4}\frac{\Delta(\Delta-4)}{24}\tilde{\phi}_{(0,0)}\phi_{(0,0)} + \cdots \\
f &\sim 1 + \frac{L^8}{r^4}f_{(4,0)} + \frac{L^{4(5-\Delta)}}{r^{2(5-\Delta)}}\frac{\mu^2 q^2}{2(\Delta-3)(\Delta-5)}\tilde{\phi}^2_{(0,0)} + \cdots \\
A_0 &\sim \mu + \frac{L^4}{r^2}A_{0(2,0)} + \frac{L^{4(4-\Delta)}}{r^{2(4-\Delta)}}\frac{\mu q^2}{8(\Delta^2-7\Delta+12)}\tilde{\phi}^2_{(0,0)} + \cdots .
\end{aligned} \tag{B8}$$

For $\Delta = 3$, the expansions are modified due to the presence of logarithmic terms, and the asymptotic behavior of the scalar field becomes

$$\phi_{r\to\infty} \sim \frac{L^2}{r}\tilde{\phi}_{(0,0)} + \frac{L^6}{r^3}\left(\tilde{\phi}_{(1,1)}\log\frac{r}{L} + \phi_{(0,0)}\right) + \cdots, \tag{B9}$$

where again we identify $\tilde{\phi}_{(0,0)}$ as the source and $\phi_{(0,0)}$ as the VEV. Due to the presence of the logarithmic term, which is leading, the near-boundary series expansions for the gauge field and warp factors differ this time from (B8),

$$f = 1 + \sum_{n\geq m}\frac{f_{(n,m)}}{r^n}\left[\log\left(\frac{r}{L}\right)\right]^m, \qquad A_0 = \mu + \sum_{n\geq m}\frac{A_{0(n,m)}}{r^n}\left[\log\left(\frac{r}{L}\right)\right]^m, \qquad A = \sum_{n\geq m}\frac{A_{(n,m)}}{r^n}\left[\log\left(\frac{r}{L}\right)\right]^m. \tag{B10}$$

We will also allow a potential that is not purely quadratic but has an expansion

$$V(\Phi^\dagger\Phi) = -\frac{12}{L^2} - \frac{3}{L^2}\Phi^\dagger\Phi + \frac{V_4}{2L^2}(\Phi^\dagger\Phi)^2 + \cdots . \tag{B11}$$

Inserting these series into the equations of motion, we fix the leading coefficients to be

$$\begin{aligned}
\phi &\sim \frac{L^2}{r}\tilde{\phi}_{(0,0)} + \frac{L^6}{r^3}\left[\tilde{\phi}_{(0,0)}\left(\frac{1}{2}\mu^2 q^2 - \left(\frac{1}{3}+\frac{V_4}{2}\right)\tilde{\phi}^2_{(0,0)}\right)\log\frac{r}{L} + \phi_{(0,0)}\right] + \cdots \\
A &\sim -\frac{L^4}{r^2}\frac{\tilde{\phi}^2_{(0,0)}}{12} + \frac{L^8}{r^4}\frac{\tilde{\phi}^2_{(0,0)}}{48}\left[\frac{1}{6}\left(-9\mu^2 q^2 + (2+3V_4)\tilde{\phi}^2_{(0,0)} - 36\frac{\phi_{(0,0)}}{\tilde{\phi}_{(0,0)}}\right) + \left((2+3V_4)\tilde{\phi}^2_{(0,0)} - 3\mu^2 q^2\right)\log\frac{r}{L}\right] + \cdots \\
f &\sim 1 + \frac{L^8}{r^4}\left[f_{(4,0)} - \frac{1}{2}(\mu q\tilde{\phi}_{(0,0)})^2\log\frac{r}{L}\right] + \cdots \\
A_0 &\sim \mu + \frac{L^4}{r^2}\left(A_{0(2,0)} - \frac{1}{4}q^2\mu\tilde{\phi}^2_{(0,0)}\log\frac{r}{L}\right) + \cdots .
\end{aligned} \tag{B12}$$

The expansion in the $u = r_H^2/r^2$ coordinate will take the form

$$\begin{aligned}
\phi &\sim \alpha_- u^{1/2} + u^{3/2}(\alpha_+\tilde{\alpha}_+\log u) + \cdots \\
f &\sim 1 + u^2(f_4 + \tilde{f}_4\log u) + \cdots \\
A_0 &\sim \mu + \mu u(A_{02} + \tilde{A}_{02}\log u) + \cdots .
\end{aligned} \tag{B13}$$

Comparing the two expansions, one finds the following relations between the coefficients:

$$\alpha_- = \frac{L^2}{r_H}\tilde{\phi}_{(0,0)} \tag{B14}$$

$$\tilde{\alpha}_+ = -\frac{1}{2}\frac{L^6}{r_H^3}\left[\tilde{\phi}_{(0,0)}\left(\frac{1}{2}\mu^2 q^2 - \left(\frac{1}{3}+\frac{V_4}{2}\right)\tilde{\phi}^2_{(0,0)}\right)\right] \quad \text{(B15)}$$

$$\alpha_+ = \frac{L^6}{r_H^3}\left[\phi_{(0,0)} - \tilde{\phi}_{(0,0)}\left(\frac{1}{2}\mu^2 q^2 - \left(\frac{1}{3}+\frac{V_4}{2}\right)\tilde{\phi}^2_{(0,0)}\right)\log\frac{r_H}{L}\right] \quad \text{(B16)}$$

$$\tilde{f}_4 = \frac{1}{4}\frac{L^8}{r_H^4}(\mu q\tilde{\phi}_{(0,0)})^2 \quad \text{(B17)}$$

$$f_4 = \frac{L^8}{r_H^4}\left[f_{(4,0)} + \frac{1}{2}(\mu q\tilde{\phi}_{(0,0)})^2\log\frac{r_H}{L}\right] \quad \text{(B18)}$$

$$\tilde{A}_{02} = \frac{1}{8}\frac{L^4}{r_H^2}q^2\tilde{\phi}^2_{(0,0)} \quad \text{(B19)}$$

$$A_{02} = \frac{L^4}{r^2}\left(\frac{1}{\mu}A_{0(2,0)} + \frac{1}{4}q^2\tilde{\phi}^2_{(0,0)}\log\frac{r_H}{L}\right). \quad \text{(B20)}$$

Since the equations of motion in the u coordinate are independent of the ratio r_H/L, we can extract the logarithmic dependence of the subleading terms explicitly,

$$\begin{aligned}\phi_{(0,0)} &= \hat{\phi}_{(0,0)} + \tilde{\phi}_{(0,0)}\left(\frac{1}{2}\mu^2 q^2 - \left(\frac{1}{3}+\frac{V_4}{2}\right)\tilde{\phi}^2_{(0,0)}\right)\log\frac{r_H}{L}\\ f_{(4,0)} &= \hat{f}_{(4,0)} - \frac{1}{2}(\mu q\tilde{\phi}_{(0,0)})^2\log\frac{r_H}{L}\\ A_{0(2,0)} &= \hat{A}_{0(2,0)} - \frac{1}{4}q^2\mu\tilde{\phi}^2_{(0,0)}\log\frac{r_H}{L},\end{aligned} \quad \text{(B21)}$$

with

$$\hat{\phi}_{(0,0)} = \alpha_+\frac{r_H^3}{L^6}, \quad \hat{f}_{(4,0)} = f_4\frac{r_H^4}{L^8}, \quad \hat{A}_{0(2,0)} = \mu A_{02}\frac{r_H^2}{L^4}. \quad \text{(B22)}$$

2. On-shell action

We can write Einstein's equations as

$$R_{MN} = T^{(A)}_{MN} + T^{\phi}_{MN} + \frac{1}{2}g_{MN}\left(\frac{L^2}{3}F^2 + |D\phi|^2 + \frac{5}{3}V\right). \quad \text{(B23)}$$

From the trace of Einstein equations, we find that the Ricci scalar is

$$R = \frac{L^2}{3}F^2 + |D\phi|^2 + \frac{5}{3}V. \quad \text{(B24)}$$

Therefore, the on-shell action (2.1) is evaluated as

$$S_{\text{on-shell}} = \frac{1}{16\pi G_5}\int d^5x\sqrt{-g}\left[\frac{2}{3}V - \frac{2}{3}L^2F^2\right]. \quad \text{(B25)}$$

Let us now use that for our solutions

$$\begin{aligned}&\Gamma^{\alpha}_{\mu\nu} = \Gamma^{r}_{r\nu} = \Gamma^{\alpha}_{rr} = 0,\\ &\Gamma^{r}_{\mu\nu} = -\frac{1}{\sqrt{g_{rr}}}K_{\mu\nu}, \qquad \Gamma^{\alpha}_{\mu r} = \sqrt{g_{rr}}K^{\alpha}_{\mu},\\ &\Gamma^{r}_{rr} = \frac{1}{2}g^{rr}\partial_r g_{rr},\end{aligned} \quad \text{(B26)}$$

where

$$K_{\mu\nu} = \frac{1}{2\sqrt{g_{rr}}}\partial_r g_{\mu\nu} \quad \text{(B27)}$$

is the extrinsic curvature and $K^{\alpha}{}_{\mu} = g^{\alpha\beta}K_{\beta\mu}$, $K = g^{\mu\nu}K_{\mu\nu}$. We will also use that

$$\frac{\partial_r\sqrt{-g}}{\sqrt{-g}} = \Gamma^{r}_{rr} + \sqrt{g_{rr}}K. \quad \text{(B28)}$$

This allows us to write

$$g^{\mu\nu}R_{\mu\nu} = -\frac{1}{\sqrt{-g}}\partial_r\left(\frac{\sqrt{-g}}{\sqrt{g_{rr}}}K\right) = -\frac{1}{\sqrt{-g}}\partial_r(\sqrt{-\gamma}K). \quad \text{(B29)}$$

We defined $\gamma_{\mu\nu} = g_{\mu\nu}$ as the boundary metric and used $\sqrt{-g} = \sqrt{g_{rr}}\sqrt{-\gamma}$. On the other hand, from Einstein's equations,

$$g^{\mu\nu}R_{\mu\nu} = -\frac{2L^2}{3}F_{0r}F^{0r} + \frac{4}{3}V + q^2g^{00}A_0^2\phi^2, \quad \text{(B30)}$$

where we only focused on the nonzero components on the solutions.

Solving for V and introducing the result in the on-shell action, one gets

$$S_{\text{on-shell}} = \frac{1}{16\pi G_5}\int d^5x\sqrt{-g}\left[-\frac{1}{2\sqrt{-g}}\partial_r(\sqrt{-\gamma}K) - L^2F_{r0}F^{r0} - \frac{q^2}{2}g^{00}A_0^2\phi^2\right]. \quad \text{(B31)}$$

Let us now use the equation of motion for the gauge field:

$$4L^2\partial_r(\sqrt{-g}F^{r0}) = 2q^2\sqrt{-g}g^{00}A_0\phi^2. \quad \text{(B32)}$$

We can then replace the q^2 term in the action by a derivative term and write the action as a total derivative:

$$S_{\text{on-shell}} = \frac{1}{16\pi G_5}\int d^5x\left[-\frac{1}{2}\partial_r(\sqrt{-\gamma}K) - L^2\sqrt{-g}\partial_r A_0 F^{r0} - L^2 A_0\partial_r(\sqrt{-g}F^{r0})\right]$$
$$= \frac{1}{16\pi G_5}\int d^5x\partial_r\left[-\frac{1}{2}\sqrt{-\gamma}K - L^2\sqrt{-g}A_0F^{r0}\right]$$
$$= -\frac{1}{16\pi G_5}\int d^4x\left[\frac{1}{2}\sqrt{-\gamma}K + L^2\sqrt{-g}A_0F^{r0}\right]^{r=r_\Lambda}_{r=r_H}. \tag{B33}$$

3. Connecting boundary and horizon values

We can rewrite the equations for f (B2) and A_0 (B3) as

$$[e^{4A}r^5f']' - L^4\left[4e^{2A}r^3(A_0')^2 + 2q^2\frac{re^{2A}A_0^2\phi^2}{f}\right] = 0 \tag{B34}$$

$$[e^{2A}r^3A_0']' - \frac{q^2}{2}\frac{re^{2A}A_0\phi^2}{f} = 0. \tag{B35}$$

We can multiply the second equation by $-4L^4A_0$ and add it to the first one, yielding

$$[e^{4A}r^5f' - 4L^4e^{2A}r^3A_0'A_0]' = 0. \tag{B36}$$

By introducing the function

$$\sigma(r) = \int_{r_H}^{r} dr_1\frac{r_1e^{2A}A_0\phi^2}{f}, \tag{B37}$$

the equations become

$$[e^{4A}r^5f' - 4L^4e^{2A}r^3A_0'A_0]' = 0 \tag{B38}$$

$$\left[e^{2A}r^3A_0' - \frac{q^2}{2}\sigma\right]' = 0. \tag{B39}$$

Let us further define

$$\beta(r) = e^{4A}r^5f' - 4L^4e^{2A}r^3A_0'A_0,$$
$$\gamma(r) = e^{2A}r^3A_0' - \frac{q^2}{2}\sigma. \tag{B40}$$

By the equations above, these are independent of the radial coordinate, and it is convenient to evaluate them at the horizon $r \to r_H$,

$$\beta(r_H) = e^{4A(r_H)}r_H^5f'(r_H) \equiv \beta_H$$
$$\gamma(r_H) = e^{2A(r_H)}r_H^3A_0'(r_H) \equiv \gamma_H. \tag{B41}$$

Note that the temperature and entropy density are given by

$$T = \frac{r_H^2f'(r_H)}{4\pi L^2}e^{A(r_H)}, \qquad s = \frac{1}{4G_5}\frac{r_H^3}{L^3}e^{3A(r_H)}. \tag{B42}$$

Then,

$$\beta_H = 16\pi G_5L^5Ts. \tag{B43}$$

The constant γ_H is related to the charge density. We should expand now the solutions (B40) close to the boundary and compare with the values at the horizon (B41). For $\Delta \neq 3$, σ has the following expansion,

$$\sigma \simeq L^{16-4\Delta}\frac{\mu\tilde{\phi}^2_{(0,0)}}{4(\Delta-3)}(r_H^{2\Delta-6} - r^{2\Delta-6}) + \sigma_b, \tag{B44}$$

where σ_b is a constant. The divergent term cancels out in the boundary expansion of $\gamma(r)$. Then, the matching of the constant terms at the boundary and the horizon leads to

$$A_{0(2,0)} = -\frac{\gamma_H}{2L^4} + q^2\left[\frac{\mu\tilde{\phi}^2_{(0,0)}}{8(\Delta-3)}\left(\frac{r_H}{L^2}\right)^{2(\Delta-3)} + \frac{\sigma_b}{2L^4}\right]$$
$$f_{(4,0)} = -\frac{1}{4}\frac{\beta_H}{L^8} + 2\mu A_{0(2,0)}. \tag{B45}$$

For $\Delta = 3$, the expansion of σ close to the boundary is

$$\sigma \simeq \mu L^4\tilde{\phi}^2_{(0,0)}\left[\log\left(\frac{r}{L}\right) - \log\left(\frac{r_H}{L}\right)\right] + \sigma_b, \tag{B46}$$

where again σ_b is a constant. The divergent term cancels out in the boundary expansion of $\gamma(r)$, and the matching of the constant terms at the boundary and the horizon leads to

$$A_{0(2,0)} = -\frac{\gamma_H}{2L^4} - q^2\left[\frac{1}{8}\mu\tilde{\phi}^2_{(0,0)}\left(1 - 2\log\frac{r_H}{L}\right) + \frac{\sigma_b}{4L^4}\right] \tag{B47}$$

$$f_{(4,0)} = -\frac{1}{4}\frac{\beta_H}{L^8} + 2\mu A_{0(2,0)} + \frac{1}{8}q^2\mu^2\tilde{\phi}^2_{(0,0)}. \tag{B48}$$

APPENDIX C: HOLOGRAPHIC RENORMALIZATION

In order to compute renormalized quantities, we follow the holographic renormalization prescription [62–64]. First, we introduce a cutoff in the radial direction r_Λ such that the divergences of the bulk action (2.1) are regulated. To this, we should add the Gibbons-Hawking term in order to have

a well-defined variational principle for the metric and boundary counterterms to remove the divergences. We distinguish between two cases, noninteger Δ and $\Delta = 3$. We assume that the form of the metric is

$$ds^2 = N^2 dr^2 + \gamma_{\mu\nu} dx^\mu dx^\nu \tag{C1}$$

and define the extrinsic curvature and Brown-York tensors in the usual way:

$$\begin{aligned} K_{\mu\nu} &= \frac{1}{2N}\partial_r \gamma_{\mu\nu}, \\ K &= \gamma^{\mu\nu} K_{\mu\nu}, \\ \Pi^{\mu\nu}_{\mathrm{BY}} &= (K^{\mu\nu} - \gamma^{\mu\nu} K). \end{aligned} \tag{C2}$$

1. Noninteger Δ

The boundary terms are

$$\begin{aligned} S_{\mathrm{GH}} &= \frac{1}{8\pi G_5}\int_{r=r_\Lambda} d^4x\sqrt{-\gamma}K \\ S_{c.t.} &= \frac{1}{16\pi G_5}\int_{r=r_\Lambda} d^4x \mathcal{L}_{c.t.} \\ \mathcal{L}_{c.t.} &= \sqrt{-\gamma}\left[-\frac{6}{L} + \frac{\Delta-4}{L}\Phi^\dagger\Phi + \frac{L}{2(\Delta-3)}\gamma^{\mu\nu}(D_\mu\Phi)^\dagger D_\nu\Phi \right. \\ &\quad \left. + \frac{1}{12L}\frac{(\Delta-4)^2}{\Delta-3}(\Phi^\dagger\Phi)^2\right]. \end{aligned}$$

The renormalized action is then

$$S_{\mathrm{ren}} = \lim_{r_\Lambda\to\infty}[S_{\mathrm{bulk}} + S_{\mathrm{GH}} + S_{c.t.}]. \tag{C3}$$

The free energy is determined by the renormalized action $\beta V_3 \mathcal{F} = -S_{\mathrm{ren}}$ (where $\beta = 1/T$ and V_3 is the spatial volume). Using the formula for the on-shell action (B33) and the boundary expansions (B8) and the relation (B45), we find

$$\begin{aligned} \mathcal{F} &= \frac{1}{16\pi G_5}\left[-\frac{1}{4}e^{4A(r_H)}\left(\frac{r_H}{L}\right)^5 f'(r_H) + 2L^3\mu A_{0(2,0)} \right. \\ &\quad \left. + L^3(\Delta-4)(\Delta-2)\tilde{\phi}_{(0,0)}\phi_{(0,0)}\right] \\ &= -\frac{L^3}{16\pi G_5}\left[-\frac{1}{4}\frac{\beta_H}{L^8} + 2\mu A_{0(2,0)} \right. \\ &\quad \left. + (\Delta-4)(\Delta-2)\tilde{\phi}_{(0,0)}\phi_{(0,0)}\right] \\ &= \frac{L^3}{16\pi G_5}[f_{(4,0)} + (\Delta-4)(\Delta-2)\tilde{\phi}_{(0,0)}\phi_{(0,0)}]. \end{aligned} \tag{C4}$$

Renormalized expectation values can be computed from variations of the action, using the same boundary terms,

$$\langle T^{\mu\nu}\rangle = \frac{1}{8\pi G_5}\lim_{r\to\infty}\frac{r^2}{L^2}\left[-\sqrt{-\gamma}\Pi^{\mu\nu}_{\mathrm{BY}} + \frac{\delta\mathcal{L}_{c.t.}}{\delta\gamma_{\mu\nu}}\right] \tag{C5}$$

$$\langle\mathcal{O}\rangle = \frac{1}{16\pi G_5}\lim_{r\to\infty}\frac{L^{2(4-\Delta)}}{r^{4-\Delta}}\left[-\sqrt{-g}g^{rr}\partial_r\phi + \frac{\delta\mathcal{L}_{c.t.}}{\delta\Phi^\dagger}\right] \tag{C6}$$

$$\langle J^\mu\rangle = \frac{1}{16\pi G_5}\lim_{r\to\infty}\left[-4L^2\sqrt{-g}g^{rr}g^{\mu\alpha}F_{r\alpha} + \frac{\delta\mathcal{L}_{c.t.}}{\delta A_\mu}\right]. \tag{C7}$$

Introducing (B8) in the formulas (C5)–(C7), we get

$$\langle T^{00}\rangle = -\frac{L^3}{16\pi G_5}[3f_{(4,0)} - (\Delta-4)(\Delta-2)\tilde{\phi}_{(0,0)}\phi_{(0,0)}] \tag{C8}$$

$$\langle T^{ii}\rangle = -\frac{L^3}{16\pi G_5}[f_{(4,0)} + (\Delta-4)(\Delta-2)\tilde{\phi}_{(0,0)}\phi_{(0,0)}] \tag{C9}$$

$$\langle\mathcal{O}\rangle = -\frac{L^3}{8\pi G_5}(\Delta-2)\phi_{(0,0)} \tag{C10}$$

$$\langle J^0\rangle = -\frac{L^3}{2\pi G_5}A_{0(2,0)}. \tag{C11}$$

Note that the Ward identity for the trace holds,

$$\langle T^\mu{}_\mu\rangle = \langle T^{\mu\nu}\rangle\eta_{\mu\nu} = -(4-\Delta)(\langle\mathcal{O}\rangle\tilde{\phi}^\dagger_{(0,0)} + \langle\mathcal{O}^\dagger\rangle\tilde{\phi}_{(0,0)}). \tag{C12}$$

2. Δ = 3

The boundary terms are

$$\begin{aligned} S_{\mathrm{GH}} &= \frac{1}{8\pi G_5}\int_{r=r_\Lambda} d^4x\sqrt{-\gamma}K \\ S_{c.t.} &= \frac{1}{16\pi G_5}\int_{r=r_\Lambda} d^4x\mathcal{L}_{c.t.} \\ \mathcal{L}_{c.t.} &= \sqrt{-\gamma}\left[-\frac{6}{L} - \frac{1}{L}\Phi^\dagger\Phi + L\left[\log\frac{r}{L} + \mathcal{W}_1\right]\gamma^{\mu\nu}(D_\mu\Phi)^\dagger D_\nu\Phi \right. \\ &\quad \left. + \frac{1}{L}\left[\left(\frac{1}{3} + \frac{V_4}{2}\right)\log\frac{r}{L} + \mathcal{W}_2\right](\Phi^\dagger\Phi)^2\right], \end{aligned}$$

where $\mathcal{W}_1$, $\mathcal{W}_2$ are finite contributions. The renormalized action is then

$$S_{\mathrm{ren}} = \lim_{r_\Lambda\to\infty}[S_{\mathrm{bulk}} + S_{\mathrm{GH}} + S_{c.t.}]. \tag{C13}$$

The free energy is determined by the renormalized action $\beta V_3\mathcal{F} = -S_{\mathrm{ren}}$ (where $\beta = 1/T$ and V_3 is the spatial volume). Using the formula for the on-shell action (B33) and the boundary expansions (B12) and the relation (B48), we find

$$\begin{aligned}\mathcal{F} &= \frac{1}{16\pi G_5}\left[-\frac{1}{4}e^{4A(r_H)}\left(\frac{r_H}{L}\right)^5 f'(r_H) + 2L^3\mu A_{0(2,0)} - L^3\tilde{\phi}_{(0,0)}\phi_{(0,0)}\right.\\ &\left. + L^3\left(\frac{1}{4}+\mathcal{W}_1\right)q^2\mu^2\tilde{\phi}^2_{(0,0)} - L^3\left(\frac{1}{12}+\frac{V_4}{8}+\mathcal{W}_2\right)\tilde{\phi}^4_{(0,0)}\right]\\ &= -\frac{L^3}{16\pi G_5}\left[-\frac{1}{4}\frac{\beta_H}{L^8} + 2\mu A_{0(2,0)} - \tilde{\phi}_{(0,0)}\phi_{(0,0)} + \left(\frac{1}{4}+\mathcal{W}_1\right)q^2\mu^2\tilde{\phi}^2_{(0,0)} - \left(\frac{1}{12}+\frac{V_4}{8}+\mathcal{W}_2\right)\tilde{\phi}^4_{(0,0)}\right]\\ &= \frac{L^3}{16\pi G_5}\left[f_{(4,0)} - \tilde{\phi}_{(0,0)}\phi_{(0,0)} + \left(\frac{1}{8}+\mathcal{W}_1\right)q^2\mu^2\tilde{\phi}^2_{(0,0)} - \left(\frac{1}{12}+\frac{V_4}{8}+\mathcal{W}_2\right)\tilde{\phi}^4_{(0,0)}\right]. \end{aligned} \tag{C14}$$

Renormalized expectation values can be computed from variations of the action, using the same boundary terms. Introducing (B12) in the formulas (C5)–(C7) (with $\Delta = 3$), we get

$$\langle T^{00}\rangle = -\frac{L^3}{16\pi G_5}\left[3f_{(4,0)} + \tilde{\phi}_{(0,0)}\phi_{(0,0)} + \left(\frac{3}{8}+\mathcal{W}_1\right)q^2\mu^2\tilde{\phi}^2_{(0,0)} + \left(\frac{1}{12}+\frac{V_4}{8}+\mathcal{W}_2\right)\tilde{\phi}^4_{(0,0)}\right] \tag{C15}$$

$$\langle T^{ii}\rangle = -\frac{L^3}{16\pi G_5}\left[f_{(4,0)} - \tilde{\phi}_{(0,0)}\phi_{(0,0)} + \left(\frac{1}{8}+\mathcal{W}_1\right)q^2\mu^2\tilde{\phi}^2_{(0,0)} - \left(\frac{1}{12}+\frac{V_4}{8}+\mathcal{W}_2\right)\tilde{\phi}^4_{(0,0)}\right] \tag{C16}$$

$$\langle \mathcal{O}\rangle = -\frac{L^3}{16\pi G_5}\left[2\phi_{(0,0)} - \left(\frac{1}{2}+\mathcal{W}_1\right)q^2\mu^2\tilde{\phi}_{(0,0)} + \left(\frac{1}{3}+\frac{V_4}{2}+2\mathcal{W}_2\right)\tilde{\phi}^3_{(0,0)}\right] \tag{C17}$$

$$\langle J^0\rangle = -\frac{L^3}{16\pi G_5}[8A_{0(2,0)} + (1+2\mathcal{W}_1)q^2\mu\tilde{\phi}^2_{(0,0)}]. \tag{C18}$$

The Ward identity for the trace has an anomalous contribution,

$$\langle T^{\mu}{}_{\mu}\rangle = \langle T^{\mu\nu}\rangle\eta_{\mu\nu} = -(\langle\mathcal{O}\rangle\tilde{\phi}^{\dagger}_{(0,0)} + \langle\mathcal{O}^{\dagger}\rangle\tilde{\phi}_{(0,0)}) + \mathcal{A}, \tag{C19}$$

where

$$\mathcal{A} = -\frac{L^3}{16\pi G_5}\left[\eta^{\mu\nu}(D_\mu\tilde{\phi}_{(0,0)})^{\dagger}D_\nu\tilde{\phi}_{(0,0)} + \left(\frac{1}{3}+\frac{V_4}{2}\right)(\tilde{\phi}^{\dagger}_{(0,0)}\tilde{\phi}_{(0,0)})^2\right]. \tag{C20}$$

It will be convenient to extract the explicit logarithmic dependence (B21) and define the finite counterterms as

$$\mathcal{W}_1 = \log(\tilde{\phi}_{(0,0)}L) + \kappa_1, \qquad \mathcal{W}_2 = \left(\frac{1}{3}+\frac{V_4}{2}\right)\log(\tilde{\phi}_{(0,0)}L) + \kappa_2. \tag{C21}$$

Then,

$$\begin{aligned}\langle T^{00}\rangle = -\frac{L^3}{16\pi G_5}&\left[3\hat{f}_{(4,0)} - \left(\mu^2q^2\tilde{\phi}^2_{(0,0)} + \left(\frac{1}{3}+\frac{V_4}{2}\right)\tilde{\phi}^4_{(0,0)}\right)\log\frac{r_H}{L^2\tilde{\phi}_{(0,0)}} + \tilde{\phi}_{(0,0)}\hat{\phi}_{(0,0)}\right.\\ &\left. + \left(\frac{3}{8}+\kappa_1\right)q^2\mu^2\tilde{\phi}^2_{(0,0)} + \left(\frac{1}{12}+\frac{V_4}{8}+\kappa_2\right)\tilde{\phi}^4_{(0,0)}\right]\end{aligned} \tag{C22}$$

$$\begin{aligned}\langle T^{ii}\rangle = -\frac{L^3}{16\pi G_5}&\left[\hat{f}_{(4,0)} - \left(\mu^2q^2\tilde{\phi}^2_{(0,0)} - \left(\frac{1}{3}+\frac{V_4}{2}\right)\tilde{\phi}^4_{(0,0)}\right)\log\frac{r_H}{L^2\tilde{\phi}_{(0,0)}} - \tilde{\phi}_{(0,0)}\hat{\phi}_{(0,0)}\right.\\ &\left. + \left(\frac{1}{8}+\kappa_1\right)q^2\mu^2\tilde{\phi}^2_{(0,0)} - \left(\frac{1}{12}+\frac{V_4}{8}+\kappa_2\right)\tilde{\phi}^4_{(0,0)}\right]\end{aligned} \tag{C23}$$

$$\langle \mathcal{O} \rangle = -\frac{L^3}{16\pi G_5}\left[2\hat{\phi}_{(0,0)} + \left(\mu^2 q^2 \tilde{\phi}_{(0,0)} - 2\left(\frac{1}{3}+\frac{V_4}{2}\right)\tilde{\phi}^3_{(0,0)}\right)\log\frac{r_H}{L^2\tilde{\phi}_{(0,0)}} - \left(\frac{1}{2}+\kappa_1\right)q^2\mu^2\tilde{\phi}_{(0,0)} + \left(\frac{1}{3}+\frac{V_4}{2}+2\kappa_2\right)\tilde{\phi}^3_{(0,0)}\right], \tag{C24}$$

$$\langle J^0 \rangle = -\frac{L^3}{16\pi G_5}\left[8\hat{A}_{0(2,0)} - 2\mu q^2 \tilde{\phi}^2_{(0,0)}\log\frac{r_H}{L^2\tilde{\phi}_{(0,0)}} + (1+2\kappa_1)q^2\mu\tilde{\phi}^2_{(0,0)}\right]. \tag{C25}$$

[1] J. M. Lattimer and M. Prakash, The physics of neutron stars, Science **304**, 536 (2004).
[2] N. Brambilla *et al.*, QCD and strongly coupled gauge theories: Challenges and perspectives, Eur. Phys. J. C **74**, 2981 (2014).
[3] A. Kurkela, P. Romatschke, and A. Vuorinen, Cold quark matter, Phys. Rev. D **81**, 105021 (2010).
[4] A. Kurkela and A. Vuorinen, Cool Quark Matter, Phys. Rev. Lett. **117**, 042501 (2016).
[5] P. de Forcrand, Simulating QCD at finite density, *Proc. Sci.*, LAT2009 (2009) 010.
[6] R. Machleidt and D. R. Entem, Chiral effective field theory and nuclear forces, Phys. Rep. **503**, 1 (2011).
[7] I. Tews, T. Kruger, K. Hebeler, and A. Schwenk, Neutron Matter at Next-to-Next-to-Next-to-Leading Order in Chiral Effective Field Theory, Phys. Rev. Lett. **110**, 032504 (2013).
[8] J. M. Maldacena, The large N limit of superconformal field theories and supergravity, Adv. Theor. Math. Phys. **2**, 231 (1998).
[9] O. Bergman, G. Lifschytz, and M. Lippert, Holographic nuclear physics, J. High Energy Phys. 11 (2007) 056.
[10] M. Rozali, H.-H. Shieh, M. Van Raamsdonk, and J. Wu, Cold nuclear matter in holographic QCD, J. High Energy Phys. 01 (2008) 053.
[11] K.-Y. Kim, S.-J. Sin, and I. Zahed, Dense holographic QCD in the Wigner-Seitz approximation, J. High Energy Phys. 09 (2008) 001.
[12] Y. Kim, C.-H. Lee, I. J. Shin, and M.-B. Wan, Holographic equations of state and astrophysical compact objects, J. High Energy Phys. 10 (2011) 111.
[13] V. Kaplunovsky, D. Melnikov, and J. Sonnenschein, Baryonic popcorn, J. High Energy Phys. 11 (2012) 047.
[14] K. Ghoroku, K. Kubo, M. Tachibana, and F. Toyoda, Holographic cold nuclear matter and neutron star, Int. J. Mod. Phys. A **29**, 1450060 (2014).
[15] S.-w. Li, A. Schmitt, and Q. Wang, From holography towards real-world nuclear matter, Phys. Rev. D **92**, 026006 (2015).
[16] M. Elliot-Ripley, P. Sutcliffe, and M. Zamaklar, Phases of kinky holographic nuclear matter, arXiv:1607.04832.
[17] P. Burikham, E. Hirunsirisawat, and S. Pinkanjanarod, Thermodynamic properties of holographic multiquark and the multiquark star, J. High Energy Phys. 06 (2010) 040.
[18] Y. Kim, I. J. Shin, C.-H. Lee, and M.-B. Wan, Explicit flavor symmetry breaking and holographic compact stars, J. Korean Phys. Soc. **66**, 578 (2015).
[19] C. Hoyos, D. Rodríguez Fernández, N. Jokela, and A. Vuorinen, Holographic Quark Matter and Neutron Stars, Phys. Rev. Lett. **117**, 032501 (2016).
[20] P. M. Hohler and M. A. Stephanov, Holography and the speed of sound at high temperatures, Phys. Rev. D **80**, 066002 (2009).
[21] A. Cherman, T. D. Cohen, and A. Nellore, A bound on the speed of sound from holography, Phys. Rev. D **80**, 066003 (2009).
[22] P. Kovtun, D. T. Son, and A. O. Starinets, Viscosity in Strongly Interacting Quantum Field Theories from Black Hole Physics, Phys. Rev. Lett. **94**, 111601 (2005).
[23] P. Demorest, T. Pennucci, S. Ransom, M. Roberts, and J. Hessels, Shapiro delay measurement of a two solar mass neutron star, Nature (London) **467**, 1081 (2010).
[24] J. Antoniadis *et al.*, A massive pulsar in a compact relativistic binary, Science **340**, 1233232 (2013).
[25] P. Bedaque and A. W. Steiner, Sound Velocity Bound and Neutron Stars, Phys. Rev. Lett. **114**, 031103 (2015).
[26] J. Casalderrey-Solana, H. Liu, D. Mateos, K. Rajagopal, and U. A. Wiedemann, Gauge/string duality, hot qcd and heavy ion collisions, arXiv:1101.0618.
[27] A. Buchel and C. Pagnutti, Exotic hairy black holes, Nucl. Phys. **B824**, 85 (2010).
[28] A. Buchel and C. Pagnutti, Correlated stability conjecture revisited, Phys. Lett. B **697**, 168 (2011).
[29] T. Sakai and S. Sugimoto, Low energy hadron physics in holographic QCD, Prog. Theor. Phys. **113**, 843 (2005).
[30] N. Jokela and A. V. Ramallo, Universal properties of cold holographic matter, Phys. Rev. D **92**, 026004 (2015).
[31] G. Itsios, N. Jokela, and A. V. Ramallo, Collective excitations of massive flavor branes, Nucl. Phys. **B909**, 677 (2016).
[32] M. Kulaxizi and A. Parnachev, Holographic responses of fermion matter, Nucl. Phys. **B815**, 125 (2009).
[33] S. Kachru, X. Liu, and M. Mulligan, Gravity duals of Lifshitz-like fixed points, Phys. Rev. D **78**, 106005 (2008).
[34] C. Hoyos-Badajoz, A. O'Bannon, and J. M. S. Wu, Zero Sound in strange metallic holography, J. High Energy Phys. 09 (2010) 086.

[35] N. Jokela, J. Järvelä, and A. V. Ramallo, Non-relativistic anyons from holography, arXiv:1605.09156.
[36] M. Taylor, Lifshitz holography, Classical Quantum Gravity **33**, 033001 (2016).
[37] A. Kurkela, E. S. Fraga, J. Schaffner-Bielich, and A. Vuorinen, Constraining neutron star matter with Quantum Chromodynamics, Astrophys. J. **789**, 127 (2014).
[38] S. S. Gubser, Breaking an Abelian gauge symmetry near a black hole horizon, Phys. Rev. D **78**, 065034 (2008).
[39] T. Faulkner, H. Liu, J. McGreevy, and D. Vegh, Emergent quantum criticality, Fermi surfaces, and AdS(2), Phys. Rev. D **83**, 125002 (2011).
[40] S. K. Domokos and J. A. Harvey, Baryon Number-Induced Chern-Simons Couplings of Vector and Axial-Vector Mesons in Holographic QCD, Phys. Rev. Lett. **99**, 141602 (2007).
[41] S. Nakamura, H. Ooguri, and C.-S. Park, Gravity dual of spatially modulated phase, Phys. Rev. D **81**, 044018 (2010).
[42] O. Bergman, N. Jokela, G. Lifschytz, and M. Lippert, Striped instability of a holographic Fermi-like liquid, J. High Energy Phys. 10 (2011) 034.
[43] M. Cvetič, M. J. Duff, P. Hoxha, J. T. Liu, H. Lü, J. X. Lu, R. Martinez-Acosta, C. N. Pope, H. Sati, and T. A. Tran, Embedding AdS black holes in ten-dimensions and eleven-dimensions, Nucl. Phys. **B558**, 96 (1999).
[44] J. McGreevy, L. Susskind, and N. Toumbas, Invasion of the giant gravitons from Anti-de Sitter space, J. High Energy Phys. 06 (2000) 008.
[45] R. C. Myers and O. Tafjord, Superstars and giant gravitons, J. High Energy Phys. 11 (2001) 009.
[46] M. Gunaydin, L. J. Romans, and N. P. Warner, Compact and noncompact gauged supergravity theories in five-dimensions, Nucl. Phys. **B272**, 598 (1986).
[47] N. Bobev, A. Kundu, K. Pilch, and N. P. Warner, Supersymmetric charged clouds in AdS5, J. High Energy Phys. 03 (2011) 070.
[48] A. Khavaev and N. P. Warner, A Class of $N = 1$ supersymmetric RG flows from five-dimensional $N = 8$ supergravity, Phys. Lett. B **495**, 215 (2000).
[49] L. J. Romans, Supersymmetric, cold and lukewarm black holes in cosmological Einstein-Maxwell theory, Nucl. Phys. **B383**, 395 (1992).
[50] A. Chamblin, R. Emparan, C. V. Johnson, and R. C. Myers, Charged AdS black holes and catastrophic holography, Phys. Rev. D **60**, 064018 (1999).
[51] U. Gursoy, E. Kiritsis, L. Mazzanti, and F. Nitti, Deconfinement and Gluon Plasma Dynamics in Improved Holographic QCD, Phys. Rev. Lett. **101**, 181601 (2008).
[52] U. Gursoy, E. Kiritsis, L. Mazzanti, and F. Nitti, Improved holographic Yang-Mills at finite temperature: Comparison with data, Nucl. Phys. **B820**, 148 (2009).
[53] O. DeWolfe, S. S. Gubser, and C. Rosen, A holographic critical point, Phys. Rev. D **83**, 086005 (2011).
[54] R. Rougemont, A. Ficnar, S. Finazzo, and J. Noronha, Energy loss, equilibration, and thermodynamics of a baryon rich strongly coupled quark-gluon plasma, J. High Energy Phys. 04 (2016) 102.
[55] R. Rougemont, J. Noronha, and J. Noronha-Hostler, Suppression of Baryon Diffusion and Transport in a Baryon Rich Strongly Coupled Quark-Gluon Plasma, Phys. Rev. Lett. **115**, 202301 (2015).
[56] T. Alho, M. Järvinen, K. Kajantie, E. Kiritsis, C. Rosen, and K. Tuominen, A holographic model for QCD in the Veneziano limit at finite temperature and density, J. High Energy Phys. 04 (2014) 124.
[57] F. Bigazzi, A. L. Cotrone, J. Mas, D. Mayerson, and J. Tarrio, D3-D7 quark-gluon plasmas at finite baryon density, J. High Energy Phys. 04 (2011) 060.
[58] F. Bigazzi, A. L. Cotrone, and J. Tarrio, Charged D3-D7 plasmas: Novel solutions, extremality and stability issues, J. High Energy Phys. 07 (2013) 074.
[59] A. F. Faedo, A. Kundu, D. Mateos, and J. Tarrio, (Super) Yang-Mills at finite heavy-quark density, J. High Energy Phys. 02 (2015) 010.
[60] A. F. Faedo, A. Kundu, D. Mateos, C. Pantelidou, and J. Tarro, Three-dimensional super Yang-Mills with compressible quark matter, J. High Energy Phys. 03 (2016) 154.
[61] C. Hoyos-Badajoz and A. Karch, Alternative large N(c) baryons and holography, Phys. Rev. D **79**, 125021 (2009).
[62] S. de Haro, S. N. Solodukhin, and K. Skenderis, Holographic reconstruction of space-time and renormalization in the AdS/CFT correspondence, Commun. Math. Phys. **217**, 595 (2001).
[63] I. Papadimitriou and K. Skenderis, Correlation functions in holographic RG flows, J. High Energy Phys. 10 (2004) 075.
[64] I. Papadimitriou and K. Skenderis, Thermodynamics of asymptotically locally AdS spacetimes, J. High Energy Phys. 08 (2005) 004.

Published for SISSA by Springer

Received: July 17, 2017
Revised: October 2, 2017
Accepted: October 23, 2017
Published: November 8, 2017

Stiff phases in strongly coupled gauge theories with holographic duals

Christian Ecker,[a] **Carlos Hoyos,**[b] **Niko Jokela,**[c,d] **David Rodríguez Fernández**[b] **and Aleksi Vuorinen**[c,d]

[a] *Institut für Theoretische Physik, Technische Universität Wien, Wiedner Hauptstr. 8-10, A-1040 Vienna, Austria*
[b] *Department of Physics, Universidad de Oviedo, c/. Federico García Lorca 18, ES-33007 Oviedo, Spain*
[c] *Department of Physics, University of Helsinki, P.O. Box 64, FI-00014 Helsinki, Finland*
[d] *Helsinki Institute of Physics, University of Helsinki, P.O. Box 64, FI-00014 Helsinki, Finland*

E-mail: christian.ecker@tuwien.ac.at, hoyoscarlos@uniovi.es, niko.jokela@helsinki.fi, rodriguezferdavid@uniovi.es, aleksi.vuorinen@helsinki.fi

Abstract: According to common lore, Equations of State of field theories with gravity duals tend to be soft, with speeds of sound either below or around the conformal value of $v_s = 1/\sqrt{3}$. This has important consequences in particular for the physics of compact stars, where the detection of two solar mass neutron stars has been shown to require very stiff equations of state. In this paper, we show that no speed limit exists for holographic models at finite density, explicitly constructing examples where the speed of sound becomes arbitrarily close to that of light. This opens up the possibility of building hybrid stars that contain quark matter obeying a holographic equation of state in their cores.

Keywords: Gauge-gravity correspondence, Holography and quark-gluon plasmas

ArXiv ePrint: 1707.00521

https://doi.org/10.1007/JHEP11(2017)031

JHEP11(2017)031

Contents

JHEP11(2017)031

1 Introduction

Astrophysical observations of neutron stars with masses up to two solar masses [1, 2] imply that the Equation of State (EoS) relating the energy density ε and pressure p of the matter inside the stars should be very stiff [3]. The stiffness can be measured by the thermodynamic derivative[1]

$$v_s^2 = \left(\frac{\partial p}{\partial \varepsilon}\right)_s , \tag{1.1}$$

where v_s can be identified as the speed of propagation of sound waves, naturally obeying the causal bound $v_s \leq 1$. According to our current understanding, the nature of this matter

[1]The symbol s denotes the entropy density here.

ranges from a relatively dilute gas of nuclei immersed in a sea of electrons in the crust of the star to dense nuclear and superdense neutron matter deep inside the star, expected to reach at least a few times the nuclear saturation density, $n_s \approx 0.16/\mathrm{fm}^3$, in the cores of the most massive stars. With the deconfinement transition of Quantum Chromodynamics (QCD) expected to take place around these densities, it is at the moment still unclear, whether quark matter should be present inside the stars or not.

There are a variety of nuclear matter EoSs that predict very high speeds of sound, some of them even exceeding the speed of light [4]. In all of these cases, the region of validity of the approach is, however, restricted to densities below (roughly) the nuclear saturation density, so that a straightforward extrapolation of the results to the large densities met in the cores of neutron stars is likely to suffer from uncontrollable systematic uncertainties (see [5] for a discussion of this topic). In particular, there is no hope of extending the description of these nuclear matter models to the quark matter phase, possibly relevant for the description of the stellar cores. At the same time, it is equally clear that approaches based on weak coupling expansions in the quark matter phase, such as perturbative QCD [6–9], cannot be used to describe the transition region, and therefore the standard approaches for the description of this regime typically include model calculations (see e.g. [10] and references therein) and interpolations between the low- and high-density regimes [11].

Considering the above difficulties, there is clearly room for alternative approaches to describing dense strongly interacting nuclear and quark matter. Such a novel approach could be provided by the gauge/gravity, or holographic, duality [12–14], which offers a way to relate problems in strongly coupled field theories in their large-N_c limit to calculations performed in classical supergravity in a curved spacetime. An interesting observation pointing towards neutron star matter indeed behaving like a strongly coupled system can be seen from the so-called Taub inequality [15] (see also [16]),[2] which states that in a relativistic kinetic theory causality imposes the condition

$$\varepsilon(\varepsilon - 3p) \geq \rho^2 \,, \tag{1.2}$$

where ρ stands for the mass density. For instance, it is easy to check that degenerate fermionic matter satisfies Taub's inequality for any value of the chemical potential. The inequality clearly implies that $\varepsilon \geq 3p$, which is saturated by conformal theories. As shown in [3], such an EoS is, however, too soft to support the heaviest observed stars, which clearly implies that one of the assumptions behind Taub's inequality must fail. The most likely culprit is the assumption of the validity of a quasiparticle description, which is far from being guaranteed for the matter found inside neutron stars. In fact, it may well be that the correct expansion point would be that of infinite (or very strong) coupling instead of a system of weakly coupled quasiparticles.

The holographic approach has already been used to describe both the confined [17–24] and deconfined [25–28] phases of QCD matter through the study of strongly coupled non-Abelian gauge field theories containing fundamental matter with a global U(1) baryon symmetry. In [27], we adopted the strategy of describing the low-density phase of QCD

[2]We thank Luciano Rezzolla for drawing our attention to this inequality.

JHEP11(2017)031

matter using the Chiral Effective Theory (CET) results of [29], supplemented by the extrapolations provided in [5], and matching them with the EoS of $\mathcal{N} = 2$ Super Yang-Mills theory at finite baryon density, corresponding to a D3-D7 brane intersection on the gravity side. While successful in providing a consistent description of dense QCD matter, this setup led to the prediction that the deconfinement transition would always be of such a strong first order type that the resulting hybrid stars become unstable as soon as even a microscopic amount of quark matter is generated in their cores. The reason for this behavior was found to be the soft nature of the holographic EoS, with $v_s^2 < 1/3$, in comparison with the stiff low-density EoSs of [5].

The softness of the holographic EoS constructed in [27] came as no surprise; in fact, already in [30, 31] it was conjectured that any field theory with a gauge/gravity dual can have a speed of sound at most as large as that of a conformal theory, i.e. $v_s \leq 1/\sqrt{3}$. In [28], we, however, showed that this conjecture is generically not valid at finite density (even though it might hold in certain theories [31]), and more recently a violation of the bound has been proposed even at zero density through the introduction of multitrace deformations in the dual gauge theory [32]. However, in both cases the violation is not nearly large enough to allow for the existence of quark matter inside neutron stars, and the question remains, whether at least a moderate softness of the EoS of strongly coupled deconfined matter is a universal prediction of holography. We should also note that a bound on the speed of sound *at fixed chemical potential* has been proposed in [33], and it seems to hold in holographic models that reproduce thermodynamic properties of QCD computed using lattice techniques at small densities [34].

In the present work, we shall demonstrate that the speeds of sound obtained in gauge/gravity models can be arbitrarily close to the speed of light by considering several examples where this turns out to be the case. On the gravity side, the models consist of Einstein-Maxwell theory minimally coupled to a scalar field, which can be either charged or neutral. These models are dual to a strongly coupled gauge theory in its large-N_c limit. The bulk gauge field is then dual to a global U(1) current on the field theory side, while the scalar field is dual to a relevant scalar operator. A relevant deformation breaking conformal invariance is introduced by turning on a coupling for the scalar operator. The first example we will study has a string theory (top-down) realization with a known field theory dual, while the rest of the cases considered form a family of bottom-up models. Interestingly, we observe that the simplest scenario including a quadratic potential for a canonically normalized scalar field does not lead to large enough values for the speed of sound. To reach higher values, it is necessary for the scalar field to possess self-interactions, which will be reflected in the properties of higher order correlators of the dual operator. This point should be a very interesting one to investigate further in the future.

Our paper is organized as follows. In section 2 we introduce both the top-down and bottom-up models we work with, and in section 3 we discuss a subtle issue related to the spontaneous generation of a scale in the top-down model. After this, we move on to presenting our main result, the EoS in both types of models, in section 4, which is followed by a thorough analysis of the stability of our solutions in section 5. Conclusions are finally drawn in section 6, while a number of computational details will be discussed in the appendices of the paper.

JHEP11(2017)031

2 Holographic models

We will use holographic models as a tool to study the EoS of strongly coupled gauge theories at finite density and temperature, although we will be more interested in low temperatures. The models will be chosen in such a way that the theory is well defined in the UV, in the sense that there is a fixed point at asymptotically large energies. If the theory was conformal, the EoS would be fixed by symmetry; here, this will be avoided by introducing a relevant deformation of the UV fixed point that breaks conformal invariance explicitly. We will consider two cases in parallel: a top-down model with a well defined string theory construction, and a family of phenomenological bottom-up models that allow a wider analysis while keeping the main ingredients of the top-down model.

2.1 Top-down model

The first case we are going to consider is a deformation of $\mathcal{N} = 4$ SU(N_c) super Yang-Mills (SYM). The theory has a global $\mathrm{SU}(4)_R \simeq \mathrm{SO}(6)_R$ R-symmetry group associated to rotations of the supercharges. $\mathcal{N} = 4$ SYM contains vector bosons, fermions, and scalars, all in the adjoint representation of the SU(N_c) gauge group. They can be listed as

fields	symbol	$\mathrm{SU}(4)_R$ representation
vector gauge bosons	$\mathcal{A}_\mu$	singlet
gauginos (fermions)	λ^a	**4**
scalars	ϕ^I	**6**

There are three mutually commuting $\mathrm{U}(1)_{i=1,2,3} \subset \mathrm{SU}(4)_R$ in the R-symmetry group. We will study states with charge for the diagonal U(1) (equal charges for all of the $\mathrm{U}(1)_i$). Since $\mathcal{N} = 4$ SYM is a conformal field theory, we will also need to turn on additional couplings that break explicitly conformal invariance. We will do this by introducing a mass for the gauginos, i.e. we will add a term to the Lagrangian of the form

$$\mathcal{L} = \mathcal{L}_{\mathcal{N}=4} + m_0 \,\mathrm{tr}\ \lambda\lambda\,. \tag{2.1}$$

As we are not adding similar mass terms for the scalars, this also breaks supersymmetry explicitly.

In the $N_c \to \infty$ limit and for very strong 't Hooft coupling $\lambda_{YM} \gg 1$, the $\mathcal{N} = 4$ SYM theory has a holographic dual description as type IIB string theory in a $\mathrm{AdS}_5 \times S^5$ geometry, at weak string coupling $g_s \sim 1/N_c$ and large curvature radius compared to the string scale $L^4/(\alpha')^2 \sim \lambda_{YM}$. The leading order behavior of the theory is thus captured by classical supergravity (SUGRA) in $\mathrm{AdS}_5 \times S^5$ [12]. Turning on a charge density and/or additional couplings in $\mathcal{N} = 4$ SYM is realized in the holographic dual by turning on dual fields that modify the background geometry.

Rather than dealing with the full ten-dimensional SUGRA description of the theory, we will restrict to a subsector that admits a consistent truncation to a simpler five-dimensional theory. The truncation is explained in more detail in [28]. The action reduces to the one of Einstein-Maxwell theory coupled to two real scalars

$$e^{-1}\mathcal{L} = \frac{1}{4}R - \frac{1}{g^2}F_{\mu\nu}F^{\mu\nu} + \frac{1}{4}(\partial_\mu\phi)^2 + \frac{1}{2}\sinh^2\left(\frac{\phi}{\sqrt{2}}\right)(\partial_\mu\theta - 2A_\mu)^2 - \frac{V(\phi)}{4}\,, \tag{2.2}$$

where e is the volume density and

$$V(\phi) = -\frac{3g^2}{4}\left(3 + \cosh(\sqrt{2}\phi)\right), \tag{2.3}$$

with the coupling constant g related to the AdS radius as $g = 2/L$. The bulk gauge field A_μ is dual to the diagonal U(1) R-current J^μ and sources for the current.

We introduce the complex field,

$$\Phi = \tanh\left(\frac{\phi}{2\sqrt{2}}\right) e^{i\theta}, \tag{2.4}$$

in such a way that the action takes the form

$$e^{-1}\mathcal{L} = \frac{1}{4}\left[R - L^2F^2 - \mathcal{K}(\Phi)|D\Phi|^2 - \mathcal{V}(\Phi)\right], \quad D_\mu\Phi = (\partial_\mu - iqA_\mu)\Phi, \tag{2.5}$$

with a charge $q = 2$ and kinetic and potential terms

$$\mathcal{K}(\Phi) = \frac{8}{(1-|\Phi|^2)^2}, \quad \mathcal{V}(\Phi) = -\frac{12}{L^2}\frac{1+|\Phi|^4}{(1-|\Phi|^2)^2}. \tag{2.6}$$

For small Φ,

$$\mathcal{K}(\Phi) \simeq 8, \quad \mathcal{V}(\Phi) \simeq -\frac{12}{L^2}\left(1 + 2|\Phi|^2\right). \tag{2.7}$$

Therefore, the canonically normalized scalar has a mass $m^2L^2 = -3$ which corresponds to a field dual to an operator of conformal dimension $\Delta = 3$, the gaugino mass operator $\mathcal{O} = \text{tr}\ \lambda\lambda$, and the associated coupling m_0. Therefore, the five-dimensional action of the truncated SUGRA subsector contains all the necessary ingredients for our analysis.

2.2 Bottom-up models

Taking the top-down model as a guide, we are going to consider a family of models with a gravity dual consisting of Einstein-Maxwell theory minimally coupled to a scalar. Thereby, we will be describing a subsector of the dual field theory including a global U(1) current J^μ and a relevant scalar operator $\mathcal{O}$. The usual large-N_c and strong coupling limits are assumed to hold for the classical gravity approximation we take to be valid.

In order to obtain different EoSs, we will allow for some freedom in the choice of the action for the scalar field. This means that in most cases the field theory dual, if it exists, is not known. We will use these models as an exploratory mean to determine whether holographic models can produce a stiff EoS, with the perspective of looking for proper holographic duals with similar properties in the future. One can in principle allow the kinetic term and the potential for the scalar to be generic functionals, although we will fix their form to be able to do explicit calculations. The five-dimensional action for these models will be as given in (2.5). For the bottom-up models we will take the charge to be zero $q = 0$, as eventually we would like to identify the U(1) symmetry with baryon symmetry, which is unbroken. For simplicity, we will fix the kinetic term to be canonically normalized $\mathcal{K}(\Phi) = 1$ and the potential to be of the form

$$\mathcal{V}(\Phi) = -\frac{12}{L^2} + m^2|\Phi|^2 + \frac{V_4}{2L^2}\left(|\Phi|^2\right)^2. \tag{2.8}$$

JHEP11(2017)031

Here, we will allow the masses to lie in the interval $0 > m^2L^2 \geq -3$, in such a way the scalar field will be dual to a scalar operator of dimension in the interval $4 > \Delta \geq 3$. We will study first the case with a purely quadratic potential $V_4 = 0$ and then the behavior when V_4 is changed.

2.3 Charged black hole solutions in the top-down model

We take an Ansatz for the metric of the form

$$ds^2 = L^2\frac{dr^2}{r^2 f(r)} + \frac{r^2}{L^2}e^{2A}\left[-f(r)dt^2 + dx_1^2 + dx_2^2 + dx_3^2\right], \tag{2.9}$$

in such a way that it is asymptotically AdS at $r \to \infty$. There is a black hole horizon at $r = r_H$, where $f(r_H) = 0$. The scalar field and the time component of the gauge field are also turned on and depend only on the radial coordinate, i.e. $\Phi_0 = \Phi_0(r)$, $A_0 = A_0(r)$.

The equations of motion and the near boundary behavior of the bulk fields are detailed in appendix A. If the fields were decoupled, their expansion at the boundary would take the form[3]

$$A_0 \sim \mu + \frac{L^4}{r^2}A_{0(0,2)}, \quad f \sim 1 + \frac{L^8}{r^4}f_{(0,4)}, \quad A \sim 0, \quad \Phi_0 \sim \frac{L^2}{r}\phi_{(0,1)} + \frac{L^6}{r^3}\left[\phi_{(1,3)}\log\left(\frac{r}{L}\right) + \phi_{(0,3)}\right]. \tag{2.10}$$

We can identify μ with the chemical potential in the dual field theory and $\phi_{(0,1)}$ with the coupling of the dual operator. If it is nonzero, this amounts to introducing a relevant deformation that breaks explicitly conformal invariance in the dual field theory. In this case, $\phi_{(0,1)}$ gives a mass to the gauginos. For $\Delta = 3$, $\phi_{(0,1)}$ has dimension one, so we can in fact identify it with a mass scale $m_0 \equiv \phi_{(0,1)}$. The coefficients $A_{0(0,2)}$, $f_{(0,4)}$, and $\phi_{(0,3)}$ determine the R-charge density, energy, and the expectation value of the scalar operator (gaugino bilinear), respectively. The coefficient of the logarithmic term $\phi_{(1,3)}$ is finally proportional to m_0.

For convenience when obtaining the numerical solutions, we will perform the variable and gauge field redefinitions

$$u = \left(\frac{r_H}{r}\right)^2, \quad A_0 \to A_0\frac{r_H}{L^2}, \tag{2.11}$$

so that the AdS boundary is now at $u \to 0$ while the horizon is at $u \to 1$. This change implies that in order to correctly match with the holographic renormalization scheme adopted, carried out in the r coordinate, one must perform the shift

$$\begin{aligned} f_{(0,4)} &\to f_{(0,4)} + 16\mu^2 m_0^2 \log\left(\frac{r_H}{L}\right) \\ \phi_{(0,3)} &\to \phi_{(0,3)} - \left(\frac{4}{3}m_0^2 + 2\mu^2\right) m_0 \log\left(\frac{r_H}{L}\right) \\ A_{0(0,2)} &\to A_{0(0,2)} + 8\mu m_0^2 \log\left(\frac{r_H}{L}\right) \end{aligned} \tag{2.12}$$

[3]We use a notation where $X_{(n,m)}$ is the coefficient of $(L^2/r)^m(\log(r/L))^n$ in the expansion of the field X.

JHEP11(2017)031

in such a way that the dependence on r_H in the near-boundary series solution is absorbed. Such a shift has to be applied also to the boundary operators (B.18). In the u coordinate, the near-boundary fields read

$$\Phi_0 \sim \alpha u^{1/2} + \left[\widehat{\beta}\log(u) + \beta\right] u^{3/2}, \quad f \sim 1 + \widehat{f}_{(0)} u^2, \quad A \sim 0, \quad A_0 \sim \frac{r_H}{L^2}\left(a_0 + a_1 u\right). \tag{2.13}$$

The map between the coefficients in both coordinates is

$$m_0 = \frac{r_H}{L^2}\alpha, \quad \phi_{(0,3)} = \frac{r_H^3}{L^6}\beta, \quad \mu = \frac{r_H}{L^2}a_0, \quad A_{0(0,2)} = \frac{r_H^3}{L^6}a_1, \quad f_{(0,4)} = \frac{r_H^4}{L^8}\widehat{f}_{(0)}\,. \tag{2.14}$$

Near the horizon we will impose regularity of the solution plus vanishing boundary conditions for the warp factor and the gauge field. Then, at leading order, we have

$$A_0 \sim A_0^{(1)}_H (1-u), \quad f \sim f_H^{(1)}(1-u), \quad A \sim A_H^{(0)} + A_H^{(1)}(1-u), \quad \Phi \sim \phi_H^{(0)}\,, \tag{2.15}$$

where the subleading terms can be found in appendix A.2.

It is convenient to define our thermodynamic variables (μ, T) in units of the mass m_0

$$\mu_r = \frac{\mu}{m_0}, \quad t_r = \frac{T}{m_0}\,, \tag{2.16}$$

so that $a_0 = \mu_r \alpha$. We will also normalize the thermodynamic potentials and expectation values of the charge and scalar operators by the mass and a common factor $\mathcal{N} = \frac{L^3}{16\pi G_5}$, such that

$$\varepsilon_r = \frac{\varepsilon}{\mathcal{N} m_0^4}, \quad p_r = \frac{p}{\mathcal{N} m_0^4}, \quad v_r = \frac{\langle \mathcal{O} \rangle}{\mathcal{N} m_0^3}, \quad n_r = \frac{n}{\mathcal{N} m_0^3}\,. \tag{2.17}$$

After defining

$$\mathcal{W}_1 = \kappa_1 - 8\log\left(m_0 L\right), \qquad \mathcal{W}_2 = \kappa_2 + \frac{32}{3}\log\left(m_0 L\right), \tag{2.18}$$

and taking the renormalized expectation values (B.18), detailed in appendix B.2, we then get

$$\begin{aligned}
\varepsilon_r &= -\frac{3\widehat{f}_0}{\alpha^4} - \frac{8\beta}{\alpha^3} + \log(\alpha)\left(32\mu_r^2 - \frac{32}{3}\right) - 4\mu_r^2\left(\kappa_1 + 3\right) - \kappa_2 - \frac{16}{3} \\
p_r &= -\frac{\widehat{f}_0}{\alpha^4} + \frac{8\beta}{\alpha^3} + \log(\alpha)\left(32\mu_r^2 + \frac{32}{3}\right) - 4\mu_r^2\left(\kappa_1 + 1\right) + \kappa_2 + \frac{16}{3} \\
v_r &= 32\frac{\beta}{\alpha^3} + \frac{64}{3}\log(\alpha)\left(3\mu_r^2 + 2\right) - 8(\kappa_1 + 4)\mu_r^2 + 4\kappa_2 + \frac{32}{3} \\
n_r &= -8\left[a_1 - 8\mu_r \log(\alpha) + (\kappa_1 + 4)\mu_r\right].
\end{aligned} \tag{2.19}$$

We have computed the solutions by means of the shooting technique, thoroughly explained in appendix A.3. We plot the results as a function of μ_r for a fixed temperature $t_r = 1$ in figure 1.

JHEP11(2017)031

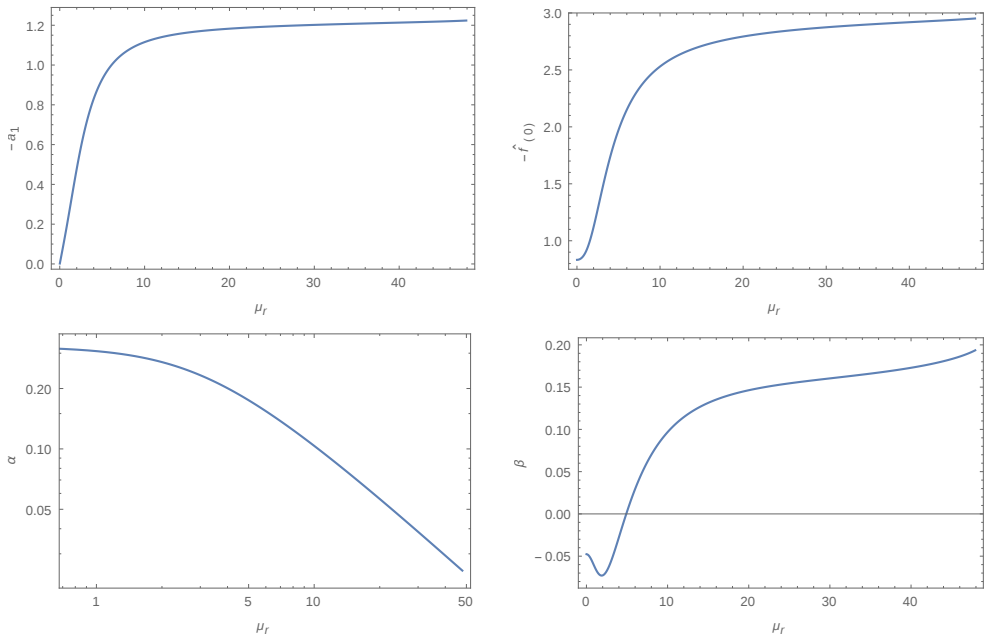

Figure 1. Coefficients of the numerical solutions defined in eq. (2.14) as functions of the reduced chemical potential μ_r. From left to right and top to bottom, $-a_1$, $-\widehat{f}_{(0)}$, α, and β.

2.4 Charged black hole solutions in bottom-up models

In the bottom-up models, we will proceed in a similar manner to the top-down one. We take an Ansatz for the metric of the form given in (2.9), and fix $q = 0$ for simplicity and because the potential application to the physics of dense nuclear matter requires the U(1) symmetry to be unbroken. The equations of motion and the near boundary behavior of the bulk fields are detailed in the appendices of [28]. For $\Delta = 3$ the equations and expansions take a similar form as in the top-down model (2.10). For $\Delta \neq 3$ only the expansion of the scalar field at the boundary changes to

$$\Phi_0 \sim \frac{L^{2(4-\Delta)}}{r^{4-\Delta}}\tilde{\phi}_{(0,0)} + \frac{L^{2\Delta}}{r^{\Delta}}\phi_{(0,0)}\,. \tag{2.20}$$

We can identify $\tilde{\phi}_{(0,0)}$ with the coupling of the dual operator. If it is nonzero, this amounts to introducing a relevant deformation that breaks explicitly conformal invariance in the dual field theory. Similarly to the top-down model, we will introduce the mass scale $m_0 = (\tilde{\phi}_{(0,0)})^{1/(4-\Delta)}$.

For convenience when obtaining the numerical solutions, we will perform the change to the u coordinate (2.11). The near-boundary expansions of the fields are given by eq. (2.13), except for the scalar field, which now reads

$$\Phi_0 \sim \alpha u^{(4-\Delta)/2} + \beta u^{\Delta/2}\,. \tag{2.21}$$

The map between the coefficients in both coordinates is given by (2.14), except for the scalar, which now takes the form

$$\tilde{\phi}_{(0)} = \left(\frac{r_H}{L^2}\right)^{4-\Delta}\alpha, \quad \phi_{(0)} = \left(\frac{r_H}{L^2}\right)^{\Delta}\beta\,. \tag{2.22}$$

JHEP11(2017)031

Near the horizon we will impose regularity of the solution plus vanishing boundary conditions for the warp factor and the gauge field as in (2.15).

It is convenient to define our thermodynamic variables (μ, T) in units of the mass m_0, as in (2.16) and (2.17). The normalization of the expectation value of the scalar operator reads in the general case

$$v_r = \frac{\langle \mathcal{O} \rangle}{\mathcal{N} m_0^{\Delta}} \,. \tag{2.23}$$

Taking the renormalized expectation values detailed in the appendix of [28], we get for $\Delta = 3$:

$$\begin{aligned}
\varepsilon_r &= -\frac{3\widehat{f}_0}{\alpha^4} - \frac{\beta}{\alpha^3} + \left(\frac{1}{3} + \frac{V_4}{2}\right)\log(\alpha) - \kappa_2 - \frac{1}{12} - \frac{V_4}{8} \\
p_r &= -\frac{\widehat{f}_0}{\alpha^4} + \frac{\beta}{\alpha^3} - \left(\frac{1}{3} + \frac{V_4}{2}\right)\log(\alpha) + \kappa_2 + \frac{1}{12} + \frac{V_4}{8} \\
v_r &= -2\frac{\beta}{\alpha^3} + 2\left(\frac{1}{3} + \frac{V_4}{2}\right)\log(\alpha) - 2\kappa_2 - \frac{1}{3} - \frac{V_4}{2} \\
n_r &= -8a_1 \,.
\end{aligned} \tag{2.24}$$

We will fix $\kappa_2 = 0$ in the following, since this parameter is irrelevant for the speed of sound. This selects $V_4 = -2/3$ as a special value, for which the logarithmic terms drop and the conformal anomaly vanishes, although there are still terms contributing to the trace of the energy-momentum tensor proportional to the expectation value of the scalar operator.

For $\Delta \neq 3$, we on the other hand get

$$\begin{aligned}
\varepsilon_r &= -\frac{3\widehat{f}_0}{\alpha^4} + (\Delta - 4)(\Delta - 2)\frac{\beta}{\alpha^3} \\
p_r &= -\frac{\widehat{f}_0}{\alpha^4} - (\Delta - 4)(\Delta - 2)\frac{\beta}{\alpha^3} \\
v_r &= -2(\Delta - 2)\frac{\beta}{\alpha^3} \\
n_r &= -8a_1 \,.
\end{aligned} \tag{2.25}$$

We have computed the solutions using the same numerical methods as for the top-down model. The results are plotted as functions of μ_r for a fixed temperature $t_r = 0.1$ in figure 2.

3 Generation of a new scale in the top-down model

There are some subtleties entering the EoS of the top-down model that we shall presently discuss. In (2.19), κ_1 and κ_2 are the coefficients of finite counterterms. These terms are scheme dependent but once the renormalization scheme has been fixed, their values are related to physical quantities such as the expectation value of the scalar operator and the charge density. This implies that the theory is not completely determined by the bulk action of the gravity dual, but it is necessary to specify the value of the finite counterterms as well.

JHEP11(2017)031

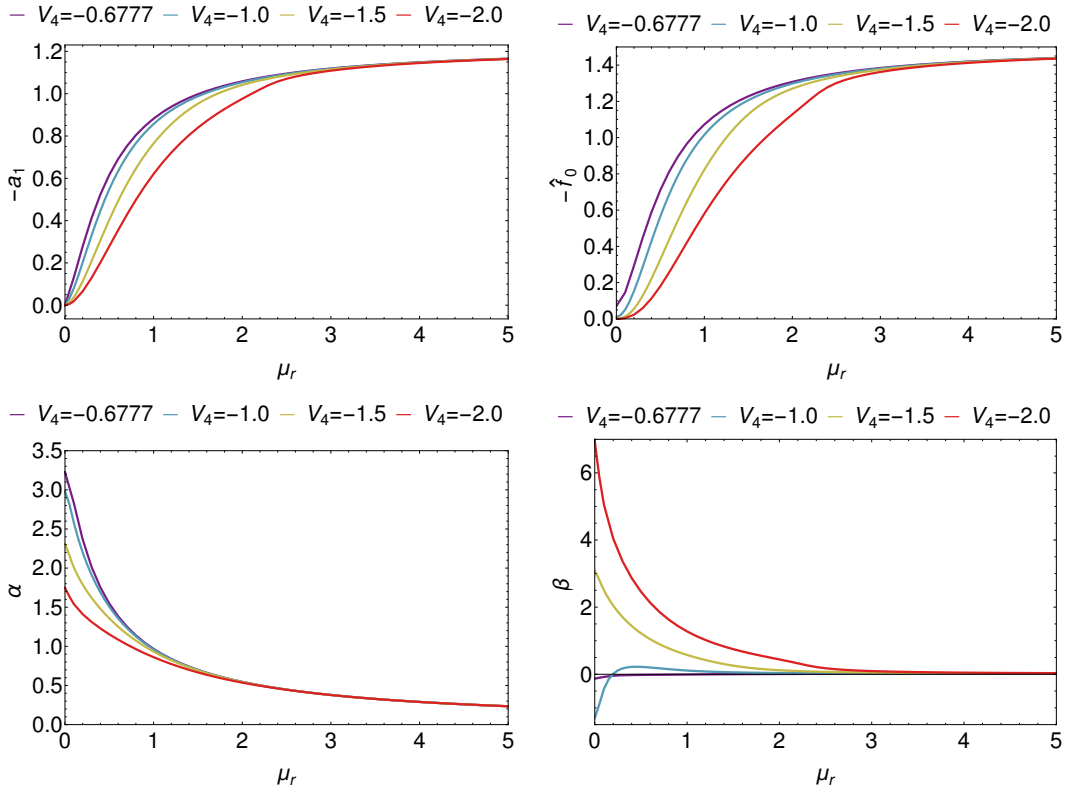

Figure 2. Coefficients of the numerical solutions in the bottom-up case as functions of the reduced chemical potential μ_r at fixed temperature $t_r = 0.1$ and different values of V_4. From left to right and top to bottom, $-a_1$, $-\widehat{f}_{(0)}$, α, and β.

From the point of view of the field theory, consider that in addition to the $\mathcal{N} = 4$ SYM fields there is a decoupled scalar field φ and a Yukawa coupling Y_φ between the scalar and the $\mathcal{N} = 4$ SYM gauginos,

$$\mathcal{L}_Y = Y_\varphi \varphi \,\mathrm{tr}\; \lambda\lambda\,. \tag{3.1}$$

In the large-N_c limit, we can treat the scalar field as quenched, neglecting loop effects from the $\mathcal{N} = 4$ SYM theory. Nevertheless, this coupling breaks conformal invariance (even though it is classically marginal) and will introduce a logarithmic dependence $\log(E/\Lambda)$ on the energy scale E in physical observables, such as scattering cross sections. In particular, a wave function renormalization of φ will show up in the kinetic term of the scalar field, having the same form as the finite counterterm associated to κ_1. The scale Λ that appears inside the log depends on the scheme, but can be fixed by measurement. After this, the value of Λ will be different in different schemes, but physical quantities will naturally have the same values in each of them.

On top of the scale appearing due to logarithmic terms, if the scalar field acquires an expectation value $\langle\varphi\rangle = m_0$, this will affect the $\mathcal{N} = 4$ SYM theory as an explicit breaking of conformal invariance. Note that in principle the scale of explicit breaking m_0 and the scale that determines the running of the coupling Λ would be completely independent, if no further condition is imposed.

JHEP11(2017)031

To illustrate the above with an example, consider the computation of a one-loop contribution to the self-energy of a scalar field due to a loop of a fermion field of mass m_0. There is a logarithmic UV divergence that in dimensional regularization in $d = 4 - 2\epsilon$ dimensions becomes a pole as $\epsilon \to 0$. Depending on the scheme, removing this divergence leaves behind different finite terms, taking the forms

$$\begin{aligned}
\Sigma_{MS}(p^2) &\sim \beta m_0^2 \left(-\gamma_E + \log(4\pi) + \log \frac{\sqrt{-p^2}}{\Lambda} \right) \\
\Sigma_{\overline{MS}}(p^2) &\sim \beta m_0^2 \log \frac{\sqrt{-p^2}}{\bar{\Lambda}} \\
\Sigma_{FS}(p^2) &\sim m_0^2 \left(\kappa_{FS} + \beta \log \frac{\sqrt{-p^2}}{m_0} \right).
\end{aligned} \tag{3.2}$$

Here, $\beta \sim Y_\varphi^2$ is a scheme-independent factor, MS and $\overline{MS}$ denote the usual (modified) minimal subtraction schemes with scale parameters Λ and $\bar{\Lambda}$, and FS stands for a fixed scale scheme with an arbitrary finite term κ_{FS}. The physical mass of the scalar M corresponds to the position of the pole in the propagator

$$p^2 + \Sigma(p^2)\Big|_{p^2=-M^2} = 0\,, \tag{3.3}$$

where m_0 is the bare mass. This can be viewed as fixing the arbitrary renormalization scales of the MS and $\overline{MS}$ schemes and the constant in the FS scheme,

$$\bar{\Lambda} = \frac{e^{\gamma_E}}{4\pi}\Lambda = M e^{-M^2/\beta m_0^2}, \quad \kappa_{FS} = \frac{M^2}{m_0^2} - \beta \log \frac{M}{m_0}\,. \tag{3.4}$$

For a given scheme, changing the renormalization scale or the finite counterterm amounts to a change of the physical scale and thus a modification of the theory.

In the holographic calculation we fix the scheme of holographic renormalization by using L as the reference scale in the asymptotic expansion of the fields and m_0 in the definition of the finite counterterms. We could have chosen a different scale, say L', in such a way that

$$\mathcal{W}_1 = \kappa_1' - 8 \log\left(m_0 L'\right), \qquad \mathcal{W}_2 = \kappa_2' + \frac{32}{3} \log\left(m_0 L'\right). \tag{3.5}$$

Physical results would be unchanged as long as we appropriately identify the values of the finite counterterms in each scheme,

$$\kappa_1' = \kappa_1 - 8\log(L/L'), \quad \kappa_2' = \kappa_2 + \frac{32}{3}\log(L/L')\,. \tag{3.6}$$

We could also have changed the scheme by using a scale different from m_0 in the logs

$$\mathcal{W}_1 = \kappa_1' - 8 \log\left(m' L\right), \qquad \mathcal{W}_2 = \kappa_2' + \frac{32}{3} \log\left(m' L\right), \tag{3.7}$$

leading to a somewhat different relation between the finite counterterms in different schemes,

$$\kappa_1' = \kappa_1 - 8\log(m_0/m'), \quad \kappa_2' = \kappa_2 + \frac{32}{3}\log(m_0/m')\,. \tag{3.8}$$

JHEP11(2017)031

This shows that an arbitrary scale can indeed be introduced through holographic renormalization.

Once we have fixed our renormalization scheme (for instance one could choose schemes where $\kappa_1' = 0$ or $\kappa_2' = 0$), different values of finite counterterms correspond to different values of physical quantities (i.e. renormalization group invariants). However, one can see that the effect of κ_2 is to add a term independent of the temperature or the chemical potential that shifts the value of the vacuum energy. It is therefore unimportant for thermodynamics, and a valid physical choice could be that the effective cosmological constant term in the dual field theory vanishes. A similar term appears in the D3/D7 model [35], where the counterterm is fixed by supersymmetry and gives a vanishing expectation value for the scalar operator [36]. In principle, the dual field theory is supersymmetric with soft-breaking terms (the gaugino mass in eq. (2.1)), and supersymmetry could then fix the value of the finite counterterm κ_2 at zero temperature and chemical potential. The value of κ_1 might also be fixed by similar considerations, but in the present context with a nonzero chemical potential, it is not known how or whether the finite counterterm is to be fixed. To our knowledge, this is still an open problem in holographic renormalization in general. This implies that giving arbitrary values to the finite counterterms might spoil the identification of the dual field theory corresponding to the consistent truncation. Nevertheless one could interpret models with different values as extensions of the original supersymmetric model with additional terms (similar to the one in eq. (3.1)) that introduce an explicit breaking of supersymmetry.

Compared to κ_2, κ_1 has a more interesting and physical effect: it changes the argument of logarithms of α according to

$$\log(\alpha) \longrightarrow \log\left(\alpha e^{-\kappa_1/8}\right) = \log\left(\frac{a_0 e^{-\kappa_1/8}}{\mu_r}\right) \equiv \log\left(\frac{\Lambda_\kappa}{\mu}\right). \tag{3.9}$$

This means that a new scale Λ_κ has been spontaneously generated in the dual field theory, and that its relative size in comparison with the scale of the explicit breaking of conformal invariance is controlled by κ_1:

$$\frac{\Lambda_\kappa}{m_0} = a_0 e^{-\kappa_1/8}. \tag{3.10}$$

In particular, for $|\kappa_1|$ sufficiently large, Λ_κ can be pushed towards the UV. In figure 3 we plot Λ_κ as a function of the reduced chemical potential for various negative values of κ_1. When the red line crosses the other curves, $\Lambda_\kappa = \mu_r$ and the argument of the logarithm in eq. (3.9) becomes unity. Note that the hierarchy is not parametrically large with N or the 't Hooft coupling, so we will remain in the realm of classical supergravity. Furthermore, as the hierarchy is introduced through finite terms in the boundary action, there is no change in the bulk supergravity equations of motion and solutions; in particular the consistent truncation is unaffected. It is still the same subset of operators in the dual field theory that close under the OPEs.

JHEP11(2017)031

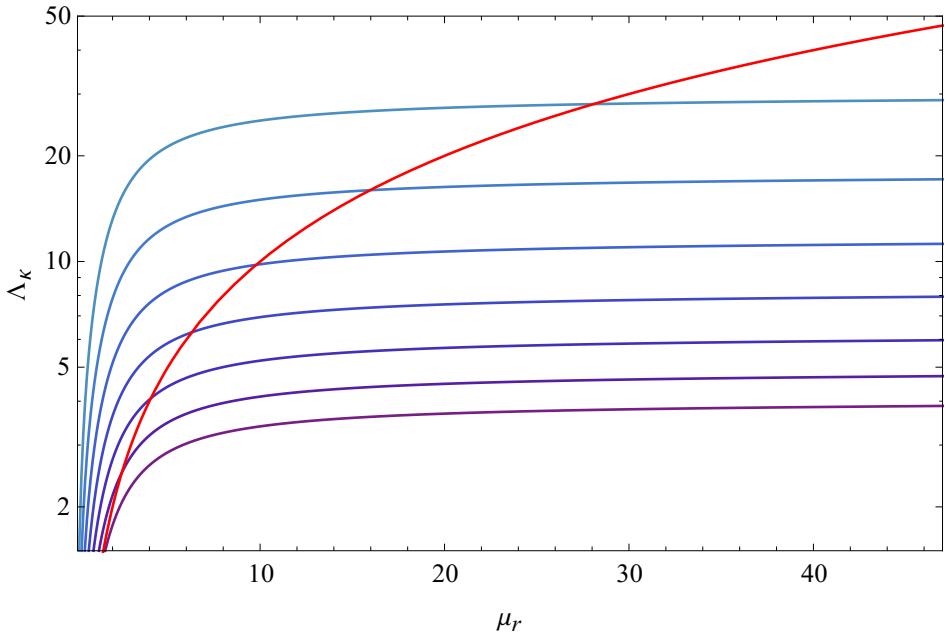

Figure 3. Λ_κ vs μ_r for different values of $\kappa_1 < 0$. The crossings with the red line correspond to points where $\Lambda_\kappa = \mu_r$. From bottom to top, $\kappa_1 = -9.49$, $\kappa_1 = -11.05$, $\kappa_1 = -12.94$, $\kappa_1 = -15.22$, $\kappa_1 = 17.99$, $\kappa_1 = -21.38$, $\kappa_1 = -25.53$.

4 Equation of State

If a weakly coupled quasiparticle description is possible for the system under study, it is appropriate to use kinetic theory to derive its Equation of State. In a relativistic theory causality then imposes a constraint, Taub's inequality [15]

$$\tau = \frac{\varepsilon(\varepsilon - 3p)}{\rho^2} \geq 1\,, \tag{4.1}$$

where ρ is the mass density. One can check for instance that for a degenerate (non-interacting) Fermi liquid $\tau = \tau_F \geq 1$, where

$$\tau_F = \frac{9}{16\,(\mu_r^2-1)^3}\left[2\mu_r^6-3\mu_r^4+\mu_r^2+\log^2\left(\mu_r+\sqrt{\mu_r^2-1}\right)-2\sqrt{\mu_r^2-1}\mu_r^3\log\left(\mu_r+\sqrt{\mu_r^2-1}\right)\right] \tag{4.2}$$

and $\mu_r = \mu/m_F$ where m_F is the mass of the fermions.

In a strongly coupled theory the above condition may easily be violated. A simple example is the D3/D7 model [35] that is used to model flavor physics at strong coupling, and that contains quarks and squarks with a mass m_q. The EoS is known analytically [37–41], and the pressure, energy density, and mass density at zero temperature read as functions of the chemical potential

$$p = \lambda(\mu^2 - m_q^2)^2, \quad \varepsilon = \lambda(\mu^2 - m_q^2)(3\mu^2 + m_q^2), \quad \rho = 4\lambda m_q \mu(\mu^2 - m_q^2)\,, \tag{4.3}$$

where λ is an unimportant constant factor. Defining the reduced chemical potential as $\mu_r = \mu/m_q$, one finds

$$\tau_{D7} = \frac{3}{4}\left(1 + \frac{1}{3\mu_r^2}\right) \;\Rightarrow\; 1 \geq \tau_{D7} \geq \frac{3}{4}\,. \tag{4.4}$$

JHEP11(2017)031

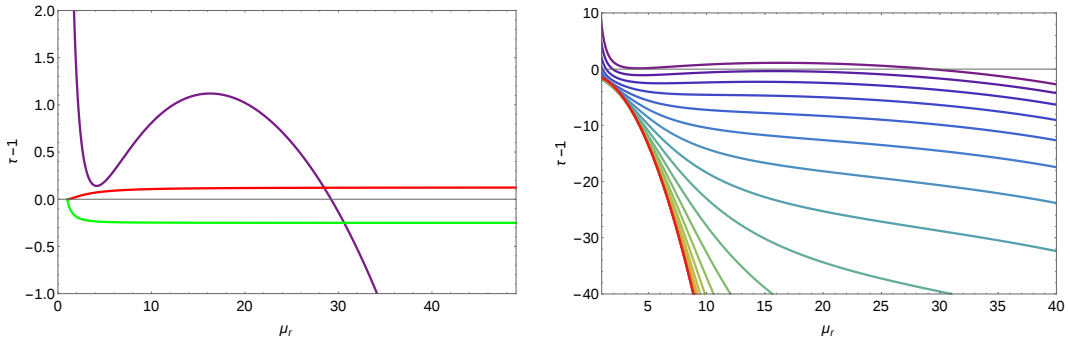

Figure 4. Left plot: the function $\tau - 1$ appearing in Taub's inequality plotted as a function of the chemical potential for a degenerate Fermi liquid (red), the D3/D7 model (green) and the top-down model for $\kappa_1 = -12.86$ (purple). Holographic models clearly violate Taub's inequality $\tau \geq 1$. At large values of μ_r, $\tau - 1$ in the D3/D7 model approaches a negative constant corresponding to $\tau = 3/4$, while the supergravity curve keeps decreasing and reaches $\tau = 0$ at $\mu_r \simeq 34$. The difference in behavior can be understood from the fact that $\varepsilon - 3p \sim m_q^2 \mu^2$ in the D3/D7 model, while $\varepsilon - 3p \sim m_0^2 \mu^2 \log(m_0/\mu)$ in the supergravity model. On the right plot we show Taub's inequality for the top-down model for different values of κ_1, spanning from -12.86 (upper curve) to -5.18×10^3 (bottom curve).

Taub's inequality is obviously violated, which indicates that the theory is indeed strongly coupled and that it possesses no good quasiparticle description. Note that there is, however, a (weaker) bound that constrains the Equation of State. Indeed, as long as $\tau \geq 0$ we will have a condition

$$\varepsilon \geq 3p\,. \tag{4.5}$$

4.1 Top-down model

We can compare the values of τ in the models we study here with those of the degenerate Fermi liquid and the D3/D7 model, see figure 4. We observe that $\tau < 0$ for a range of values of the chemical potential ($\mu_r \gtrsim 32$ for $\kappa_1 = -10$; for even more negative values of κ_1 the curve of the top-down model goes further down). It thus appears that in these regions the EoS is stiffer than in a conformal theory, but how stiff can it be? In order to answer this question we would need to compute the adiabatic speed of sound (1.1). However, it is technically easier to work at fixed temperature and compute the isothermal speed of sound

$$v^2_{s\,\mathrm{isot}} = \left(\frac{\partial p}{\partial \varepsilon}\right)_T = \frac{\left(\frac{\partial p_r}{\partial \mu_r}\right)_{t_r}}{\left(\frac{\partial \varepsilon_r}{\partial \mu_r}\right)_{t_r}}\,, \tag{4.6}$$

which is closely related to the adiabatic one through the standard thermodynamic relations

$$\begin{aligned} v^2_{s\,\mathrm{isot}} &= \frac{\rho_r}{\mu_r \left(\frac{\partial \rho_r}{\partial \mu_r}\right)_{t_r} + t_r \left(\frac{\partial s_r}{\partial \mu_r}\right)_{t_r}} \\ v^2_{s\,\mathrm{adiab}} &= \frac{1}{\mu_r} \frac{\rho_r \left(\frac{\partial s_r}{\partial t_r}\right)_{\mu_r} - s_r \left(\frac{\partial s_r}{\partial \mu_r}\right)_{t_r}}{\left(\frac{\partial \rho_r}{\partial \mu_r}\right)_{t_r} \left(\frac{\partial s_r}{\partial t_r}\right)_{\mu_r} - \left(\frac{\partial \rho_r}{\partial t_r}\right)_{\mu_r} \left(\frac{\partial s_r}{\partial \mu_r}\right)_{t_r}}\,. \end{aligned} \tag{4.7}$$

JHEP11(2017)031

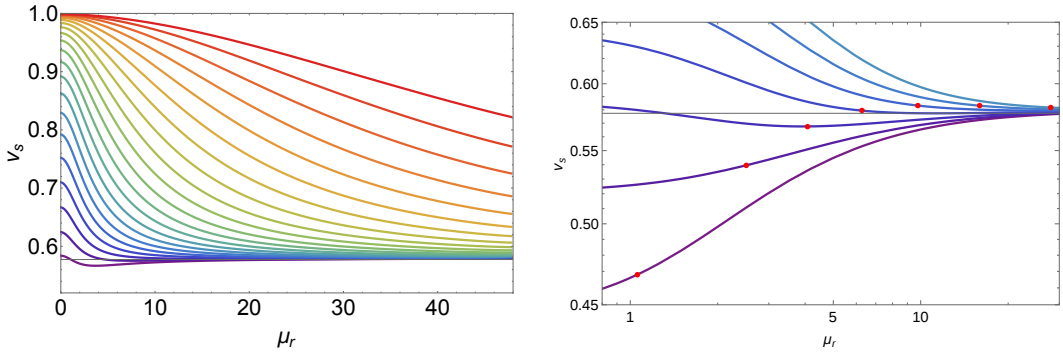

Figure 5. v_s as a function of the reduced chemical potential at $t_r = 1$ at different values of κ_1. The thin horizontal line corresponds to the value of the speed of sound in the conformal theory $v_s = 1/\sqrt{3}$. In the left plot the values of κ_1 span from -12.84 (bottom curve) to -5.18×10^3 (upper curve). In the right plot we have marked the points where $\mu_r = \Lambda_\kappa$ for different curves, which are at the same values of κ_1 than in figure 3.

If the pressure has an analytic expansion in T/μ for $T/\mu \ll 1$ (as it will be the case in our models) and the entropy goes to zero at zero temperature, one can neglect the terms proportional to $\left(\frac{\partial s_r}{\partial \mu_r}\right)_{t_r}$ and the two speeds become the same. At non-zero temperature, the difference is suppressed by a factor of at least $O(T/\mu)$. Moreover, in many practical applications the temperature is taken to be zero as a good approximation. Therefore, we will study the isothermal speed of sound in the following and drop the label.

The behavior of the speed of sound v_s in the top-down model is depicted in figure 5.[4] We observe that, for $\kappa_1 < 0$, when $|\kappa_1|$ is increased the speed of sound becomes larger at low values of the chemical potential, eventually becoming quite close to the speed of light, and the region where the speed of sound is large also grows. A possible way to understand this is to recall that the scale Λ_κ defined in (3.10) that controls the contribution of the logarithmic terms in (2.19) increases with increasing $|\kappa_1|$. When this happens, the logarithmic terms become large in magnitude. If the logarithmic terms in (2.19) dominate, the EoS becomes stiff but remains compatible with causality, as $\varepsilon_r \sim p_r$. Therefore, there is no fundamental obstacle towards obtaining a stiff EoS for a large interval of chemical potentials, as long as a significant separation of scales is present.

An important issue to consider is the possibility that the theory might become unstable in the stiff regime. A necessary but not sufficient condition for thermodynamic stability is that the charge susceptibility be positive,

$$\chi = \frac{\partial^2 p}{\partial \mu^2} > 0\,. \tag{4.8}$$

In figure 6 we plot $\chi|_{t_r=1}$ for different values of κ_1. For large enough values of $|\kappa_1|$, the susceptibility is positive and the theory is thermodynamically stable with respect to density fluctuations. There is a critical value $\kappa_1 = \kappa_c \approx -6.44$, for which the theory becomes

[4]These plots correspond to values of the chemical potential that are much below the regime of validity of the probe approximation used in [28]. For $t_r = 1$ one should go at least to values $\mu_r > 150$ before we reach the probe limit.

JHEP11(2017)031

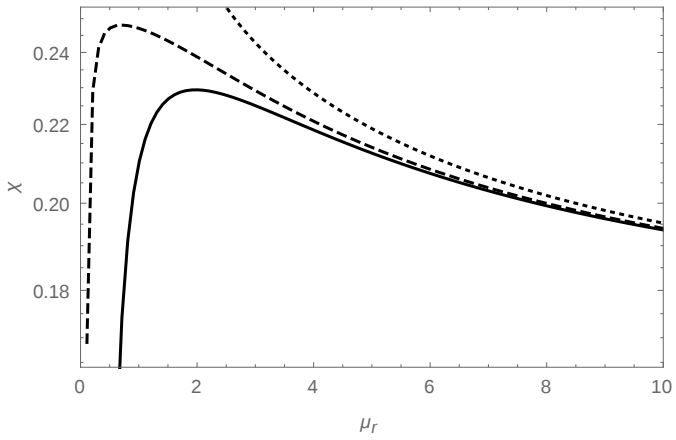

Figure 6. The charge susceptibility χ as a function of the reduced chemical potential μ_r for $t_r = 1$ and for different values of κ_1. From top to bottom, $\kappa_1 = -8$ (black dotted line), $\kappa_1 = \kappa_c$ (black dashed line) and $\kappa_1 = -6$ (black solid line). The central curve marks the onset of the thermodynamic instability, i.e., $\chi(0)|_{\kappa=\kappa_c} = 0$. For larger values of κ_1, one gets $\chi < 0$ up to some finite μ_r.

unstable at low values of the chemical potential. Therefore, the models with a large speed of sound are thermodynamically stable in the stiff regime. We will study their dynamical stability in section 5.

4.2 Bottom-up models

Moving again to the bottom-up models, we first consider the case without a quartic term in the potential $V_4 = 0$. The results are summarized in figure 7. We find that the speed of sound can be larger than the one in a conformal theory, and that larger deviations occur for operators of lower dimensions, close to $\Delta = 3$ for our allowed range. The left plot of figure 7 reflects this: there, we have fixed the temperature, computed the speed of sound as function of the chemical potential, and plotted the largest value we have found for each dimension of the scalar operator. This behavior holds for a range of low temperatures. The right plot of figure 7 shows the largest value of the speed of sound for a fixed dimension $\Delta \sim 3$ as we vary the temperature. We see that the magnitude increases as we lower the temperature, but it seems to saturate at an absolute maximum. The maximum value is just slightly larger than the conformal value by some 3 %, while for phenomenological purposes it should be at least ca. 30 % larger.

Next, we turn on the quartic term in the potential, i.e. let $V_4 \neq 0$. In figure 8 we plot the speed of sound as a function of the chemical potential for a fixed temperature $t_r = 0.1$ and different values of V_4. We observe that making V_4 more negative increases the value of the speed of sound, while making V_4 more positive has the opposite effect. It is possible to reach values of the speed of sound 20–40 % larger than the conformal value for $V_4 \sim -1.5$ and $\mu_r \sim 0.6$–0.75. The speed of sound seems to be growing further at lower values of the chemical potential. This shows that stiff phases are possible in generic holographic models.

However, in contrast to the top-down model, we find that in most cases there are violations of causality ($v_s > 1$) or thermodynamic instabilities ($v_s^2 < 0$) at small values of

JHEP11(2017)031

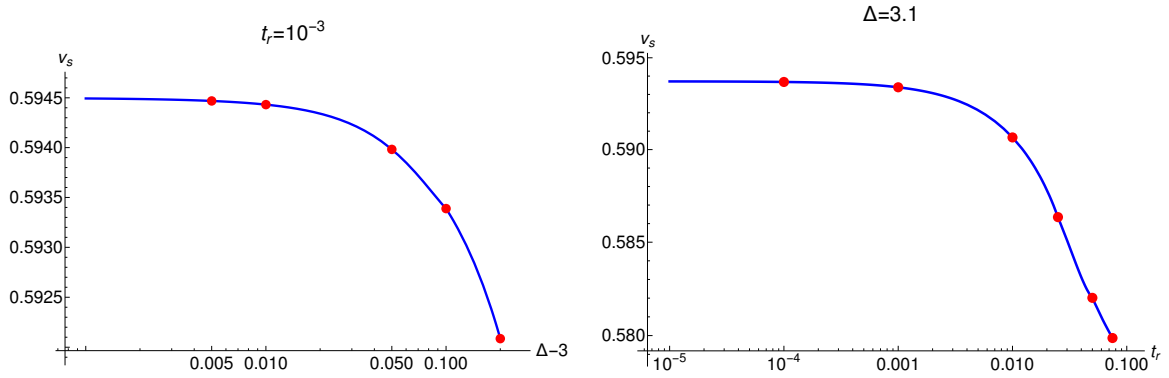

Figure 7. Left plot: maximum speed of sound at a given isotherm as a function of the conformal dimension. The isotherm was taken to be $t_r = 10^{-3}$. Right plot: maximum speed of sound as a function of the reduced chemical potential at a fixed conformal dimension $\Delta = 3.1$.

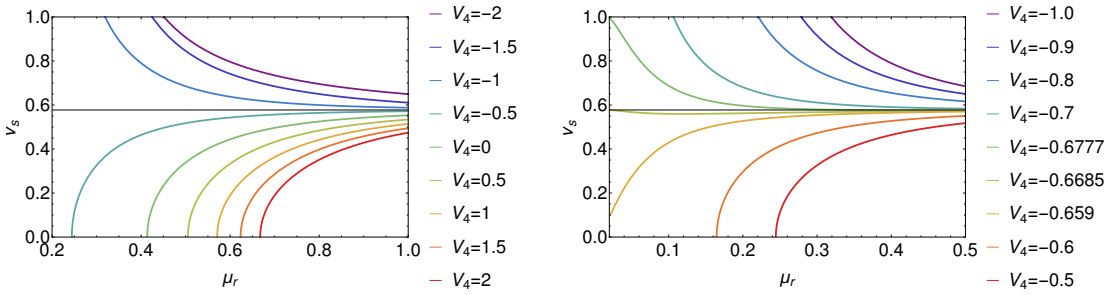

Figure 8. The speed of sound as a function of the reduced chemical potential μ_r for fixed temperature $t_r = 0.1$. The charge and dimension of the dual scalar operator are $q = 0$ and $\Delta = 3$.

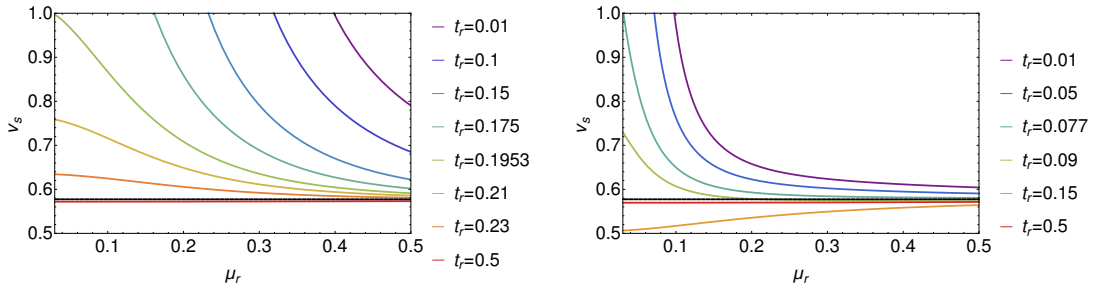

Figure 9. The speed of sound as a function of the reduced chemical potential μ_r for different temperatures and for a fixed quartic potential $V_4 = -1$ (left) and $V_4 = -0.67$ (right). The charge and dimension of the dual scalar operator are $q = 0$ and $\Delta = 3$.

the chemical potential, so there is likely a phase transition between the high temperature, zero density phase and the low temperature, non-zero density one. Nevertheless, as we show in figure 9, for any given temperature there is a range of values of V_4 where the speed of sound remains in the physical range $1 \geq v_s^2 \geq 0$. This happens around the special value of $V_4 = -2/3$, for which the conformal anomaly vanishes; we even observe that near the special value the speed of sound becomes very close to its conformal limit and almost independent of the chemical potential.

JHEP11(2017)031

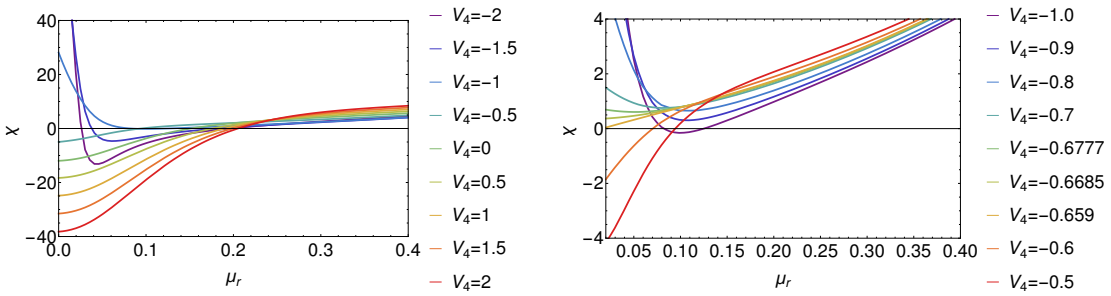

Figure 10. The charge susceptibility χ as a function of the reduced chemical potential μ_r for $t_r = 0.1$ and for different values of V_4.

To inspect thermodynamic stability, we have plotted the charge susceptibility in figure 10. In the cases where $v_s^2 < 0$ we also find that the susceptibility becomes negative, although this appears to happen at lower values of the chemical potential, so it may correspond to a different kind of instability. When the speed of sound becomes superluminal there can also be a small interval with $\chi > 0$ for $V_4 \gtrsim -1$. In the window where $1 \geq v_s^2 > 0$ for all values of the chemical potential we find that $\chi > 0$, so these correspond to thermodynamically stable phases. Numerically, it seems that the values of V_4 for which $v_s^2 = 0$ and $\chi = 0$ at zero chemical potential coincide.

5 Stability

The aim of this section is to determine whether the stiff phases we have found are indeed local minima of the free energy in the space of homogeneous configurations. To this end, we will introduce a small time-dependent perturbation, expecting that if the equilibrium configuration is unstable we will witness the exponential growth of some of the modes. Otherwise, we expect the perturbation to oscillate and/or decay back to equilibrium. As we are considering only homogeneous configurations, we can suppress the spatial dependence. On the gravity side, this translates into studying a linear perturbation around the previously obtained background solution[5]

$$\Phi \to \Phi(r) + \delta\Phi(r,t), \quad A_0 \to A_0(r) + \delta A_0(r,t), \quad g_{\mu\nu} \to g_{\mu\nu}(r) + \delta g_{\mu\nu}(r,t)\,. \tag{5.1}$$

Since our background is stationary, we can expand in plane waves of a given frequency ω,

$$\delta\Phi(r,t) = \varphi(r)e^{-i\omega t}, \quad \delta A_0(r,t) = a_0(r)e^{-i\omega t}, \quad \delta g_{\mu\nu}(r,t) = h_{\mu\nu}(r)e^{-i\omega t}\,. \tag{5.2}$$

Dynamical modes are normalizable and satisfy an ingoing boundary condition at the horizon. This is possible typically only for a discrete set of complex frequencies, the quasinormal frequencies ω_n. If the imaginary part of the quasinormal frequency is negative or zero, $\mathrm{Im}\,\omega_n \leq 0$, the associated quasinormal mode decays in time or is oscillatory, and the background is stable. On the other hand, if $\mathrm{Im}\,\omega_n > 0$ is positive, the quasinormal mode grows exponentially in time and the background is unstable.

[5]We work in the $\delta g_{r\mu} = A_r = 0$ gauge.

JHEP11(2017)031

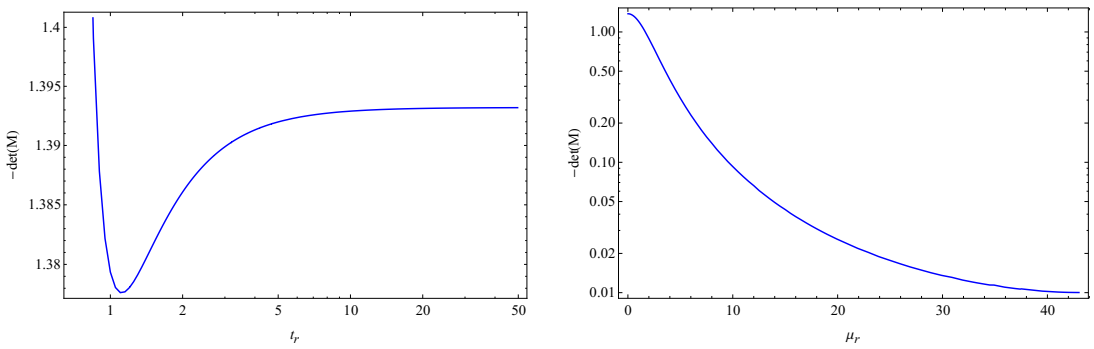

Figure 11. Left figure: $\det(M)$ at zero density as a function of the reduced temperature. Right figure: $\det(M)$ as a function of the reduced chemical potential at $t_r = 1$.

An important piece of information is that at zero chemical potential and high temperatures — $\mu_r = 0$, $t_r \gg 1$ — the model is known to be stable, as the quasinormal modes should approximate those of a probe scalar in an AdS black hole background, all of which are on the lower half of the complex frequency plane [42]. As the background changes continuously, a quasinormal mode has to cross the real axis to the upper half plane in order to develop an instability. Physically we expect that if the background becomes unstable there will be another *stationary* solution corresponding to the true vacuum of the theory. In that case the crossing should happen at the origin of the complex plane. Therefore, the onset of the instability can be determined from the appearance of a quasinormal mode at zero frequency.

We study the appearance of a zero frequency quasinormal mode using the determinant method of e.g. [43, 44] and standard techniques, most details of which can be found in appendix C. First, we introduce gauge invariant combinations of the fields under diffeomorphisms that preserve the condition $g_{\mu r} = 0$. There are two independent scalar modes

$$\begin{aligned} z_1 &= \varphi + \varphi^\dagger - \frac{r\Phi_0'}{1+rA'}h \\ z_2 &= \omega\left(\varphi - \varphi^\dagger\right) + q\Phi_0\left[\frac{A_0}{f}h_{00} + 2a_0 + \left(A_0 + \frac{r}{1+rA'}\left(A_0' - \frac{f'}{2f}A_0\right)\right)h\right], \end{aligned} \tag{5.3}$$

where $h = \delta^{ij}h_{ij}/3$ is the trace of the spatial components of the metric fluctuation. If $q \neq 0$, the two modes are coupled

$$0 = z_i'' + \mathcal{A}_{ij}z_j + \mathcal{B}_{ij}z_j', \qquad i,j = 1,2\,, \tag{5.4}$$

with coefficients $\mathcal{A}_{ij}, \mathcal{B}_{ij}$ that depend on the background fields. If $q = 0$, the off-diagonal components of $\mathcal{A}$ and $\mathcal{B}$ are zero and the two modes decouple.

We impose that the solutions are ingoing at the horizon. There are two independent solutions $z_i^{(I)}$, $z_i^{(II)}$ corresponding to making z_1 or z_2 zero at the horizon. When these solutions are taken to the boundary, a linear combination of them will be normalizable for the values of the frequency corresponding to the quasinormal modes. In the u coordinate,

JHEP11(2017)031

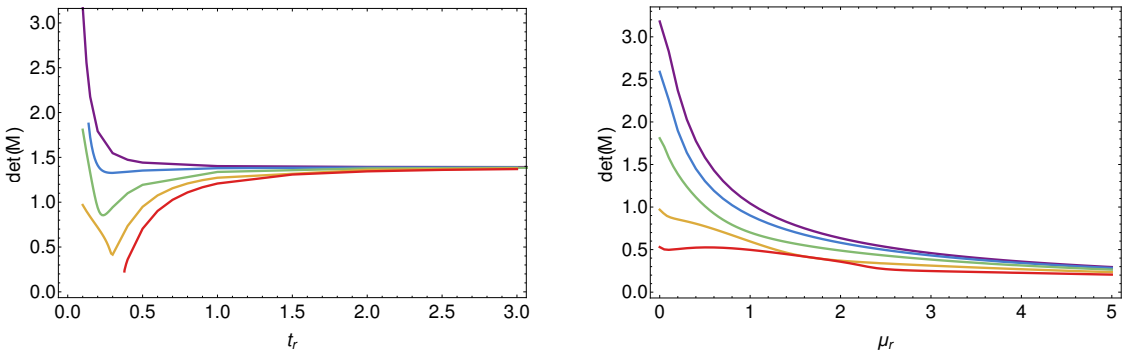

Figure 12. Left figure: $\det(M)$ at zero density as a function of the reduced temperature for the bottom-up model with quartic term (top to bottom) $V_4 = -0.5, -0.6777, -1, -1.5, -2$. Right figure: $\det(M)$ as a function of the reduced chemical potential at $t_r = 0.1$.

the expansion of the solutions at the boundary $u \to 0$ is, to leading order,

$$z_i \sim \sqrt{u}\left(z_i^{(nn)} + u\, z_i^{(n)}\right) , \tag{5.5}$$

where we identify the coefficients of the non-normalizable (nn) and normalizable (n) solutions. We arrange the solutions in a matrix with constant entries at the boundary

$$M = \lim_{u\to 0} \frac{1}{\sqrt{u}} \begin{pmatrix} z_1^{(I)} & z_2^{(I)} \\ z_1^{(II)} & z_2^{(II)} \end{pmatrix} . \tag{5.6}$$

M depends on the frequency, and a normalizable solution exists when $M(\omega)$ has a zero eigenvalue, i.e. $\det(M(\omega)) = 0$.

For the top-down model we have computed the determinant at zero frequency $\omega = 0$ first for a zero chemical potential $\mu_r = 0$ starting at high temperatures and decreasing the temperature to values $t_r < 1$ (left plot in figure 11). As the determinant never vanishes, the background is stable for $\mu_r = 0, t_r = 1$. We then repeat the same calculation but keeping $t_r = 1$ fixed and increasing the chemical potential μ_r. We find that the determinant is non-vanishing in the range we are interested $0 \leq \mu_r \leq 50$ (right plot in figure 11). Therefore, the theory remains dynamically stable in the regime where the EoS is stiff.

For the bottom-up model we do a similar stability analysis, we first compute the determinant at zero frequency $\omega = 0$ at zero chemical potential $\mu_r = 0$ starting at high temperatures and decreasing the temperature to values $t_r < 0.1$ (left plot in figure 12). We then fix the temperature to $t_r = 0.1$ and increase the chemical potential μ_r (right plot in figure 12). We find that the determinant is non-vanishing for values of V_4 where the speed of sound remains in the physical window, even when the speed of sound is close to the speed of light. Therefore, these models have sensible physical behavior and no obvious instabilities even in the regime where the EoS is stiff.

6 Conclusions

In the paper at hand, we studied the thermodynamics of cold and dense strongly coupled matter via simple holographic models. The models include the minimal ingredients of finite

JHEP11(2017)031

charge density and breaking of conformal invariance through a coupling for a relevant scalar operator of conformal dimension $4 > \Delta \geq 3$. We find that for some of these cases it is possible to find very stiff Equations of State, with the speed of sound almost reaching the speed of light. A simple stability analysis of the models furthermore showed no obvious thermodynamic or dynamic instabilities.

We observe that the simplest models possessing a quadratic action for the scalar field do not reach speeds of sound significantly larger than the conformal limit of $v_s = 1/\sqrt{3}$. In bottom-up models with a quartic potential, the speed of sound can on the other hand reach the speed of light if the quartic term has a negative coefficient $V_4 < 0$ with large enough magnitude. However, except for a small range of values around $V_4 = -2/3$, the isothermal speed of sound becomes superluminal or imaginary (indicating the presence of an instability) at low values of the chemical potential. Concerning the superluminal behavior, it should, however, be noted that when the chemical potential is of the same order or smaller than the temperature, one should rather consider the adiabatic speed of sound, which may affect to the range of values of V_4, for which causality is respected.

In addition to the bottom-up models, we also studied a top-down model with a more complicated action for the scalar, determined by a consistent truncation of supergravity. The issues of superluminal or imaginary speeds of sound do not appear in this case, which suggests that adding higher powers of the scalar field to the scalar potential might ameliorate the behavior of these quantities also in the bottom-up models. On the other hand, a stiff EoS is achieved in the top-down model only when there is a large separation between the scale of explicit breaking of conformal invariance and another scale that is spontaneously generated due to logarithmic divergences. The conclusion seems to be that although there is no fundamental obstruction to achieving a stiff EoS, this may not be possible in the simplest models and/or for the most "natural" values of the parameters of the system. On the positive side, the conditions required to achieve a stiff and physically consistent EoS may prove to be quite restrictive and thus turn out to be useful in constraining possible holographic models of QCD.

An interesting question is if the increase in stiffness is due to some underlying physical mechanism involving microscopic degrees of freedom in the dual field theory, at least for the top-down model where the dual is known. However, microscopic fields are not gauge invariant and therefore not directly accessible using the duality. So far we can just make a broad qualitative statement, it appears that one needs a combination of explicit and anomalous breaking of conformal invariance, with a hierarchy between these scales such that the scale of anomalous breaking is the larger.

An obvious phenomenological application of our results lies in the physics of neutron stars, where a holographic quark matter EoS has previously been matched to nuclear matter EoSs in [27]. The fact that very stiff EoSs can be obtained from holography opens up the possibility to construct matched EoSs exhibiting a weakly first order or even a cross-over deconfinement transition, thus allowing for the existence of a macroscopic amount of quark matter in the cores of the stars. Recalling the ease, with which quantities such as neutrino emissitivities and transport coefficients can be computed in holography, this paves the way for very interesting astrophysical studies.

JHEP11(2017)031

Acknowledgments

We would like to thank Daniel Grumiller, Alexander Haber, Ville Keränen, Esko Keski-Vakkuri, Elias Kiritsis, Aleksi Kurkela, David Müller, Ayan Mukhopadhyay, Francesco Nitti, Florian Preis, Anton Rebhan, Luciano Rezzolla, and Andreas Schmitt for useful discussions. C.E. is supported by the Austrian Science Fund (FWF), project no. P27182-N27 and DKW1252-N27. C.H. is supported by the Ramon y Cajal fellowship RYC-2012-10370 and the Spanish national grant MINECO-16-FPA2015-63667-P. C.H. and D.R.F. are supported by the Asturian grant FC-15-GRUPIN14-108. N.J. is supported by the Academy of Finland, grant no. 1297472. A.V. is supported by the Academy of Finland, grant no. 1303622, as well as the European Research Council, grant no. 725369. N.J. and A.V. thank the organizers of the CERN workshop *From quarks to gravitational waves: Neutron stars as a laboratory for fundamental physics* for warm hospitality.

A Background solutions

Varying the action (2.5) of the top-down model (2.6) with respect to the bulk metric, gauge, and scalar fields yields the equations of motion

$$\begin{aligned}
0 &= \frac{\Phi'}{fr}\left[f\left(4rA'+5\right)+rf'\right]-\frac{\Phi^2+1}{\Phi^2-1}\frac{e^{-2A}\Phi}{f^2r^4}\left(3e^{2A}fr^2+A_0^2L^4q^2\right)+\frac{2\Phi\left(\Phi'\right)^2}{1-\Phi^2}+\Phi''\\
0 &= A_0'\left(2A'+\frac{3}{r}\right)-\frac{4A_0q^2\Phi^2}{fr^2\left(1-\Phi^2\right)^2}+A_0''\\
0 &= f'\left(4A'+\frac{5}{r}\right)-\frac{16e^{-2A}A_0^2L^4q^2\Phi^2}{fr^4\left(1-\Phi^2\right)^2}-\frac{4L^4}{r^2}e^{-2A}A_0'^2+f''\\
0 &= A''+\frac{A'}{r}+\frac{8}{3\left(1-\Phi^2\right)^2}\left(\Phi'^2+\frac{L^4q^2}{f^2r^4}e^{-2A}A_0^2\Phi^2\right)\\
0 &= A'\left(\frac{3f'}{2f}+\frac{12}{r}+6A'\right)+\frac{1}{2fr^2}\left[2e^{-2A}L^4A_0'^2+3\left(rf'-4\frac{1+\Phi^4}{\left(1-\Phi^2\right)^2}\right)\right]+\\
&\quad\frac{6}{r^2}-\frac{4}{\left(1-\Phi^2\right)^2}\left(\Phi'^2+\frac{L^4q^2}{f^2r^4}e^{-2A}A_0^2\Phi^2\right).
\end{aligned}\tag{A.1}$$

A.1 Near boundary series expansions

The near boundary behavior for the scalar field is

$$\Phi\sim\frac{L^2}{r}\phi_{(0,1)}+\frac{L^6}{r^3}\left[\phi_{(1,3)}\log\left(\frac{r}{L}\right)+\phi_{(0,3)}\right]. \tag{A.2}$$

We shall assume the following series expansions for the other fields

$$\begin{aligned}
f &= 1+\sum_{n,m}\frac{L^{2n}}{r^n}f_{(n,m)}\log\left(\frac{r}{L}\right)^m, & A &= \sum_{n,m}\frac{L^{2n}}{r^n}A_{(n,m)}\log\left(\frac{r}{L}\right)^m\\
A_0 &= \mu+\sum_{n,m}\frac{L^{2n}}{r^n}A_{0(n,m)}\log\left(\frac{r}{L}\right)^m, & \Phi &= \sum_{n,m}\frac{L^{2n}}{r^n}\phi_{(n,m)}\log\left(\frac{r}{L}\right)^m
\end{aligned}\tag{A.3}$$

JHEP11(2017)031

which upon implementing the equations of motion become

$$
\begin{aligned}
A_0(r) \sim{}& \mu + \frac{L^4}{r^2}\left[\mathrm{A}_{0(0,2)} - 8\mu\phi_{(0,1)}^2 \log\left(\frac{r}{L}\right)\right] + \\
& \frac{L^8}{3r^4}\Bigg\{2\phi_{(0,1)}\left[\phi_{(0,1)}\left(4\mathrm{A}_{0(0,2)} + 9\mu^3\right) - 8\mu\phi_{(0,1)}^3 + 6\mu\phi_{(0,3)}\right] + \\
& 24\log\left(\frac{r}{L}\right)\mu\phi_{(0,1)}^2\left(\mu^2\phi_{(0,1)}^2 - 2\phi_{(0,1)}^2\right)\Bigg\} \\
f(r) \sim{}& 1 + \frac{L^8}{r^4}\left[f_{0,4} - 16\mu^2 L^4\phi_{(0,1)}^2 \log\left(\frac{r}{L}\right)\right] \\
A(r) \sim{}& -\frac{2L^4\phi_{(0,1)}^2}{3r^2} - \frac{L^8}{9r^4}\phi_{(0,1)}\Bigg\{9\mu^2\phi_{(0,1)}\left[2\log\left(\frac{r}{L}\right) + 1\right] + \phi_{(0,1)}^3\left[12\log\left(\frac{r}{L}\right) + 5\right] + 9\phi_{(0,3)}\Bigg\} \\
\Phi(r) ={}& \frac{L^2}{r}\phi_{(0,1)} + \frac{L^6}{r^3}\left[\phi_{(0,1)}\log\left(\frac{r}{L}\right)\left(\frac{4}{3}\phi_{(0,1)}^2 + 2\mu^2\right) + \phi_{(0,3)}\right]
\end{aligned}
\tag{A.4}
$$

plus sub-leading terms that we do not put here.

A.2 Near horizon series expansions

As stated before, we will demand regularity of the solutions near the horizon. Thus, in the u coordinate,

$$
(\Phi, A) = \sum_{n=0}\left(\phi_H^{(n)}, A_H^{(n)}\right)(1-u)^n, \quad (f, A_0) = \sum_{n=1}\left(f_H^{(n)}, {A_0}_H^{(n)}\right)(1-u)^n \,. \tag{A.5}
$$

Again, combining this with the equations of motion, we obtain

$$
\begin{aligned}
A_H^{(1)} ={}& \frac{1}{f_H^{(1)}}\left[\frac{1+\phi_H^{(0)4}}{\left(\phi_H^{(0)2}-1\right)^2} - \frac{2}{3}A_{0H}^{(1)2}e^{-2A_H^{(0)}}\right] - \frac{1}{2} \\
A_H^{(2)} ={}& \frac{1}{f_H^{(1)}\left(\phi_H^{(0)2}-1\right)^2}\left[-\frac{4A_{0H}^{(1)2}e^{-2A_H^{(0)}}\phi_H^{(0)2}}{3f_H^{(1)}} + \frac{\phi_H^{(0)4}}{2} + \frac{1}{2}\right] - \frac{A_{0H}^{(1)2}e^{-2A_H^{(0)}}}{3f_H^{(1)}} \\
& - \frac{\phi_H^{(0)2}}{2f_H^{(1)2}\left(\phi_H^{(0)2}-1\right)^4}\left[\frac{3\phi_H^{(0)4}}{2} + 3\phi_H^{(0)2} + \frac{3}{2}\right] - \frac{1}{4} \\
{A_0}_H^{(2)} ={}& \frac{1}{6}A_{0H}^{(1)}\left(\frac{4A_{0H}^{(1)2}e^{-2A_H^{(0)}} - 6}{f_H^{(1)}} + 3\right)
\end{aligned}
\tag{A.6}
$$

JHEP11(2017)031

and

$$f_H^{(2)} = \frac{10}{3} A_{0H}^{(1)\,2} e^{-2A_H^{(0)}} + \frac{f_H^{(1)}}{2} - \frac{2\left(\phi_H^{(0)\,4}+1\right)}{\left(\phi_H^{(0)\,2}-1\right)^2} \tag{A.7}$$

$$\phi_H^{(1)} = \frac{3\left(\phi_H^{(0)\,2}+1\right)}{4 f_H^{(1)}\left(\phi_H^{(0)\,2}-1\right)}\phi_H^{(0)}$$

$$\phi_H^{(2)} = \frac{\phi_H^{(0)}\left(\phi_H^{(0)\,2}+1\right)}{64 f_H^{(1)\,2}\left(\phi_H^{(0)\,2}-1\right)^2}\left\{3\left[(8f_H^{(1)}+9)\phi_H^{(0)\,2} - 8f_H^{(1)}+3\right] - 32 e^{2A_H^{(0)}} A_{0H}^{(1)\,2}\left(\phi_H^{(0)\,2}-1\right)\right\}$$

plus higher-order terms.

A.3 Numerical integration

We will solve the system of equations (A.1) through the *shooting technique* to determine the independent boundary and horizon constants. At given values (μ_r, t_r), one starts with a trial set of independent boundary and horizon data,

$$X = \left(A_{0H}^{(1)}, A_H^{(0)}, A_{0(0,2)}, \alpha, \beta, \phi_H^{(0)}\right), \tag{A.8}$$

Note that $f_H^{(1)}$ can be fixed in terms of t_r and $A_H^{(0)}$ alone and the constrain fixes the value of $A_H^{(1)}$.

The algorithm is as follows: we compute the numerical solution and construct some object made out of the fields and their derivatives

$$V(u) = \left(f, A_0, \phi, A, A_0', \phi'\right), \tag{A.9}$$

note that it is not necessary to account for the derivatives of f or A_0 since their equations of motion turn out to be first order. We perform the numerical integration from some near horizon value $u_{\rm hor}$, using as boundary conditions the near-horizon series expansions from (A.6) and (A.7), down to some intermediate point u_*. Evaluating the fields and their derivatives at this point produces a vector $V(u_*)|_{\rm hor\to bulk}$. Repeating the analogous procedure, this time employing the near-boundary series as boundary conditions, from some near-boundary value $u_{\rm boun}$ down to the same intermediate point u_* produces $V(u_*)|_{\rm boun\to bulk}$.[6] The mismatch vector M is constructed by the difference

$$M(X) = V(u_*)|_{\rm hor\to bulk} - V(u_*)|_{\rm boun\to bulk}\,. \tag{A.10}$$

The correct choice of X must lead to $M = 0$. By thinking of $M(X)$ as a vector-valued function, the problem becomes a root finding in six dimensions. We apply the Newton-Raphson method. It works by a generalization of the familiar one-dimensional method of

[6] Nevertheless, both for the near horizon and near boundary series expansions, in order to enhance the accuracy and shorten the overall integration time, we have truncated the series at a much larger order.

JHEP11(2017)031

tracking tangent lines. For a guess X, compute the Jacobian J of partial derivatives of the mismatch vector. The new vector X shall be

$$X = X^{\text{guess}} - J^{-1}M\,. \tag{A.11}$$

The Jacobian is computed through finite differences, once the solutions in a neighborhood of the guess point (on each direction on the constants space) are known. In particular, as step in the Jacobian we will take 10^{-10}. On each numerical integration, $u_{\text{hor}} = 1 - \epsilon_0$, $u_{\text{boun}} = \epsilon_0$, ϵ_0 being some sensitive cut-off; we use 10^{-8} and $u_* = 1/2$. As for the initial data X^{guess}, a sensitive choice for mild reduced chemical potential and temperature is the solution inherited from the scalar field in probe approximation, wherein the geometry reduced to an AdS-RN [28],

$$X^{\text{guess}} = X_{\text{AdS-RN}} = \left(\mu, 0, 0, \alpha^P, \beta^P, \phi_H^P\right)\,, \tag{A.12}$$

where $\left(\alpha^P, \beta^P\right)$ are obtained from integration of the scalar equation in this approximation, once ϕ_H^P is set. If the norm of the mismatch $||M||$ lies above some threshold fixed a priori, the iteration starts once again, but taking X as the new starting point and stops if otherwise. In our computations, we will fix the threshold to be 10^{-9}. Our attempt to connect the model to neutron star physics implies that we will focus in regimes at which $X_{\text{AdS-RN}}$ works not very well, but luckily, thanks to the smoothness of the solutions, if for some choice $X_{(\mu_0,t_0)}$, $||M|| < 10^{-9}$, then we can take this vector as initial guess on the next computation, i.e., $X_{(\mu_0,t_0)} \to X^{\text{guess}}_{(\mu_0+\delta\mu,t_0)}$.

B Calculation of thermodynamic quantities

B.1 On-shell action

For the holographic models we consider, one can write Einstein's equations in the form

$$R_{MN} = T^{(A)}_{MN} + T^{\phi}_{MN} + \frac{1}{2}g_{MN}\left(\frac{L^2}{3}F^2 + \mathcal{K}_\Phi|D\phi|^2 + \frac{5}{3}\mathcal{V}_\Phi\right)\,. \tag{B.1}$$

From the trace of these equations, we find that the Ricci scalar reads

$$R = \frac{L^2}{3}F^2 + \mathcal{K}_\Phi|D\phi|^2 + \frac{5}{3}\mathcal{V}_\Phi\,, \tag{B.2}$$

implying that the on-shell action (2.5) evaluates to

$$S_{\text{on-shell}} = \frac{1}{16\pi G_5}\int d^5x\sqrt{-g}\left[\frac{2}{3}\mathcal{V}_\Phi - \frac{2}{3}L^2F^2\right]\,. \tag{B.3}$$

Let us now use the fact that for our solutions

$$\Gamma^\alpha_{\mu\nu} = \Gamma^r_{r\nu} = \Gamma^\alpha_{rr} = 0\,,\ \Gamma^r_{\mu\nu} = -\frac{1}{\sqrt{g_{rr}}}K_{\mu\nu}\,,\ \Gamma^\alpha_{\mu r} = \sqrt{g_{rr}}K^\alpha_{\ \mu}\,,\ \Gamma^r_{rr} = \frac{1}{2}g^{rr}\partial_r g_{rr}\,, \tag{B.4}$$

where

$$K_{\mu\nu} = \frac{1}{2\sqrt{g_{rr}}}\partial_r g_{\mu\nu} \tag{B.5}$$

JHEP11(2017)031

is the extrinsic curvature and $K^{\alpha}_{\ \mu} = g^{\alpha\beta}K_{\beta\mu}$, $K = g^{\mu\nu}K_{\mu\nu}$. Using also the simple result

$$\frac{\partial_r\sqrt{-g}}{\sqrt{-g}} = \Gamma^r_{rr} + \sqrt{g_{rr}}K\,, \tag{B.6}$$

we can write

$$g^{\mu\nu}R_{\mu\nu} = -\frac{1}{\sqrt{-g}}\partial_r\left(\frac{\sqrt{-g}}{\sqrt{g_{rr}}}K\right) = -\frac{1}{\sqrt{-g}}\partial_r\left(\sqrt{-\gamma}K\right)\,. \tag{B.7}$$

Here, we defined $\gamma_{\mu\nu} = g_{\mu\nu}$ as the boundary metric and used $\sqrt{-g} = \sqrt{g_{rr}}\sqrt{-\gamma}$.

On the other hand, from Einstein's equations we obtain

$$g^{\mu\nu}R_{\mu\nu} = -\frac{2L^2}{3}F_{0r}F^{0r} + \frac{4}{3}\mathcal{V}_\Phi + q^2 g^{00}\mathcal{K}_\Phi A_0^2\phi^2\,, \tag{B.8}$$

where we only focused on the nonzero components of the solutions. Solving now for $\mathcal{V}_\Phi$ and introducing the result in the on-shell action, one gets

$$S_{\rm on-shell} = \frac{1}{16\pi G_5}\int d^5x\sqrt{-g}\left[-\frac{1}{2\sqrt{-g}}\partial_r\left(\sqrt{-\gamma}K\right) - L^2F_{r0}F^{r0} - \frac{q^2}{2}g^{00}\mathcal{K}_\phi A_0^2\phi^2\right]. \tag{B.9}$$

Finally, we use the equation of motion for the gauge field,

$$4L^2\partial_r\left(\sqrt{-g}F^{r0}\right) = 2q^2\sqrt{-g}g^{00}\mathcal{K}_\phi A_0\phi^2\,. \tag{B.10}$$

We can then replace the q^2 term in the action by a derivative term and write the action as a total derivative:

$$\begin{aligned} S_{\rm on-shell} &= \frac{1}{16\pi G_5}\int d^5x\left[-\frac{1}{2}\partial_r\left(\sqrt{-\gamma}K\right) - L^2\sqrt{-g}\partial_r A_0F^{r0} - L^2A_0\partial_r\left(\sqrt{-g}F^{r0}\right)\right] \\ &= \frac{1}{16\pi G_5}\int d^5x\,\partial_r\left[-\frac{1}{2}\sqrt{-\gamma}K - L^2\sqrt{-g}A_0F^{r0}\right] \\ &= \frac{1}{16\pi G_5}\int d^4x\left[\frac{1}{2}\sqrt{-\gamma}K + L^2\sqrt{-g}A_0F^{r0}\right]^{r=r_\Lambda}_{r=r_H}\,. \end{aligned} \tag{B.11}$$

B.2 Holographic renormalization

In order to be able to read off the speed of sound, we need the energy density ε and pressure p, which can be read from the diagonal components of the expectation value of the stress energy tensor, $\langle T_{\mu\nu}\rangle$. We can decompose the line element (2.9) into its transverse and longitudinal components,

$$dS^2 = N^2dr^2 + \gamma_{\mu\nu}dx^\mu dx^\nu\,, \qquad N^2 = \frac{L^2}{r^2f}\,. \tag{B.12}$$

We will now determine, which counterterms we need to consider in order to obtain finite one point correlation functions. Together with the cosmological constant term

$$\mathcal{I}_\Lambda = -\frac{1}{8\pi G_5}\int d^4x\sqrt{-\gamma}\Lambda\,, \tag{B.13}$$

JHEP11(2017)031

which will cancel out the volume divergence, we need to include also the Gibbons-Hawking term,

$$\mathcal{I}_{\rm GH} = \frac{1}{8\pi G_5}\int d^4x\sqrt{-\gamma}K\ . \tag{B.14}$$

The details of the holographic renormalization of bottom-up models can be found in [28]. In the following we focus on the top-down model, that present some small differences due to the more complicated form of the kinetic term and the potential for the scalar field.

From the near boundary behavior of the metric field,

$$\begin{aligned}
\gamma_{00} &= -\frac{r^2}{L^2} + \frac{4}{3}L^2\phi_{(0,1)}^2 + \frac{L^6}{9r^2}\Bigg\{\left[2\phi_{(0,1)}\left(9\mu^2\phi_{(0,1)} + \phi_{(0,1)}^3 + 9\phi_{(0,3)}\right) - 9f_{0,4}\right] \\
&\quad + 12\phi_{(0,1)}^2\left(15\mu^2 + 2\phi_{(0,1)}^2\right)\log\left(\frac{r}{L}\right)\Bigg\} \\
\gamma_{ii} &= \frac{r^2}{L^2} - \frac{4}{3}L^2\phi_{(0,1)}^2 - \frac{2L^6}{9r^2}\Bigg\{\phi_{(0,1)}\left(9\mu^2\phi_{(0,1)} + \phi_{(0,1)}^3 + 9\phi_{(0,3)}\right) \\
&\quad + 6\phi_{(0,1)}^2\left(3\mu^2 + 2\phi_{(0,1)}^2\right)\log\left(\frac{r}{L}\right)\Bigg\},
\end{aligned} \tag{B.15}$$

we note that it is necessary to add the following counterterm that will cancel out divergences due to the backreaction of the scalar field,

$$\mathcal{I}_{\rm c} = -\frac{1}{8\pi G_5}\int d^4x\,\sqrt{-\gamma}\left\{\frac{32}{4}L|D\Phi|^2\log\left(\frac{r}{L}\right) - \left[8 + \frac{32}{3}\Phi^2\log\left(\frac{r}{L}\right)\right]\frac{\Phi^2}{L}\right\}. \tag{B.16}$$

Another counterterm may also be added,

$$\mathcal{I}_{\rm f} = -\frac{L}{8\pi G_5}\int d^4x\,\sqrt{-\gamma}\left[\mathcal{W}_1|D_\alpha\Phi|^2 + \frac{\mathcal{W}_2}{L^2}\Phi^4\right], \tag{B.17}$$

which will introduce non-trivial finite contributions to our QFT.

After varying the action with respect to the boundary metric, and inserting the near boundary series expansions (A.4), we get the boundary vev's

$$\begin{aligned}
\langle T^{00}\rangle = \varepsilon &= -\frac{L^3}{16\pi G_5}\left[3f_{(0,4)} + 8\phi_{(0,1)}\phi_{(0,3)} + 4\mu^2\phi_{(0,1)}^2(\mathcal{W}_1+3) + \phi_{(0,1)}^4\left(\mathcal{W}_2 + \frac{16}{3}\right)\right] \\
\langle T^{ii}\rangle = p &= -\frac{L^3}{16\pi G_5}\left[f_{0,4} - 8\phi_{(0,1)}\phi_{(0,3)} + 4\mu^2\phi_{(0,1)}^2(\mathcal{W}_1+1) - \phi_{(0,1)}^4\left(\mathcal{W}_2 + \frac{16}{3}\right)\right] \\
\langle\mathcal{O}\rangle = v &= -\frac{2L^3}{\pi G_5}\left[\phi_{(0,3)} - \frac{1}{4}\mu^2\phi_{(0,1)}(\mathcal{W}_1+4) + \phi_{(0,1)}^3\left(\frac{\mathcal{W}_2}{8} - \frac{2}{3}\right)\right] \\
\langle j^0\rangle = n &= -\frac{L^3}{2\pi G_5}\left[A_{0(0,2)} + \mu\phi_{(0,1)}^2(\mathcal{W}_1+4)\right],
\end{aligned} \tag{B.18}$$

which satisfy

$$\langle T^{\mu\nu}\rangle\,\eta_{\mu\nu} = -\langle\mathcal{O}\rangle\,\phi_{(0,1)} + \mathcal{A}\,, \tag{B.19}$$

JHEP11(2017)031

with the anomaly

$$\mathcal{A} = \frac{L^3}{\pi G_5}\phi_{(0,1)}^2\left(\frac{\mu^2}{2}+\frac{2}{3}\phi_{(0,1)}^2\right). \tag{B.20}$$

Combining expressions (B.18) and (B.25), one can straightforwardly verify that the thermodynamic relation

$$\varepsilon + p = n\mu + TS \tag{B.21}$$

holds. Moreover, the renormalized action at the boundary is equal to the free energy in the macrocanonical ensemble,

$$\begin{aligned} S_{\text{ren}} &= S_{\text{on-shell}} + \mathcal{I}_\Lambda + \mathcal{I}_{\text{GH}} + \mathcal{I}_{\text{c}} + \mathcal{I}_{\text{f}} \\ &= \Omega = \frac{L^3}{16\pi G_5}\left[f_{0,4} - 8\phi_{(0,1)}\phi_{(0,3)} + 4\mu^2\phi_{(0,1)}^2(\mathcal{W}_1+1) - \phi_{(0,1)}^4\left(\mathcal{W}_2+\frac{16}{3}\right)\right] \\ &= -p\,, \end{aligned} \tag{B.22}$$

where we have made use of (B.27) when expressing $S_{\text{on-shell}}$ at the horizon r_H in terms of the boundary coefficients.

We can now examine the equations of motion in order to see if some sort of relation between the near boundary/horizon coefficients can be set. If we define

$$\beta(r) = e^{4A}r^5 f' - 4L^4 e^{2A} r^3 A_0' A_0\,, \tag{B.23}$$

we notice that due to equations (A.1), this quantity is independent of the radial coordinate. It is convenient to evaluate it at the horizon, $r \to r_H$, giving

$$\beta(r_H) = e^{4A(r_H)} r_H^5 f'(r_H) \equiv \beta_H\,. \tag{B.24}$$

Note also that the temperature and entropy density are given by

$$T = \frac{r_H^2 f'(r_H)}{4\pi L^2} e^{A(r_H)}\,,\quad s = \frac{1}{4G_5}\frac{r_H^3}{L^3}e^{3A(r_H)}\,, \tag{B.25}$$

so that

$$\beta_H = 16\pi G_5 L^5 T s\,. \tag{B.26}$$

The above steps enable us to find the relation

$$\widehat{f}_{(0)} = \alpha\left(2\mu_r a_1 + 4\mu_r^2\alpha^3 - \pi e^{3A_H^{(0)}} t_r\right). \tag{B.27}$$

Moreover, another relation can be obtained from the constraint equation in the bulk,

$$A_H^{(1)} = \frac{1}{f_H^{(1)}}\left[\frac{1+\phi_H^{(0)4}}{\left(\phi_H^{(0)2}-1\right)^2} - \frac{2}{3}A_{0H}^{(1)2} e^{-2A_H^{(0)}}\right] - \frac{1}{2}\,. \tag{B.28}$$

Both relations (B.27) and (B.28) can be employed to enhance the numeric integration of the set of equations (A.1).

JHEP11(2017)031

C Fluctuations

C.1 Equations for gauge invariant combinations

We will use radial gauge $\delta g_{\mu r} = \delta a_r = 0$. At zero spatial momentum fluctuations split in decoupled sectors according to their representation under the group of spatial rotations. There are three sectors:

- Tensor: $h_{ij} - \frac{1}{3}\delta_{ij}\delta^{kl}h_{kl}$.
- Vector: a_i, h_{0i} .
- Scalar: φ, $\varphi^\dagger$, h_{00}, a_0, $h = \delta^{ij}h_{ij}/3$.

In principle we expect instabilities to be related to changes in the scalar, thus we will restrict the analysis to the scalar sector. We see that there are five components of the fields in the scalar sector. The equations of motion (Einstein, Maxwell, and the equation of motion for the scalar) include a second order (dynamical) equation for each mode plus three first order (constraints) equations. This adds up to eight coupled equations for the five modes. However, the actual number of independent dynamical modes is just two and the system can be reduced to two coupled differential equations (of second order). We will do this in the following.

In the radial gauge there are residual diffeomorphisms $\xi^M(x)$ and gauge transformations $\lambda(x)$. The linear variations of the fields are

$$\begin{aligned}\delta\Phi &= \xi^M\partial_M\Phi + iq\Phi\lambda \\ \delta\Phi^\dagger &= \xi^M\partial_M\Phi^\dagger - iq\Phi^\dagger\lambda \\ \delta A_M &= \xi^N\partial_N A_M + \partial_M\xi^N A_N + \partial_M\lambda\,.\end{aligned} \tag{C.1}$$

For homogeneous fluctuations we can expand in plane waves $\xi^M = e^{-i\omega t}\eta^M(r)$, $\lambda = e^{-i\omega t}\chi(r)$, in such a way that the allowed transformations are

$$\eta^r = c_0 r\sqrt{f},\ \ \eta^{0\prime} = -i\omega c_0\frac{L^4 e^{-2A}}{r^3 f^{3/2}},\quad \chi' = i\omega c_0\frac{L^4 e^{-2A}}{r^3 f^{3/2}}A_0,\quad \eta^i = c_i\,, \tag{C.2}$$

where c_0, c_i are arbitrary functions of the frequency. We can construct a basis of two independent combinations of the scalar components that are invariant under these gauge transformations z_1, z_2; these are the expressions given in (5.3). The equations of motion can be found in a straightforward way by taking radial derivatives of z_i and using the equations of motion of the scalar modes. They take the generic form (5.4). The result with $q \neq 0$ is quite cumbersome, so we will give here expressions for the bottom-up models with $q = 0$ and canonical kinetic term, but generic potential. The off-diagonal coefficients

JHEP11(2017)031

vanish $\mathcal{A}_{12}=\mathcal{A}_{21}=\mathcal{B}_{12}=\mathcal{B}_{21}=0$ and the diagonal ones take the values:

$$\begin{aligned}\mathcal{A}_{11}=\mathcal{A}_{22}&=-4A'-\frac{f'}{f}-\frac{5}{r}\\ \mathcal{B}_{11}&=-\frac{e^{-2A}L^4\omega^2}{f^2r^4}+\frac{4\Phi_0\Phi_0'\partial\mathcal{V}_\Phi}{3fr^2A'+3fr}-\frac{2rf'\left(\Phi_0'\right)^2}{3f\left(rA'+1\right)}-\frac{8}{3}\left(\Phi_0'\right)^2\\ &\quad+\frac{\partial\mathcal{V}_\Phi+2\Phi_0^2\partial^2\mathcal{V}_\Phi}{fr^2}+\frac{2r^2\left(\Phi_0'\right)^4}{9\left(rA'+1\right)^2}\\ \mathcal{B}_{22}&=\frac{\partial\mathcal{V}_\Phi}{fr^2}-\frac{e^{-2A}L^4\omega^2}{f^2r^4}\,.\end{aligned}\tag{C.3}$$

C.2 Solutions

The method that we will follow here to find a solution for the quasi-normal modes is valid for any number of coupled or decoupled linear differential equations. Expanding the system (5.4) around $u\to 1$,

$$0=z_j''-\frac{z_j'}{1-u}+\frac{e^{-2A_H^{(0)}}\omega^2}{4f_H^{(1)}(1-u)^2}z_j\,,\tag{C.4}$$

we infer that the leading order behavior at the horizon is given by

$$z_j|_{u\to1}\sim z_j^{(\text{out})}(1-u)^{i\omega c_I}+z_j^{(\text{ing})}(1-u)^{-i\omega c_I}\tag{C.5}$$

with $c_I=e^{A_H^{(0)}}/2f_H^{(1)}$, and we have labeled the outgoing and infalling pieces as $z_j^{(\text{out})}$ and $z_j^{(\text{ing})}$, respectively. Imposing causality means that we pick the ingoing solution. From here, we can construct a solution valid throughout the whole bulk,

$$z_j\sim(1-u)^{-i\omega c_I}z_{j(\text{reg})}\,,\tag{C.6}$$

with

$$z_{j(\text{reg})}=\sum_{m=0}z_j^{(m)}(1-u)^m\,,\tag{C.7}$$

regular at the horizon. At leading order and taking $\omega=0$,

$$\begin{aligned}z_{1(\text{reg})}&=z_1^{(1)}(1-u)+\cdots\\ z_{2(\text{reg})}&=z_2^{(0)}-\left\{\frac{\left(\phi_H^{(0)2}-1\right)\left(\phi_H^{(0)2}+1\right)}{2\left(\phi_H^{(0)4}+1\right)f_H{}^{(0)}}z_1{}^{(1)}e^{-2A_H{}^{(0)}}A_{0H}{}^{(1)}\right.\\ &\quad\left.+\frac{3\left(\phi_H^{(0)8}+8\phi_H^{(0)4}-1\right)z_2{}^{(0)}}{4\left(\phi_H^{(0)2}-1\right)^2\left(\phi_H^{(0)4}+1\right)f_H{}^{(0)}}\right\}(1-u)+\cdots\,.\end{aligned}\tag{C.8}$$

A normalizable solution at $u\to0$ can be obtained by means of the determinant method. First, we choose a set of linearly independent boundary conditions at the horizon, that is,

$$\left\{z_{1(reg)},z_{2(\text{reg})}\right\}=\left\{\,(1,0)\,,(0,1)\,\right\},\tag{C.9}$$

JHEP11(2017)031

and for each of these boundary conditions, we solve numerically the system (5.4) by means of a single shooting from the horizon, where we impose

$$z_j(1-\epsilon_0) = z_{j\,(\mathrm{reg})}(1-\epsilon_0), \quad z_j'(1-\epsilon_0) = z_{j\,(\mathrm{reg})}{}'(1-\epsilon_0)\,, \tag{C.10}$$

to the boundary, taking as cutoff the same as in the background computation ($\epsilon_0 = 10^{-8}$), although there is a high robustness against this choice. Furthermore, since we now deal with a linear differential equation system, there is no need to demand the same accuracy as for the background computation, so we set $m = 2$ in eq. (C.7). Near the boundary, the solutions have the following expansion to leading order,

$$z_{1,2} \sim \sqrt{u}\left(z_{1,2}^{(nn)} + u\, z_{1,2}^{(n)}\right), \tag{C.11}$$

where we identify the non-normalizable (nn) as the leading term while the normalizable (n) as the sub-leading one. Normalizable solutions will have $z_1^{(nn)} = z_2^{(nn)} = 0$. The numerical solutions can be arranged as elements of a matrix M,

$$M = \frac{1}{\sqrt{u}}\begin{pmatrix} z_1^{(I)}{}_{(\mathrm{reg})} & z_2^{(I)}{}_{(\mathrm{reg})} \\ z_1^{(II)}{}_{(\mathrm{reg})} & z_2^{(II)}{}_{(\mathrm{reg})} \end{pmatrix}, \tag{C.12}$$

which, if evaluated at the AdS boundary gives zero determinant, then, a normalizable solution exists. This will happen at a certain frequency $\omega \in \mathbb{C}$, for fixed chemical potential and temperature. If we were about to determine such frequency, the problem amounts to find the root of a certain equation, $\det(M(\omega)) = 0$, which can be searched using Newton's method. Nevertheless, this might not even be necessary, since we can dial the chemical potential and compute the determinant at zero frequency.

References

[1] P. Demorest, T. Pennucci, S. Ransom, M. Roberts and J. Hessels, *Shapiro Delay Measurement of A Two Solar Mass Neutron Star*, *Nature* **467** (2010) 1081 [arXiv:1010.5788] [INSPIRE].

[2] J. Antoniadis et al., *A Massive Pulsar in a Compact Relativistic Binary*, *Science* **340** (2013) 6131 [arXiv:1304.6875] [INSPIRE].

[3] P. Bedaque and A.W. Steiner, *Sound velocity bound and neutron stars*, *Phys. Rev. Lett.* **114** (2015) 031103 [arXiv:1408.5116] [INSPIRE].

[4] N.K. Glendenning, *Compact Stars. Nuclear Physics, Particle Physics and General Relativity*, Springer (1997).

[5] K. Hebeler, J.M. Lattimer, C.J. Pethick and A. Schwenk, *Equation of state and neutron star properties constrained by nuclear physics and observation*, *Astrophys. J.* **773** (2013) 11 [arXiv:1303.4662] [INSPIRE].

JHEP11(2017)031

[6] B.A. Freedman and L.D. McLerran, *Fermions and Gauge Vector Mesons at Finite Temperature and Density. 3. The Ground State Energy of a Relativistic Quark Gas*, *Phys. Rev.* **D 16** (1977) 1169 [INSPIRE].

[7] A. Vuorinen, *The Pressure of QCD at finite temperatures and chemical potentials*, *Phys. Rev.* **D 68** (2003) 054017 [hep-ph/0305183] [INSPIRE].

[8] A. Kurkela, P. Romatschke and A. Vuorinen, *Cold Quark Matter*, *Phys. Rev.* **D 81** (2010) 105021 [arXiv:0912.1856] [INSPIRE].

[9] A. Kurkela and A. Vuorinen, *Cool quark matter*, *Phys. Rev. Lett.* **117** (2016) 042501 [arXiv:1603.00750] [INSPIRE].

[10] M. Buballa, *NJLS model analysis of quark matter at large density*, *Phys. Rept.* **407** (2005) 205 [hep-ph/0402234] [INSPIRE].

[11] A. Kurkela, E.S. Fraga, J. Schaffner-Bielich and A. Vuorinen, *Constraining neutron star matter with Quantum Chromodynamics*, *Astrophys. J.* **789** (2014) 127 [arXiv:1402.6618] [INSPIRE].

[12] J.M. Maldacena, *The large-N limit of superconformal field theories and supergravity*, *Int. J. Theor. Phys.* **38** (1999) 1113 [hep-th/9711200] [INSPIRE].

[13] S.S. Gubser, I.R. Klebanov and A.M. Polyakov, *Gauge theory correlators from noncritical string theory*, *Phys. Lett.* **B 428** (1998) 105 [hep-th/9802109] [INSPIRE].

[14] E. Witten, *Anti-de Sitter space and holography*, *Adv. Theor. Math. Phys.* **2** (1998) 253 [hep-th/9802150] [INSPIRE].

[15] A.H. Taub, *Relativistic Rankine-Hugoniot Equations*, *Phys. Rev.* **74** (1948) 328 [INSPIRE].

[16] L. Rezzolla and O. Zanotti, *Relativistic Hydrodynamics*, Oxford University Press (2013).

[17] O. Bergman, G. Lifschytz and M. Lippert, *Holographic Nuclear Physics*, *JHEP* **11** (2007) 056 [arXiv:0708.0326] [INSPIRE].

[18] M. Rozali, H.-H. Shieh, M. Van Raamsdonk and J. Wu, *Cold Nuclear Matter In Holographic QCD*, *JHEP* **01** (2008) 053 [arXiv:0708.1322] [INSPIRE].

[19] K.-Y. Kim, S.-J. Sin and I. Zahed, *Dense holographic QCD in the Wigner-Seitz approximation*, *JHEP* **09** (2008) 001 [arXiv:0712.1582] [INSPIRE].

[20] Y. Kim, C.-H. Lee, I.J. Shin and M.-B. Wan, *Holographic equations of state and astrophysical compact objects*, *JHEP* **10** (2011) 111 [arXiv:1108.6139] [INSPIRE].

[21] V. Kaplunovsky, D. Melnikov and J. Sonnenschein, *Baryonic Popcorn*, *JHEP* **11** (2012) 047 [arXiv:1201.1331] [INSPIRE].

[22] K. Ghoroku, K. Kubo, M. Tachibana and F. Toyoda, *Holographic cold nuclear matter and neutron star*, *Int. J. Mod. Phys.* **A 29** (2014) 1450060 [arXiv:1311.1598] [INSPIRE].

[23] S.-w. Li, A. Schmitt and Q. Wang, *From holography towards real-world nuclear matter*, *Phys. Rev.* **D 92** (2015) 026006 [arXiv:1505.04886] [INSPIRE].

[24] M. Elliot-Ripley, P. Sutcliffe and M. Zamaklar, *Phases of kinky holographic nuclear matter*, *JHEP* **10** (2016) 088 [arXiv:1607.04832] [INSPIRE].

[25] P. Burikham, E. Hirunsirisawat and S. Pinkanjanarod, *Thermodynamic Properties of Holographic Multiquark and the Multiquark Star*, *JHEP* **06** (2010) 040 [arXiv:1003.5470] [INSPIRE].

JHEP11(2017)031

[26] Y. Kim, I.J. Shin, C.-H. Lee and M.-B. Wan, *Explicit flavor symmetry breaking and holographic compact stars*, *J. Korean Phys. Soc.* **66** (2015) 578 [arXiv:1404.3474] [INSPIRE].

[27] C. Hoyos, D. Rodríguez Fernández, N. Jokela and A. Vuorinen, *Holographic quark matter and neutron stars*, *Phys. Rev. Lett.* **117** (2016) 032501 [arXiv:1603.02943] [INSPIRE].

[28] C. Hoyos, N. Jokela, D. Rodríguez Fernández and A. Vuorinen, *Breaking the sound barrier in AdS/CFT*, *Phys. Rev.* **D 94** (2016) 106008 [arXiv:1609.03480] [INSPIRE].

[29] I. Tews, T. Krüger, K. Hebeler and A. Schwenk, *Neutron matter at next-to-next-to-next-to-leading order in chiral effective field theory*, *Phys. Rev. Lett.* **110** (2013) 032504 [arXiv:1206.0025] [INSPIRE].

[30] P.M. Hohler and M.A. Stephanov, *Holography and the speed of sound at high temperatures*, *Phys. Rev.* **D 80** (2009) 066002 [arXiv:0905.0900] [INSPIRE].

[31] A. Cherman, T.D. Cohen and A. Nellore, *A Bound on the speed of sound from holography*, *Phys. Rev.* **D 80** (2009) 066003 [arXiv:0905.0903] [INSPIRE].

[32] A. Anabalon, T. Andrade, D. Astefanesei and R. Mann, *Universal Formula for the Holographic Speed of Sound*, arXiv:1702.00017 [INSPIRE].

[33] Y. Yang and P.-H. Yuan, *Universal Behaviors of Speed of Sound from Holography*, arXiv:1705.07587 [INSPIRE].

[34] R. Rougemont, R. Critelli, J. Noronha-Hostler, J. Noronha and C. Ratti, *Dynamical versus equilibrium properties of the QCD phase transition: A holographic perspective*, *Phys. Rev.* **D 96** (2017) 014032 [arXiv:1704.05558] [INSPIRE].

[35] A. Karch and E. Katz, *Adding flavor to AdS/CFT*, *JHEP* **06** (2002) 043 [hep-th/0205236] [INSPIRE].

[36] A. Karch, A. O'Bannon and K. Skenderis, *Holographic renormalization of probe D-branes in AdS/CFT*, *JHEP* **04** (2006) 015 [hep-th/0512125] [INSPIRE].

[37] A. Karch and A. O'Bannon, *Holographic thermodynamics at finite baryon density: Some exact results*, *JHEP* **11** (2007) 074 [arXiv:0709.0570] [INSPIRE].

[38] A. Karch, D.T. Son and A.O. Starinets, *Zero Sound from Holography*, arXiv:0806.3796 [INSPIRE].

[39] A. Karch, M. Kulaxizi and A. Parnachev, *Notes on Properties of Holographic Matter*, *JHEP* **11** (2009) 017 [arXiv:0908.3493] [INSPIRE].

[40] M. Ammon, M. Kaminski and A. Karch, *Hyperscaling-Violation on Probe D-branes*, *JHEP* **11** (2012) 028 [arXiv:1207.1726] [INSPIRE].

[41] G. Itsios, N. Jokela and A.V. Ramallo, *Collective excitations of massive flavor branes*, *Nucl. Phys.* **B 909** (2016) 677 [arXiv:1602.06106] [INSPIRE].

[42] A. Núñez and A.O. Starinets, *AdS/CFT correspondence, quasinormal modes and thermal correlators in $N = 4$ SYM*, *Phys. Rev.* **D 67** (2003) 124013 [hep-th/0302026] [INSPIRE].

[43] I. Amado, M. Kaminski and K. Landsteiner, *Hydrodynamics of Holographic Superconductors*, *JHEP* **05** (2009) 021 [arXiv:0903.2209] [INSPIRE].

[44] O. Bergman, N. Jokela, G. Lifschytz and M. Lippert, *Striped instability of a holographic Fermi-like liquid*, *JHEP* **10** (2011) 034 [arXiv:1106.3883] [INSPIRE].

JHEP11(2017)031

4 Results

Now we shall summarize the results obtained in the articles presented in this thesis, leaving for Sec. 5, a more detailed discussion.

Results of the article "Ward identities and relations between conductivities and viscosities in holography":

The near boundary analysis in holographic models with UV fixed point is not enough to determine all the Ward identities that arise from the existing symmetries of the system, although there are no arguments a priori to avoid their derivation from the gauge/gravity duality. The missing information is still present, although hidden in a "subtle" way. In this work, we developed a procedure to determine, up to possible inherent ambiguities, the remaining Ward identities. Our approach relied on the construction of a conserved probability current in the bulk, J, i.e. independent of the AdS coordinate, and parity symmetry. We gave a general prescription on how to construct such probability current for any linear system of second order ordinary differential equations and applied it to a specific set of theories consisting of $3+1$-dimensional gravity dual theory coupled to a scalar field. From there, we could establish the relation between the parity even components of the conductivities and the shear and bulk viscosities.

It is however worthwhile to mention that the current J contains two kinds of contributions, one is coming from the evaluation of the probability current at the boundary and it is ambiguous because the probability current we have constructed depends on auxiliary fields whose boundary conditions can be fixed in different ways. The second kind of contribution depends on the value of the current at the horizon and it cannot be determined without explicitly solving the equations of motion. Since the correlators Γ are defined only in terms of the original fluctuations, the horizon and boundary ambiguities should cancel each other, but we cannot determine completely the Ward identity from parity invariance of the current alone. The situation is somewhat improved when only parity even or parity odd sources are turned on, in this case there are no spurious contributions from the horizon. Nevertheless, the results are consistent with the already known relations between conductivities and viscosities from standard field theory analysis [66], posing therefore a novel and more complete way to derive transport relations from the Ward identities in the gauge/gravity duality.

Results of the article "Holographic quark matter and neutron stars":

By means of an extrapolation of top-down theory [50], we studied in [67] a quantum field theory at strong coupling which could be identified as cold quark matter at finite density. Flavor was introduced by adding $D7$ branes in the probe approximation, so that the overall action can be split into two contributions, $S = S_{\mathcal{N}=4} + S_{D7}$, wherein $S_{\mathcal{N}=4}$ vanishes when one sets $T/\mu \to 0$[4]. Both the energy density and the pressure have been determined analytically. With this, we described the core of a neutron star, made out of deconfined matter at zero temperature. In order to model a full hybrid neutron star, we combined the information gained from holography with an extrapolation of soft/intermediate and stiff equations of state from chiral effective field theories, employed to model the outer layer, made out of confined matter. In addition, we integrated out the TOV equations and obtained the $M - R$ curves. From comparing the free energies both of the holographic and CET models, we found that at the crossing point, the difference between their derivatives was rather large, signaling thus a strong first order phase transition between confined and deconfined matter. The underlying reason of is related to the softness on the equation of state from the $D3 - D7$ model. Based on all of these results, we concluded that *no significant amount of quark matter can exist at the interior of a neutron star.*

Results of the article "Breaking the sound barrier in holography":

In this work, we studied a simple class of models involving RG flows triggered by relevant scalar operators charged under a global Abelian symmetry, particularized to the case where the charged scalar field was in the probe approximation (no backreaction). The gravity geometry was thus reduced to an AdS-RN. At a particular choice of scalar charge q and conformal dimension Δ, we reproduced a simplified model from a string theory example: a charged black hole dual to a $\mathcal{N} = 4$ theory at finite R-charge density, deformed by a gaugino mass term in the probe approximation. We found solutions to the scalar field, both numerical and even analytical at low temperatures, where the black hole is near extremal and the geometry of the gravitational theory reduces to an $AdS_2 \times \mathbb{R}_3$. Since at very large densities an instability toward the formation of a homogeneous condensate develops (the scalar field would acquire an expectation value at zero source), we made sure that the violation occurs in the stable regime, which occurred at an extremely large ratio μ/T. We proved that the conjectured bound for holographic theories in four dimensions, $v_s < 1/\sqrt{3}$, was not correct, as the holographic models found realized UV complete four dimensional field theories that could describe stable systems, both thermodynam-

[4]Strictly speaking, the temperature inside a neutron star is evidently not zero, but since the densities are much larger compared to the temperature, $\mu/T \sim 10^3 - 10^4$, thermal contributions can be neglected.

ically and dynamically and hence susceptible to be applied to phenomenology. From the results of this work, we conclude that *there is no universal bound for the speed of sound in holographic models dual to ordinary four-dimensional relativistic field theories.*

Results of the article "Stiff phases in strongly coupled gauge theories with holographic duals":

In [68], we studied the thermodynamics of cold and dense strongly coupled matter via simple holographic models, following a natural extension of [69], consisting of going beyond the approximation of a small breaking of conformal invariance, namely, including backreaction of the scalar field onto the geometry. The models included the minimal ingredients of finite charge density and breaking of conformal invariance through a coupling for a relevant scalar operator of conformal dimension $4 > \Delta \geq 3$. A simple stability analysis of the models furthermore showed no obvious thermodynamic or dynamic instabilities. In addition to the bottom-up models, we also studied a top-down model with a more complicated action for the scalar, determined by a consistent truncation of supergravity. We studied how large can be the value of the speed of sound in holography. We showed that the speeds of sound obtained in gauge/gravity models can be arbitrarily close to the speed of light, providing several examples. On the gravity side, the models consisted of an Einstein-Maxwell theory coupled to a scalar field, which can be either charged or neutral. These models are dual to a strongly coupled gauge theory in its large-N_c limit. The bulk gauge field is then dual to a global $U(1)$ current on the field theory side, while the addition of the scalar field induces a relevant deformation (meaning that the UV is a fixed point). We focused on two particular models: The first one had a string theory (top-down) realization with a known field theory dual, while the the second case consisted of a family of bottom-up models. Interestingly, we observed that the simplest scenario including a quadratic potential for a canonically normalized scalar field does not lead to large enough values for the speed of sound. To reach higher values, it has been necessary for the scalar field to possess self-interactions, which are reflected in the properties of higher order correlators of the dual operator. In any case, both the bottom-up and top-down theories violated the Taub's inequality (2.6) in (stable) regimes where the speed of sound was clearly above the conformal value.

While it is true that in what concerns the top-down model, its applicability to phenomenology is not straightforward (the chemical potential in this case is related to the R-density, instead of a baryonic density), it described a well-known relativistic field theory, wherein the only (natural) bound that arises is causality. A seizable speed of sound was found, driven by the emergence of a new scale from the boundary renormalization, and because of the fact that the scalar field

was charged under the $U(1)$ gauge group. Such new scale did not appear for the bottom-up family models. Instead, the source for the seizable speed of sound in this last kind of models was essentially the (unfixed) coefficient that multiplies the ϕ^4 term in the bulk potential, which, if led to be large enough, can lead to the emergence of (thermo)dynamic instabilities.

5 Conclusions

Now we shall detail the conclusions of the present thesis, making a distinction whether are referred to systems in $2+1$ dimensions [32] or in $3+1$ dimensions [67–69].

5.1 Systems in $2+1$ dimensions

Regarding the relations for the stress-tensor transport coefficients from the Ward identities, some non-trivial information has been derived in the context of holography for systems with parity invariance. In relation to the ambiguities that enter in the Ward identities in [32], a naïve comparison with the Ward identity (2.23) at zero magnetic field in [66] would fix the imaginary part to zero. Although this probably holds in the holographic model, the correlators computed using holographic renormalization can differ by contact terms from the correlators that enter in the Ward identity in [66], so there might be additional contributions. It would be interesting to look for a general argument that fixes the aforementioned ambiguity in holographic models.

A natural generalization of this work would be to derive similar Ward identities in holographic models with broken parity, in particular the relation between Hall viscosity and Hall conductivity. This is a direction that has not been explored much, even though there are a large variety of models that exhibit a non-zero Hall conductivity: dyonic black holes [25, 70–74], D-brane intersections of different types [75–79] and others [80, 81]. However, the value of the Hall viscosity has been determined in a different class of holographic models dual to parity breaking superfluids [82–85]. It would be interesting to check if and when the models that have a Hall conductivity also have a Hall viscosity, since this is mostly the case in Quantum Hall systems and other topological states in condensed matter.

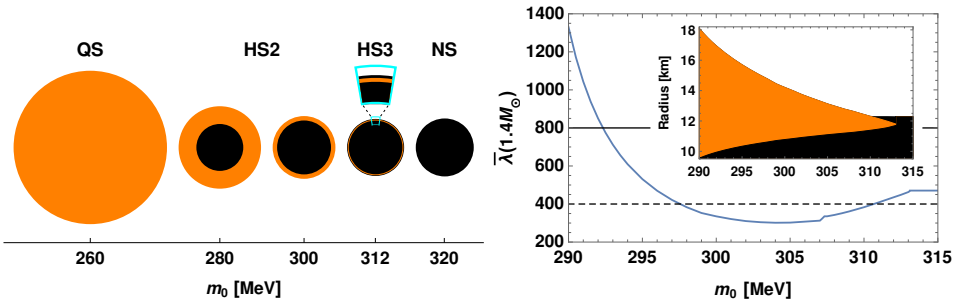

Figure 1: Left plot: Types of neutron stars predicted by the combined $D3-D7$ brane intersection and CEF models from [67] as a function of m_0. Right plot: Tidal deformability (blue line) and allowed radii for a neutron star as a function of m_0. For both plots, the orange region denotes strange quark matter while the black one hadronic matter.

5.2 Systems in $3+1$ dimensions

The validity regime for treating the stack of $D7$ branes in a $D3-D7$ brane intersection as if they are in the probe approximation, is restricted to the case when $N_c \gg N_f$. Since in [67], we have set $N_f = N_c = 3$, the model has thus been regarded as a phenomenological extrapolation from a former top-down model with one parameter to fix (the t'Hooft coupling). This extrapolation might have entailed an additional systematic uncertainty, which perhaps can be ameliorated if one departs from the probe approximation and considers a fully-backreacted solution. Moreover, we have set the constituent quark mass m_0 to be a fixed parameter, but one can explore the phenomenology that arises when such restriction is lifted. This has already been carried out in [86], being able to model not only pure neutron stars and pure quark stars, but also exotic hybrid stars that accommodate either an outer crust composed of quark matter and a core of hadronic matter (HS2s), or another type (HS3s) that have both a quark mantle and a nuclear crust on top of a nuclear matter core. For all types of stars constructed, we were able to determine not only their mass-radius relations, but we also computed the tidal deformabilities (see figure 1), as well as moments of inertia and the mass distribution, finding that there exists a range of parameter values in the $D3-D7$ model, for which the novel hybrid stars have properties in very good agreement with all existing bounds on the stationary properties of compact stars. In particular, the tidal deformabilities of these solutions are smaller than those of ordinary neutron stars of the same mass, implying that they provide an excellent fit to the gravitational data GW170817 of LIGO and Virgo.

Regarding our analysis in [69], it is worthwhile to mention that only for the near-extremal case we were able to find an analytic formula for the speed of sound. It would be interesting to examine whether there exists a general formula, or more precisely, under what specific conditions one can get an speed of sound larger than its conformal value for holographic theories, more or less in the same lines than in [87], but for theories with relevant deformations instead.

In [68] we found out that the issues of superluminal or imaginary speeds of sound do not appear for the top-down model, which suggests that adding higher powers of the scalar field to the scalar potential might ameliorate the behavior of these quantities also in the bottom-up models. On the other hand, a stiff EoS is achieved in the top-down model only when there is a large separation between the scale of explicit breaking of conformal invariance and another scale that is spontaneously generated due to the inclusion of finite counterterms from renormalization. An interesting question is if the increase in stiffness is due to some underlying physical mechanism involving microscopic degrees of freedom in the dual field theory, at least for the top-down model where the dual is known. However, microscopic fields are not gauge invariant and therefore not directly accessible using the duality. So far we could just make a broad qualitative statement, it appears that one needs a combination of explicit and anomalous breaking of conformal invariance, with a hierarchy between these scales such that the scale of anomalous breaking is the larger. Moreover, while it is true that the bottom-up constructions are limited to some finite density and temperature windows, the applications to phenomenology are rich and wide. Response under external tidal deformations (parametrized by the so–called Love numbers), or even computer simulations of hybrid neutron star binary merging with EoS for the deconfined portion governed by stiff holographic models is at hand, opening up a wide spectrum of possibilities to study.

A different but equally interesting study would be to find a top-down model with finite baryon (rather than R-charge) density. Quark matter is typically introduced by embedding probe branes in the geometry, and in the known examples where the theory is truly $(3+1)$-dimensional, the bound on the speed of sound is satisfied even at finite density. This might change upon considering the backreaction of the branes. Solutions with backreacted flavors at finite density have been recently constructed in [88–91]. Another possibility is to take an alternative large-N limit where (anti) fundamental fields are extrapolated to two-index antisymmetric representations [92] and where operators with baryon charge map to gravitational modes.

6 Conclusiones

Ahora detallaremos las conclusiones de la presente tesis, haciendo una distinción si están referidas a sistemas en $2+1$ dimensiones [32] o a $3+1$ dimensiones [67–69].

6.1 Sistemas en $2+1$ dimensiones

Con respecto a las relaciones para los coeficientes de transporte que se obtienen por medio de las identidades de Ward, se extrajo información no trivial de acuerdo con la dualidad holográfica para sistemas con invariancia bajo paridad. En relación a las ambigüedades existentes en las identidades de Ward que aparecen en [32], una ingenua comparación con la identidad de Ward derivada en (2.23) en ausencia de campo magnético en [66] fijaría la parte imaginaria de corriente de probabilidad a cero. Aunque esto posiblemente sea cierto, los correladores obtenidos por medio de la renormalización holográfica pueden diferir en términos de contacto con respecto a los que intervienen en la identidad de Ward en [66], por lo que pueden haber contribuciones adicionales. Sería interesante buscar un argumento general que fijase por completo la incertidumbre anteriormente mencionada en modelos holográficos.

Una generalización natural de este trabajo sería el derivar identidades de Ward en modelos holográficos con ruptura de paridad, en particular examinando la relación entre la viscosidad de Hall y la conductividad de Hall. Esta es una dirección no muy explorada, aunque existen una gran variedad de modelos holográficos que exhiben una conductividad Hall no nula: agujeros negros diónicos [25,70–74], intersecciones de D-branas de distintas clases [75–79] entre otros [80,81]. No obstante, el valor de la viscosidad Hall ha sido determinado en una clase diferente de modelos holográficos duales a superfluidos que presentan ruptura de paridad [82–85]. Sería de interés examinar cuando, y bajo qué circunstancias, los modelos que presentan conductividad Hall puedan también presentar viscosidad de Hall, dado que este es el caso en sistemas cuánticos Hall y otros estados topológicos en materia condensada.

6.2 Sistemas en $3+1$ dimensiones

El régimen de validez para tratar el conjunto de $D7$ branas en la intersección $D3-D7$ bajo la aproximación sonda, está restringida al caso en donde $N_c \gg N_f$. Dado que en [67] hemos establecido que $N_f = N_c = 3$, el modelo ha sido por tanto considerado como una extrapolación fenomenológica de un modelo top-down original, con un parámetro a fijar (el acoplo t'Hooft).

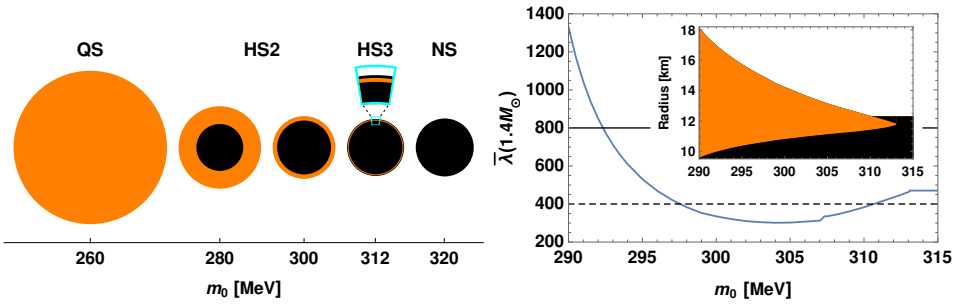

Figure 2: Gráfico izquierdo: Clases de estrellas de neutrones predichas por la combinación de modelos $D3-D7$ y CEF empleada en [67] como función de m_0. Gráfico derecho: Deformación de marea (línea azul) y radios permitidos para una estrella de neutrones estable como función de m_0. Para ambos gráficos, las regiones naranja y negra denotan materia quarkiónica extraña y materia hadrónica respectivamente.

Esta extrapolación puede haber originado una incertidumbre sistemática adicional, que quizás se puede aliviar si uno abandona la aproximación sonda y uno considera una solución con back-reaction. Por otra parte, hemos fijado la masa quark constituyente m_0, pero uno puede explorar la fenomenología que surge cuando tal restricción es eliminada. Esto se realizó en particular en [86], siendo capaces de modelizar no sólo estrellas de neutrones o de quarks, sino también estrellas híbridas que pueden contener una corteza exterior de materia quarkiónica y un núcleo de materia hadrónica (HS2), u otro tipo (HS3) que contienen tanto un manto de materia quarkionica así como una corteza exterior de materia hadrónica. Para todos los modelos de estrellas construidos, pudimos determinar no sólo las relaciones masa-radio, sino además determinar las deformaciones de marea (ver figura 2), así como momentos de inercia y la distribución de masa, encontrando que existe un rango de parámetros concerniente al modelo $D3-D7$ para el cual los modelos de estrellas híbridas exóticas tienen propiedades en muy buen acuerdo con todas las restricciones necesarias para existencia de estrellas compactas estacionarias. En particular, las deformaciones de marea de estos modelos son menores a con respecto las de estrellas de neutrones ordinarias de igual masa, implicando por tanto que poseen un excelente acuerdo con respecto a las observaciones gravitacionales de Ligo GW170817 y Virgo.

Relacionado con nuestro análisis de la velocidad del sonido en [69], cabe destacar que solamente en el caso extremal fuimos capaces de derivar una fórmula para la velocidad del sonido. Sería interesante examinar si existe una fórmula general, o para ser más preciso, bajo qué cir-

cunstancias uno puede tener una velocidad del sonido mayor que la dada por el valor conforme en teorías holográficas, más o menos en la misma línea que en [87], pero para teorías con deformaciones relevantes.

En [68] encontramos que el modelo top-down está exento de problemas relacionados con velocidad del sonido superluminal o compleja, lo cual sugiere que añadir órdenes superiores en el campo escalar al potencial puede mejorar el comportamiento de estas cantidades en lo concerniente a los modelos bottom-up. Por otra parte, una ecuación de estado rígida es alcanzada en el modelo top-down solo cuando hay una amplia separación entre la escala de ruptura explícita de simetría conforme y otra escala que es espontáneamente generada debido a la inclusión de términos finitos desde la renormalización holográfica. Una cuestión interesante es si el incremento de la rigidez es debido a algún mecanismo físico subyacente que involucre grados de libertad microscópicos en la teoría dual, al menos en lo que respecta al modelo top-down, en donde su dual es conocido. No obstante, los campos microscópicos no son invariantes gauge y por tanto no accesibles por medio de la dualidad holográfica. Hasta el momento solo hemos podido establecer una afirmación cualitativa amplia; parece ser que uno necesita la combinación de ruptura de invariancia conforme tanto explícita como anómala, con una jerarquía entre ambas escalas, de tal manera que la escala de ruptura anómala es considerablemente más grande. Por otra parte, si bien es cierto que la viabilidad de los modelos bottom-up está limitada en un cierto intervalo de temperatura y potencial químico, sus aplicaciones fenomenológicas son ricas y amplias. Respuesta bajo deformaciones de marea externas (parametrizadas por medio de los llamados números Love), o incluso simulaciones por ordenador de fusiones de estrellas de neutrones híbridas, cuyas equaciones de estado estén governadas por modelos holográficos, son posibles, abriendo un amplio espectro de posibilidades para estudiar.

Enfocado en otra línea de estudio, pero igualmente provechosa, se podría encontrar un modelo top-down que describiese un estado a densidad bariónica finita (en vez de a densidad R finita). Materia quarkiónica es introducida mediante el embebimiento de branas en la geometría bajo la aproximación sonda, y el los casos conocidos en donde la teoría es verdaderamente en $(3+1)$ dimensiones, el límite para la velocidad del sonido es satisfecho incluso para estados a densidad finita. Esto podría cambiar tras considerar el backreaction de las branas. Soluciones con sabores en backreaction a densidad finita han sido recientemente construidas en [88–91]. Otra posibilidad es considerar un límite de gran N alternativo, en donde campos en la representación (anti) fundamental son extrapolados a representaciones asimétricas con dos índices [92] y en donde operadores con carga bariónica son relacionados con modos gravitacionales.

7 Report on the impact factor

Below we give some details, taken from the Journal Citation Reports database, of the journals wherein the articles of this thesis have been published. The impact factors date from 2016, the most updated one at the moment. The date of acceptance is also specified. This thesis project started in September 1, 2014.

Article	Journal	Date of acceptance	Impact factor	Field
1	Journal of High Energy Physics	December 16, 2015	6.603	Particles & Fields
2	Physical Review Letters	June 16, 2016	8.462	Multidisciplinary Physics
3	Physical Review D	October 19, 2016	4.568	Particles & Fields Astronomy & Astrophysics
4	Journal of High Energy Physics	October 23, 2017	6.603	Particles & Fields